

Supporting Information

Changes in molecular film metallicity with minor modifications of their constitutive quinonoid zwitterions

Lucie Routaboul^{1,*} Iori Tanabe,² Juan Colon Santana,² Minghui Yuan,¹ Alessio Ghisolfi,¹

William Serrano Garcia,² Peter A. Dowben,^{2,*} Bernard Doudin,³ and Pierre Braunstein^{1,*}

¹ Université de Strasbourg, CNRS, CHIMIE UMR 7177, Laboratoire de Chimie de
Coordination, 4 rue Blaise Pascal, 67081 Strasbourg, France

² Dept. of Physics and Astronomy, Nebraska Center for Materials and Nanoscience,
University of Nebraska-Lincoln, Lincoln NE 68588, USA

³ Institut de Physique et Chimie des Matériaux de Strasbourg (UMR 7504 CNRS),
Université de Strasbourg, 23 rue du Loess B.P. 43, 67034 Strasbourg, France

Content of the Supporting Information

1 Synthesis of new zwitterionic molecules	S-4
1.1. Generalities	S-4
1.2. Optimized procedure	S-4
1.3. Synthetic procedure and characterization	S-10
1.3.1. Synthesis of zwitterion 6	S-11
1.3.2. Synthesis of zwitterion 7	S-11
1.3.3. Synthesis of zwitterion 8	S-12
1.3.4. Synthesis of zwitterion 9	S-13
1.3.5. Synthesis of zwitterion 10	S-13
1.3.6. Synthesis of zwitterion 11	S-14
1.3.7. Synthesis of zwitterion 12	S-15
1.3.8. Synthesis of zwitterion 13	S-16
1.3.9. Synthesis of zwitterion 14	S-17
1.3.10. Synthesis of zwitterion 15	S-18
1.3.11. Synthesis of zwitterion 16	S-18
1.3.12. Synthesis of zwitterion 17	S-19
1.3.13. Synthesis of zwitterion 18	S-20
1.3.14. Synthesis of zwitterion 19	S-20
1.3.15. Synthesis of zwitterion 20	S-21
1.3.16. Synthesis of zwitterion 21	S-22
1.3.17. Synthesis of zwitterion 22	S-23
1.3.18. Synthesis of zwitterion 23	S-24
1.3.19. Synthesis of zwitterion 24	S-24
1.3.20. Synthesis of zwitterion 25	S-25
1.3.21. Synthesis of zwitterion 26	S-26
2 Crystal structures determined by X-ray diffraction	S-28
Table S3. Selected X-ray data of zwitterions 6, 7 and 8	S-29
Table S4. Selected X-ray data of zwitterions 9, 12 and 13	S-30

Table S5. Selected X-ray data of zwitterions 15 , 19 and 24	S-31
2.1. Metrical data	S-32
2.2. Molecular arrangement in the solid state	S-33
2.2.1. Molecular arrangement of zwitterion 5	S-33
2.2.2. Influence of the length of the linker between the phenyl group and the zwitterionic core	S-36
2221. <i>Molecular arrangement of zwitterion 7</i>	S-37
2222. <i>Molecular arrangement of zwitterion 8</i>	S-38
2223. <i>Molecular arrangement of zwitterion 9</i>	S-39
2224. <i>Molecular arrangement of zwitterion 6</i>	S-42
2.2.3. Influence of a substituent on the linker	S-47
2231. <i>Molecular arrangement of zwitterion 12</i>	S-47
2232. <i>Molecular arrangement of zwitterion 13</i>	S-47
2.2.4. Influence of the functional groups on the aromatic part	S-49
2241. <i>Molecular arrangement of zwitterion 24</i>	S-49
2242. <i>Molecular arrangement of zwitterion 19</i>	S-52
2243. <i>Molecular arrangement of zwitterion 15</i>	S-56
2.2.5. Characteristics of the molecular rows	S-58
3. References	S-70
NMR spectra of zwitterion 6	S-71
NMR spectra of zwitterion 7	S-79
NMR spectra of zwitterion 8	S-86
NMR spectra of zwitterion 9	S-94
NMR spectra of zwitterion 10	S-103
NMR spectra of zwitterion 11	S-111

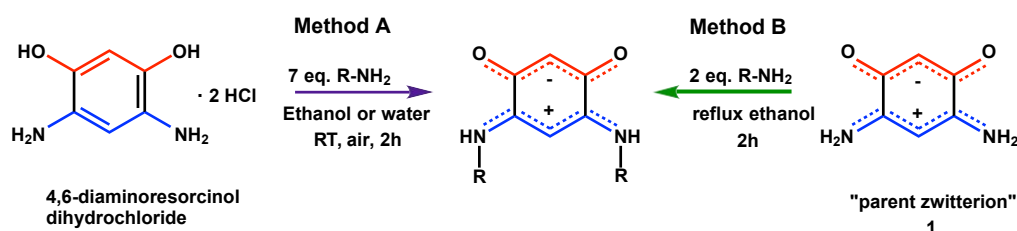
NMR spectra of zwitterion 12	S-121
NMR spectra of zwitterion 13	S-130
Figure S91. Comparison of the IR spectra of zwitterion 13 .	S-138
NMR spectra of zwitterion 14	S-139
NMR spectra of zwitterion 15	S-151
NMR spectra of zwitterion 16	S-156
NMR spectra of zwitterion 17	S-162
NMR spectra of zwitterion 18	S-170
NMR spectra of zwitterion 19	S-174
NMR spectra of zwitterion 20	S-181
NMR spectra of zwitterion 21	S-192
NMR spectra of zwitterion 22	S-199
NMR spectra of zwitterion 23	S-206
NMR spectra of zwitterion 24	S-215
NMR spectra of zwitterion 25	S-224
NMR spectra of zwitterion 26	S-232

1. Synthesis of new zwitterionic molecules

1.1. Generalities

The quinonoid zwitterions were isolated in good yields, using synthetic methods previously described in the literature.¹ They can be typically prepared by two different methods (Scheme S1). Following method A, they are directly obtained by reaction of an excess primary amine with 4,6-diaminoresorcinol dihydrochloride (commercially available). This one-pot reaction, performed in the presence of air and at room temperature, yields in 2 h the desired product. Following method B, the desired compound is obtained by a trans-amination reaction from the « parent zwitterion » **1**. The latter is readily prepared following the published procedure.¹ This method has the advantage to require the use of only two equivalents of primary amine per « parent zwitterion » **1**. We have recently demonstrated that the trans-amination reaction (method B) can be performed under microwave irradiation.² This activation method offers a fast (2 min. reaction time) and efficient access to several zwitterions and afforded a significantly increase in the yields of sterically-hindered zwitterions.

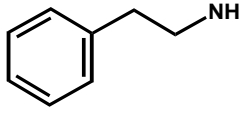
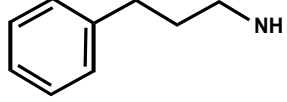
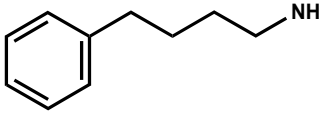
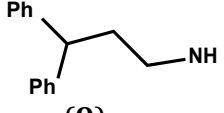
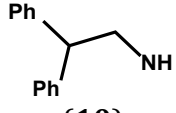
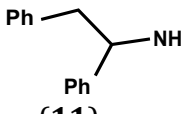
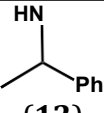
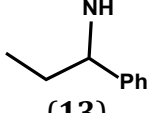
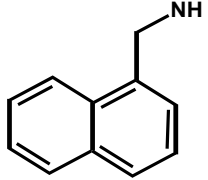
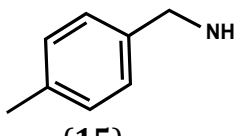
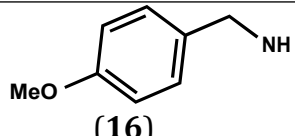
Scheme S1. General scheme of the two synthetic methods leading to quinonoid zwitterions ^{1,2}

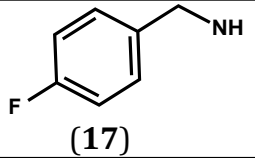
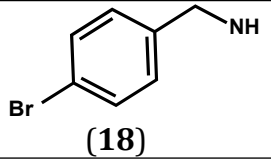
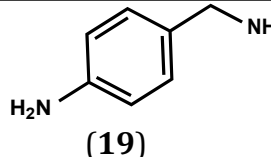
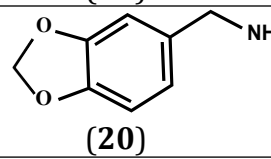
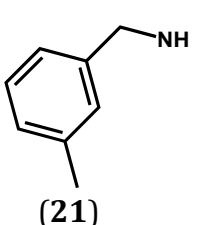
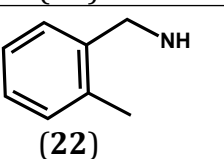
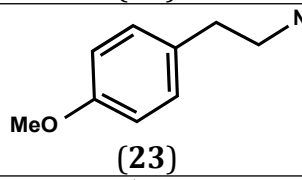
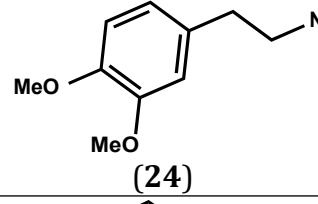
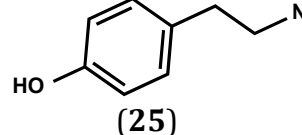
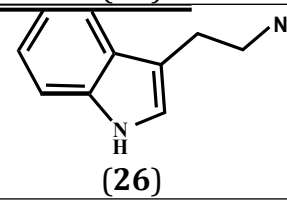


1.2. Optimized procedure

The best conditions for the syntheses of new zwitterions contained in this manuscript are summarized in Table S1.

Table S1. Synthesis of zwitterions with N-substituent

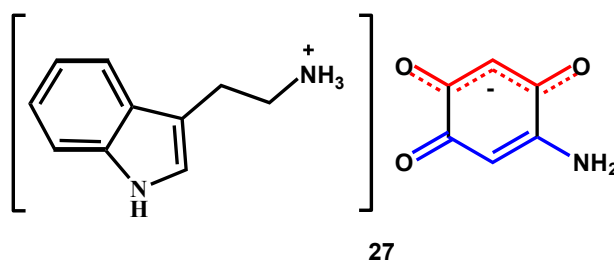
Entry	R-NH (Zwitterion)	Optimal experimental conditions	Yield (%)
1	 (6)	Method B Microwave irradiation ^a Solvent: water	> 95
2	 (7)	Method B Microwave irradiation ^a Solvent: water	> 95
3	 (8)	Method B Microwave irradiation ^a Solvent: water	92
4	 (9)	Method B Microwave irradiation ^a Solvent: ethanol	24
5	 (10)	Method B Microwave irradiation ^a Solvent: water	67
6	 (11)	Method B Microwave irradiation ^a Solvent: water Temperature: 130°C	30
7	 (12)	Method B Thermal conditions (oil bath) ^b Solvent: water	40
8	 (13)	Method B Thermal conditions (oil bath) ^b Solvent: water	71
9	 (14)	Method B Microwave irradiation ^a Solvent: water Temperature: 130°C	73
10	 (15)	Method B Thermal conditions (oil bath) ^b Solvent: water	82
11	 (16)	Method A Solvent: water	92

12	 (17)	Method B Thermal conditions (oil bath) ^b Solvent: water	> 95
13	 (18)	Method B Thermal conditions (oil bath) ^b Solvent: water	ND
14	 (19)	Method B Microwave irradiation ^a Solvent: water	90
15	 (20)	Method B Microwave irradiation ^a Solvent: water	50
16	 (21)	Method B Thermal conditions (oil bath) ^b Solvent: water	47
17	 (22)	Method B Thermal conditions (oil bath) ^b Solvent: water	57
18	 (23)	Method A Solvent: water	> 95
19	 (24)	Method A Solvent: water	> 95
20	 (25)	Method B Microwave irradiation ^a Solvent: water	77
21	 (26)	Method B Microwave irradiation ^a Solvent: ethanol	35

a) Reaction performed in a closed system (sealed CEM 10 ml reactor), 2.5 ml of water, power up to 80 W, 2 min at 100 °C. b) Preheated oil bath, 10 ml of solvent. ND (Not Determined, the expected product is obtained but all purification attempts failed)

The best yields of compounds having different linkers between the zwitterionic core and the phenyl substituent (Table S1, entries 1-8) were obtained when the trans-amination reaction was performed under microwave irradiation and water was used as solvent (except for zwitterions **9** and **13**). The lower yield obtained for zwitterion **9** compared to **10** may be due to the low solubility of the corresponding amine in water. The zwitterion **11** was only obtained when the reaction was performed under microwave irradiation at 130 °C (Table S1, entry 6). Zwitterions **11-13** are chiral compounds and **12** and **13** are enantiopure (Table S1, entries 6-8). Concerning the synthesis of zwitterions having a functional group on the aromatic substituent, no general rule can be identified and various tests should be carried out in order to determine the best solvent (Table S1, entries 9-21). For example, it is necessary to perform the reaction in water in order to obtain pure zwitterion **25** (when ethanol was used as a solvent, the crude mixture contained zwitterion **25** and unreacted parent zwitterion **1**, and since the solubility of both compounds is very low in organic solvents, we did not succeed to separate them). In the case of **26**, ethanol was the best solvent and we observed the formation of a by-product when the reaction was performed in water, which is probably the ion-pair **27** (Scheme S2), and all purification attempts failed.

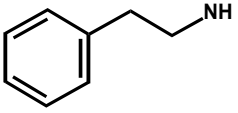
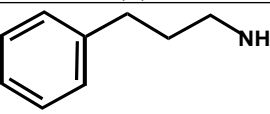
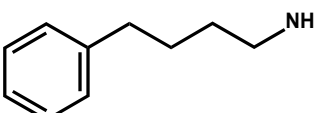
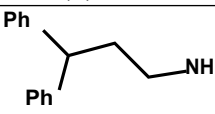
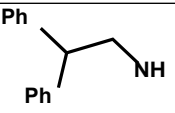
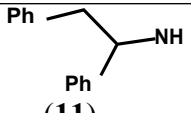
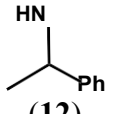
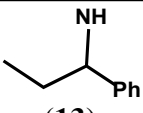
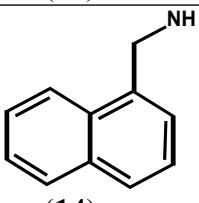
Scheme S2. Proposed chemical structure of the ion-pair **27**

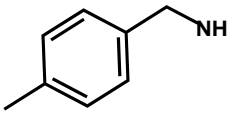
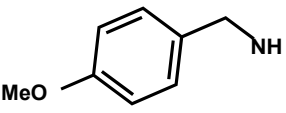
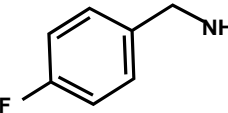
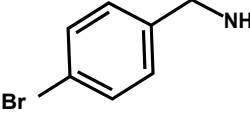
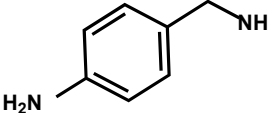
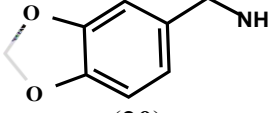
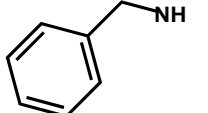
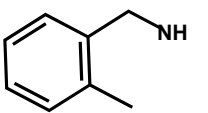
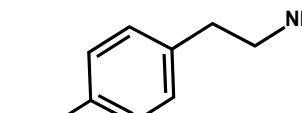


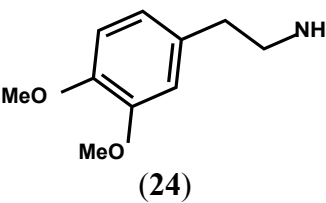
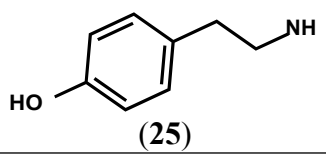
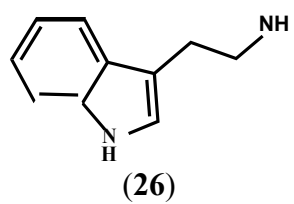
Finally, we succeeded in synthesizing a range of compounds having different steric bulk and functional groups. The presence of electron-donating or electron-withdrawing substituents allows to modulate the molecular electronic properties.

All syntheses performed are given in Table S2 and compared with the optimized conditions detailed in Table S1.

Table S2. Results concerning syntheses of new zwitterions. Yields in %.

entry	R-NH (Zwitterion)	Method B				Method A
		thermal		microwave		
		water	ethanol	water	ethanol	
1	 (6)	83	NP	>95	33	91
2	 (7)	80	55	>95	64	63
3	 (8)	72	49	92	NP	61
4	 (9)	NP	NP	17	24	NP
5	 (10)	50	NP	67	NP	50
6	 (11)	/	/	100°C: / 130°C: 30 150°C: /	/	/
7	 (12)	40	NP	NP	NP	NP
8	 (13)	71	6	65	NP	66
9	 (14)	NP	NP	130°C: 73	NP	NP

10	 (15)	82	18	42	NP	NP
11	 (16)	80	NP	69	NP	92
12	 (17)	>95	NP	76	NP	60
13	 (18)	ND	NP	NP	NP	NP
14	 (19)	78	82	90	NP	NP
15	 (20)	NP	NP	50	NP	NP
16	 (21)	47	NP	NP	NP	NP
17	 (22)	57	NP	NP	NP	NP
18	 (23)	83	45	78	NP	>95

19	 (24)	64	NP	37	37	>95
20	 (25)	36	ND	77	ND	NP
21	 (26)	ND	24	ND	35	NP

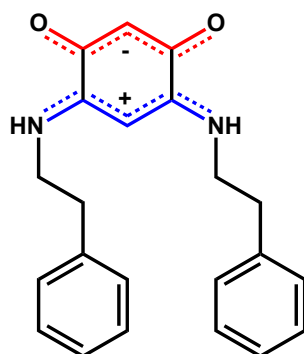
a) Preheated oil bath, 10 ml of solvent, 2 h at 80 or 100 °C. b) Reaction performed in a close system (sealed CEM 10 ml reactor), 2.5 ml of water, power up to 80 W, 2 min at 100 °C. NP (Not Performed), ND (Not Determined, the expected product is obtained but all purification attempts failed) and / (the presence of the expected product is not observed).

1.3. Synthetic procedure and characterization

General. Commercial 4,6-diaminoresorcinol dihydrochloride and functional amines were used directly without further purification. Solvents were freshly distilled under argon prior to use. Reactions under microwave irradiations were performed in a closed system (10 ml CEM reactor) and using a microwave CEM discover SP2011. ¹H NMR spectra were recorded in CDCl₃ on a Bruker 500 MHz instrument, operating at 125 MHz for ¹³C spectra and 500 MHz for ¹H spectra. Chemical shifts are given in δ units, in parts per million (ppm) relative to the singlet at δ = 7.26 for CHCl₃. The splittings were designated as s, singlet; d, doublet; t, triplet; m, multiplet; br, broad.

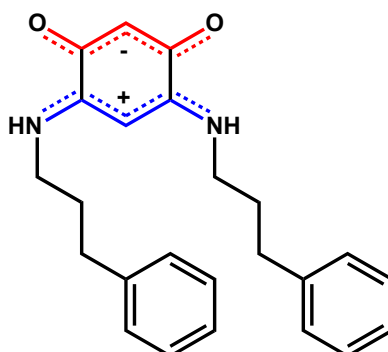
All relevant spectra are given in pages from S-71 to S-243.

1.3.1. Synthesis of (6Z)-4-(2-(phenyl)ethylamino)-6-(2-(phenyl)ethyliminio)-3-oxocyclohexa-1,4-dien-1-olate (6).



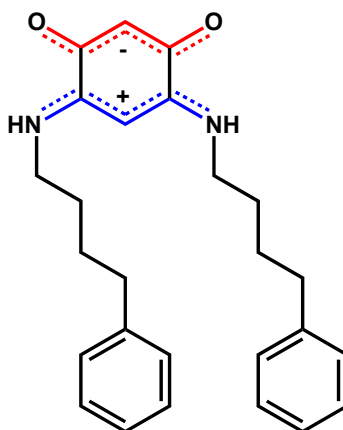
To a suspension of the parent zwitterion **1** (0.067 g, 0.485 mmol) in water (2.5 mL) was added 2-phenylethylamine (0.122 mL, 0.970 mmol). After microwave irradiation (the maximum power fixed at 80 Watts, 2 min at 100 °C), the reaction mixture was filtered and the solid collected was washed with water (5 ml) and then several times with diethyl ether and pentane (0.162 g, >95%). ¹H NMR (500 MHz, CDCl₃): δ 3.01 (t, ³J_{HH} = 7.2 Hz, 4H, CH₂), 3.57 (m, 4H, N-CH₂), 4.88 (s, 1H, N···C···CH), 5.44 (s, 1H, O···C···CH), 7.22-7.37 (m, 10H, CH aromatic), 8.46 (br s, 2H, NH). ¹³C{¹H} NMR (125 MHz, CDCl₃): δ 34.76 (s, CH₂), 44.76 (s, N-CH₂), 80.98 (s, N···C···CH), 98.80 (s, O···C···CH), 127.26 (s, CH Ar), 128.72 (s, CH Ar), 129.08 (s, CH Ar), 137.18 (s, C Ar), 156.73 (s, N···C), 172.22 (s, O···C).

1.3.2. Synthesis of (6Z)-4-(3-(phenyl)propylamino)-6-(3-(phenyl)propyliminio)-3-oxocyclohexa-1,4-dien-1-olate (7).



To a suspension of the parent zwitterion **1** (0.300 g, 2.17 mmol) in water (2.5 mL) was added 3-phenylpropylamine (0.615 mL, 4.34 mmol). After microwave irradiation (the maximum power fixed at 80 Watts, 2 min at 100 °C), the reaction mixture was filtered and the solid collected was washed with water (5 ml) and then several times with diethyl ether (0.800 g, >95%). ¹H NMR (500 MHz, CDCl₃): δ 1.97 (m, 4H, N-CH₂-CH₂), 2.65 (t, ³J_{HH} = 7.2 Hz, 4H, CH₂-CAr), 3.22 (m, 4H, N-CH₂), 4.78 (s, 1H, N···C···CH), 5.37 (s, 1H, O···C···CH), 7.07-7.25 (m, 10H, CH aromatic), 8.34 (br s, 2H, NH). ¹³C{¹H} NMR (125 MHz, CDCl₃): δ 29.45 (s, CH₂), 32.66 (s, CH₂), 42.21 (s, N-CH₂), 80.61 (s, N···C···CH), 98.86 (s, O···C···CH), 126.44 (s, CH Ar), 128.35 (s, CH Ar), 128.67 (s, CH Ar), 139.98 (s, C Ar), 156.63 (s, N···C), 172.30 (s, O···C).

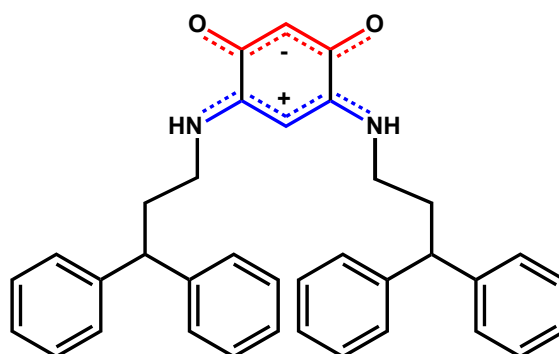
1.3.3. Synthesis of (6Z)-4-(4-(phenyl)-butylamino)-6-(4-(phenyl)-butyliminio)-3-oxocyclohexa-1,4-dien-1-olate (**8**).



To a suspension of the parent zwitterion **1** (0.130 g, 0.94 mmol) in water (2.5 mL) was added 4-phenyl-1-butylamine (0.300 mL, 1.88 mmol). After microwave irradiation (the maximum power fixed at 80 Watts, 2 min at 100 °C), the reaction mixture was filtered and the solid collected was washed with water (5 ml) and then several times with diethyl ether (0.350 g, 92%). ¹H NMR (500 MHz, CDCl₃): δ 1.70 (m, 8H, N-CH₂-CH₂ and N-CH₂-CH₂-CH₂), 2.62 (m, 4H, CH₂-CAr), 3.27 (m, 4H, N-CH₂), 4.99 (s, 1H, N···C···CH), 5.39

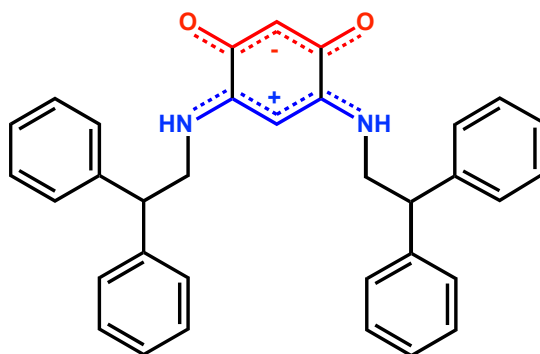
(s, 1H, O···C···CH), 7.11-7.26 (m, 10H, CH aromatic), 8.23 (br s, 2H, NH). $^{13}\text{C}\{^1\text{H}\}$ NMR (125 MHz, CDCl_3): δ 29.45 (s, CH_2), 32.66 (s, CH_2), 42.21 (s, N- CH_2), 80.61 (s, N···C···CH), 98.86 (s, O···C···CH), 126.44 (s, CH Ar), 128.35 (s, CH Ar), 128.67 (s, CH Ar), 139.98 (s, C Ar), 156.63 (s, N···C), 172.30 (s, O···C).

1.3.4. Synthesis of (6Z)-4-(3,3-(diphenyl)propylamino)-6-(3,3-(diphenyl)propyliminio)-3-oxocyclohexa-1,4-dien-1-olate (**9**).



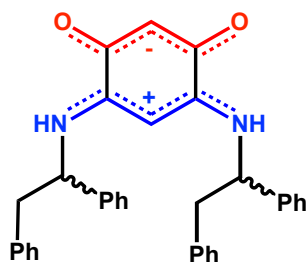
To a suspension of the parent zwitterion **1** (0.067 g, 0.485 mmol) in ethanol (2.5 mL) was added 3,3-diphenylpropylamine (0.206 g, 0.97 mmol). After microwave irradiation (the maximum power fixed at 80 Watts, 2 min at 100 °C), the reaction mixture was filtered and the violet solid collected was washed with water (5 ml) and then several times successively with ethanol and diethyl ether (0.062 g, 24%). ^1H NMR (500 MHz, CDCl_3): δ 2.45 (m, 4H, N- CH_2 - CH_2), 3.24 (m, 4H, N- CH_2), 3.97 (t, $^3J_{\text{HH}} = 8.0$ Hz, 2H, CH), 4.65 (s, 1H, N···C···CH), 5.46 (s, 1H, O···C···CH), 7.20-7.33 (m, 20H, CH aromatic), 8.32 (br s, 2H, NH). $^{13}\text{C}\{^1\text{H}\}$ NMR (125 MHz, CDCl_3): δ 33.95 (s, CH_2), 41.59 (s, N- CH_2), 48.31 (s, CH), 80.66 (s, N···C···CH), 98.80 (s, O···C···CH), 126.92 (s, CH Ar), 127.63 (s, CH Ar), 128.91 (s, CH Ar), 143.07 (s, C Ar), 156.67 (s, N···C), 172.17 (s, O···C).

1.3.5. Synthesis of (6Z)-4-(2,2-(diphenyl)ethylamino)-6-(2,2-(diphenyl)ethyliminio)-3-oxocyclohexa-1,4-dien-1-olate (**10**).



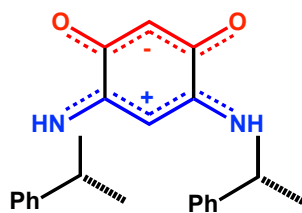
To a suspension of the parent zwitterion **1** (0.067 g, 0.485 mmol) in water (2.5 mL) was added 2,2-diphenylethylamine (0.195 g, 0.97 mmol). After microwave irradiation (the maximum power fixed at 80 Watts, 2 min at 100 °C), the reaction mixture was filtered and the solid collected was washed with water (5 ml) and then several times successively with ethanol and diethyl ether. It was solubilized in dichloromethane and this solution was washed with water, dried over magnesium sulfate, and filtered through Celite. The solution was concentrated under reduced pressure and addition of ether led to precipitation of the zwitterion **10** as a pink solid which was washed several times and successively with ether and pentane (0.164 g, 67%). ¹H NMR (500 MHz, CDCl₃): δ 3.86 (m, 4H, N-CH₂), 4.27 (m, 2H, CH), 4.90 (s, 1H, N...C...CH), 5.33 (s, 1H, O...C...CH), 7.20-7.33 (m, 20H, CH aromatic), 8.23 (br s, 2H, NH). ¹³C{¹H} NMR (125 MHz, CDCl₃): δ 47.91 (s, N-CH₂), 49.86 (s, CH), 81.14 (s, N...C...CH), 98.59 (s, O...C...CH), 127.62 (s, CH Ar), 127.87 (s, CH Ar), 129.20 (s, CH Ar), 140.35 (s, C Ar), 156.84 (s, N...C), 171.77 (s, O...C).

1.3.6. Synthesis of (6Z)-4-(1,2-(diphenyl)ethylamino)-6-(1,2-(diphenyl)ethyliminio)-3-oxocyclohexa-1,4-dien-1-olate (**11**).



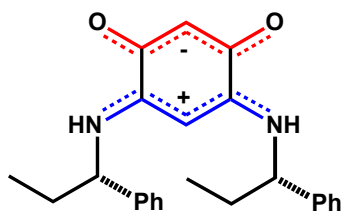
To a suspension of the parent zwitterion **1** (0.067 g, 0.485 mmol) in water (2.5 mL) was added 1,2-diphenylethylamine (0.190 ml, 0.97 mmol). After microwave irradiation (the maximum power fixed at 80 Watts, 2 min at 100 °C), the reaction mixture was filtered and the solid collected was washed with water. It was solubilized in dichloromethane and this solution was washed with water, dried over magnesium sulfate, and filtered through Celite. The solution was concentrated under reduced pressure and addition of pentane led to precipitation of the zwitterion **11** as a pink-violet solid which was washed several times with pentane (0.072 g, 30%). We observed by ¹H NMR an equimolar ratio of meso and racemic mixture of compounds. ¹H NMR (500 MHz, CDCl₃): δ 3.05–3.15 (m, 8H, CH₂), 4.36 (m, 4H, N–CH), 4.42 (m, 4H, N–CH), 4.52 (s, 1H, N···C···CH), 4.62 (s, 1H, N···C···CH), 5.34 (s, 1H, O···C···CH), 5.35 (s, 1H, O···C···CH), 6.88–7.08 (m, 16H, CH aromatic), 7.17–7.36 (m, 24H, CH aromatic), 8.54 (br s, 2H, NH). ¹³C{¹H} NMR (125 MHz, CDCl₃): δ 43.22 (s, CH₂), 43.25 (s, CH₂), 59.75 (s, N–CH), 83.75 (s, N···C···CH), 83.97 (s, N···C···CH), 98.46 (s, O···C···CH), 98.54 (s, O···C···CH), 126.22 (s, CH Ar), 126.62 (s, CH Ar), 127.37 (s, CH Ar), 127.43 (s, CH Ar), 128.40 (s, CH Ar), 128.55 (s, CH Ar), 128.82 (s, CH Ar), 128.95 (s, CH Ar), 129.12 (s, CH Ar), 129.14 (s, CH Ar), 129.19 (s, CH Ar), 129.27 (s, CH Ar), 135.44 (s, C Ar), 135.86 (s, C Ar), 138.37 (s, C Ar), 138.61 (s, C Ar), 155.93 (s, N···C), 155.96 (s, N···C), 171.89 (s, O···C).

1.3.7. Synthesis of (R,R)-(6Z)-4-(1-(phenyl)ethylamino)-6-(1-(phenyl)ethyliminio)-3-oxocyclohexa-1,4-dien-1-olate (**12**).



To a suspension of the parent zwitterion **1** (0.250 g, 1.81 mmol) in water (10 mL) was added (R)-(+)-1-phenylethylamine (0.638 mL, 3.62 mmol). The solution was heated at 100 °C for 2 h (preheated oil bath). After cooling to room temperature, the reaction mixture was filtered and the solid was washed several times with water. It was solubilized in dichloromethane and the organic phase was washed with water, dried over magnesium sulfate, and filtered through Celite. The solution was concentrated under reduced pressure and addition of pentane led to precipitation of the zwitterion **10** as a violet solid which was washed successively with ether and pentane (0.250 g, 40%). ¹H NMR (500 MHz, CDCl₃): δ 1.52 (d, ³J_{HH} = 6.9 Hz, 6H, CH₃), 4.37 (m, 2H, CH), 4.78 (s, 1H, N···C···CH), 5.43 (s, 1H, O···C···CH), 7.15–7.18 (m, 4H, CH aromatic), 7.32–7.41 (m, 6H, CH aromatic), 8.36 (br s, 2H, NH). ¹³C{¹H} NMR (125 MHz, CDCl₃): δ 22.87 (s, CH₃), 54.02 (s, N-CH), 84.17 (s, N···C···CH), 98.80 (s, O···C···CH), 125.92 (s, CH Ar), 128.41 (s, CH Ar), 129.29 (s, CH Ar), 140.55 (s, C Ar), 155.96 (s, N···C), 172.06 (s, O···C).

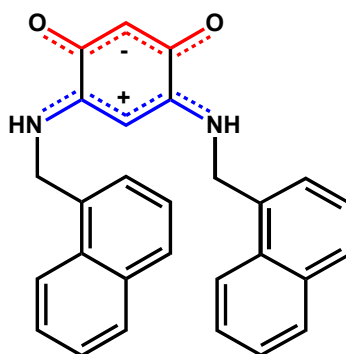
1.3.8. Synthesis of (R,R)-(6Z)-4-[(1-(phenyl)propylamino)-6-(1-(phenyl)propyliminio)-3-oxocyclohexa-1,4-dien-1-olate (**13**).



To a suspension of the parent zwitterion **1** (0.300 g, 2.17 mmol) in water (10 mL) was added (R)-(+)-1-phenylpropylamine (0.634 mL, 4.34 mmol). The solution was heated at 80 °C for 2 h (preheated oil bath). After cooling to room temperature, the reaction

mixture was filtered and the solid was washed several times with water. It was solubilized in dichloromethane and this solution was washed with water, dried over magnesium sulfate, and filtered through Celite. The solution was concentrated under reduced pressure and addition of pentane led to precipitation of the zwitterion **13** as a brown solid which was washed successively with ether and pentane (0.569 g, 71%). ¹H NMR (500 MHz, CDCl₃): δ 0.82 (t, ³J_{HH} = 7.3 Hz, 6H, CH₃), 1.85 (m, 4H, CH₂), 4.08 (m, 2H, N-CH), 4.78 (s, 1H, N···C···CH), 5.42 (s, 1H, O···C···CH), 7.14–7.16 (m, 4H, CH aromatic), 7.32–7.41 (m, 6H, CH aromatic), 8.41 (br s, 2H, NH). ¹³C{¹H} NMR (125 MHz, CDCl₃): δ 10.49 (s, CH₃), 29.90 (s, CH₂), 60.13 (s, N-CH), 84.15 (s, N···C···CH), 98.68 (s, O···C···CH), 126.58 (s, CH Ar), 128.41 (s, CH Ar), 129.16 (s, CH Ar), 139.25 (s, C Ar), 156.12 (s, N···C), 172.12 (s, O···C).

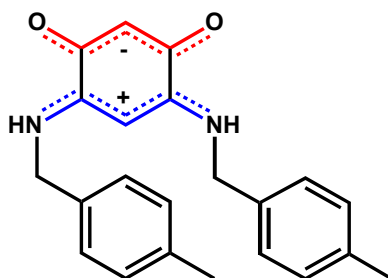
1.3.9. Synthesis of (6Z)-4-((naphthalen-1-ylmethyl)amino)-6-((naphthalen-1-ylmethyl)iminio)-3-oxocyclohexa-1,4-dien-1-olate (**14**).



To a suspension of the parent zwitterion **1** (0.067 g, 0.485 mmol) in water (2.5 mL) was added 1-naphthalenemethylamine (0.145 ml, 0.97 mmol). After microwave irradiation (the maximum power fixed at 80 Watts, 2 min at 100 °C), the reaction mixture was filtered and the brown solid collected was washed with water and then several times successively with ethanol, diethyl ether and pentane (0.148 g, 73%). ¹H NMR (500 MHz, DMSO d₆): δ 5.00 (s, 1H, O···C···CH), 5.04 (m, 4H, N-CH₂), 5.70 (s, 1H, N···C···CH), 7.14–

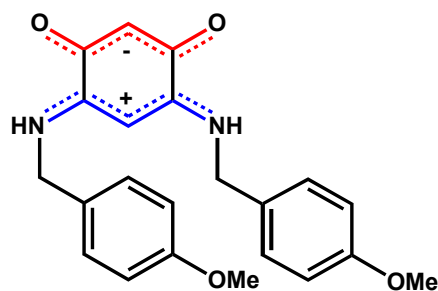
7.15 (m, 4H, CH naphthyl), 7.53–7.55 (m, 4H, CH naphthyl), 7.80–7.82 (m, 2H, CH naphthyl), 7.94–7.96 (m, 2H, CH naphthyl), 8.12–8.14 (m, 2H, CH naphthyl), 9.59 (br s, 2H, NH). $^{13}\text{C}\{^1\text{H}\}$ NMR (125 MHz, DMSO d_6): δ 44.64 (s, N-CH₂), 83.68 (s, N \cdots C \cdots CH), 98.12 (s, O \cdots C \cdots CH), 123.89 (s, CH naphthyl), 125.70 (s, CH naphthyl), 125.75 (s, CH naphthyl), 126.51 (s, CH naphthyl), 126.94 (s, CH naphthyl), 128.52 (s, CH naphthyl), 129.11 (s, CH naphthyl), 131.00 (s, C naphthyl), 131.96 (s, C naphthyl), 133.87 (s, C naphthyl), 157.29 (s, N \cdots C), 172.39 (s, O \cdots C).

1.3.10. Synthesis of (6Z)-4-(1-(4-(methyl)-phenyl)-methylamino)-6-(1-(4-(methyl)-phenyl)-methyliminio)-3-oxocyclohexa-1,4-dien-1-olate (**15**).



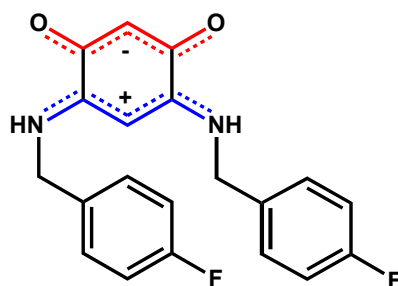
To a suspension of the parent zwitterion **1** (0.300 g, 2.17 mmol) in water (10 mL) was added 4-methylbenzylamine (0.555 mL, 4.34 mmol). The solution was heated at 100 °C for 2 h (preheated oil bath). After cooling to room temperature, the reaction mixture was filtered and the brown solid was washed several times and successively with water, ethanol, ether and pentane (0.618 g, 82%). ^1H NMR (500 MHz, CDCl₃): δ 2.34 (s, 6H, CH₃), 4.46 (m, 4H, N-CH₂), 5.27 (s, 1H, N \cdots C \cdots CH), 5.46 (s, 1H, O \cdots C \cdots CH), 7.09–7.15 (m, 8H, CH aromatic), 8.61 (br s, 2H, NH). $^{13}\text{C}\{^1\text{H}\}$ NMR (125 MHz, CDCl₃): δ 21.23 (s, CH₃), 47.29 (s, N-CH₂), 82.04 (s, N \cdots C \cdots CH), 99.20 (s, O \cdots C \cdots CH), 127.78 (s, CH Ar), 129.90 (s, CH Ar), 131.10 (s, C Ar), 138.53 (s, C Ar), 156.79 (s, N \cdots C), 172.21 (s, O \cdots C).

1.3.11. Synthesis of (6Z)-4-(1-(4-(methoxy)-phenyl)-methylamino)-6-(1-(4-(methoxy)-phenyl)-methyliminio)-3-oxocyclohexa-1,4-dien-1-olate (**16**).



4-methoxybenzylamine (4.3 mL, 33 mmol) was added to a solution of 4,6-diaminoresorcinol dihydrochloride (1.00 g, 4.7 mmol) in water (20 mL). Within a few minutes the color of the solution changed from brown to violet. After 2 h at room temperature in the presence of air, the reaction mixture was filtered. The red solid was washed successively and several times with water, ether and pentane (1.64 g, 92%).¹H NMR (500 MHz, DMSO d₆): δ 3.73 (s, 6H, CH₃), 4.52 (m, 4H, N-CH₂), 4.96 (s, 1H, N-C-CH), 5.57 (s, 1H, O-C-CH), 6.83-6.86 (m, 4H, CH aromatic), 7.18-7.21 (m, 4H, CH aromatic), 9.51 (br s, 2H, NH). ¹³C{¹H} NMR (125 MHz, DMSO d₆): δ 45.10 (s, N-CH₂), 55.01 (s, CH₃), 82.72 (s, N-C-CH), 97.69 (s, O-C-CH), 113.93 (s, CH Ar), 128.53 (s, C Ar), 129.09 (s, CH Ar), 155.96 (s, N-C), 158.58 (s, C Ar), 172.10 (s, O-C).

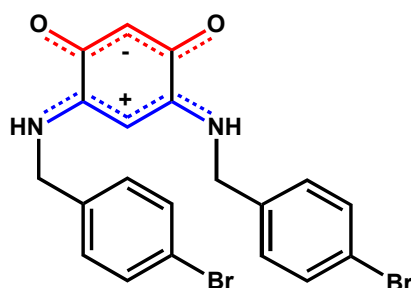
1.3.12. Synthesis of (6Z)-4-(1-(4-(fluoro)phenyl)methylamino)-6-(1-(4-(fluoro)phenyl)methyliminio)-3-oxocyclohexa-1,4-dien-1-olate (**17**).



To a suspension of the parent zwitterion **1** (0.300 g, 2.17 mmol) in water (2.5 mL) was added 4-fluorobenzylamine (0.500 mL, 4.34 mmol). After microwave irradiation (the maximum power fixed at 80 Watts, 2 min at 100 °C), the reaction mixture was filtered and the violet solid collected was washed with and then several times with ethanol,

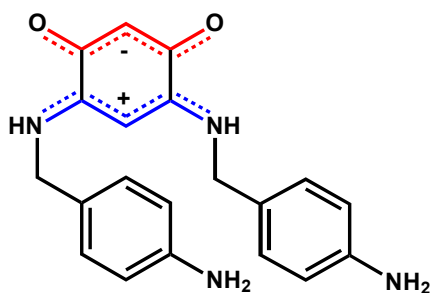
diethyl ether and pentane (0.770 g, >95%). ^1H NMR (500 MHz, DMSO d_6): δ 4.58 (m, 4H, N-CH₂), 4.97 (s, 1H, O...C...CH), 5.54 (s, 1H, N...C...CH), 7.09–7.14 (m, 4H, CH aromatic), 7.28–7.31 (m, 4H, CH aromatic), 9.72 (br s, 2H, NH). $^{13}\text{C}\{^1\text{H}\}$ NMR (125 MHz, DMSO d_6): δ 45.30 (s, N-CH₂), 83.22 (s, N...C...CH), 98.21 (s, O...C...CH), 115.79 (d, $J_{\text{CF}} = 21.5$ Hz, CH Ar), 130.14 (d, $J_{\text{CF}} = 8.2$ Hz, CH Ar), 133.27 (s, C Ar), 156.80 (s, N...C), 161.90 (d, $^1J_{\text{CF}} = 243.4$ Hz, C-F), 172.47 (s, O...C). $^{19}\text{F}\{^1\text{H}\}$ NMR (282 MHz, DMSO d_6): δ -115.02.

1.3.13. Synthesis of (6Z)-4-(1-(4-(bromo)-phenyl)-methylamino)-6-(1-(4-(bromo)-phenyl)-methyliminio)-3-oxocyclohexa-1,4-dien-1-olate (**18**).



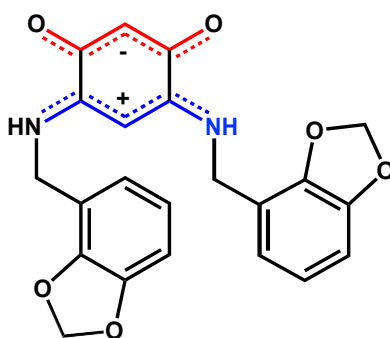
To a suspension of the parent zwitterion **1** (0.300 g, 2.17 mmol) in water (10 mL) was added 4-bromobenzylamine (0.545 mL, 4.34 mmol). The solution was heated at 100 °C for 2 h (preheated oil bath). After cooling to room temperature, the reaction mixture was filtered and the dark grey solid was washed several times and successively with water, ethanol, ether and pentane (0.66 g). ^1H NMR (500 MHz, DMSO d_6): δ 4.57 (m, 4H, N-CH₂), 4.97 (s, 1H, O...C...CH), 5.49 (s, 1H, N...C...CH), 7.17–7.20 (m, 4H, CH aromatic), 7.47–7.49 (m, 4H, CH aromatic), 9.73 (br s, 2H, NH). $^{13}\text{C}\{^1\text{H}\}$ NMR (125 MHz, DMSO d_6): δ 45.41 (s, N-CH₂), 83.41 (s, N...C...CH), 98.20 (s, O...C...CH), 121.12 (s, C Ar), 130.26 (s, CH Ar), 131.92 (s, CH Ar), 156.95 (s, N...C), 158.58 (s, C Ar), 172.40 (s, O...C).

1.3.14. Synthesis of (6Z)-4-(1-(4-(amino)-phenyl)-methylamino)-6-(1-(4-(amino)-phenyl)-methyliminio)-3-oxocyclohexa-1,4-dien-1-olate (**19**).



To a suspension of the parent zwitterion **1** (0.300 g, 2.17 mmol) in water (2.5 mL) was added 4-aminobenzylamine (0.495 mL, 4.34 mmol). After microwave irradiation (the maximum power fixed at 80 Watts, 2 min at 100 °C), the reaction mixture was filtered and the solid collected was washed with water, ether and pentane (0.680 g, 90%). ¹H NMR (500 MHz, DMSO d₆): δ 4.39 (m, 4H, N-CH₂), 4.94 (s, 1H, O···C···CH), 5.04 (br s, 4H, NH₂), 5.62 (s, 1H, N···C···CH), 6.51 (m, 4H, CH aromatic), 6.97 (m, 4H, CH aromatic), 9.32 (br s, 2H, NH). ¹³C{¹H} NMR (125 MHz, DMSO d₆): δ 45.62 (s, N-CH₂), 82.29 (s, N···C···CH), 97.55 (s, O···C···CH), 113.88 (s, CH Ar), 123.30 (s, C Ar), 128.87 (s, CH Ar), 148.14 (s, C Ar), 155.53 (s, N···C), 172.13 (s, O···C).

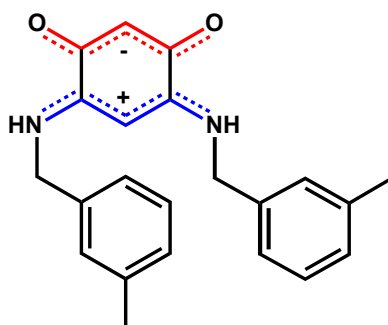
1.3.15. Synthesis of (6Z)-4-((benzo[d][1,3]dioxol-4-ylmethyl)amino)-6-((benzo[d][1,3]dioxol-4-ylmethyl)iminio)-3-oxocyclohexa-1,4-dien-1-olate (**20**).



To a suspension of the parent zwitterion **1** (0.067 g, 0.485 mmol) in water (2.5 mL) was added 3,4-(methylenedioxy)benzylamine (0.125 ml, 0.97 mmol). After microwave irradiation (the maximum power fixed at 80 Watts, 2 min at 100 °C), the reaction mixture was filtered and the solid collected was washed with water. It was solubilized in

dichloromethane and this solution was washed with water, dried over magnesium sulfate, and filtered through Celite. The solution was concentrated under reduced pressure and addition of pentane led to precipitation of the zwitterion **20** as a green solid which was washed successively with ether and pentane (0.098 g, 50%). ¹H NMR (500 MHz, DMSO d₆): δ 4.50 (m, 4H, N-CH₂), 4.95 (s, 1H, O-CH), 5.61 (s, 1H, N-CH), 5.90 (s, 4H, O-CH₂), 6.79-6.81 (m, 4H, CH aromatic), 6.89 (m, 4H, CH aromatic), 9.59 (br s, 2H, NH). ¹³C{¹H} NMR (125 MHz, DMSO d₆): δ 45.10 (s, N-CH₂), 55.01 (s, CH₃), 82.72 (s, N-CH), 97.69 (s, O-CH), 113.93 (s, CH Ar), 128.53 (s, C Ar), 129.09 (s, CH Ar), 155.96 (s, N-C), 158.58 (s, C Ar), 172.10 (s, O-C).

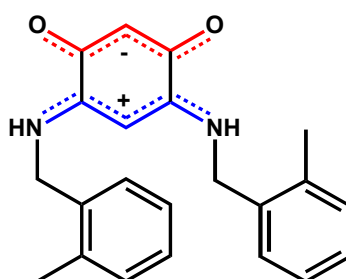
1.3.16. Synthesis of (6Z)-4-(1-(3-(methyl)phenyl)methylamino)-6-(1-(3-(methyl)phenyl)methyliminio)-3-oxocyclohexa-1,4-dien-1-olate (**21**).



To a suspension of the parent zwitterion **1** (0.200 g, 1.45 mmol) in water (15 mL) was added 2-methylbenzylamine (0.360 mL, 2.90 mmol). The solution was heated at 100 °C for 2 h (preheated oil bath). After cooling to room temperature, the reaction mixture was filtered and the brown solid was washed several times with water. It was solubilized in dichloromethane and this solution was washed with water, dried over magnesium sulfate, and filtered through Celite. The solution was concentrated under reduced pressure and addition of ether led to precipitation of the zwitterion **21** as a brown solid which was washed several times and successively with ether and pentane (0.236 g, 47%). ¹H NMR (500 MHz, CDCl₃): δ 2.33 (s, 6H, CH₃), 4.46 (m, 4H, N-CH₂), 5.27

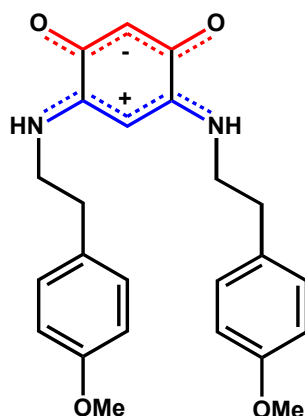
(s, 1H, N \cdots C \cdots CH), 5.47 (s, 1H, O \cdots C \cdots CH), 7.00–7.03 (m, 4H, CH aromatic), 7.13–7.25 (m, 4H, CH aromatic), 8.39 (br s, 2H, NH). $^{13}\text{C}\{^1\text{H}\}$ NMR (125 MHz, CDCl_3): δ 21.43 (s, CH_3), 47.49 (s, N- CH_2), 81.82 (s, N \cdots C \cdots CH), 98.94 (s, O \cdots C \cdots CH), 124.82 (s, CH Ar), 128.41 (s, CH Ar), 129.14 (s, CH Ar), 129.46 (s, CH Ar), 134.00 (s, C Ar), 139.19 (s, C Ar), 157.06 (s, N \cdots C), 172.16 (s, O \cdots C).

1.3.17. Synthesis of (6Z)-4-(1-(2-(methyl)phenyl)methylamino)-6-(1-(2-(methyl)phenyl)methyliminio)-3-oxocyclohexa-1,4-dien-1-olate (**22**).



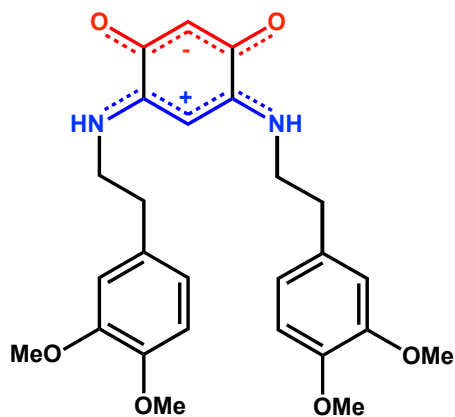
To a suspension of the parent zwitterion **1** (0.200 g, 1.45 mmol) in water (15 mL) was added 2-methylbenzylamine (0.360 mL, 2.90 mmol). The solution was heated at 100 °C for 2 h (preheated oil bath). After cooling to room temperature, the reaction mixture was filtered and the solid was washed several times with water. It was solubilized in dichloromethane and this solution was washed with water, dried over magnesium sulfate, and filtered through Celite. The solution was concentrated under reduced pressure and addition of ether led to precipitation of the zwitterion **22** as a violet solid which was washed several times and successively with ether and pentane (0.284 g, 57%). ^1H NMR (500 MHz, CDCl_3): δ 2.29 (s, 6H, CH_3), 4.49 (m, 4H, N- CH_2), 5.29 (s, 1H, N \cdots C \cdots CH), 5.47 (s, 1H, O \cdots C \cdots CH), 7.14–7.27 (m, 8H, CH aromatic), 8.39 (br s, 2H, NH). $^{13}\text{C}\{^1\text{H}\}$ NMR (125 MHz, CDCl_3): δ 19.22 (s, CH_3), 45.86 (s, N- CH_2), 81.59 (s, N \cdots C \cdots CH), 98.91 (s, O \cdots C \cdots CH), 126.78 (s, CH Ar), 128.71 (s, CH Ar), 129.10 (s, CH Ar), 131.13 (s, CH Ar), 131.83 (s, C Ar), 136.42 (s, C Ar), 157.00 (s, N \cdots C), 172.02 (s, O \cdots C).

1.3.18. Synthesis of (6Z)-4-(2-(4-(methoxy)-phenyl)-ethylamino)-6-(2-(4-(methoxy)-phenyl)-ethyliminio)-3-oxocyclohexa-1,4-dien-1-olate (**23**).



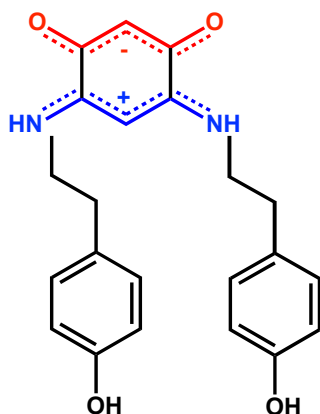
4-methoxyphenethylamine (4.8 mL, 33 mmol) was added to a solution of 4,6-diaminoresorcinol dihydrochloride (1.00 g, 4.7 mmol) in water (20 mL). After 2 h at room temperature in the presence of air, the reaction mixture was filtered and the brown solid was washed successively and several times with water, ether and pentane (1.87 g, >95%). ¹H NMR (500 MHz, CDCl₃): δ 2.89 (t, ³J_{HH} = 7.1 Hz, 4H, CH₂), 3.48 (m, 4H, N-CH₂), 3.75 (s, 6H, CH₃), 4.82 (s, 1H, N···C···CH), 5.38 (s, 1H, O···C···CH), 6.82–6.85 (m, 4H, CH aromatic), 7.08–7.10 (m, 4H, CH aromatic), 8.33 (br s, 2H, NH). ¹³C{¹H} NMR (125 MHz, CDCl₃): δ 33.90 (s, CH₂), 44.91 (s, N-CH₂), 55.33 (s, CH₃), 80.97 (s, N···C···CH), 98.76 (s, O···C···CH), 114.47 (s, CH Ar), 129.04 (s, C Ar), 129.73 (s, CH Ar), 156.69 (s, N···C), 158.83 (s, C Ar), 172.22 (s, O···C).

1.3.19. Synthesis of (6Z)-4-(2-(3,4-(dimethoxy)-phenyl)-ethylamino)-6-(2-(3,4-(dimethoxy)-phenyl)-ethyliminio)-3-oxocyclohexa-1,4-dien-1-olate (**24**).



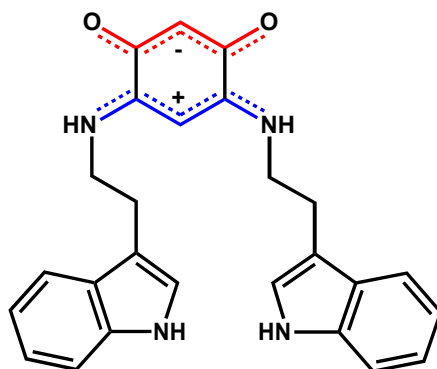
3,4-dimethoxyphenethylamine (5.6 mL, 33 mmol) was added to a solution of 4,6-diaminoresorcinol dihydrochloride (1.00 g, 4.7 mmol) in water (20 mL). Within a few minutes the color of the solution changed from brown to violet. After 2 h at room temperature in the presence of air, the reaction mixture was filtered. The violet solid was washed successively and several times with water, ether and pentane (2.26 g, >95%). ^1H NMR (500 MHz, CDCl_3): δ 2.90 (t, $^3J_{\text{HH}} = 7.1$ Hz, 4H, CH_2), 3.50 (m, 4H, N- CH_2), 3.82 (s, 6H, CH_3), 3.84 (s, 6H, CH_3), 4.86 (s, 1H, N \cdots C \cdots CH), 5.42 (s, 1H, O \cdots C \cdots CH), 6.82–6.85 (m, 4H, CH aromatic), 6.67 (m, 2H, CH aromatic), 6.70–6.73 (m, 2H, CH aromatic), 6.78–6.80 (m, 2H, CH aromatic), 8.30 (br s, 2H, NH). $^{13}\text{C}\{^1\text{H}\}$ NMR (125 MHz, CDCl_3): δ 33.90 (s, CH_2), 44.91 (s, N- CH_2), 55.33 (s, CH_3), 80.97 (s, N \cdots C \cdots CH), 98.76 (s, O \cdots C \cdots CH), 114.47 (s, CH Ar), 129.04 (s, C Ar), 129.73 (s, CH Ar), 156.69 (s, N \cdots C), 158.83 (s, C Ar), 172.22 (s, O \cdots C).

1.3.20. Synthesis of (6Z)-4-(2-(4-(hydroxy)phenyl)ethylamino)-6-(2-(4-(hydroxy)phenyl)ethyliminio)-3-oxocyclohexa-1,4-dien-1-olate (**25**).



To a suspension of the parent zwitterion **1** (0.135 g, 0.97 mmol) in water (2.5 mL) was added Tyramine (0.266 g, 1.94 mmol). After microwave irradiation (the maximum power fixed at 80 Watts, 2 min at 100 °C), the reaction mixture was filtered and the solid collected was washed several times and successively with water ethanol and diethyl ether (0.281 g, 77%). ¹H NMR (500 MHz, DMSO d₆): δ 2.77 (m, 4H, CH₂), 3.53 (m, 4H, N-CH₂), 3.75 (s, 6H, CH₃), 4.90 (s, 1H, N···C···CH), 5.24 (s, 1H, O···C···CH), 6.66-6.68 (m, 4H, CH aromatic), 7.03-7.05 (m, 4H, CH aromatic), 8.92 (br s, 2H, NH), 9.25 (br s, 2H, OH). ¹³C{¹H} NMR (125 MHz, DMSO d₆): δ 33.61 (s, CH₂), 44.60 (s, N-CH₂), 82.06 (s, N···C···CH), 97.90 (s, O···C···CH), 115.67 (s, CH Ar), 128.85 (s, C Ar), 130.25 (s, CH Ar), 156.33 (s, C Ar), 156.42 (s, N···C), 172.46 (s, O···C).

1.3.21. Synthesis of (6Z)-4-(2-(1H-indol-3-yl)-ethylamino)-6-(2-(1H-indol-3-yl)-ethyliminio)-3-oxocyclohexa-1,4-dien-1-olate (**26**).



To a suspension of the parent zwitterion **1** (0.067 g, 0.485 mmol) in ethanol (2.5 mL) was added tryptamine (0.145 ml, 0.97 mmol). After microwave irradiation (the maximum power fixed at 80 Watts, 2 min at 100 °C), the reaction mixture was filtered and the solid collected was extracted with ethanol. The solution was concentrated under reduced pressure and addition of diethyl ether precipitated the zwitterion **26** as a green solid which was washed successively with ether and pentane (0.073 g, 35%). ¹H NMR (500 MHz, DMSO d₆): δ 2.96 (m, 4H, CH₂), 3.46 (m, 4H, N-CH₂), 4.89 (s, 1H, O-C-CH), 5.07 (s, 1H, N-C-CH), 6.94 (m, 2H, CH aromatic), 7.04 (m, 2H, CH aromatic), 7.13 (m, 2H, N-CH), 7.31-7.34 (m, 2H, CH aromatic), 7.55-7.57 (m, 2H, CH aromatic), 8.89 (br s, 2H, NH), 10.87 (br s, 2H, NH). ¹³C{¹H} NMR (125 MHz, DMSO d₆): δ 23.98 (s, CH₂), 42.83 (s, N-CH₂), 81.33 (s, N-C-CH), 97.40 (s, O-C-CH), 110.57 (s, C quat.), 111.43 (s, CH Ar), 118.22 (s, CH Ar), 118.40 (s, CH Ar), 121.04 (s, CH Ar), 123.33 (s, N-CH), 127.01 (s, C Ar), 136.25 (s, C Ar), 155.73 (s, N-C), 171.98 (s, O-C).

2. Crystal structures determined by X-ray diffraction

Single crystals of zwitterions **6-9**, **12**, **13**, **15**, **19** and **24** were obtained and their molecular structures (Figures S1) were elucidated by X-ray diffraction. Crystallographic details are given in Tables S3- S5.

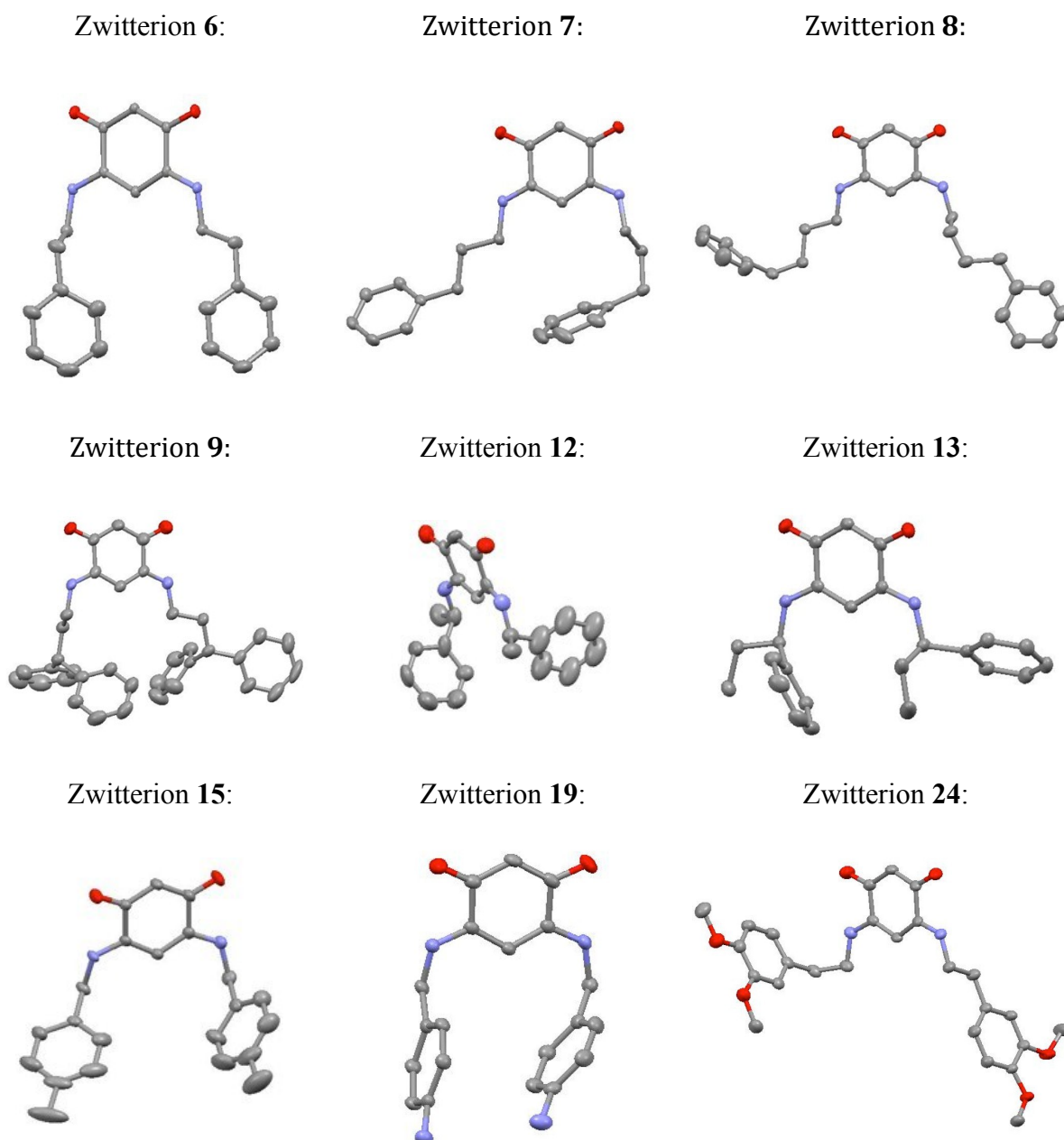


Figure S1. Mercury views of **6-9**, **12**, **13**, **15** and **24**. Thermal ellipsoids are drawn at the 50% probability level. H atoms are not shown for clarity.

Table S3. Selected X-ray data of zwitterions **6,7** and **8**

Compound	6	7	8
Chemical formula	C ₂₂ H ₂₂ N ₂ O ₂	C ₂₄ H ₂₆ N ₂ O ₂	C ₂₆ H ₃₀ N ₂ O ₂ ·H ₂ O
Formula Mass	346.42	374.47	420.54
Crystal system	Triclinic	Triclinic	Triclinic
<i>a</i> /Å	5.0542(5)	7.9425(3)	9.1007(11)
<i>b</i> /Å	9.8327(9)	11.2305(5)	9.4113(11)
<i>c</i> /Å	18.1540(17)	12.3864(5)	15.0880(18)
α /°	97.826(2)	69.7420(10)	97.591(3)
β /°	91.725(2)	88.5510(10)	90.128(3)
γ /°	96.982(2)	74.2780(10)	116.126(2)
Unit cell volume/Å ³	886.16(15)	994.85(7)	1147.4(2)
Temperature/K	173(2)	173(2)	173(2)
Space group	<i>P</i> -1	<i>P</i> -1	<i>P</i> -1
<i>Z</i>	2	2	2
Absorption coefficient, μ /mm ⁻¹	0.084	0.080	0.609
No. of reflections measured	13229	15982	11458
No. of independent reflections	4968	5808	3631
<i>R</i> _{int}	0.0583	0.0302	0.0225
Final <i>R</i> _I values (<i>I</i> > 2σ(<i>I</i>))	0.0727	0.0439	0.0899
Final <i>wR</i> (<i>F</i> ²) values (<i>I</i> > 2σ(<i>I</i>))	0.1620	0.1079	0.2579
Final <i>R</i> _I values (all data)	0.1351	0.0788	0.0923
Final <i>wR</i> (<i>F</i> ²) values (all data)	0.1941	0.1208	0.2608
Goodness of fit on <i>F</i> ²	1.022	1.026	1.072

Table S4. Selected X-ray data of zwitterions **9**, **12** and **13**

Compound	9	12	13
Chemical formula	C ₃₆ H ₃₄ N ₂ O ₂	C ₂₂ H ₂₂ N ₂ O ₂	C ₂₄ H ₂₆ N ₂ O ₂
Formula Mass	526.65	346.41	374.47
Crystal system	Monoclinic	Orthorhombic	Monoclinic
<i>a</i> /Å	8.284(9)	12.666(2)	6.0492(4)
<i>b</i> /Å	30.84(3)	13.200(3)	13.9149(9)
<i>c</i> /Å	11.178(13)	13.728(3)	12.3077(8)
α /°	90.00	90.00	90.00
β /°	98.85(3)	90.00	97.355(4)
γ /°	90.00	90.00	90.00
Unit cell volume/Å ³	2822(5)	2295.2(8)	1027.46(12)
Temperature/K	173(2)	173(2)	173(2)
Space group	<i>P</i> 2(1)/ <i>C</i>	<i>P</i> 2 ₁ 2 ₁ 2 ₁	<i>P</i> 2 ₁
<i>Z</i>	4	4	2
Absorption coefficient, μ /mm ⁻¹	0.076	0.065	0.609
No. of reflections measured	16427	16743	6751
No. of independent reflections	6552	5471	3057
<i>R</i> _{int}	0.1031	0.0797	0.0379
Final <i>R</i> _{<i>I</i>} values (<i>I</i> > 2σ(<i>I</i>))	0.0996	0.0921	0.0372
Final <i>wR</i> (<i>F</i> ²) values (<i>I</i> > 2σ(<i>I</i>))	0.2065	0.2355	0.0983
Final <i>R</i> _{<i>I</i>} values (all data)	0.2266	0.2113	0.0384
Final <i>wR</i> (<i>F</i> ²) values (all data)	0.2609	0.2808	0.0999
Goodness of fit on <i>F</i> ²	1.028	0.927	1.034

Table S5. Selected X-ray data of zwitterions **15**, **19** and **24**

Compound	15	19	24
Chemical formula	C ₂₂ H ₂₂ N ₂ O ₂	C ₂₀ H ₂₀ N ₄ O ₂	C ₂₆ H ₃₀ N ₂ O ₆
Formula Mass	346.41	348.40	466.52
Crystal system	Triclinic	Triclinic	Monoclinic
<i>a</i> /Å	4.7968(8)	9.4739(8)	12.5230(4)
<i>b</i> /Å	12.304(2)	10.4564(10)	9.9321(3)
<i>c</i> /Å	16.302(2)	10.8136(16)	20.2298(7)
α /°	101.238(8)	109.389(3)	90.00
β /°	95.761(8)	110.956(2)	111.348(2)
γ /°	95.785(13)	104.273(2)	90.00
Unit cell volume/Å ³	931.8(3)	858.68(17)	2343.53(13)
Temperature/K	173(2)	173(2)	173(2)
Space group	<i>P</i> -1	<i>P</i> -1	<i>P</i> 2 ₁ /c
<i>Z</i>	2	2	4
Absorption coefficient, μ /mm ⁻¹	0.632	0.090	0.094
No. of reflections measured	8622	10895	11737
No. of independent reflections	2978	4555	5334
<i>R</i> _{int}	0.0717	0.0328	0.0473
Final <i>R</i> _I values (<i>I</i> > 2σ(<i>I</i>))	0.1053	0.0476	0.0530
Final <i>wR</i> (<i>F</i> ²) values (<i>I</i> > 2σ(<i>I</i>))	0.2521	0.0988	0.1282
Final <i>R</i> _I values (all data)	0.1349	0.1021	0.0740
Final <i>wR</i> (<i>F</i> ²) values (all data)	0.2991	0.1178	0.1418
Goodness of fit on <i>F</i> ²	1.202	1.003	1.054

2.1. Metrical data

The bond lengths within the “C₆ core” of zwitterions **6**, **13** and **19** (Figure S2) are given in Table S6 and are representative of all zwitterions described in this paper.

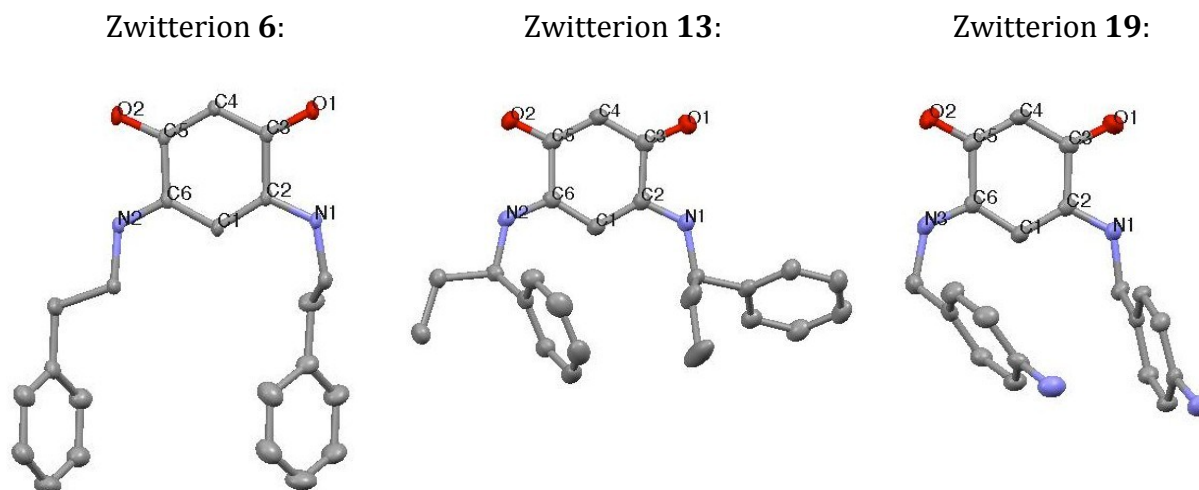


Figure S2. Mercury views of **6**, **13** and **19**. Thermal ellipsoids are drawn at the 50% probability level. H atoms are not shown for clarity.

Table S6. Selected interatomic distances (Å) in zwitterions **6**, **13** and **19**

Zwitterion 6		Zwitterion 13		Zwitterion 19	
C(1)-C(2)	1.386(3)	C(1)-C(2)	1.391(3)	C(1)-C(2)	1.383(2)
C(2)-C(3)	1.520(3)	C(2)-C(3)	1.532(2)	C(2)-C(3)	1.526(2)
C(3)-C(4)	1.395(3)	C(3)-C(4)	1.391(3)	C(3)-C(4)	1.402(2)
C(4)-C(5)	1.396(3)	C(4)-C(5)	1.397(3)	C(4)-C(5)	1.388(2)
C(5)-C(6)	1.513(3)	C(5)-C(6)	1.537(2)	C(5)-C(6)	1.521(2)
C(6)-C(1)	1.386(3)	C(6)-C(1)	1.386(3)	C(6)-C(1)	1.391(2)
C(3)-O(1)	1.249(2)	C(3)-O(1)	1.247(2)	C(3)-O(1)	1.2432(19)
C(5)-O(2)	1.249(2)	C(5)-O(2)	1.241(2)	C(5)-O(2)	1.2549(17)
C(2)-N(1)	1.316(3)	C(2)-N(1)	1.315(2)	C(2)-N(1)	1.3191(18)
C(6)-N(2)	1.319(3)	C(6)-N(2)	1.317(2)	C(6)-N(3)	1.314(2)

They are also similar to those observed in related zwitterions.^{1,2,3} Interestingly, the bond lengths C(3)-C(4) / C(4)-C(5) and C(3)-O(1) / C(5)-O(2), respectively, are almost equal. Likewise C(1)-C(6) / C(1)-C(2) as well as C(2)-N(1) / C(6)-N(2) are similar, respectively (Table S6). Their values are intermediate between those for single and double bonds. However, the C(2)-C(3) and C(5)-C(6) distances are much longer and are consistent with single bonds. Based on these metrical data, these zwitterions are best described as containing two fully delocalized 6π electrons systems (trimethyne oxonol part: O...C...CH...C...O and the trimethyne cyanine part: N...C...CH...C...N) connected by two C-C single bonds.

2.2. Molecular arrangement in the solid-state

In this section we describe the main features associated with the three-dimensional arrangement of various zwitterions as a function of the R group. The underlying motivation is to try to correlate the molecular packing with the structure of the thin films obtained by deposition of these molecules on a gold substrate.

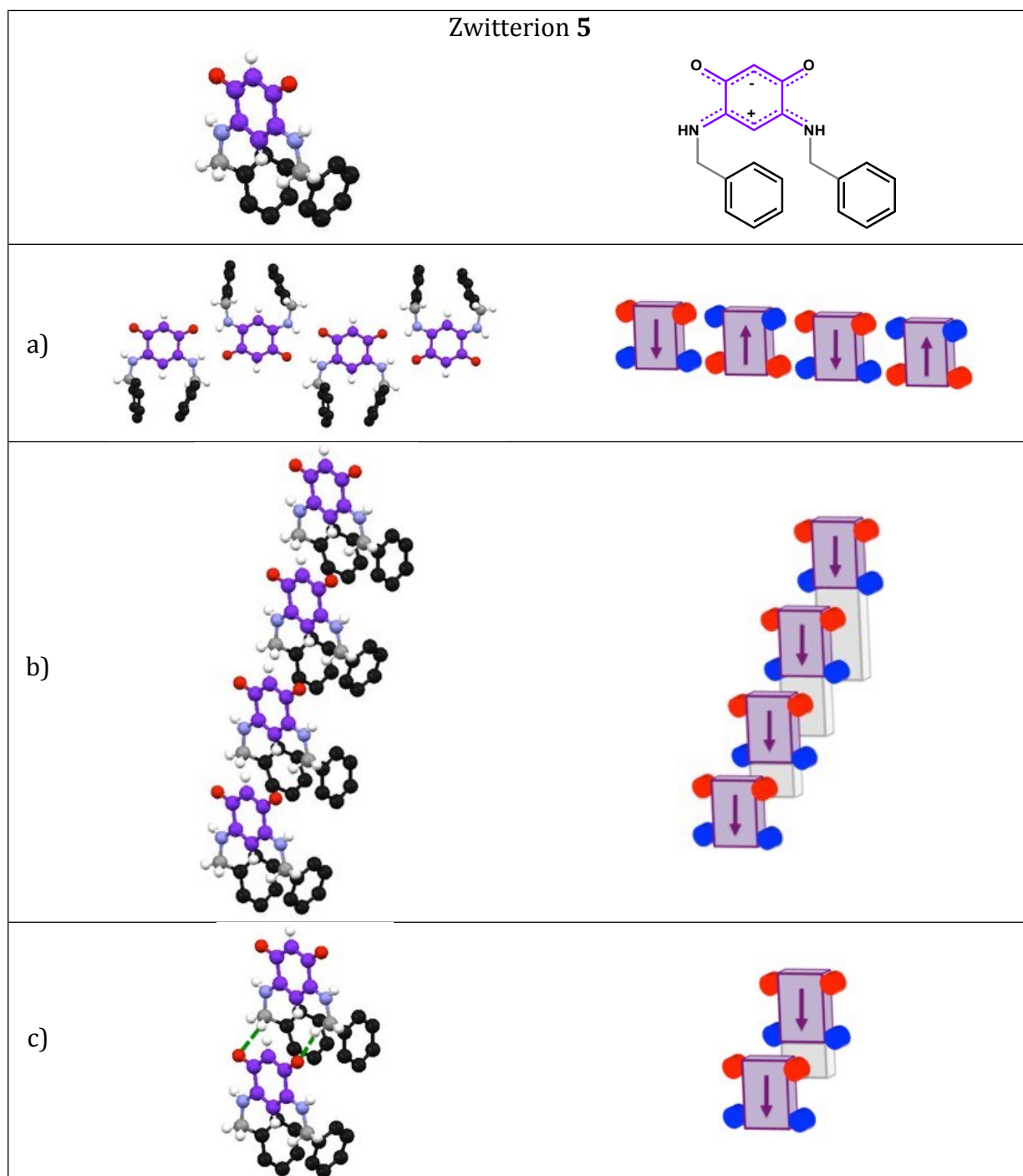
In order to facilitate comparisons between the various zwitterions, the full analysis of molecular arrangements will be presented (elements concerning the molecular arrangements of zwitterions **5**, **13** and **15** are discussed in the main text and are duplicated in the ESI for consistency).

For comparative purpose, we should recall the molecular arrangement of **5** observed in the solid state.

2.2.1. Molecular arrangement of zwitterion **5**

As usual for these quinonoid zwitterions, **5** forms an infinite 1-D ribbon in which the molecules adopt a coplanar head-to-tail arrangement due to hydrogen bonding and

dipolar interactions (Figure S3a).^{Erreur ! Signet non défini.} Figure S3b shows that an infinite row of molecules is formed in a direction orthogonal to the C6 core.



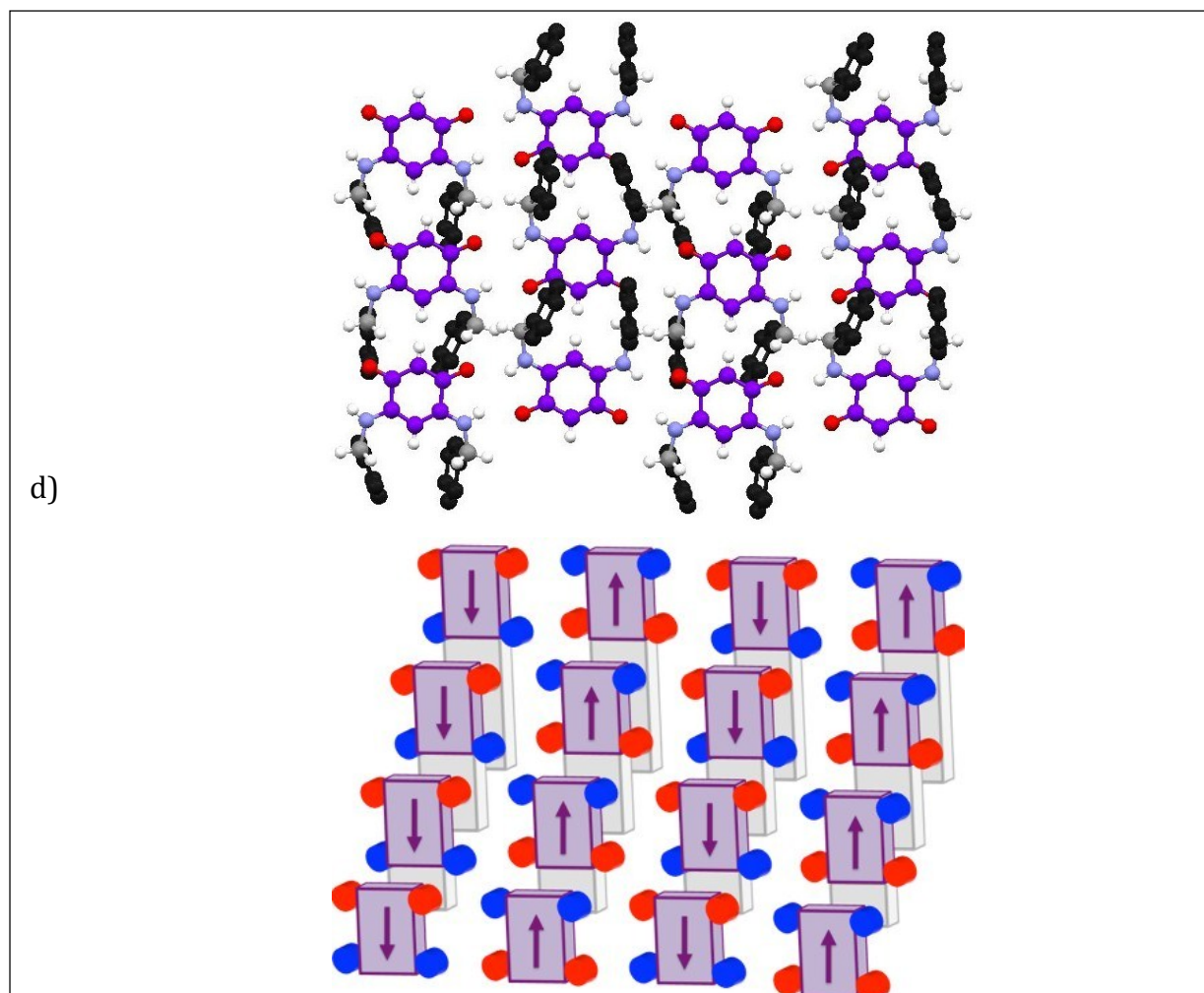


Figure S3. Molecular arrangement of zwitterions **5** in the crystalline state. a) A head-to-tail arrangement. b) A row of molecules **5**. c) Hydrogen bonding between two neighboring molecules. d) A succession of 4 molecular rows. For clarity, quinonoid cores are indicated in violet and phenyl substituents in black. Parallelepipeds represent the quinonoid core and the arrows indicate the dipole direction. Red and blue spheres represent oxygen and nitrogen atoms, respectively. Light grey parallelepipeds are indicated to facilitate the visualization of the molecular arrangement of quinonoid zwitterions. Figures S3b and S3c are taken from the main text.

Similar rows are observed on the gold substrate (Scheme 2, main text)³ and this stacking is crucial for the electronic behavior of the film on surface. Within a row, we observe hydrogen bonding interactions between methylene groups and the anionic system of the nearest neighbor (Figure S3c). This hydrogen bonding contributes to maintain the

cationic system of one molecule in close proximity to the anionic system of a neighboring molecule and this favors interactions between them. We have attributed the semi-metallic character of the benzyl zwitterion **5** to these interactions.⁴ Within a row, molecules of **5** are shifted upward (Figure S3b). Each row interacts via hydrogen bonding with an adjacent one to form a head-to-tail arrangement (Figure S3d).

For all new compounds described in this manuscript, we were particularly looking for infinite molecular rows, which are primordial for electronic transport. The following section is focused on the identification of molecular rows.

2.2.2. Influence of the length of the linker between the phenyl group and the zwitterionic core

The number of carbon atoms between the zwitterionic core and the phenyl group drastically influences the molecular arrangement. Based on this X-ray study, we decided that zwitterions with a linker longer than 2 carbon atoms (C-C) would not be selected in priority for the study on the electronic transport of their molecular films on gold.

2.2.2.1. *Molecular arrangement of zwitterion 7*

In the case of **7**, we did not observe any formation of molecular rows in a direction orthogonal to the C6 core. Thus, the propyl linker is flexible enough to allow interactions between the phenyl and the zwitterionic core and the latter suppresses all possible stacking interactions between zwitterionic cores (Figure S4). Therefore the molecular arrangement of zwitterion **7** is drastically different from that observed for **5** (Figure S5b).

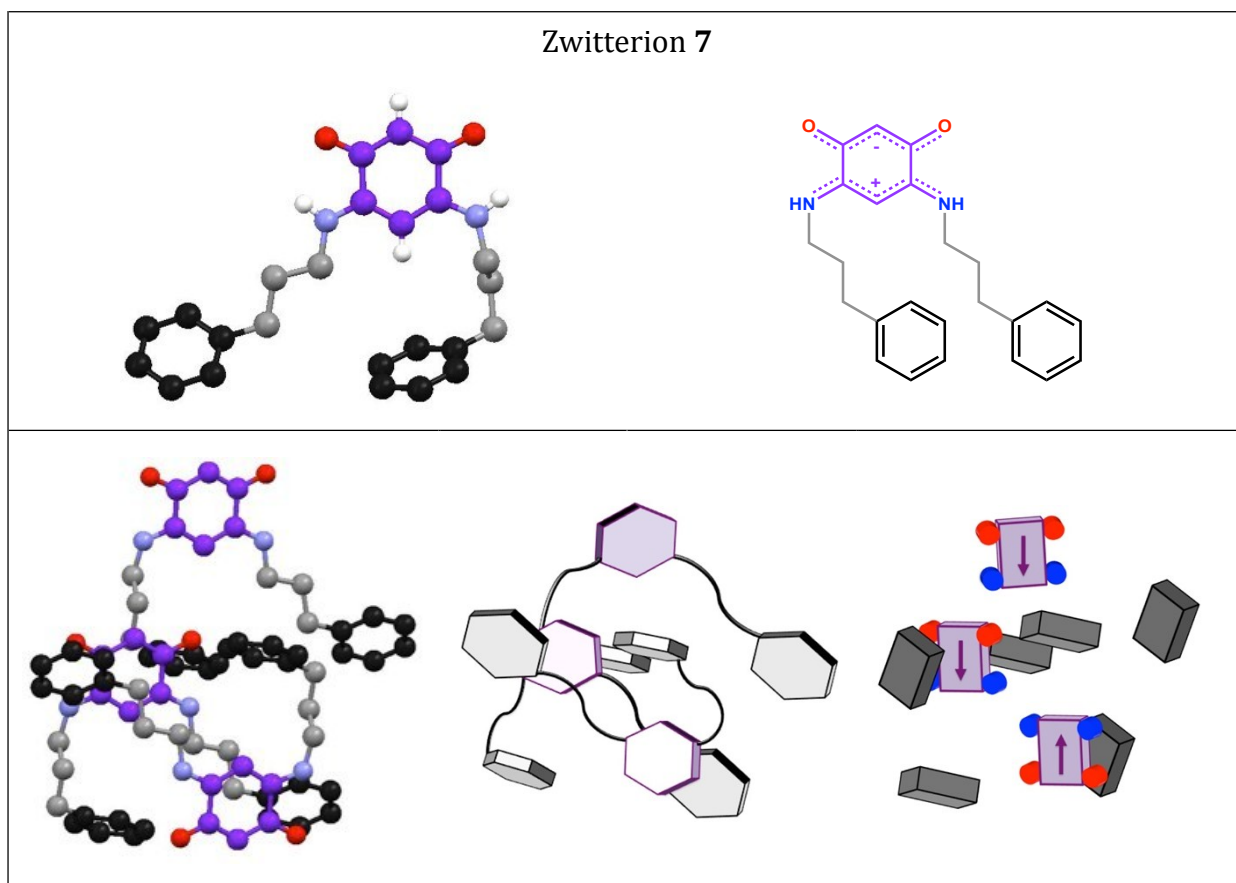
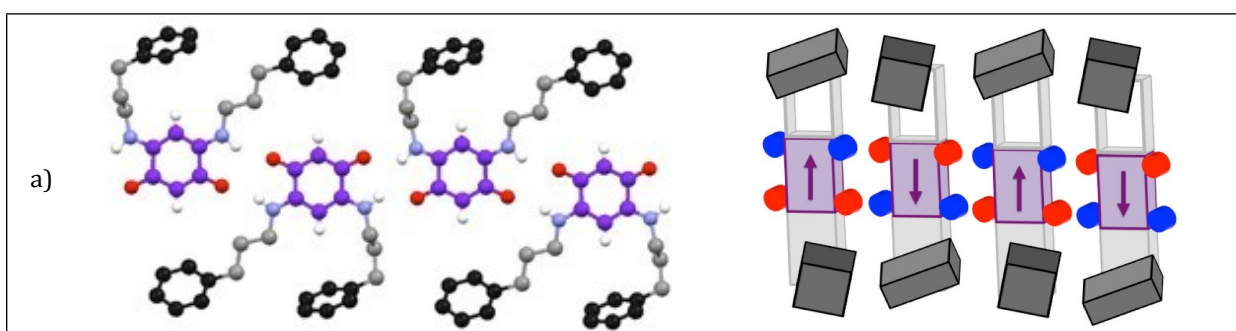


Figure S4. View of the interactions between the phenyl substituent and the zwitterionic core of compound 7. For clarity, quinonoid cores are indicated in violet and phenyl substituents in black. In the sketch, violet and black hexagons/parallelepipeds represent the quinonoid core and the phenyl ring, respectively. The arrows indicate the dipole direction. Red and blue spheres represent oxygen and nitrogen atoms, respectively.



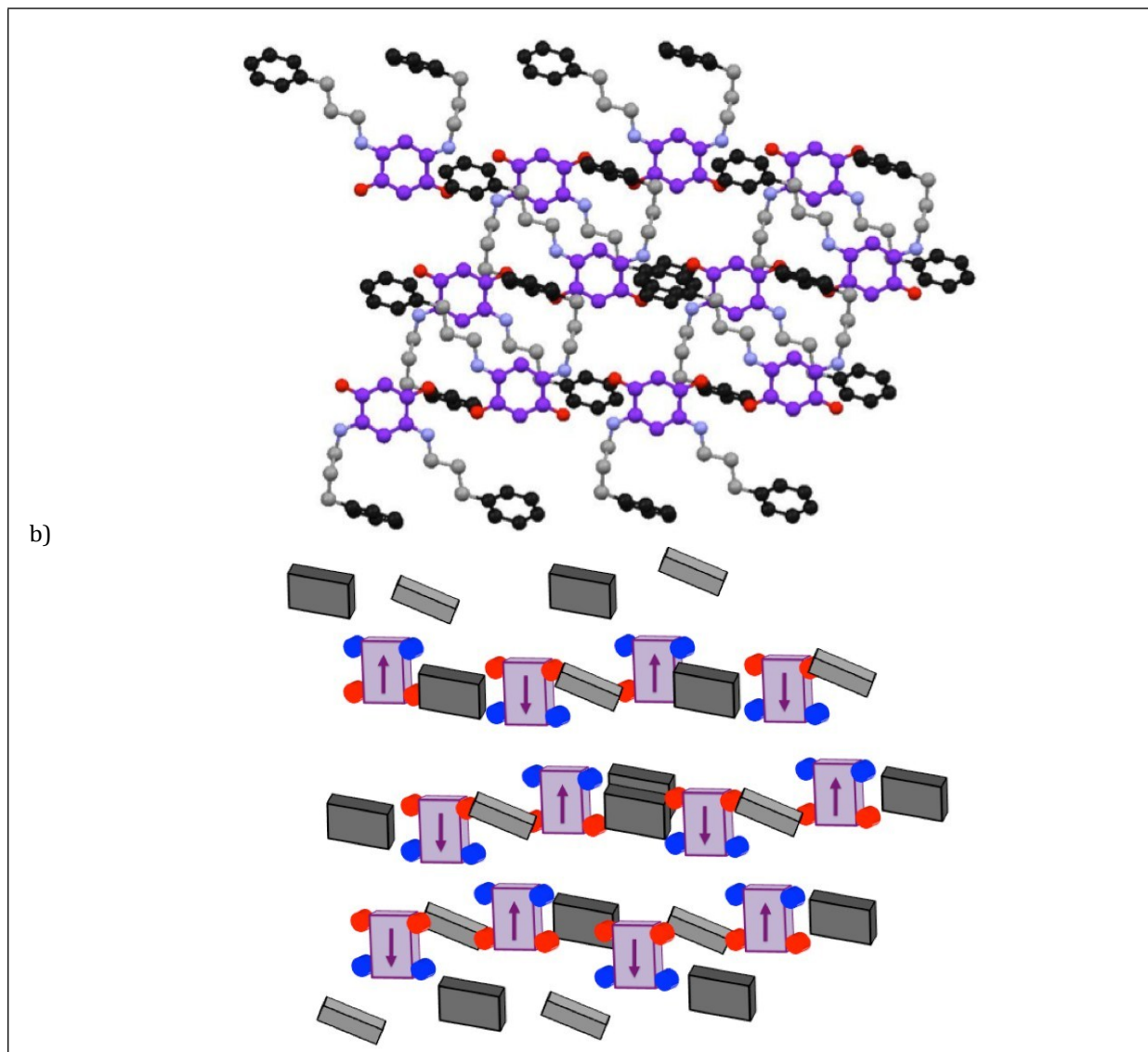


Figure S5. Molecular arrangement of zwitterions **7** in the crystalline state. Molecules of **7** form a head-to-tail arrangement (Figure S5a) similar to that observed for **5** (Figure S3a). Figure S5b represents the molecular arrangement which associates the head-to-tail ribbon with the interaction between aryl substituent and the quinonoid core (Figure S4). For clarity, quinonoid cores are indicated in violet and phenyl substituents in black. In the sketch, violet and black parallelepipeds represent the quinonoid core and the phenyl ring, respectively. The arrows indicate the dipole direction. Red and blue spheres represent oxygen and nitrogen atoms, respectively. Light grey parallelepipeds are indicated to facilitate the visualization of the molecular arrangement of quinonoid zwitterions.

2.2.2.2. Molecular arrangement of zwitterion **8**

This compound co-crystalizes with water molecules, which interact via H-bonds with the zwitterions and thereby modify the molecular arrangement of **8** (Figure S6).

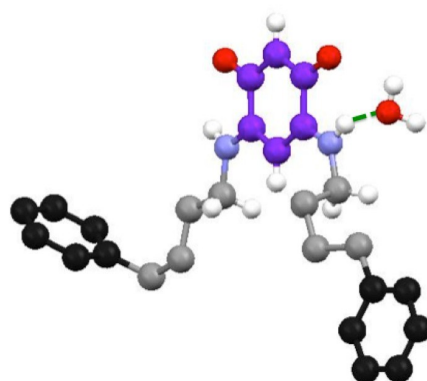
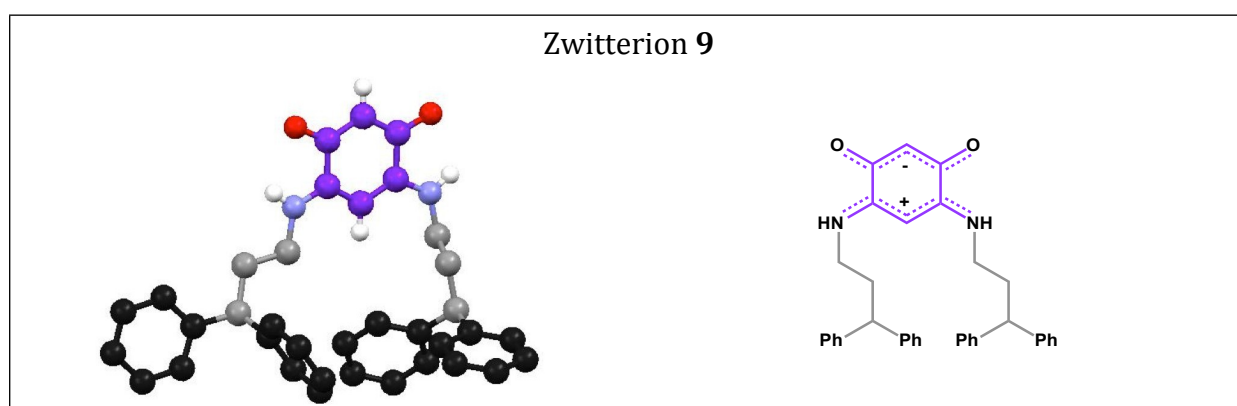
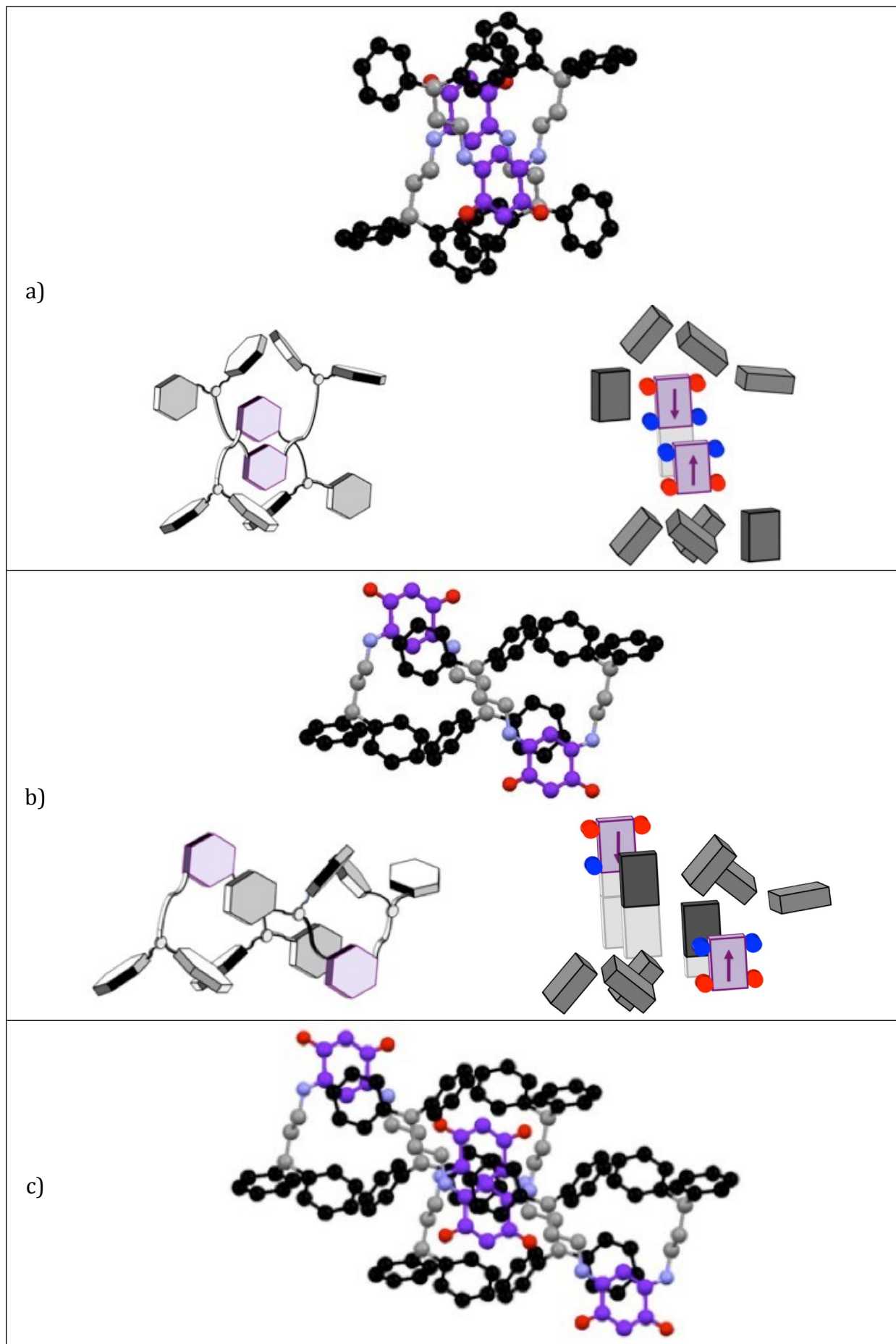


Figure S6. Hydrogen bonding between zwitterion **8** and a molecule of water

2.2.2.3. Molecular arrangement of zwitterion **9**

In the case of **9**, a stacking in a direction orthogonal to the C6 core is observed (Figure S7a). However, the presence of distinct pairs of molecules (Figure S7c) contrasts with the infinite molecular rows found in **5** (Figure S3b). Interactions between the quinonoid core and the aryl substituent are observed (Figure S7b), which limit the number of interactions between quinonoid cores. The head-to-tail arrangement of **9** is indicated and discussed in Figure S8. This compound does not appear to us as the best candidate for electronic transport studies on gold substrate since we do not observe infinite molecular row in solid state.





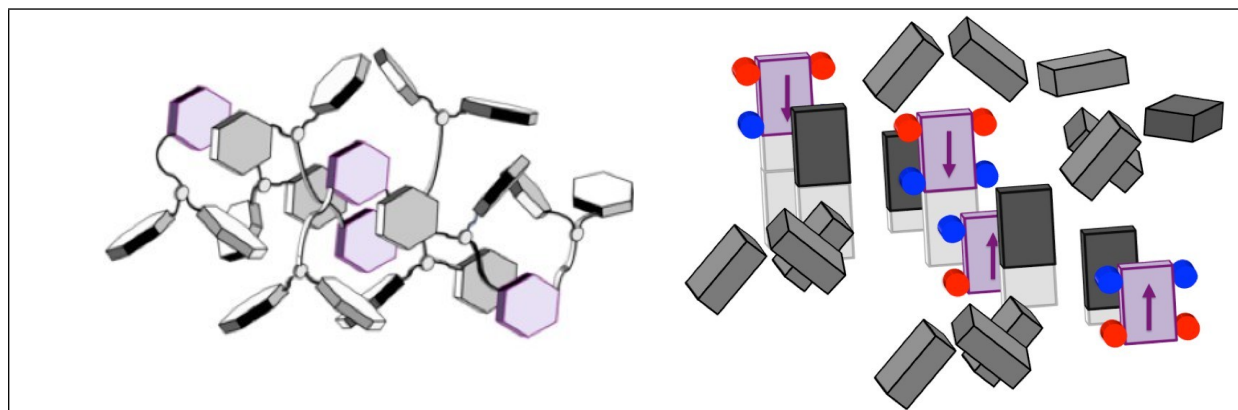
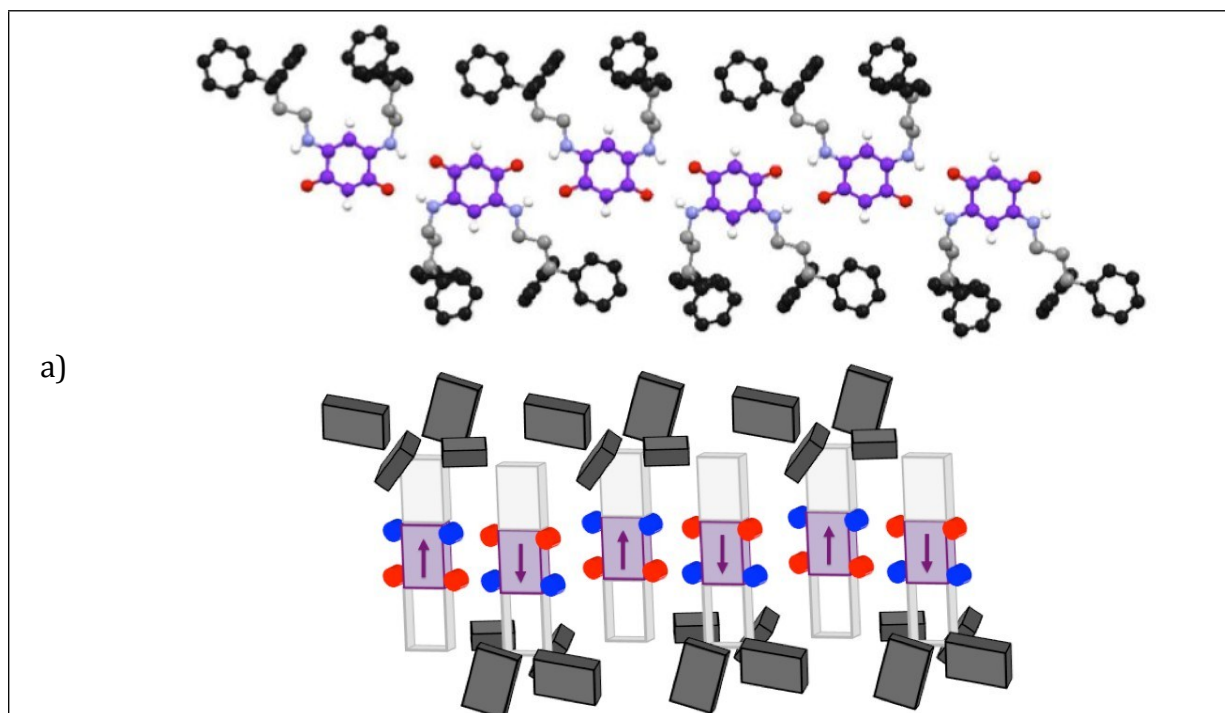


Figure S7. a) View of the stacking of two quinonoid cores in **9**. b) View of the interactions between the phenyl substituent and the zwitterionic core of **9**. c) View of the intermolecular arrangement of **9**. For clarity, quinonoid cores are indicated in violet and phenyl substituents in black. In the sketch, violet and black hexagons/parallelepipeds represent the quinonoid core and the phenyl ring, respectively. The arrows indicate the dipole direction. Red and blue spheres represent oxygen and nitrogen atoms, respectively. Light grey parallelepipeds are indicated to facilitate the visualization of the molecular arrangement of quinonoid zwitterions.



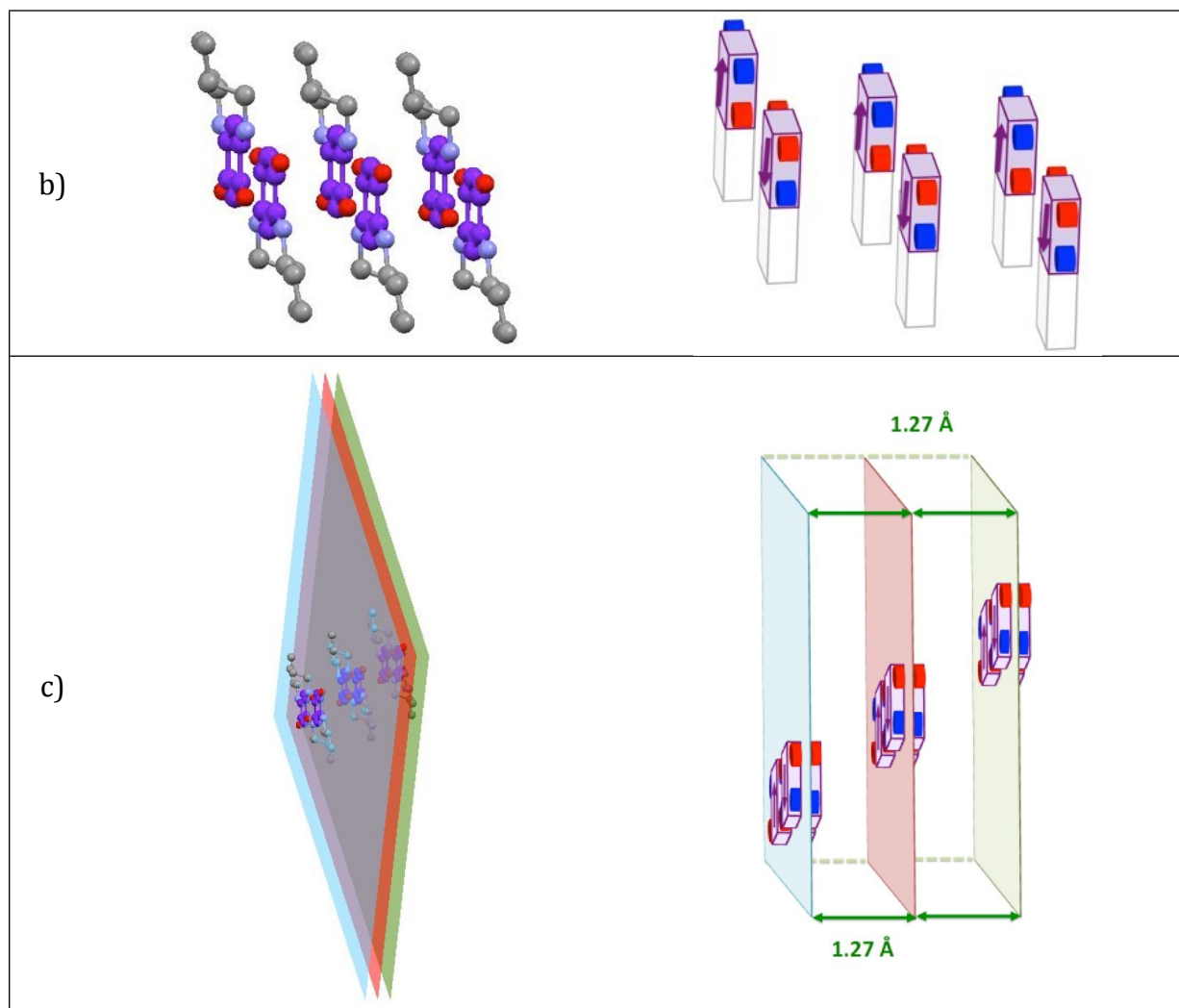
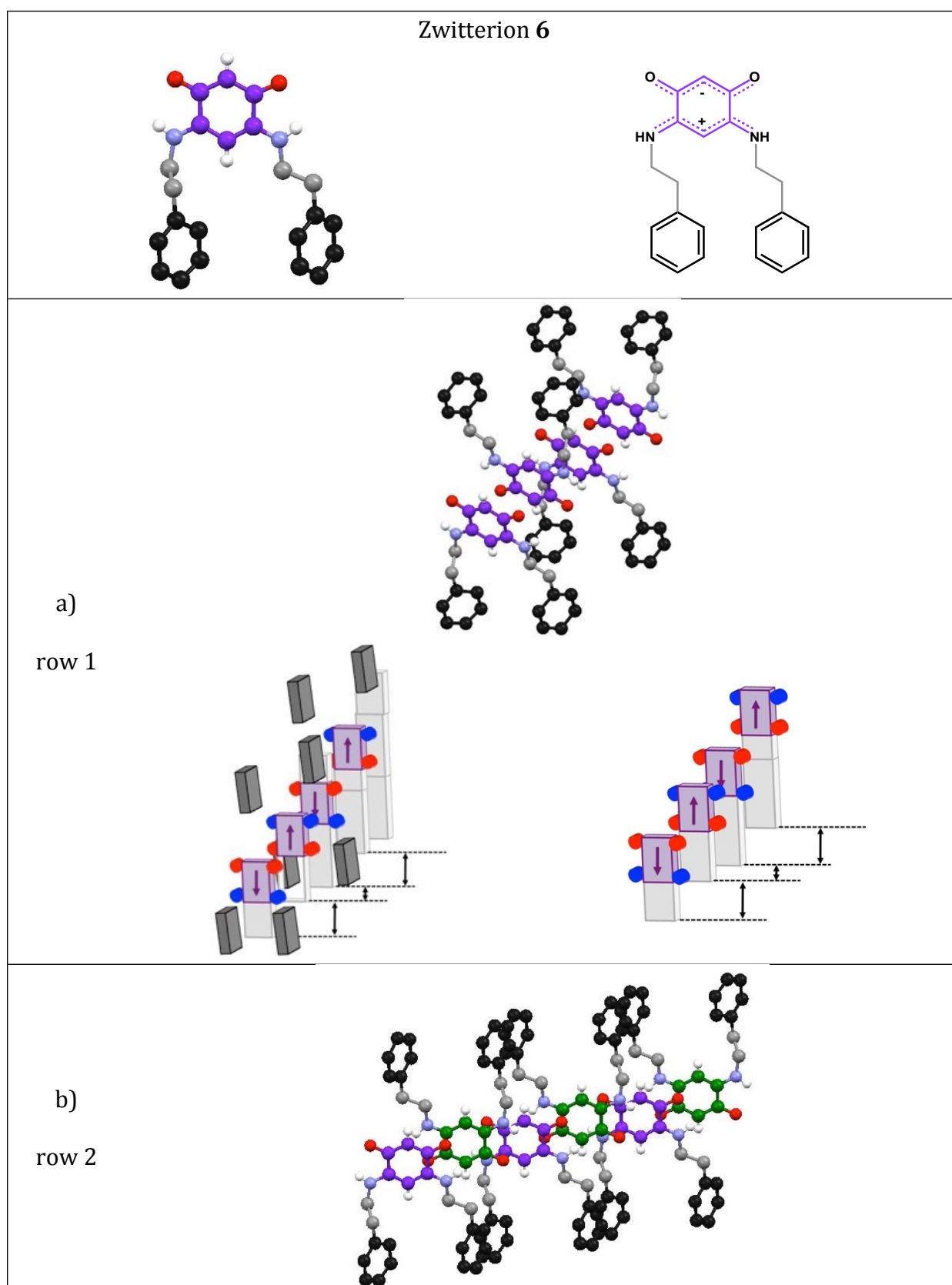


Figure S8. Molecules of **9** form an infinite head-to-tail ribbon (Figure S8a). Whereas in **5**, molecules are coplanar (Figure S3a), pairs of molecules **9** form in parallel planes (Figure 8b). The spacing between two consecutive mean planes (plane containing the two quinonoid cores) is 1.27 Å (Figure 8c). For clarity, quinonoid cores are indicated in violet and phenyl substituents in black (a) or were omitted (b-c). In the sketch, violet and black parallelepipeds represent the quinonoid core and the phenyl ring, respectively. The arrows indicate the dipole direction. Red and blue spheres represent oxygen and nitrogen atoms, respectively. Blue, pink and Green parallelepipeds represent three consecutive mean planes. Light grey parallelepipeds are indicated to facilitate the visualization of the molecular arrangement of quinonoid zwitterions.

2.2.2.4. Molecular arrangement of zwitterion **6**

The structure of zwitterion **6** is significantly different from those of zwitterions **5** and **7**.

Molecular rows are formed in a direction orthogonal to the C6 core (Figure S9a).



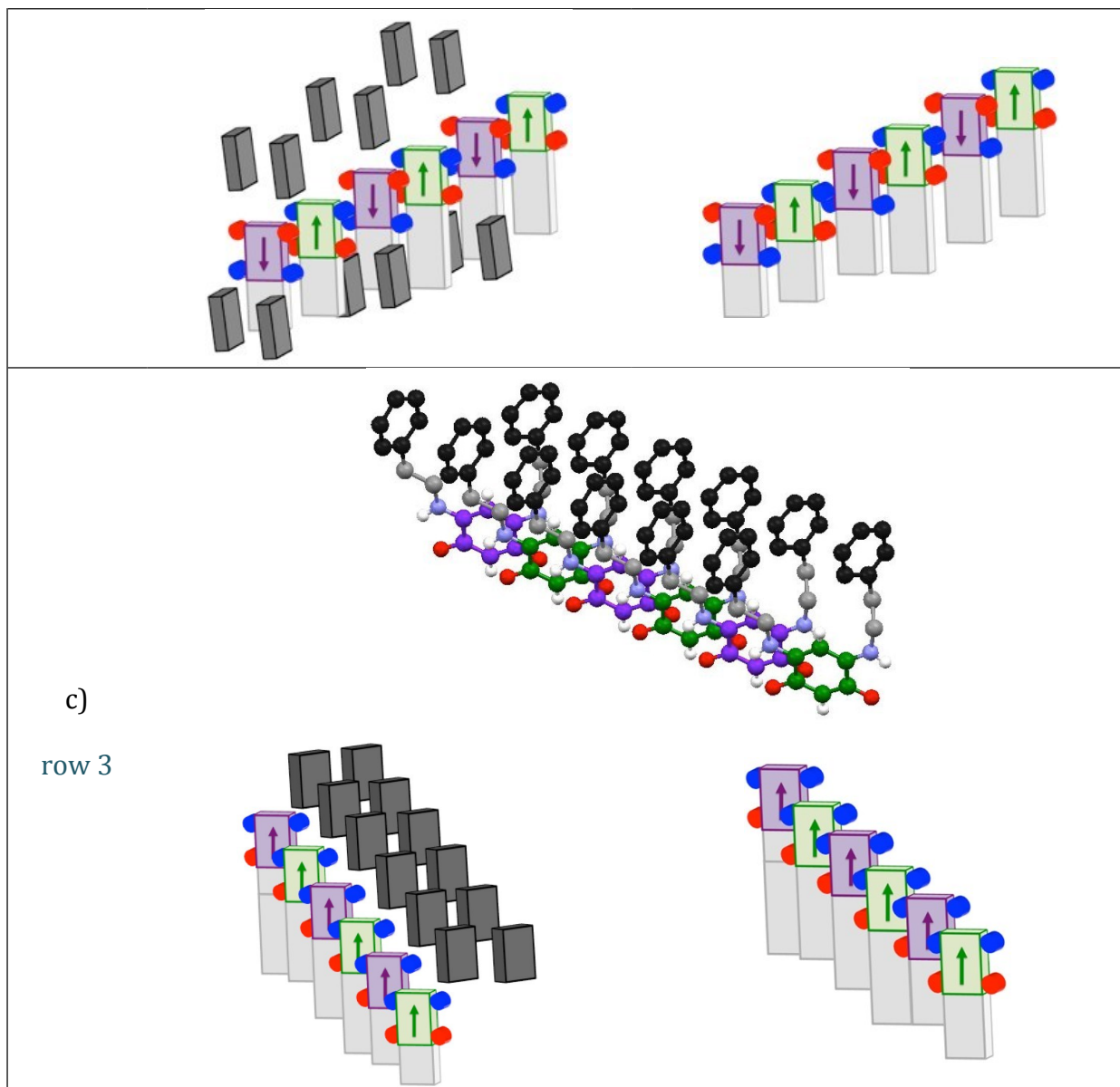
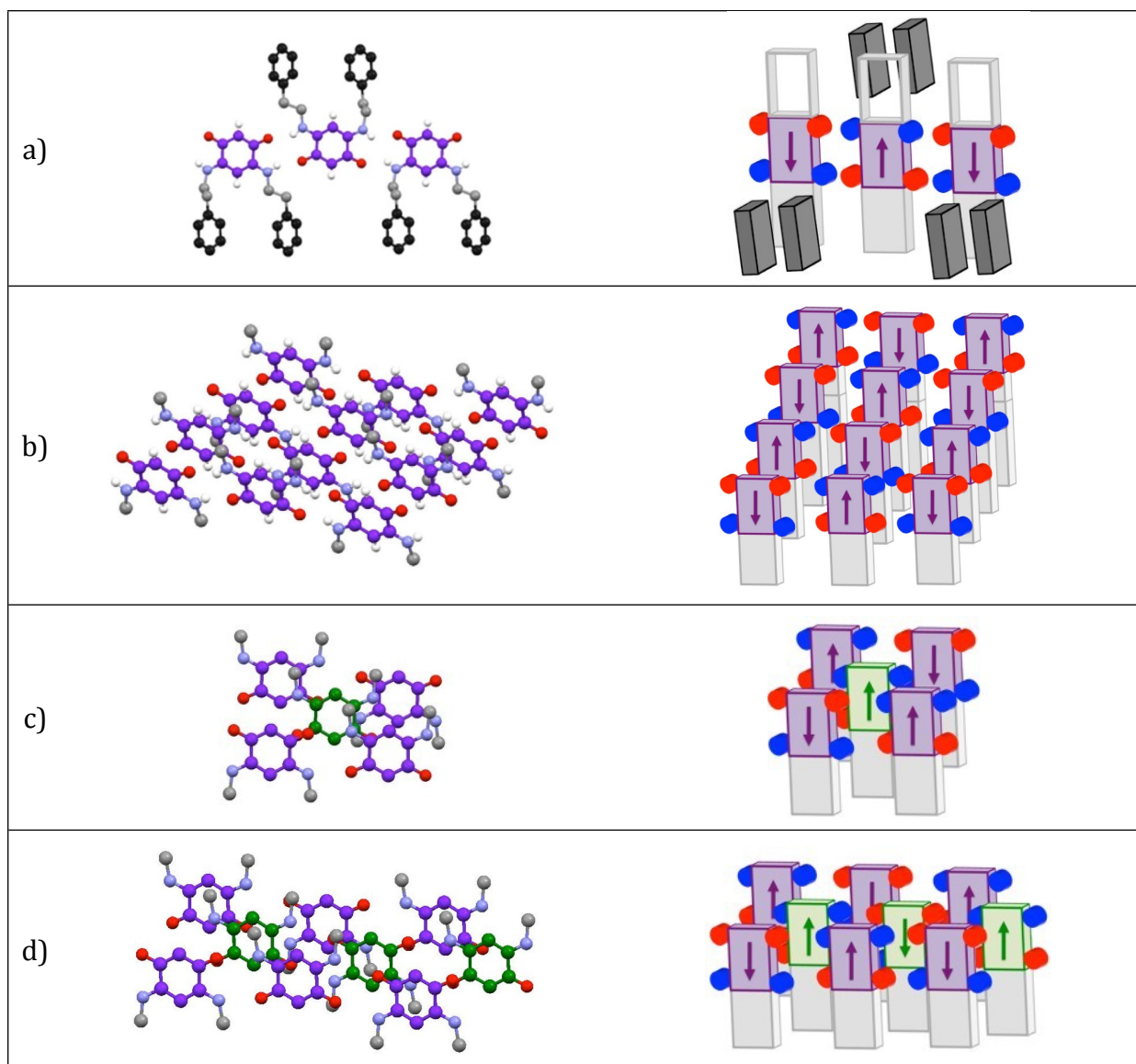


Figure S9. Molecular arrangement of zwitterion **6** in the crystalline state. a) First type of molecular row. b) Second type of molecular row. c) Third type of molecular row. For clarity, quinonoid cores are indicated in violet or in green and the phenyl substituents in black. In the sketch, green and violet parallelepipeds represent the quinonoid core and the arrows indicate the orientation of the electric dipole. Black parallelepipeds represent the phenyl substituent. Light grey parallelepipeds are indicated to facilitate the visualization of the molecular arrangement of quinonoid zwitterions.

We observe two different spacings between molecules and in contrast to **5**, molecular dipole moments are alternatively oriented up and down (Figure S9a). The study of the

full molecular arrangement (Figure S10e) reveals two additional types of rows. In row 3, all dipole moments are oriented in the same direction (Figure S9c) whereas in row 2, they are alternatively up and down (Figure S9b). Therefore, three distinct types of molecular rows are observed against only one for the benzyl zwitterion **5**. The zwitterion **6** appears as a potentially interesting candidate for the study of electronic properties of its molecular film on gold.



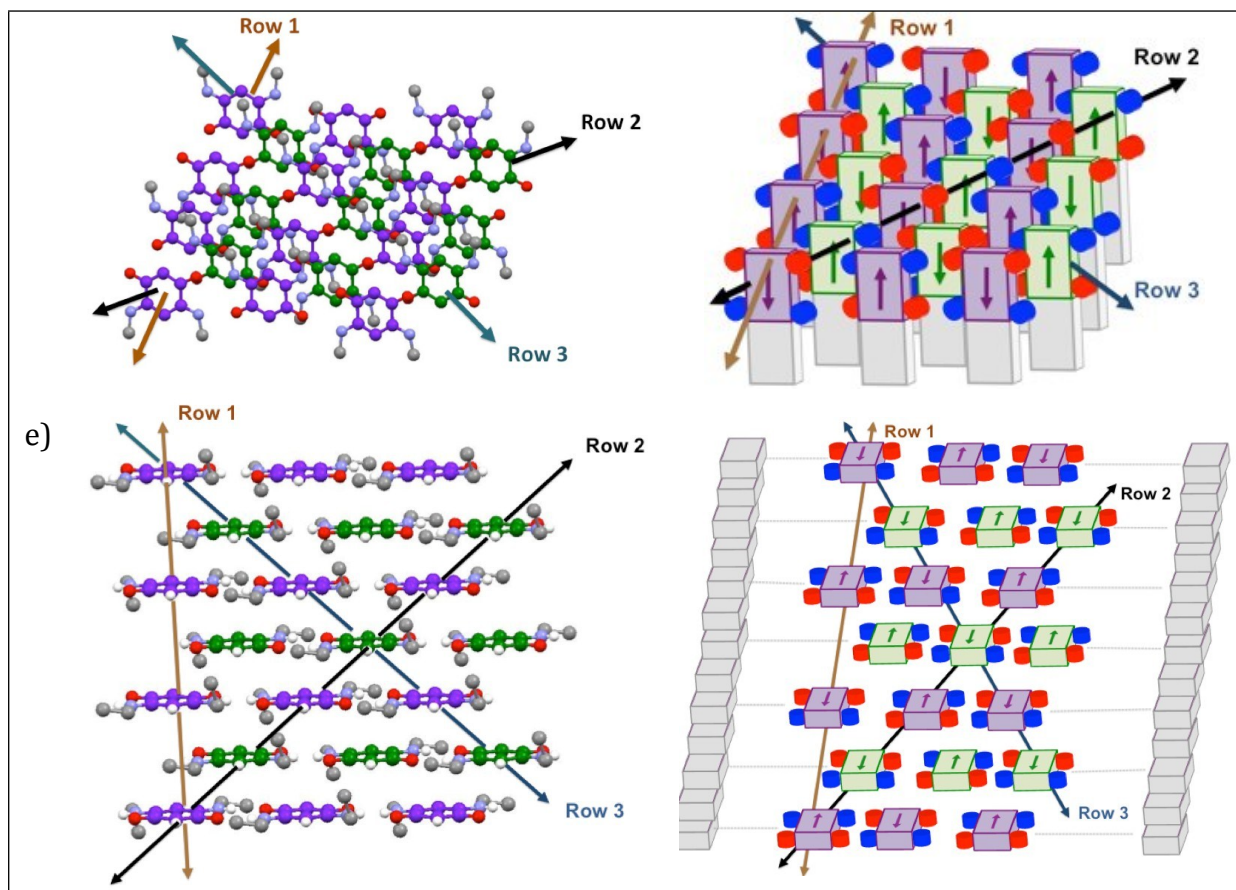


Figure S10. Molecular arrangement of zwitterion **6** in the crystalline state. This structure is complex as it results from a close combination of two molecular arrangements. In the first one, zwitterion **6** forms an infinite 1-D ribbon in which the molecules adopt a head-to-tail arrangement (Figure S10a). A molecular row is formed in a direction orthogonal to the C6 core (Figure S9a). Each row interacts via hydrogen bonding with an adjacent head-to-tail row (Figure S10b). If we consider the first two molecules of two successive rows, they surround the molecule with the zwitterionic core colored in green (Figure S10c). From this molecule begins a new arrangement (Figure S10d) which is identical to that described in Figures S9a and S10a. Figure S10e represents two views of the full molecular arrangement of zwitterion **6**. For clarity, quinonoid cores are indicated in violet or in green and the phenyl substituents in black (a) or were omitted (b-e). In the sketch, green and violet parallelepipeds represent the quinonoid core and the arrows indicate the orientation of the electric dipole. Black parallelepipeds represent the phenyl substituent. Light grey parallelepipeds are indicated to facilitate the visualization of the molecular arrangement of quinonoid zwitterions.

2.2.3. Influence of a substituent on the linker

2.2.3.1. Molecular arrangement of zwitterion 12

The compound co-crystalizes with molecules of pentane. Therefore, these data cannot be used in the present context.

2.2.3.2. Molecular arrangement of zwitterion 13

Interestingly zwitterion 13 (Figure S11a) forms molecular rows similar to those of 5 (Figure S3b). The hydrogen bonding depicted in the Figure S3c is also observed for 13 (Figure S11b).

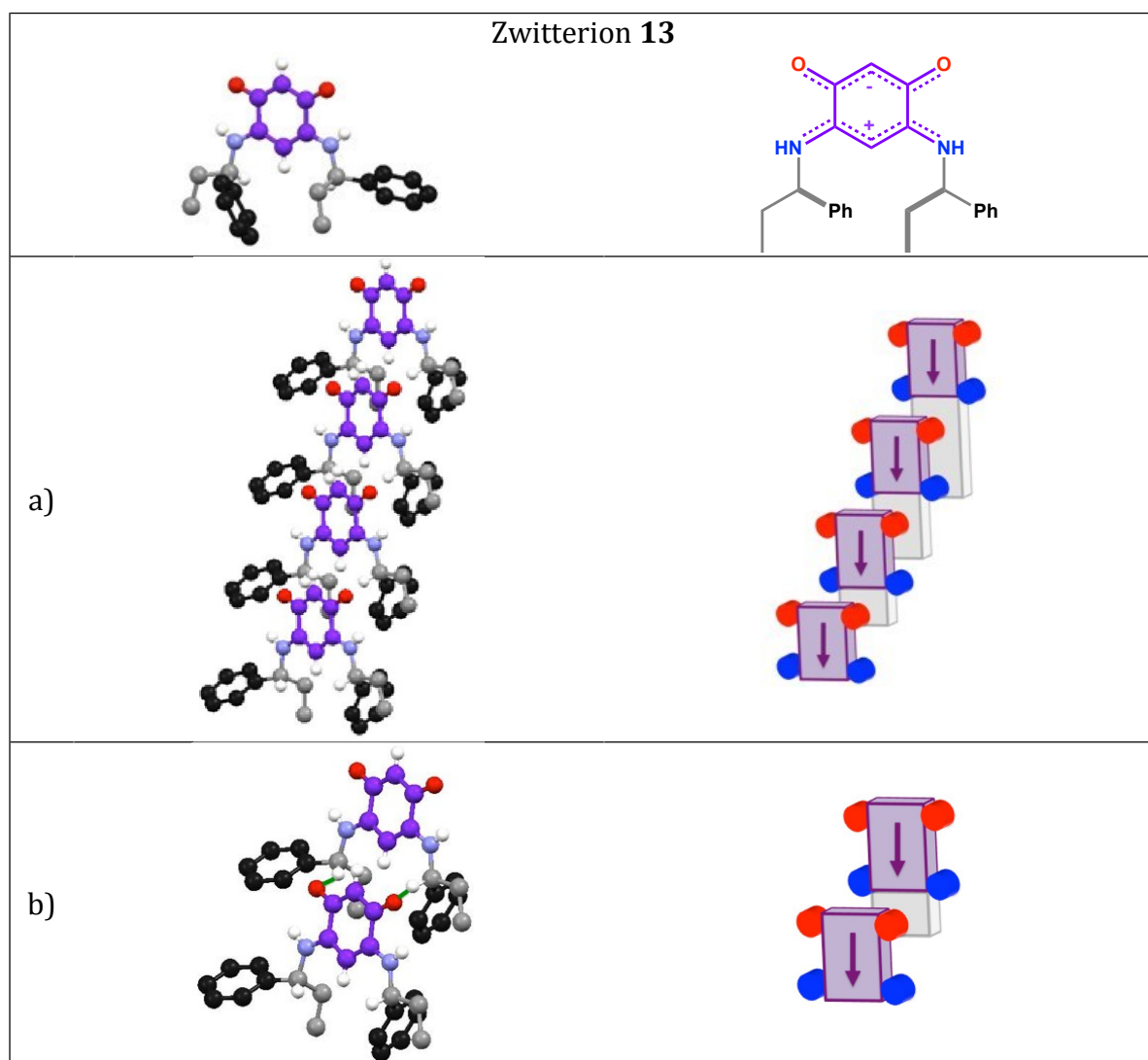


Figure S11. The molecular arrangement of zwitterions **13** in the crystalline state. a) A row of molecules. b) Hydrogen bonding between two neighboring molecules. For clarity, quinonoid cores are indicated in violet and phenyl substituents in black. In the sketch, parallelepipeds represent the quinonoid core and the arrows indicate the dipole direction. Red and blue spheres represent oxygen and nitrogen atoms, respectively. Light grey parallelepipeds are indicated to facilitate the visualization of the molecular arrangement of quinonoid zwitterions. Figure S11 is taken from the main text.

Zwitterion **13** forms an infinite head-to-tail ribbon (Figure S12a). As observed for other zwitterions without a methylene substituent in α -position to the nitrogen, the quinonoid cores in this ribbon are not coplanar.² Therefore the molecular arrangement of **13** indicated in Figure S12b is significantly different from that observed for **5** (Figure S3d). It is therefore possible that the steric hindrance of **13** could affect the structure of the molecular film on the gold surface. An increase of the distance between adjacent molecular rows or a molecular structure in which adjacent rows would not be parallel would be detrimental (like Figure S12b).

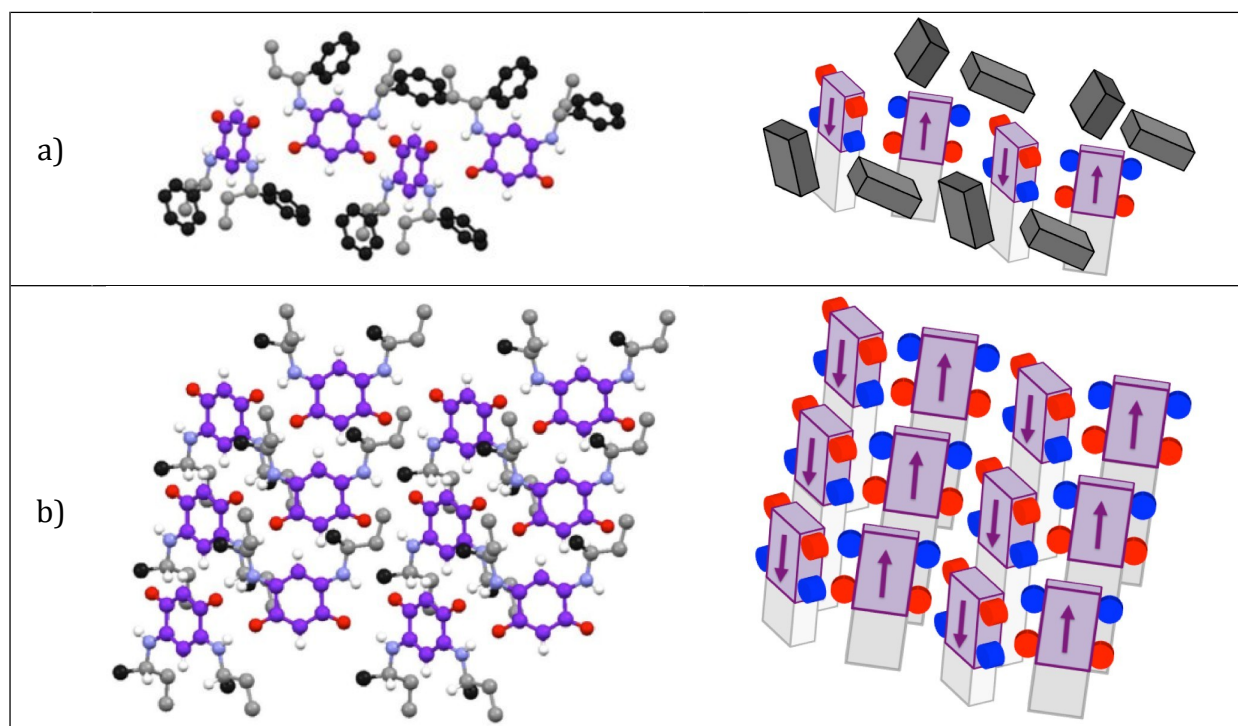


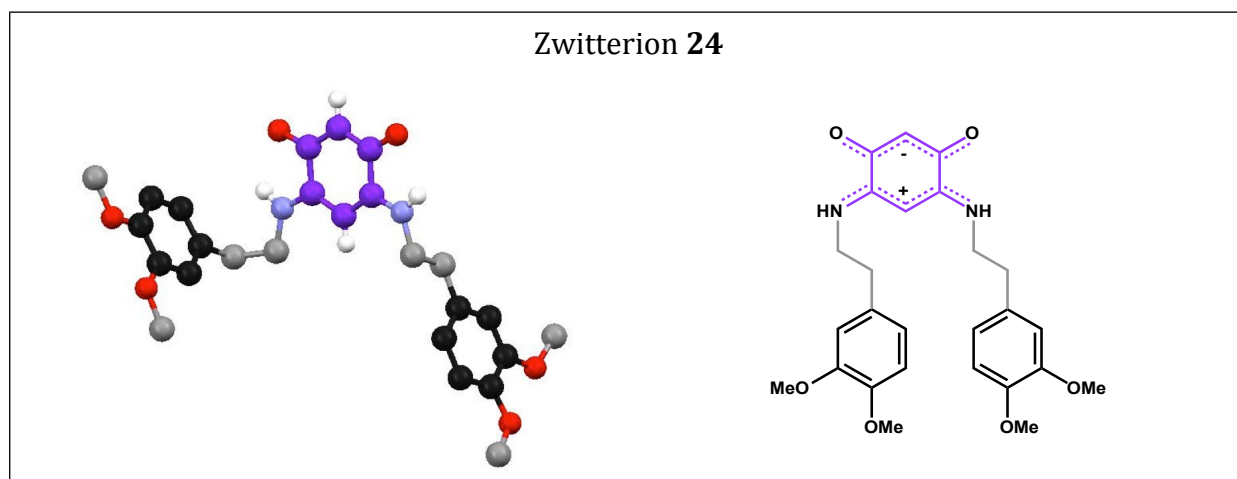
Figure S12. The molecular arrangement of zwitterions **13** in the crystalline state. a) A head-to-tail arrangement. b) A succession of 4 molecular rows. For clarity, quinonoid cores are indicated in violet and

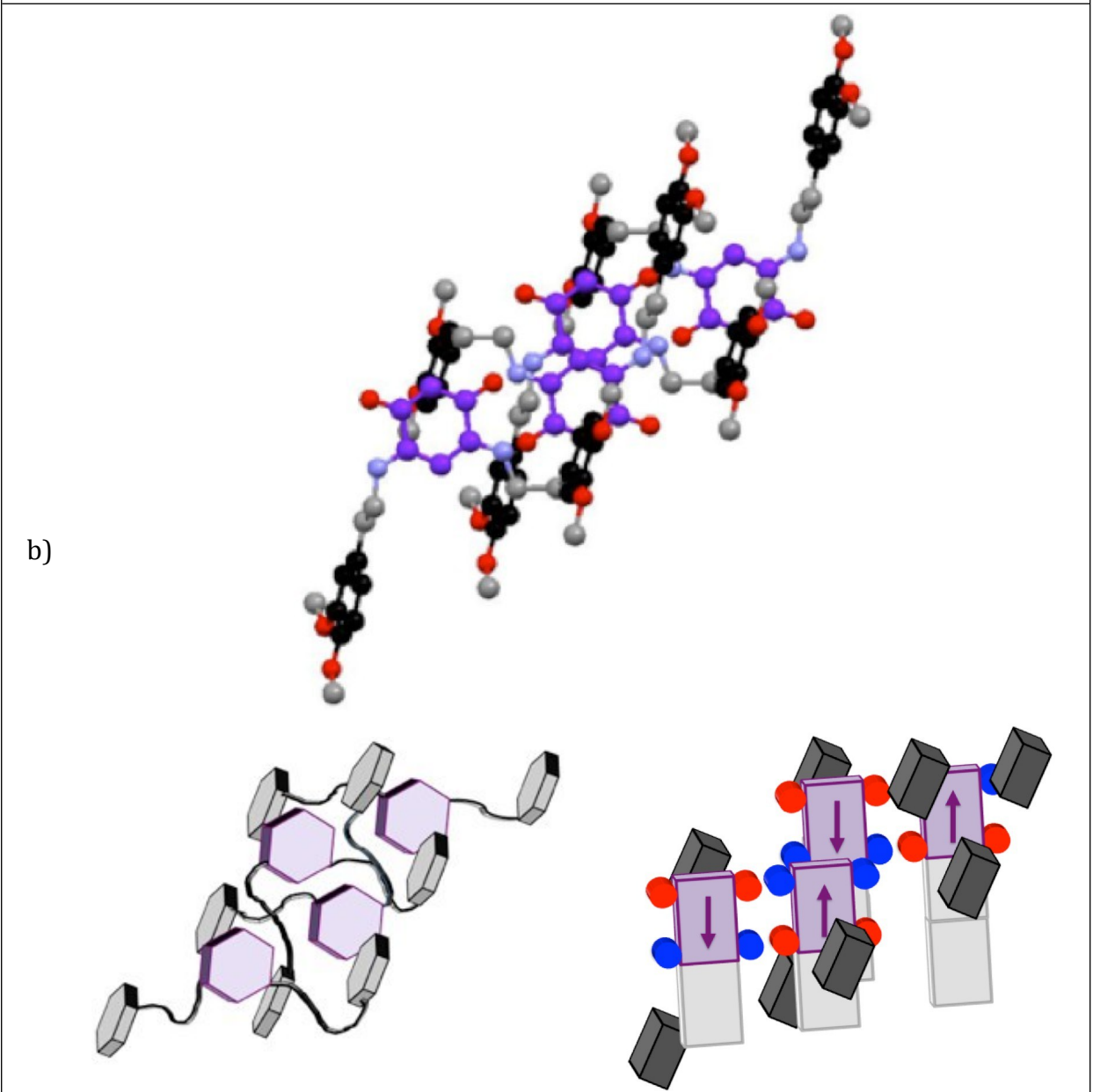
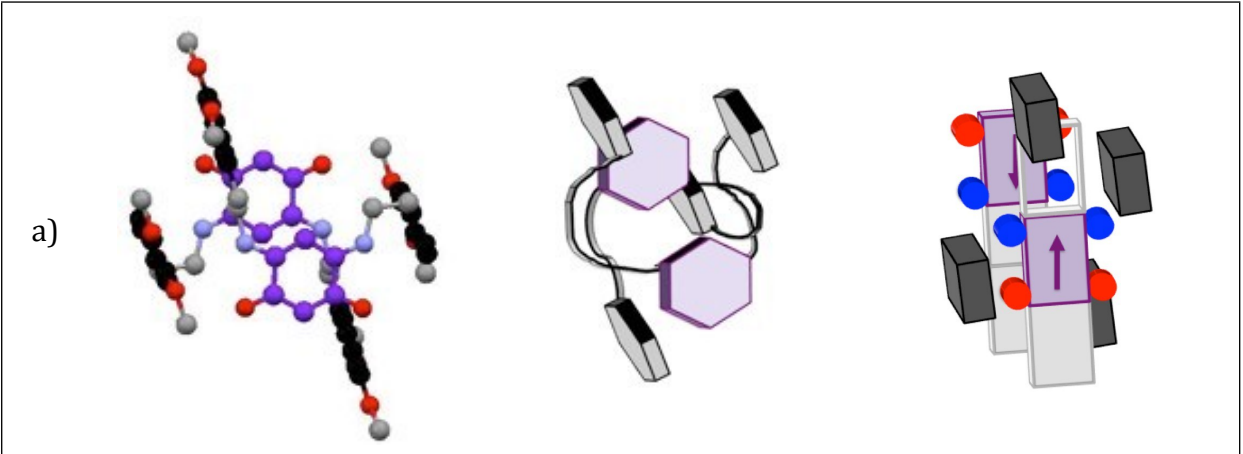
phenyl substituents in black or were omitted (b). In the sketch, violet parallelepipeds represent the quinonoid core and the arrows indicate the dipole direction. Red and blue spheres represent oxygen and nitrogen atoms, respectively. Black parallelepipeds represent the phenyl substituent. Light grey parallelepipeds are indicated to facilitate the visualization of the molecular arrangement of quinonoid zwitterions.

2.2.4. Influence of the functional groups on the aromatic part.

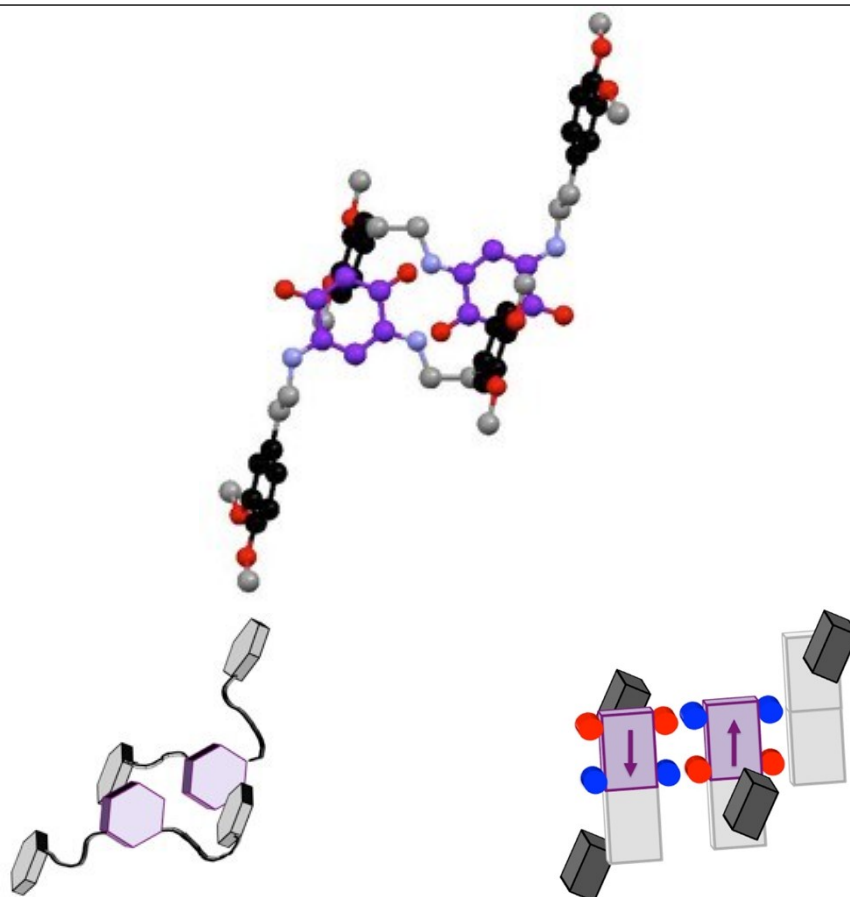
2.2.4.1. Molecular arrangement of zwitterion **24**

The stacking between quinonoid cores is shown in Figure S13a. However, zwitterion **24** does not appear to us as a promising candidate for electronic transport. Although a molecular stacking in a direction orthogonal to the C6 core is present (Figure S13a), interactions between the quinonoid core and the aryl substituent (Figure S13c) results in the formation of distinct pairs of molecules (Figure S13b). Moreover, the presence of distinct pair of molecules (Figure S13d) contrasts with the infinite head-to-tail arrangement generally observed for this family of molecules (for example see Figure S3a). A similar observation was made for the molecule studied in reference 5 and we hypothesized that strong intermolecular interactions result in a weak anchoring of the molecule on the surface and hamper the formation of N-Au interactions.⁵ Therefore, we anticipate difficulties to anchor the zwitterion **24** on a gold substrate.





c)



d)

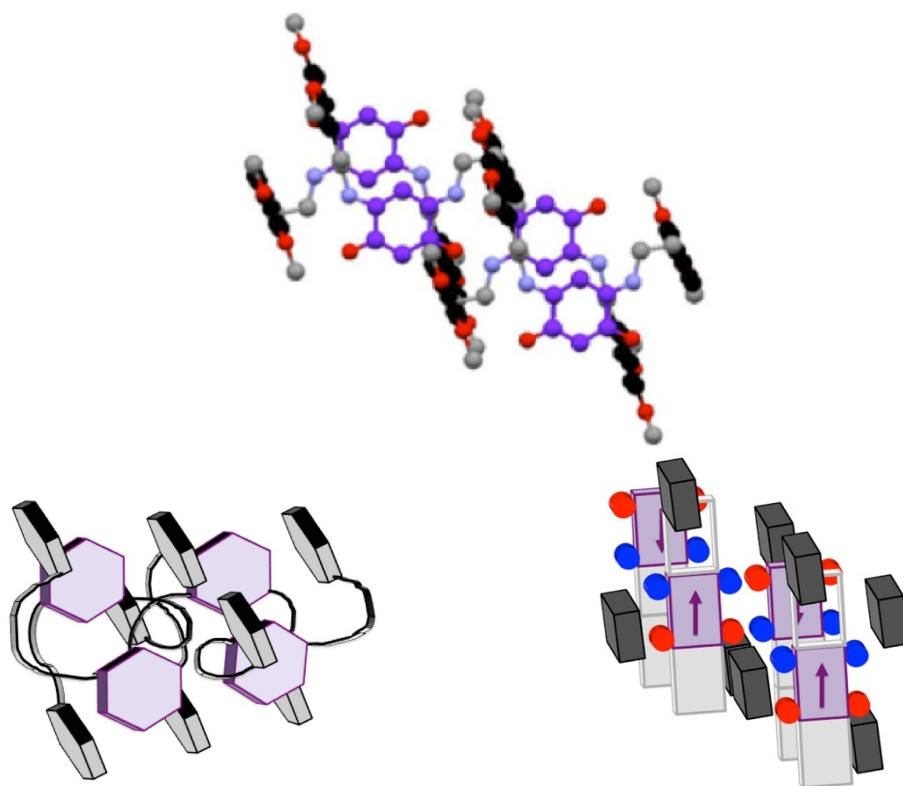
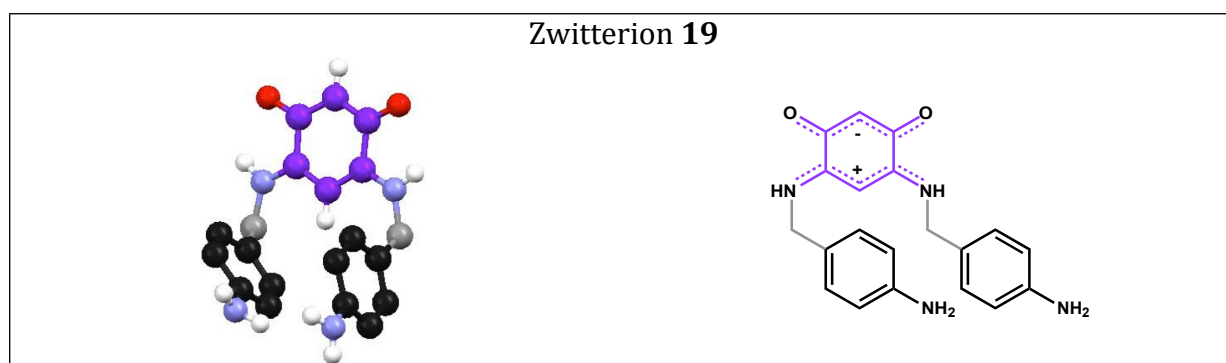


Figure S13. Molecular arrangement of zwitterions **24** in the crystalline state. a) View of the stacking of two quinonoid cores. b) View of the arrangement which results from the stacking interaction of quinonoid cores and the interaction between the quinonoid core and the aryl substituent. c) View of the interactions between the phenyl substituent and the zwitterionic core. d) View of the head-to-tail pair of molecules associates to the interaction between the quinonoid core and the aryl substituent. For clarity, the quinonoid cores are indicated in violet and the phenyl substituents in black. In the sketch, violet and black hexagons/ parallelepipeds represent the quinonoid core and the phenyl ring, respectively. The arrows indicate the dipole direction. Red and blue spheres represent oxygen and nitrogen atoms, respectively. Light grey parallelepipeds are indicated to facilitate the visualization of the molecular arrangement of quinonoid zwitterions.

2.2.4.2. Molecular arrangement of zwitterion **19**

Molecular rows are formed in a direction orthogonal to the C6 core (Figure S14a). These rows result from two distinct molecular interactions: 1) between a methylene group and the anionic system (Figure S14b) and 2) between an amino group and the anionic system (Figure S14c). As formed with zwitterion **24**, pairs of molecules **19** are arranged in a head-to-tail manner (Figure S15b).



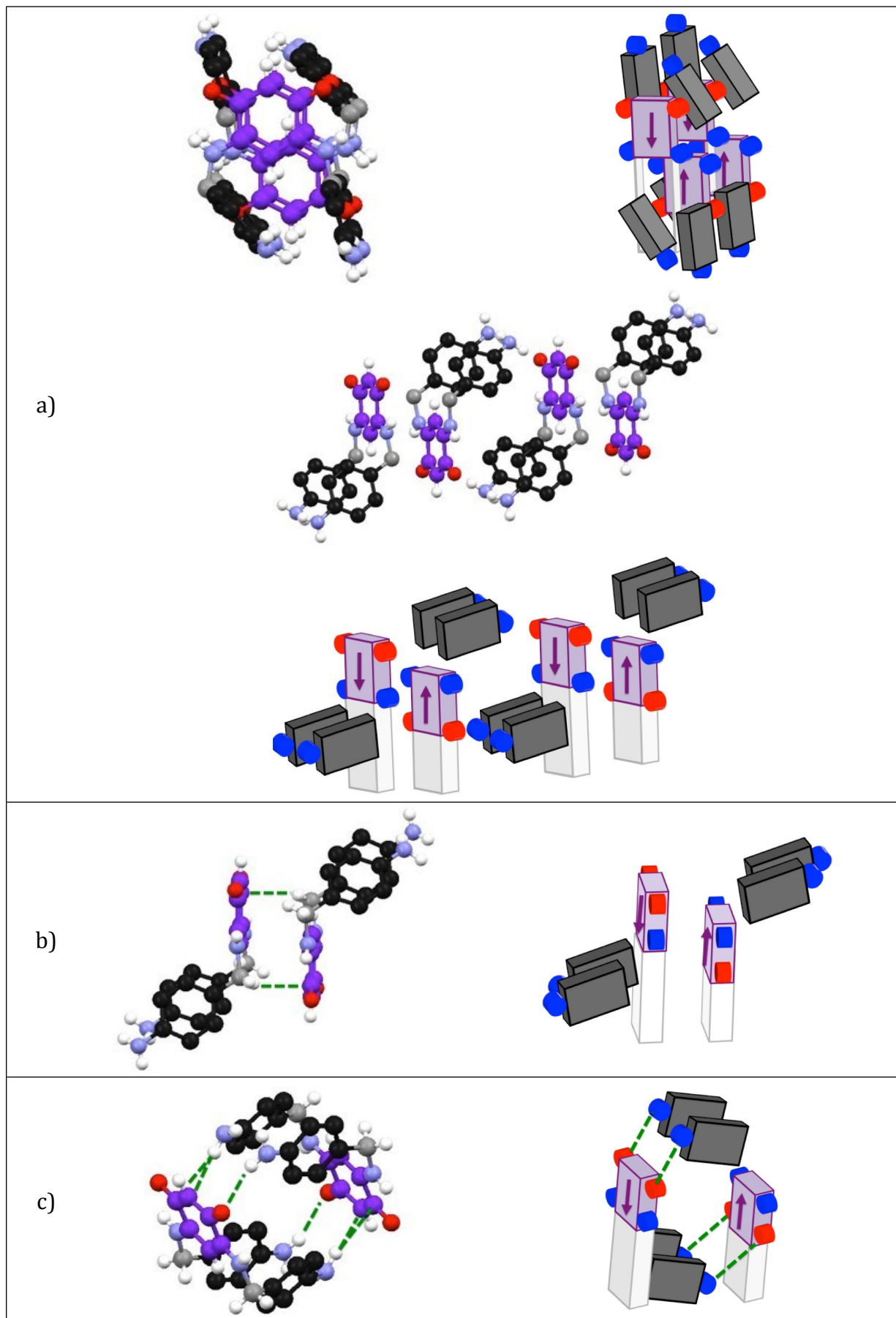
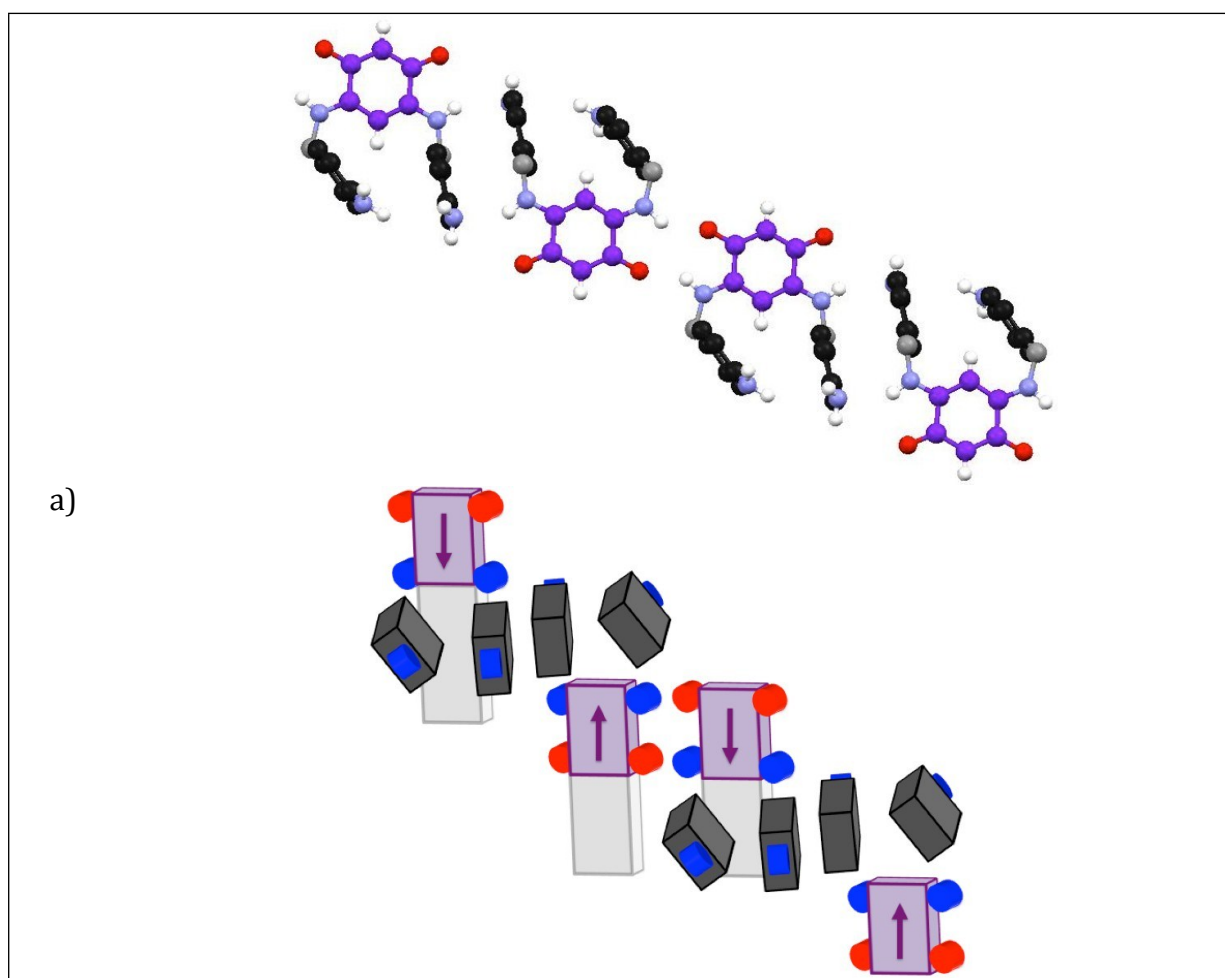


Figure S14. Molecular arrangement of zwitterions **19** in the crystalline state. a) Two views of the same molecular row. b) View of the interactions between the anionic system and the methylene group. c) View of the interactions between the anionic system and the NH₂ group. For clarity, quinonoid cores are indicated in violet and phenyl substituents in black. In the sketch, violet parallelepipeds represent the quinonoid core and the arrows indicate the dipole direction. Red and blue spheres represent oxygen and nitrogen atoms, respectively. Black parallelepipeds represent the phenyl substituent. Light grey parallelepipeds are indicated to facilitate the visualization of the molecular arrangement of quinonoid zwitterions.



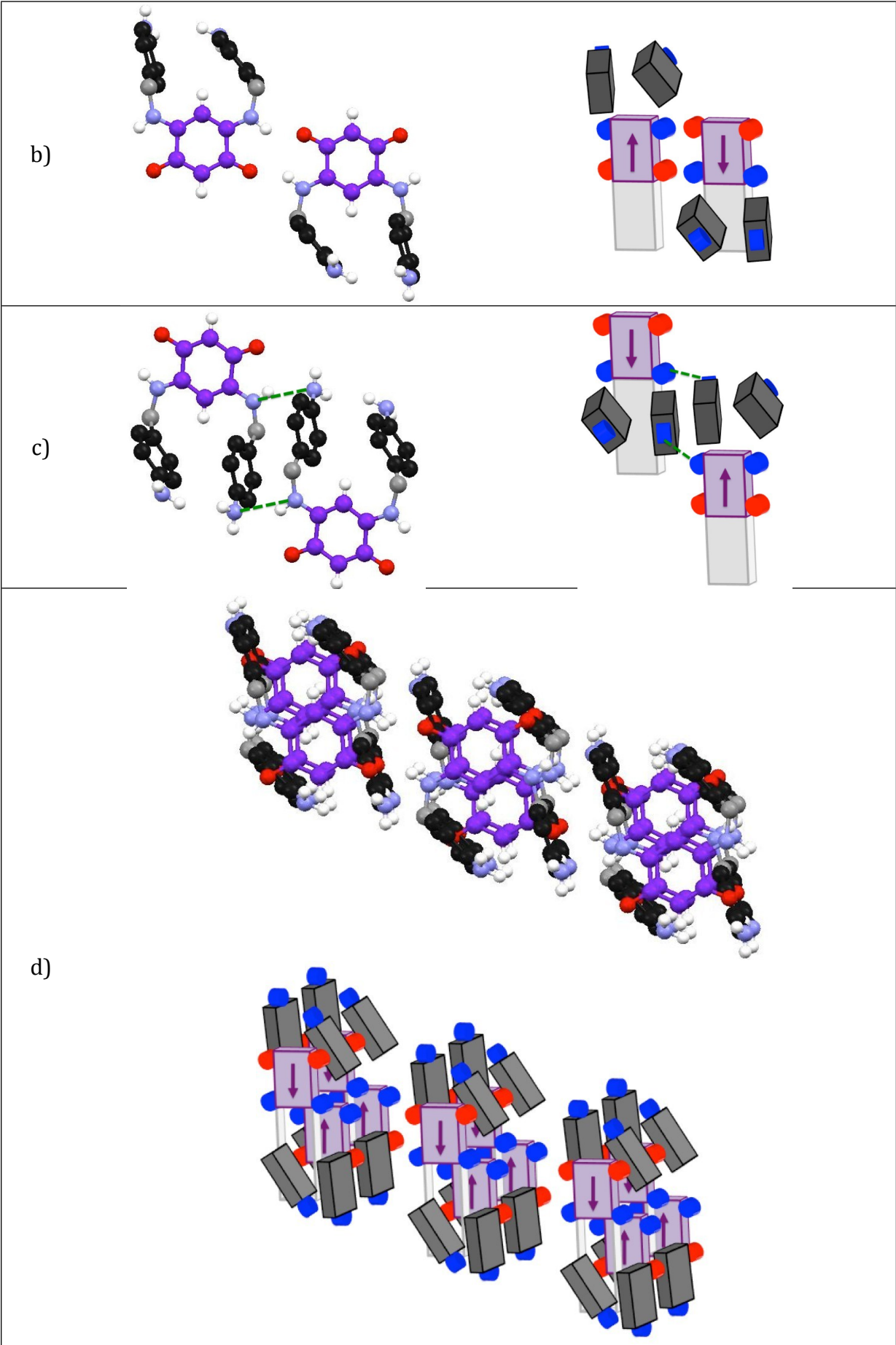
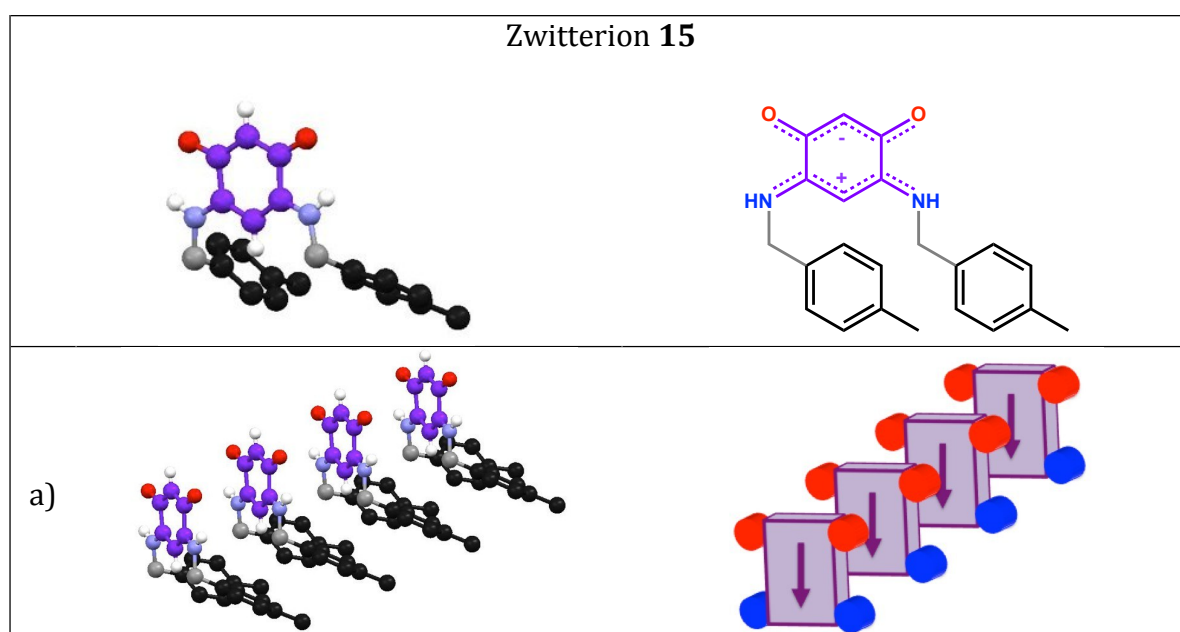


Figure S15. Molecular arrangement of zwitterions **19** in the crystalline state. a) View of the arrangement which associates the head-to-tail pair of molecule to the hydrogen bonding between the NH₂ function and the cationic system. b) Pair of molecules arranged in a head-to-tail manner. c) Hydrogen bonding between the NH₂ group and the cationic system. d) A succession of 3 molecular rows. For clarity, quinonoid cores are indicated in violet and phenyl substituents in black. In the sketch, violet parallelepipeds represent the quinonoid core and the arrows indicate the dipole direction. Red and blue spheres represent oxygen and nitrogen atoms, respectively. Black parallelepipeds represent the phenyl substituent. Light grey parallelepipeds are indicated to facilitate the visualization of the molecular arrangement of quinonoid zwitterions.

2.2.4.3. Molecular arrangement of zwitterion **15**

In the case of **15**, we observe the formation of a molecular row in a direction orthogonal to the C6 core (Figure S16a) where a methylene group interacts with the aryl substituent (Figure S16b). These interactions are drastically different from those observed in **5** (Figure S3c). Molecules of **15** are shifted horizontally (Figure S16a) whereas molecules of **5** are shifted upward (Figure S3b). The succession of three molecular rows of **15** (Figure S16d) is similar to that observed for zwitterions **3** (HN-R: HN-CH₂-CH₂-CH₂-OMe) and **4** (HN-R: HN-CH₂-CH₂-CH₂-SMe).³



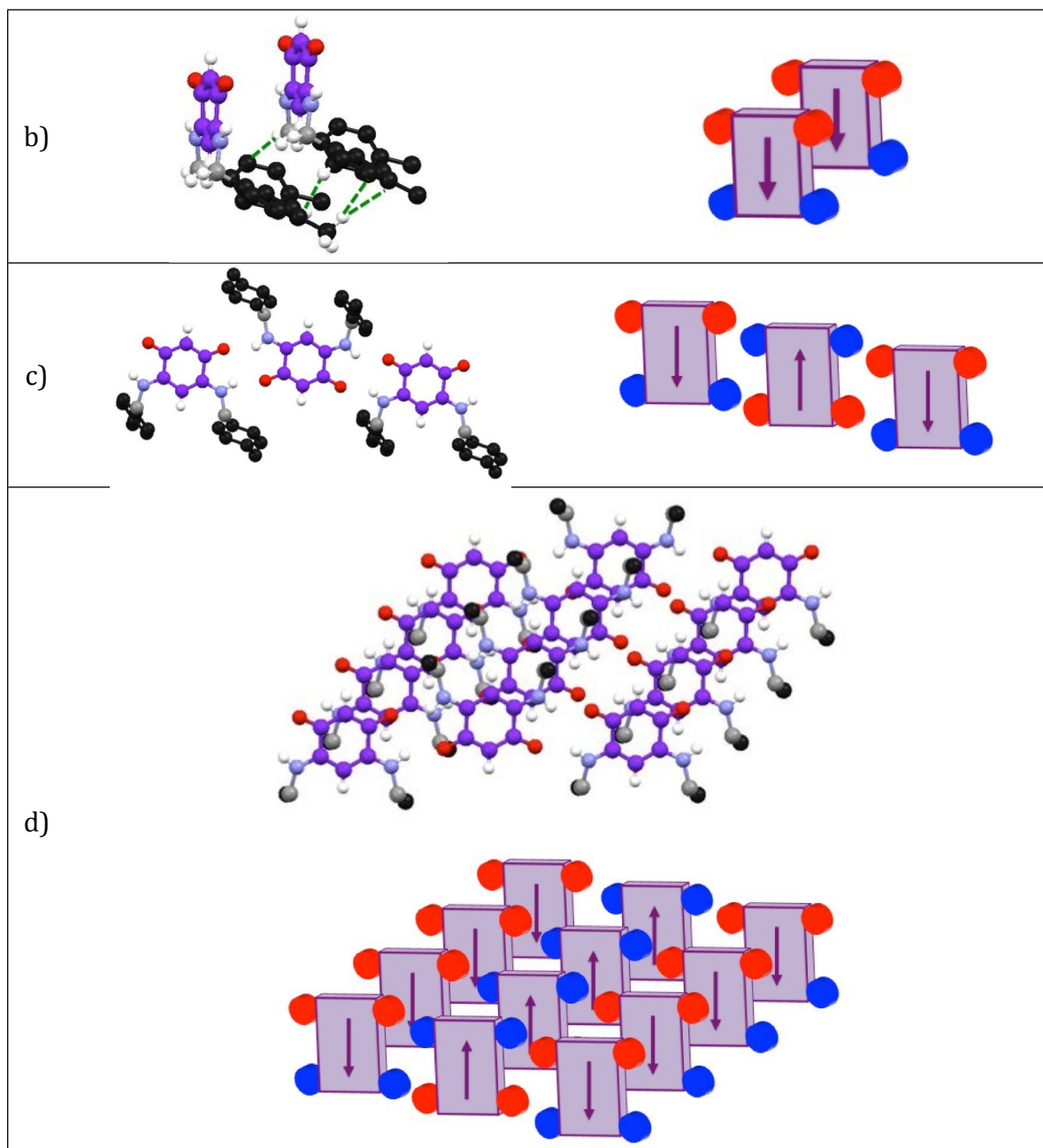


Figure S16. The molecular arrangement of zwitterions **15** in the crystalline state. a) A row of molecules. b) Hydrogen bonding between two neighboring molecules. c) A head-to-tail ribbon of **15**. d) A succession of 3 molecular rows. For clarity, quinonoid cores are indicated in violet and phenyl substituents in black (a-c) or were omitted (d). Parallelepipeds represent the quinonoid core and the arrows indicate the dipole direction. Red and blue spheres represent oxygen and nitrogen atoms, respectively. Figures S16a and S16b are taken from the main text.

2.2.5. Characteristics of the molecular rows

From the analysis of seven X-ray structures, it appears that only four candidates fulfill the crucial criteria needed for interesting electronic properties by having infinite molecular rows in a direction orthogonal to the C6 core. In order to gain potential information on the electronic properties of the film on substrate, we need to study in more detail the arrangement within the molecular row. The latter is characterized by three spacings: 1) the spacing between mean-planes containing quinonoid core, 2) the interatomic D^{0-0} and D^{0-N} distances and 3) the distance D^{0-N} between neighboring molecules.

Different spacings of zwitterions **6**, **13**, **15** and **19** are compared to those of the benzyl zwitterion **5** as well as **3** of which the molecular film on a gold surface exhibited semiconductor behavior (Table S7).³

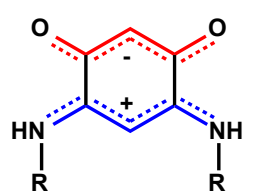
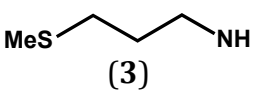
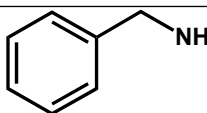
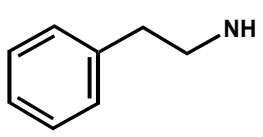
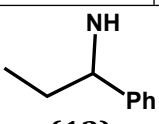
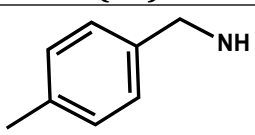
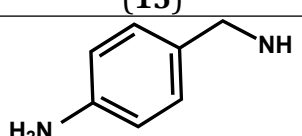
In the case of **19** (Table S7 and Figure S17), for each type of spacing we observe two very different sets of values (for example spacing between two planes are 3.39 and 7.38 Å). This can be easily rationalized by the presence within a molecular row of two distinct types of interactions (Figure S14). The separations between the anionic core and the amino group (Figure S14c) are very large and therefore not favorable for efficient electronic transport properties of molecular film of **19**.

Interestingly, the spacings observed for **13** (Table S7 and Figure S18) are very close to those with the benzyl zwitterion **5**. Surprisingly, the comparison between zwitterions **5** (Table S7 and Figure S19) and **13** shows that an increase of steric hindrance of the R substituent does not automatically yield to an increase of the intermolecular spacing.

The first row of zwitterion **6** (Table S7 and Figure S20) does not appear interesting for electronic transport since all the spacings are too large. The spacings measured for the other two rows of **6** (Table S7, Figures S21 and S22) are in the range of those of

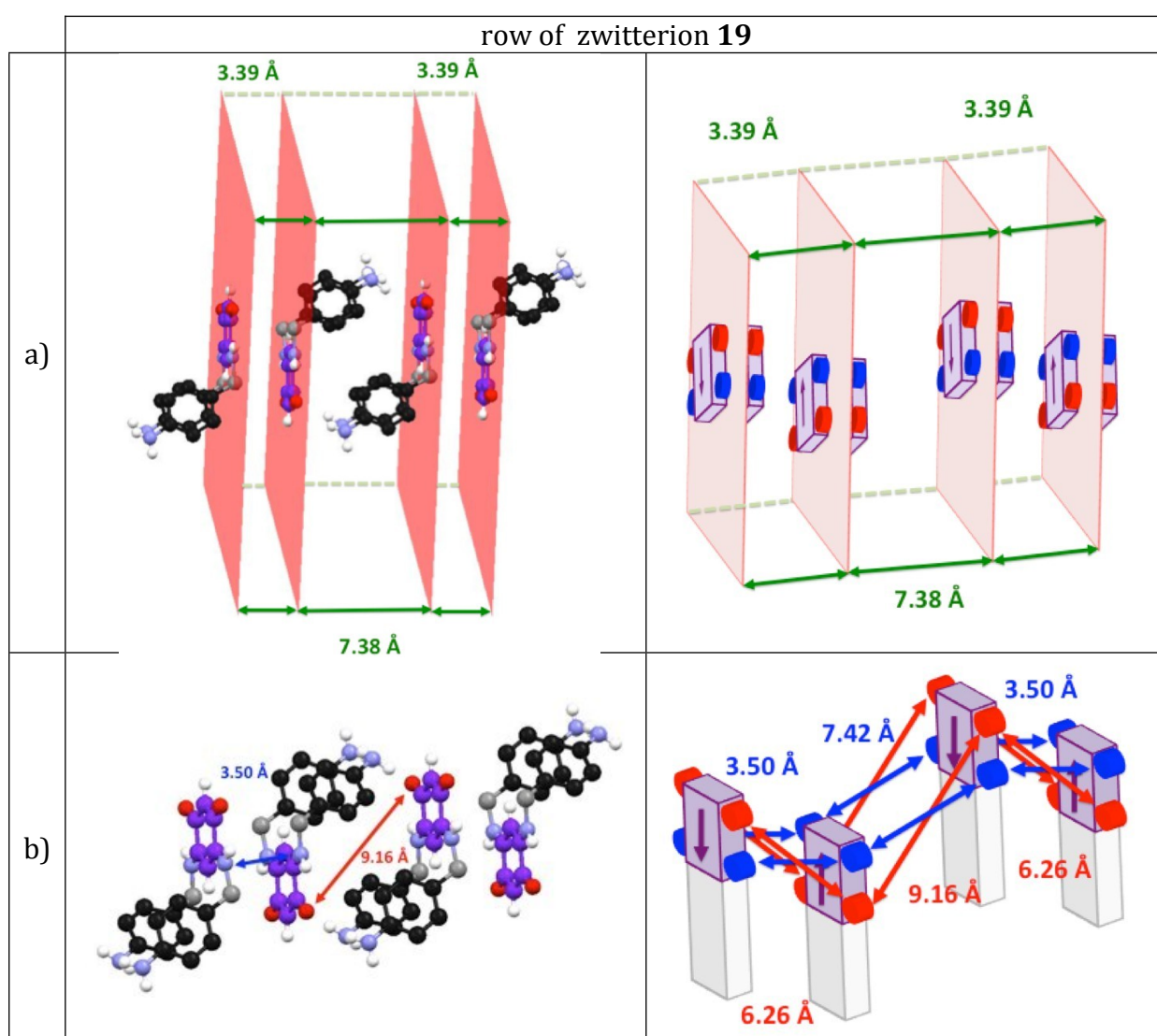
molecules **3** and **5**. Therefore we can expect that molecular films formed from these zwitterions would be conductor. The D^{O-N} distances are close to those of **3** and we can expect that the molecular film of **6** on the gold surface would probably not have semi-metallic character.

Table S7. Different spacing (\AA) measured within molecular row of zwitterions **3**, **5**, **6**, **13**, **15** and **19**

		Spacing D^{PL} between mean- planes (\AA)	Range of Interatomic Distances D^{O-O} and D^{N-N} (\AA)	Distances D^{O-N} between consecutive molecules (\AA)
 (3)		3.24	5.30	5.27 5.29
 (5)		2.91 3.05	6.35 --- 6.40	4.22; 4.27
 (6)	Row 1	6.30	7.65; 6.41	6.64; 6.44
		6.04	6.08; 8.24	6.83; 6.65
	Row 2	2.92	4.86; 6.40	4.95; 5.11
		3.17	5.39; 5.73	4.98; 4.80
	Row 3	3.12	5.05	5.03 5.12
 (13)		3.01	6.05	3.99 4.21
 (15)		3.46	4.80	4.4 4.60
 (19)		3.39 7.38	3.50, 6.26 7.42, 9.16	4.35, 4.32 7.95, 7.87

The D^{O-O} (or D^{N-N}) distance in **15** (Table S7 and Figure S23) is considerably shorter than in **5**, whereas the D^{O-N} distance in **15** is significantly larger than in **5**. We also note that

the D^{O-N} distance of 5.2 Å in zwitterions **3** and **4** is significantly larger than in **15**. Therefore, we can be relatively confident about the potential electronic transport properties of a molecular film of zwitterion **15** on a gold surface. Since the spacing D^{PL} in **15** is larger than in **5** and molecules are horizontally shifted, we can hypothesize that interactions between the anionic and cationic π -systems would be less favored than in **5**. The arrangement found in **15** is more similar to that of **3** than of **5**.



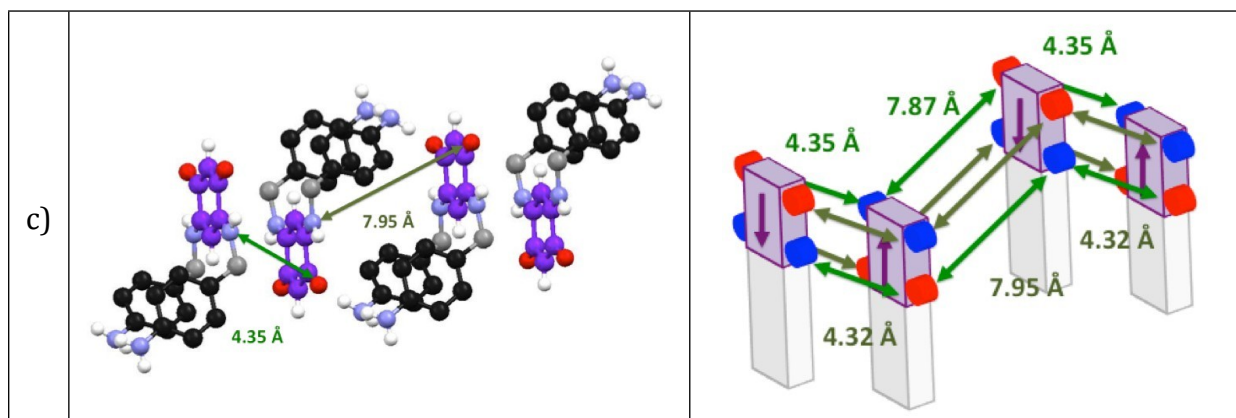
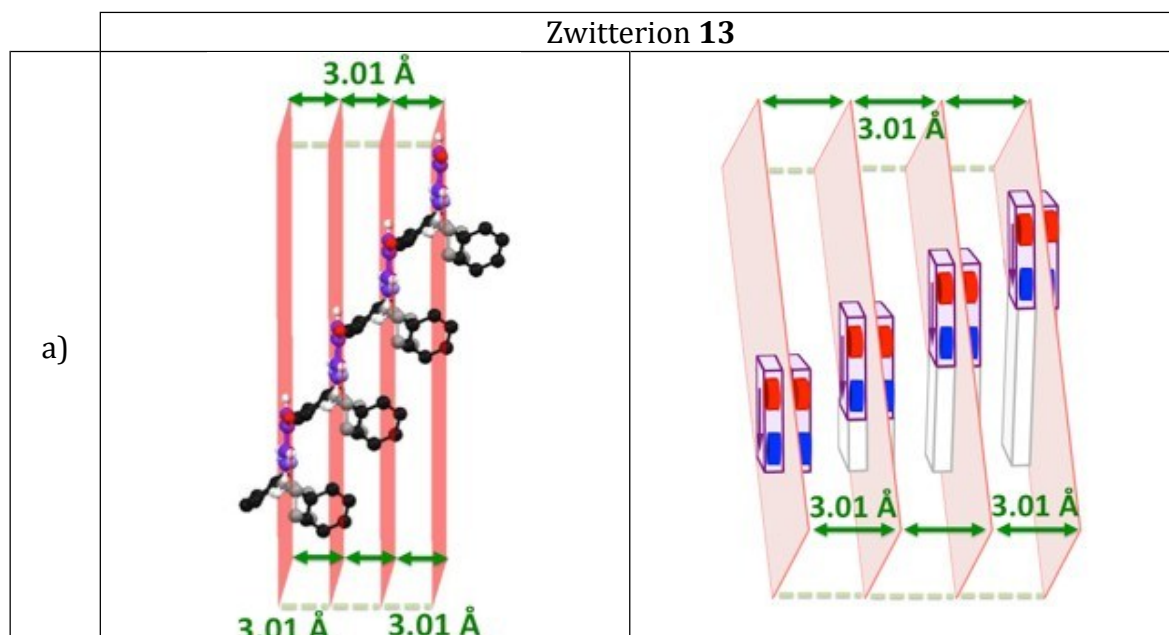


Figure S17. The characteristic intermolecular spacings in a molecular row of **19**. a) The spacing D^{PL} between mean-planes. b) Interatomic distances $D^{\text{O-O}}$ and $D^{\text{N-N}}$ between two consecutive molecules. c) Distances $D^{\text{O-N}}$ between two consecutive molecules. For clarity, quinonoid cores are indicated in violet and phenyl substituents in black. Parallelepipeds represent the quinonoid core and the arrows indicate the dipole direction. Red and blue spheres represent oxygen and nitrogen atoms, respectively. Light pink parallelepipeds represent mid-planes of quinonoid cores. Light grey parallelepipeds are indicated to facilitate the visualization of the molecular arrangement of quinonoid zwitterions.



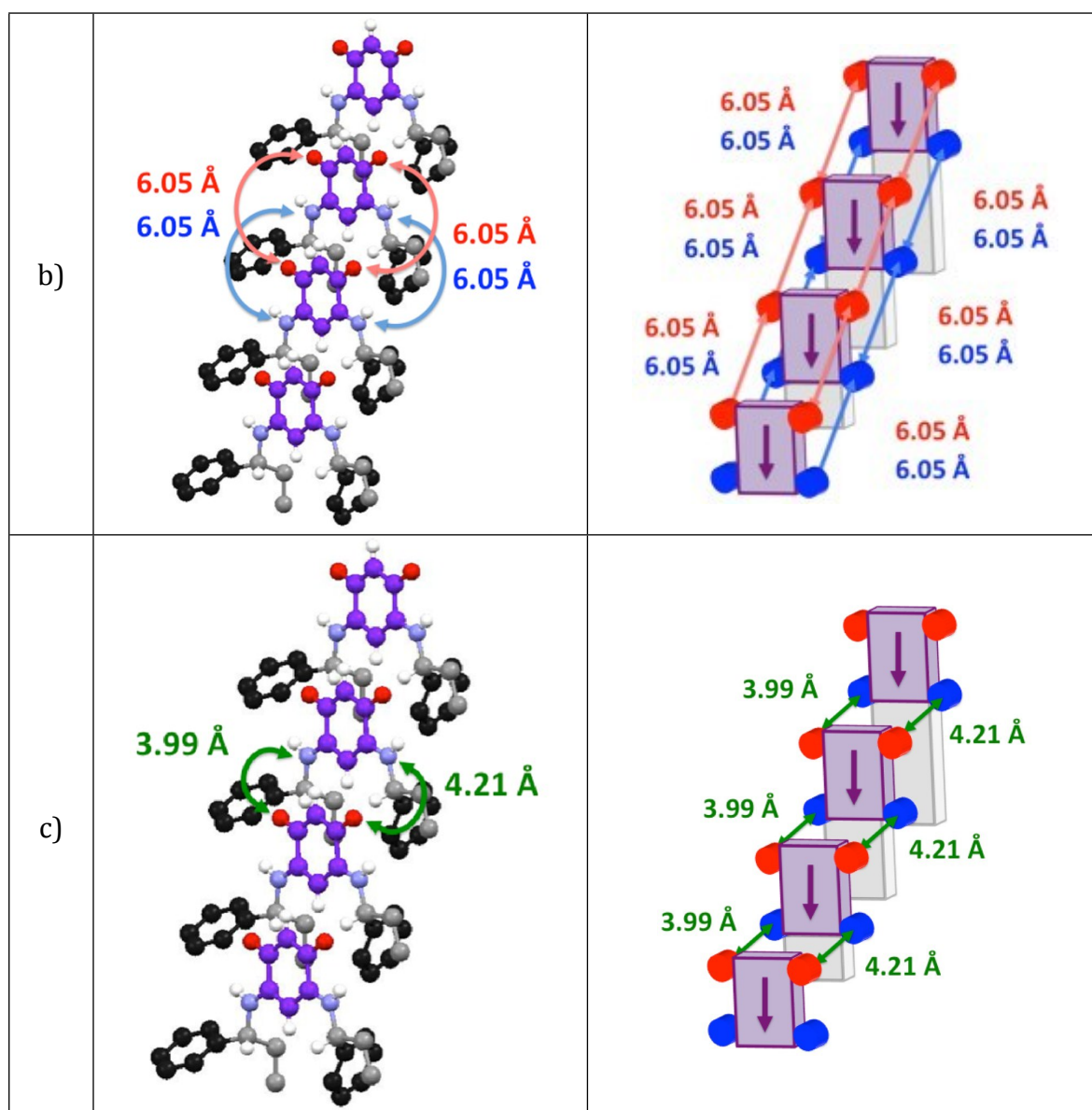


Figure S18. The characteristic intermolecular spacings in a molecular row of **13**. a) The spacing D^{PL} between mean-planes. b) Interatomic distances $D^{\text{O-O}}$ and $D^{\text{N-N}}$ between two consecutive molecules. c) Distances $D^{\text{O-N}}$ between two consecutive molecules. For clarity, quinonoid cores are indicated in violet and phenyl substituents in black. Parallelepipeds represent the quinonoid core and the arrows indicate the dipole direction. Red and blue spheres represent oxygen and nitrogen atoms, respectively. Light pink parallelepipeds represent mid-planes of quinonoid cores. Light grey parallelepipeds are indicated to facilitate the visualization of the molecular arrangement of quinonoid zwitterions. Figure S18 is taken from the main text.

Zwitterion 5

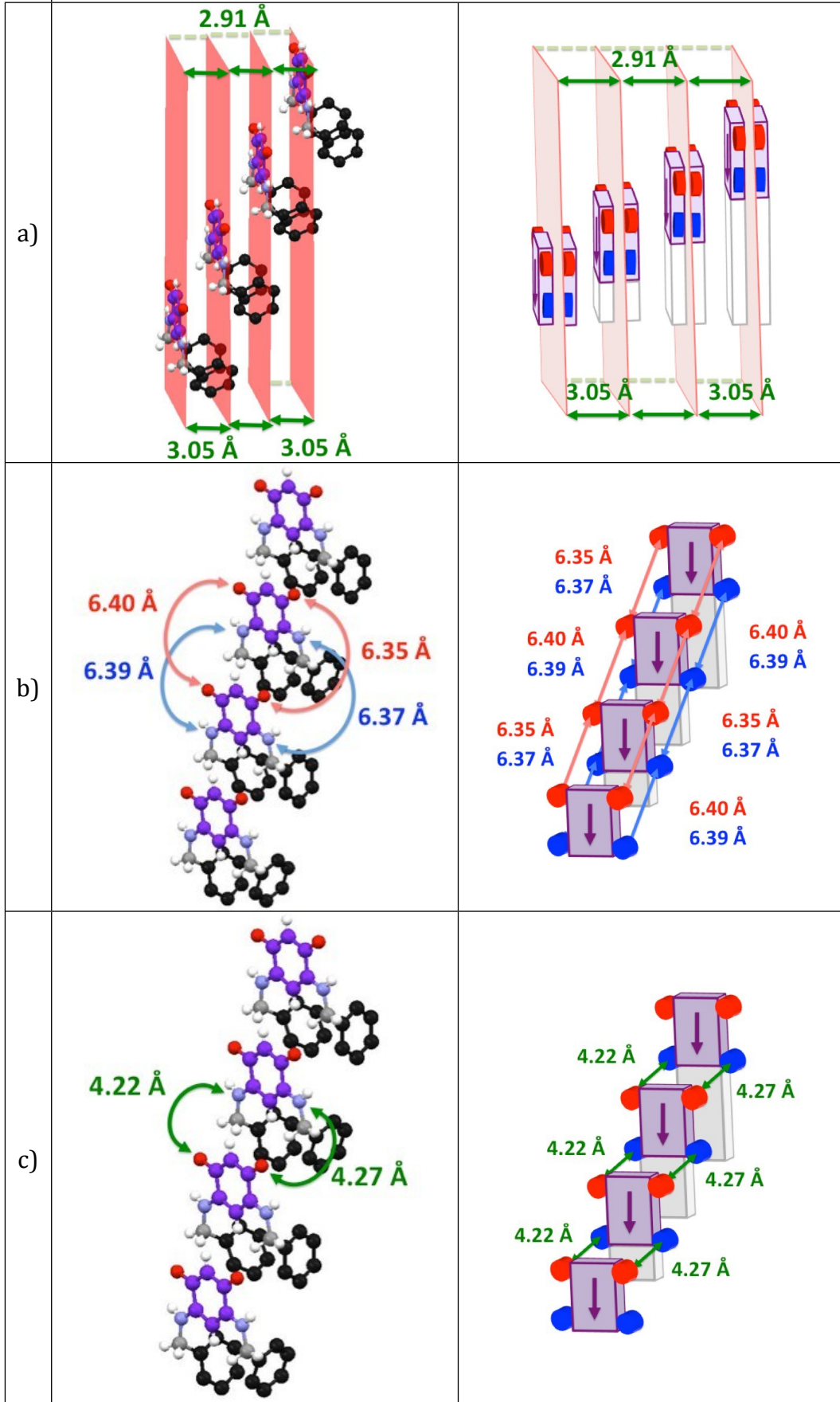
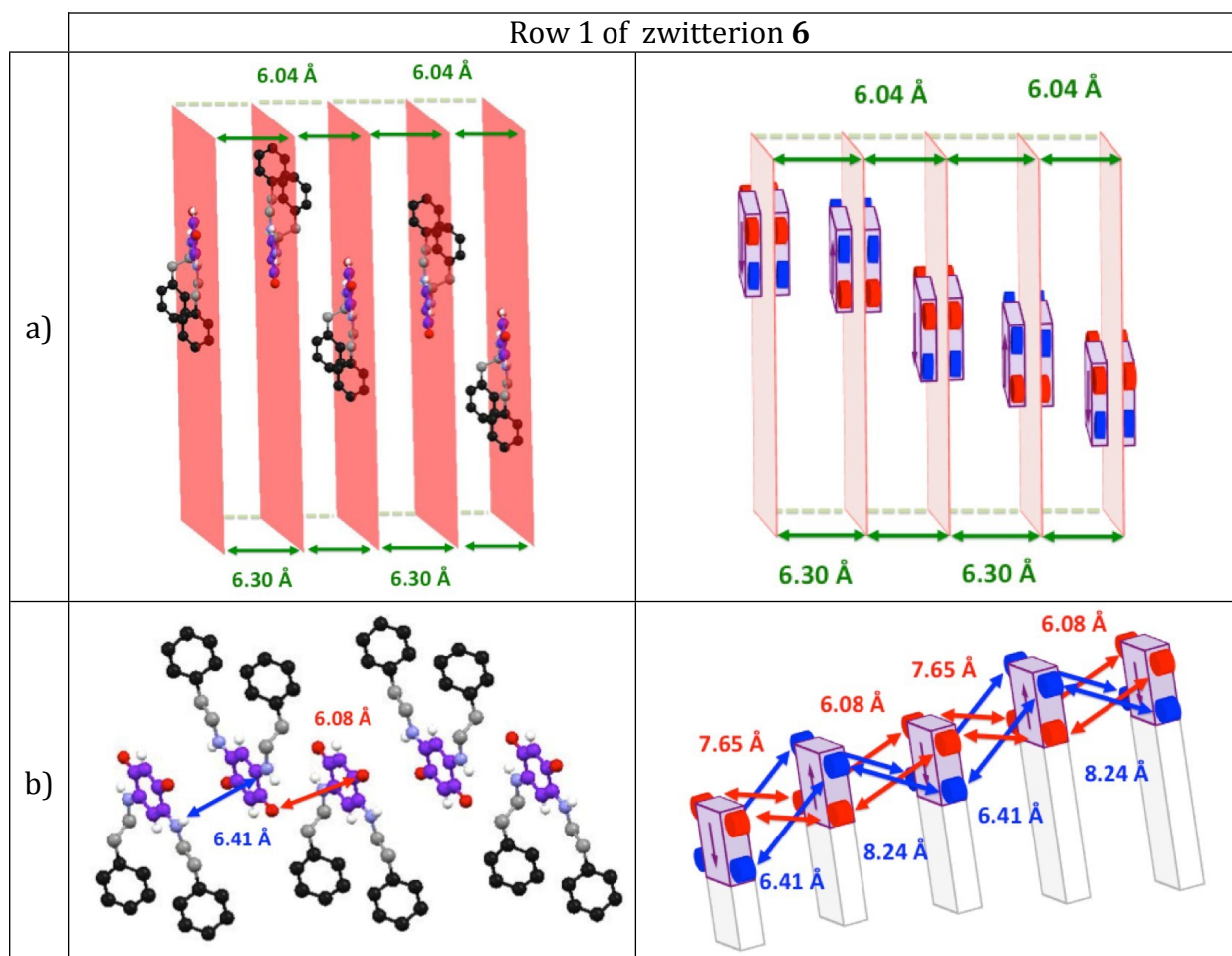


Figure S19. The characteristic intermolecular spacings in a molecular row of **5**. a) The spacing D^{PL} between mean-planes. b) Interatomic distances $D^{\text{O-O}}$ and $D^{\text{N-N}}$ between two consecutive molecules. c) Distances $D^{\text{O-N}}$ between two consecutive molecules. For clarity, quinonoid cores are indicated in violet and phenyl substituents in black. Parallelepipeds represent the quinonoid core and the arrows indicate the dipole direction. Red and blue spheres represent oxygen and nitrogen atoms, respectively. Light pink parallelepipeds represent mid-planes of quinonoid cores. Light grey parallelepipeds are indicated to facilitate the visualization of the molecular arrangement of quinonoid zwitterions. Figure S19 is taken from the main text.



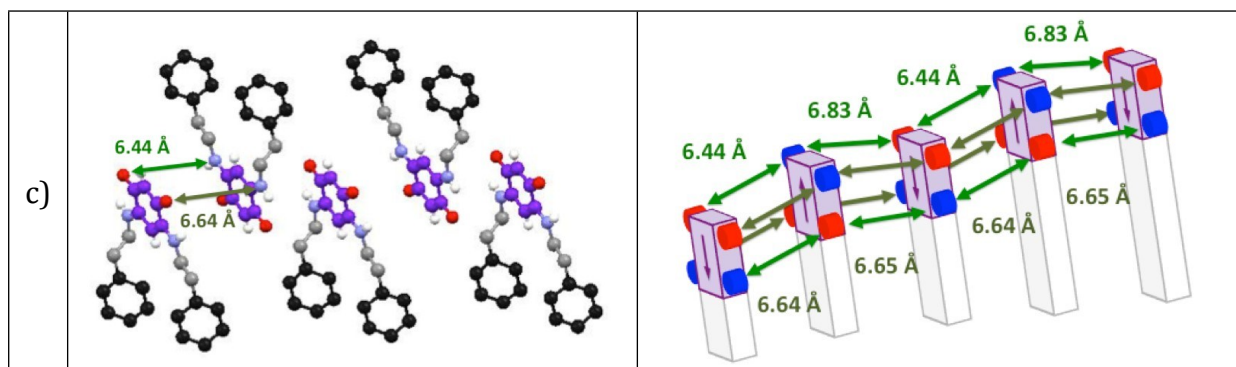
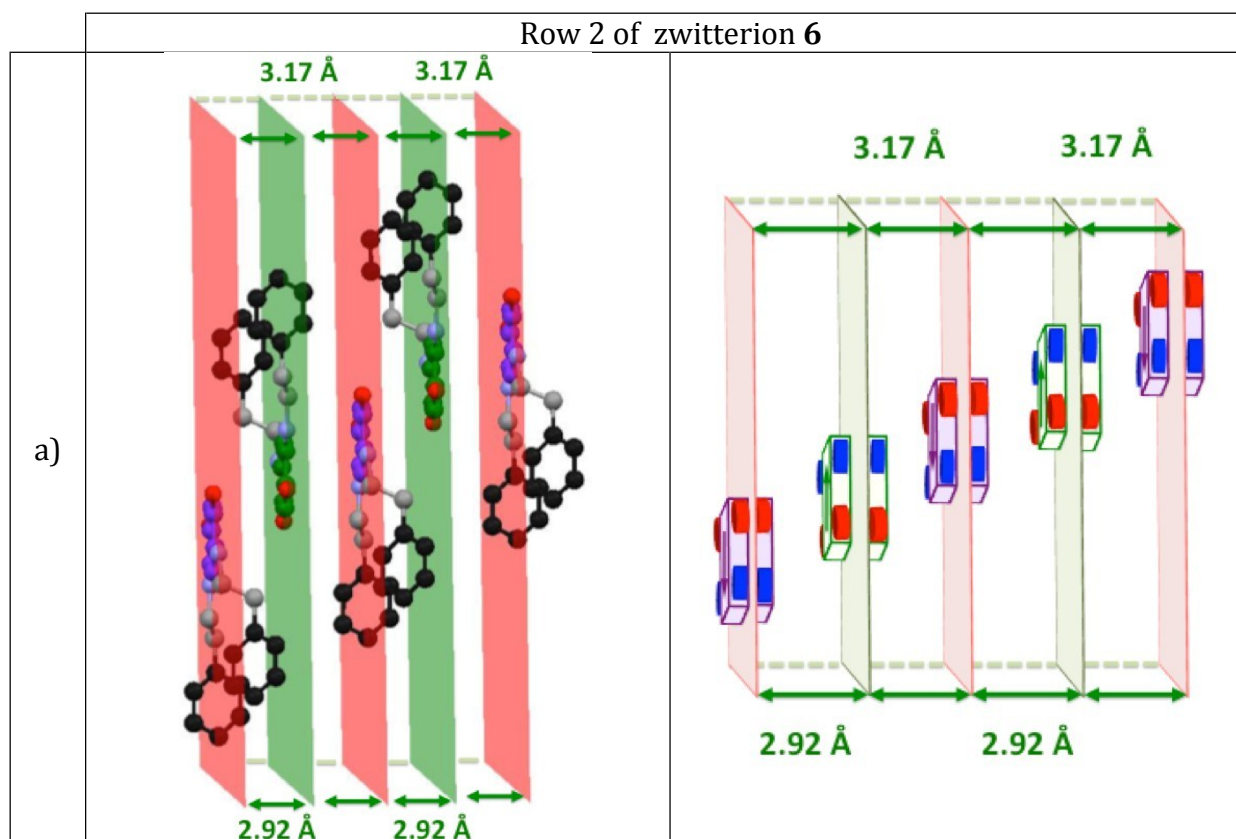


Figure S20. The characteristic intermolecular spacings in a molecular row 1 of **6**. a) The spacing D^{PL} between mean-planes. b) Interatomic distances $D^{\text{O-O}}$ and $D^{\text{N-N}}$ between two consecutive molecules. c) Distances $D^{\text{O-N}}$ between two consecutive molecules. For clarity, quinonoid cores are indicated in violet and phenyl substituents in black. Parallelepipeds represent the quinonoid core and the arrows indicate the dipole direction. Red and blue spheres represent oxygen and nitrogen atoms, respectively. Light pink parallelepipeds represent mid-planes of quinonoid cores. Light grey parallelepipeds are indicated to facilitate the visualization of the molecular arrangement of quinonoid zwitterions.



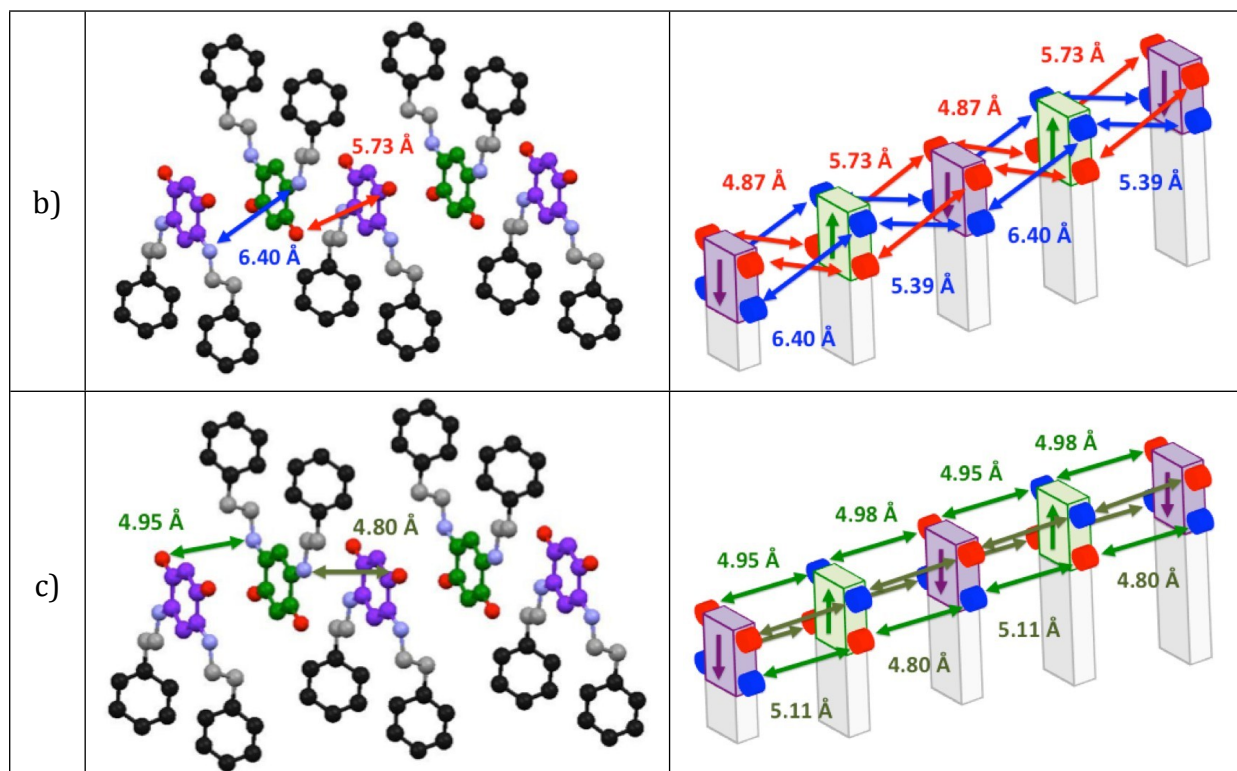


Figure S21. The characteristic intermolecular spacings in a molecular row 2 of 6. a) The spacing D^{PL} between mean-planes. b) Interatomic distances $D^{\text{O-O}}$ and $D^{\text{N-N}}$ between two consecutive molecules. c) Distances $D^{\text{O-N}}$ between two consecutive molecules. For clarity, quinonoid cores are indicated in violet and green. Phenyl substituents are indicated in black. Green and violet parallelepipeds represent the quinonoid core and the arrows indicate the dipole direction. Red and blue spheres represent oxygen and nitrogen atoms, respectively. Light pink and green parallelepipeds represent mid-planes of quinonoid cores. Light grey parallelepipeds are indicated to facilitate the visualization of the molecular arrangement of quinonoid zwitterions.

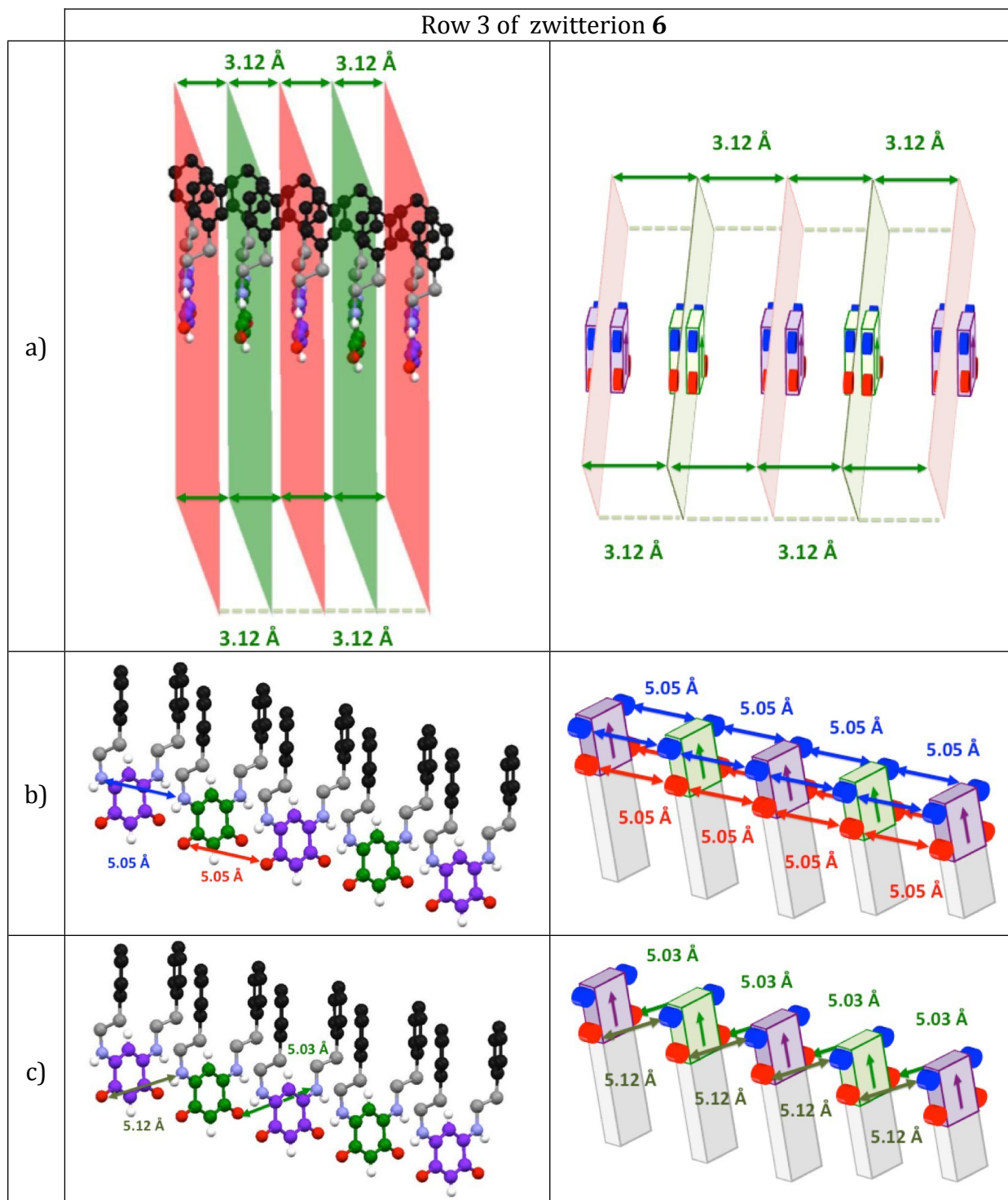


Figure S22. The characteristic intermolecular spacings in a molecular row 3 of **6**. a) The spacing D^{PL} between mean-planes. b) Interatomic distances D^{O-O} and D^{N-N} between two consecutive molecules. c) Distances D^{O-N} between two consecutive molecules. For clarity, quinonoid cores are indicated in violet and green. Phenyl substituents are indicated in black. Green and violet parallelepipeds represent the quinonoid core and the arrows indicate the dipole direction. Red and blue spheres represent oxygen and

nitrogen atoms, respectively. Light pink and green parallelepipeds represent mid-planes of quinonoid cores. Light grey parallelepipeds are indicated to facilitate the visualization of the molecular arrangement of quinonoid zwitterions.

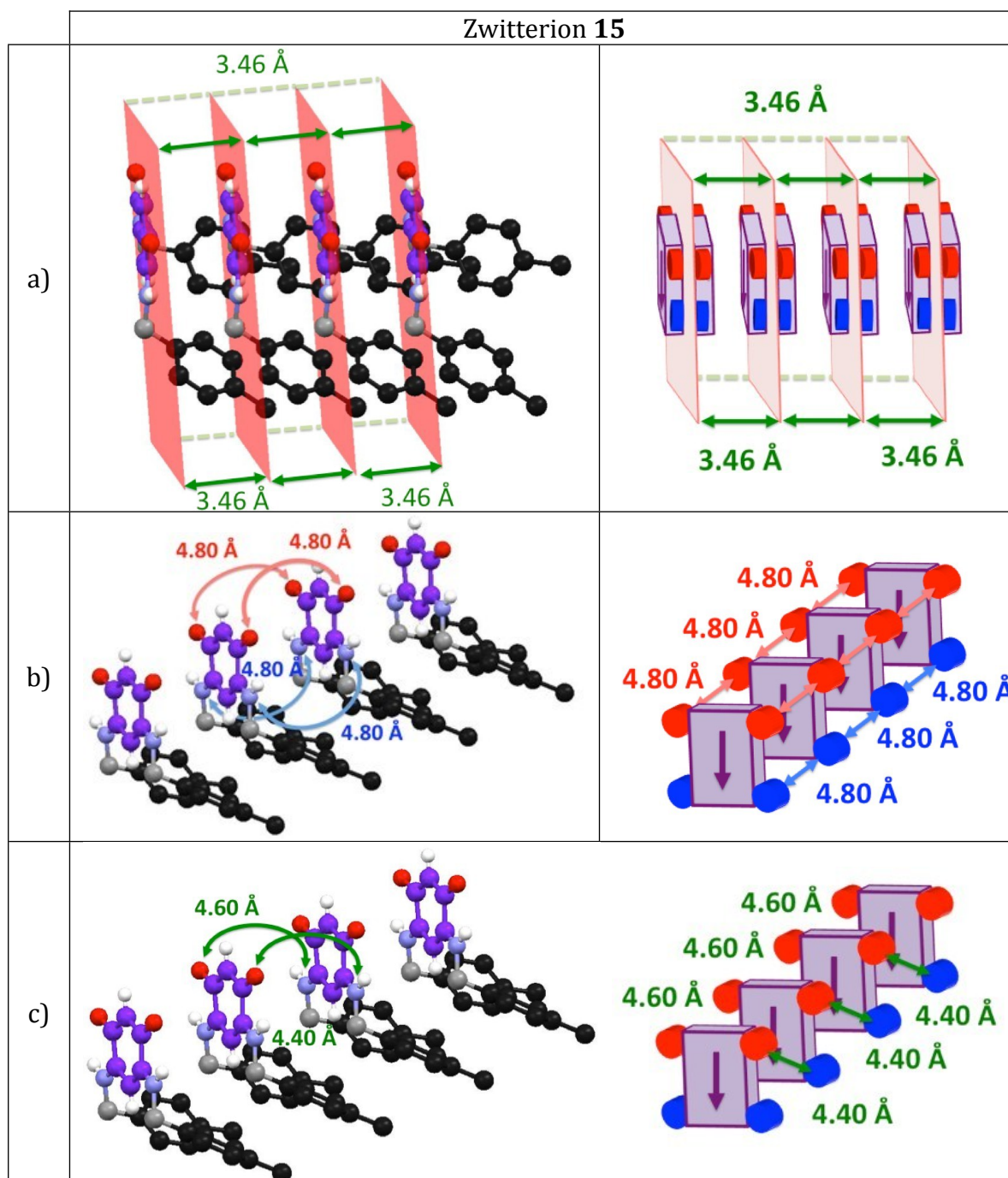


Figure S23. The characteristic intermolecular spacings in a molecular row of **15**. a) The spacing D^{PL} between mean-planes. b) Interatomic distances $D^{\text{O-O}}$ and $D^{\text{N-N}}$ between two consecutive molecules. c) Distances $D^{\text{O-N}}$ between two consecutive molecules. For clarity, quinonoid cores are indicated in violet and

phenyl substituents in black. Parallelepipeds represent the quinonoid core and the arrows indicate the dipole direction. Red and blue spheres represent oxygen and nitrogen atoms, respectively. Light pink parallelepipeds represent mid-planes of quinonoid cores. Figure S23 is taken from main text.

3. References

-
- ¹ a) P. Braunstein, O. Siri, J.-P. Taquet, M.-M. Rohmer, M. Benard and R. Welter, *J. Am. Chem. Soc.*, 2003, **125**, 12246-12256. b) P. Braunstein, O. Siri, J. P. Taquet, WO 2004009534 A1, **2004**. c) Q.-Z. Yang, O. Siri and P. Braunstein, *Chem. Eur. J.*, 2005, **11**, 7237-7246.
- ² M. Yuan, I. Tanabe, J.-M. Bernard-Schaaf, Q.-Y. Shi, V. Schlegel, R. Schurhammer, P. A. Dowben, B. Doudin, L. Routaboul and P. Braunstein, *New J. Chem.*, 2016, **40**, 5782-5796.
- ³ L. Routaboul, P. Braunstein, J. Xiao, Z. Zhang, P. A. Dowben, G. Dalmas, V. Da Costa, O. Felix, G. Decher, L. G. Rosa and B. Doudin, *J. Am. Chem. Soc.* **2012**, *134*, 8494-8506.
- ⁴ L. G. Rosa, J. Velez, Z. Zhang, J. Alvira, O. Vega, G. Diaz, L. Routaboul, P. Braunstein, B. Doudin, Y. B. Losovyj, and P. A. Dowben, *Phys Status Solidi B*, 2012, **249**, 1571-1576.
- ⁵ L. Kong, L. Routaboul, P. Braunstein, H.-G. Park, J. Choi, J. P. C. Cordova, E. Vega, L. G. Rosa, B. Doudin and P. A. Dowben, *RSC Adv.* **2013**, *3*, 10956-10961.

Figure S24. ^1H NMR spectrum of zwitterion **6** (CDCl_3 ; 500 MHz)

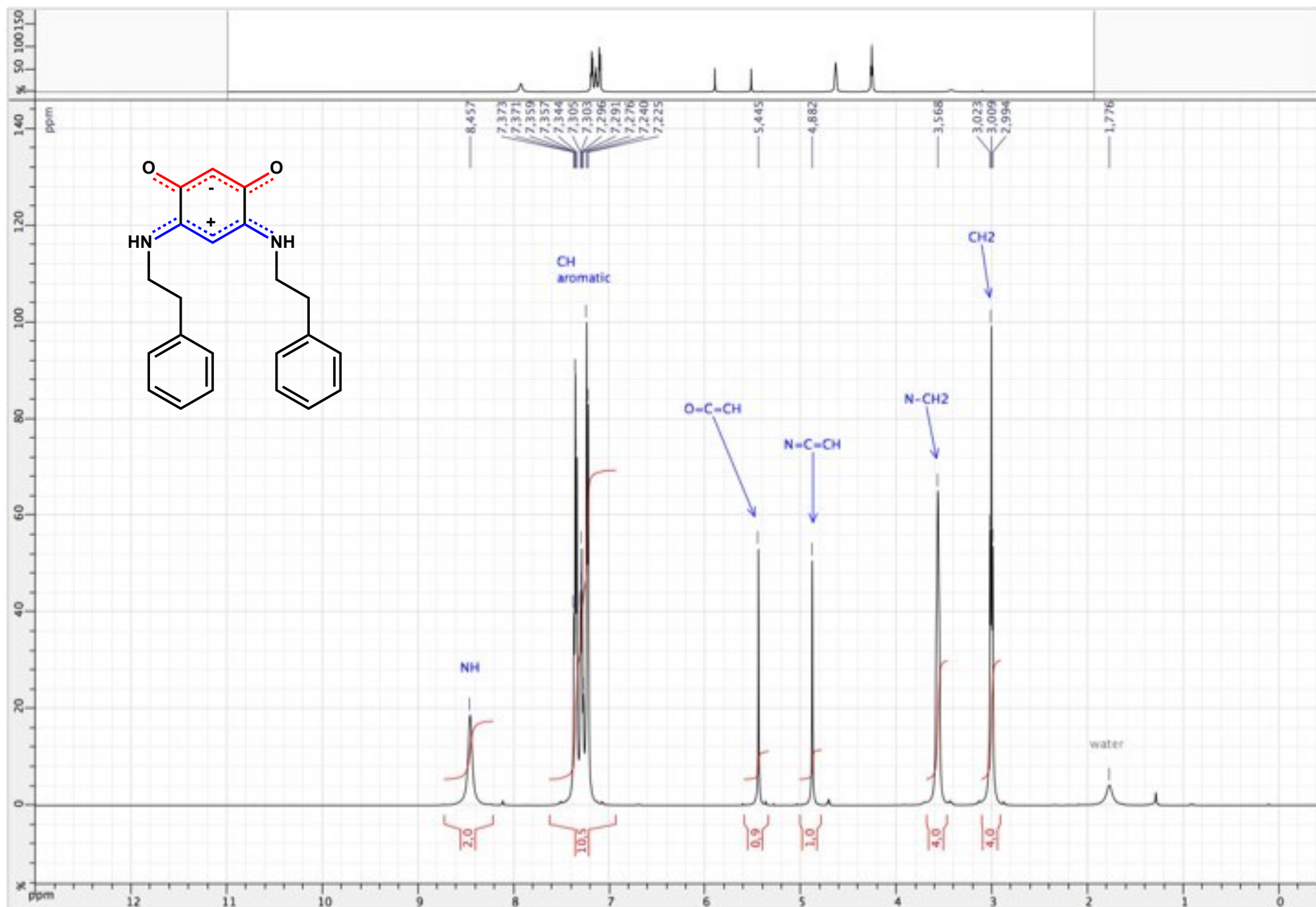


Figure S25. ^1H NMR spectrum of zwitterion **6** (CDCl_3 ; 500 MHz)

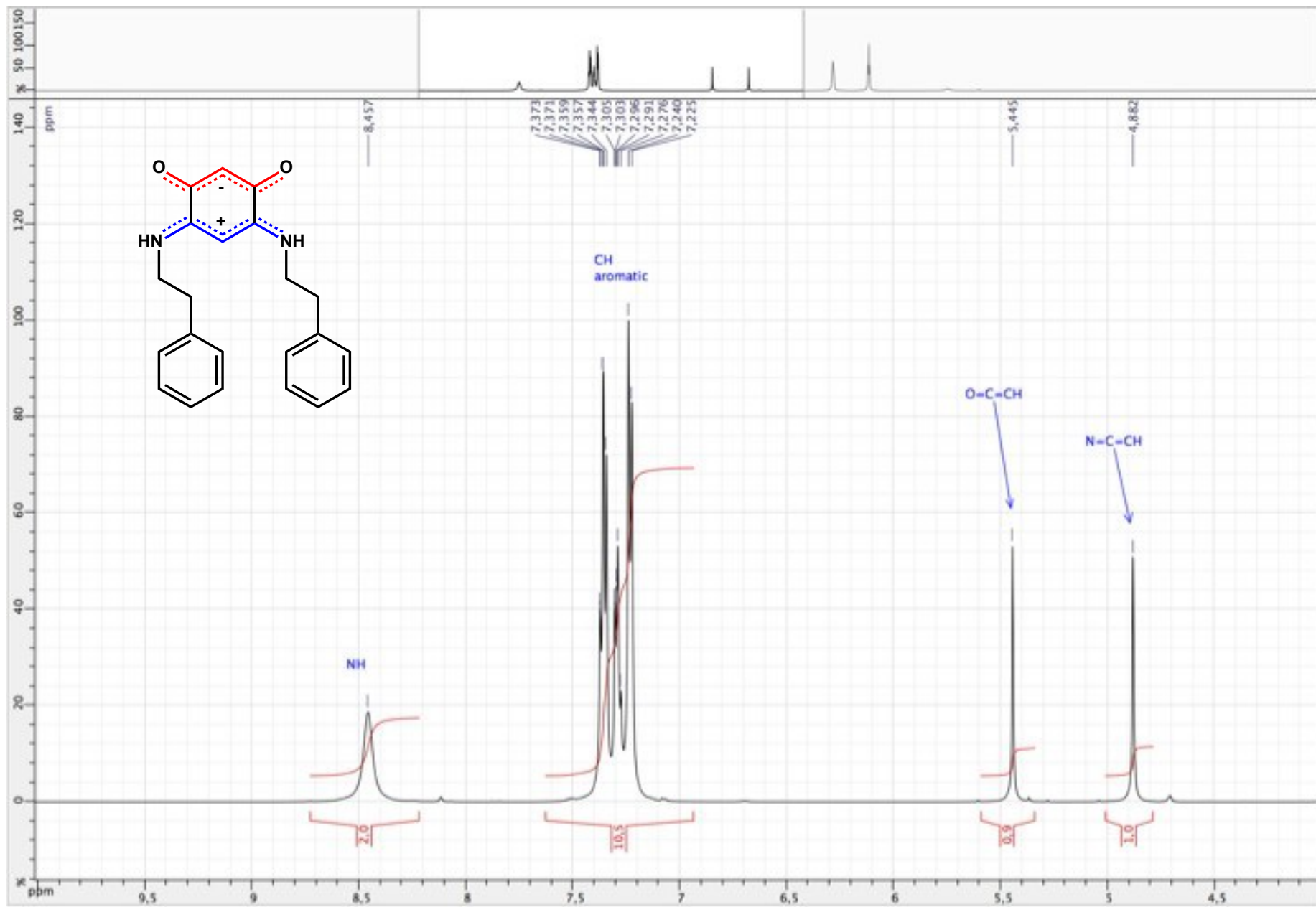


Figure S26. ^1H NMR spectrum of zwitterion **6** (CDCl_3 ; 500 MHz)

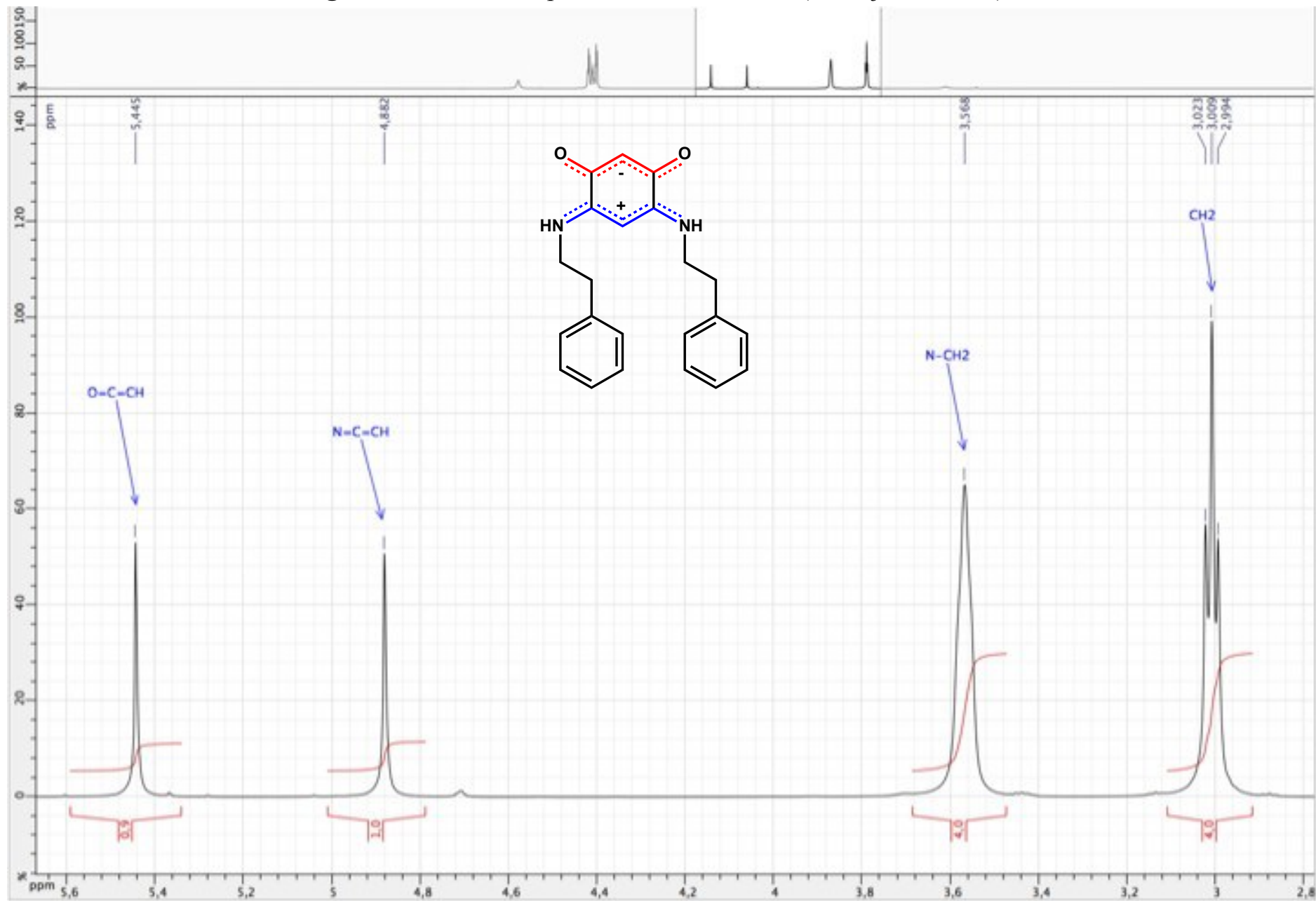


Figure S27. ^1H NMR spectrum of zwitterion **6** (CDCl_3 ; 500 MHz)

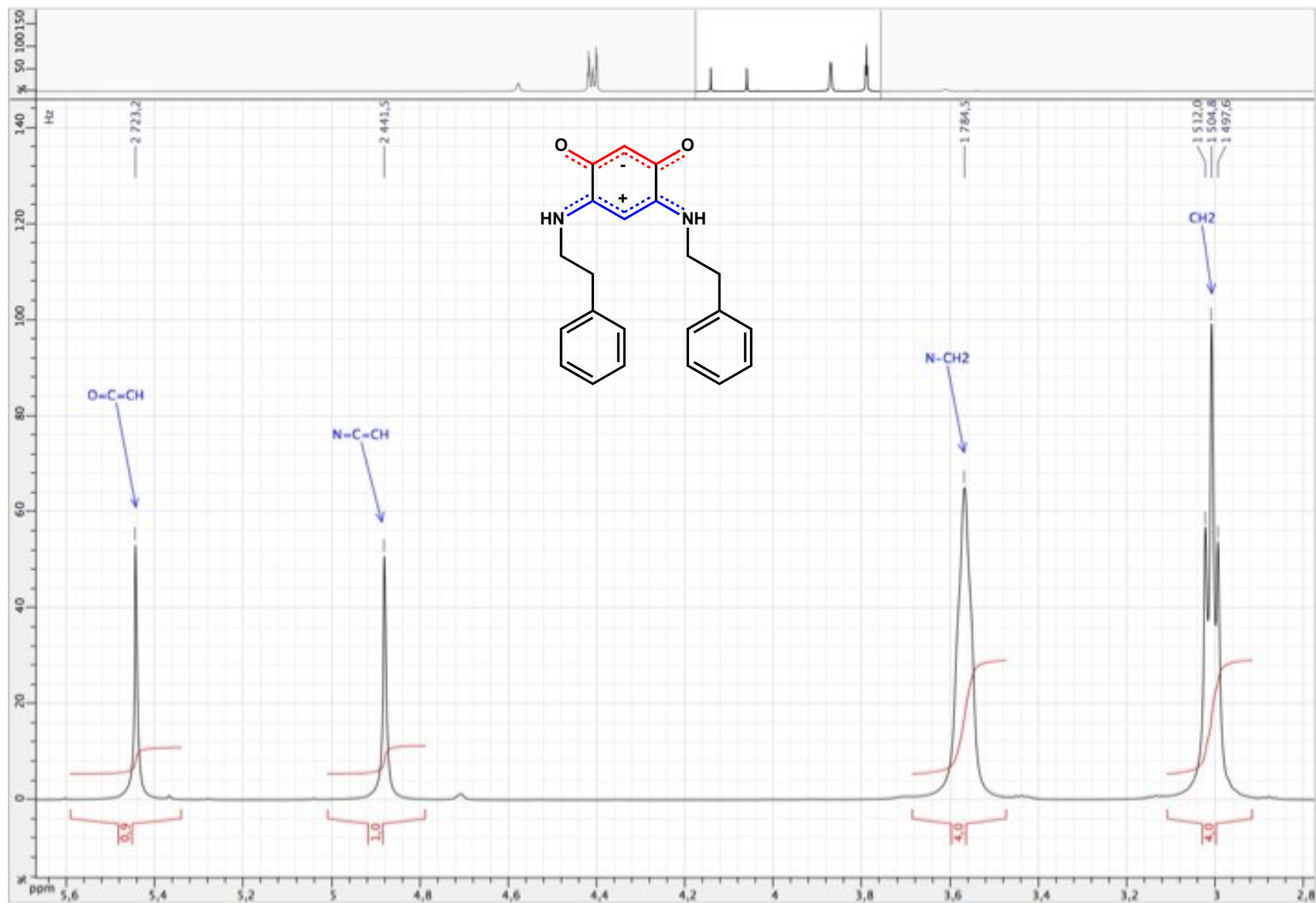


Figure S28. ^{13}C $\{^1\text{H}\}$ NMR spectrum of zwitterion **6** (CDCl_3 ; 125 MHz)

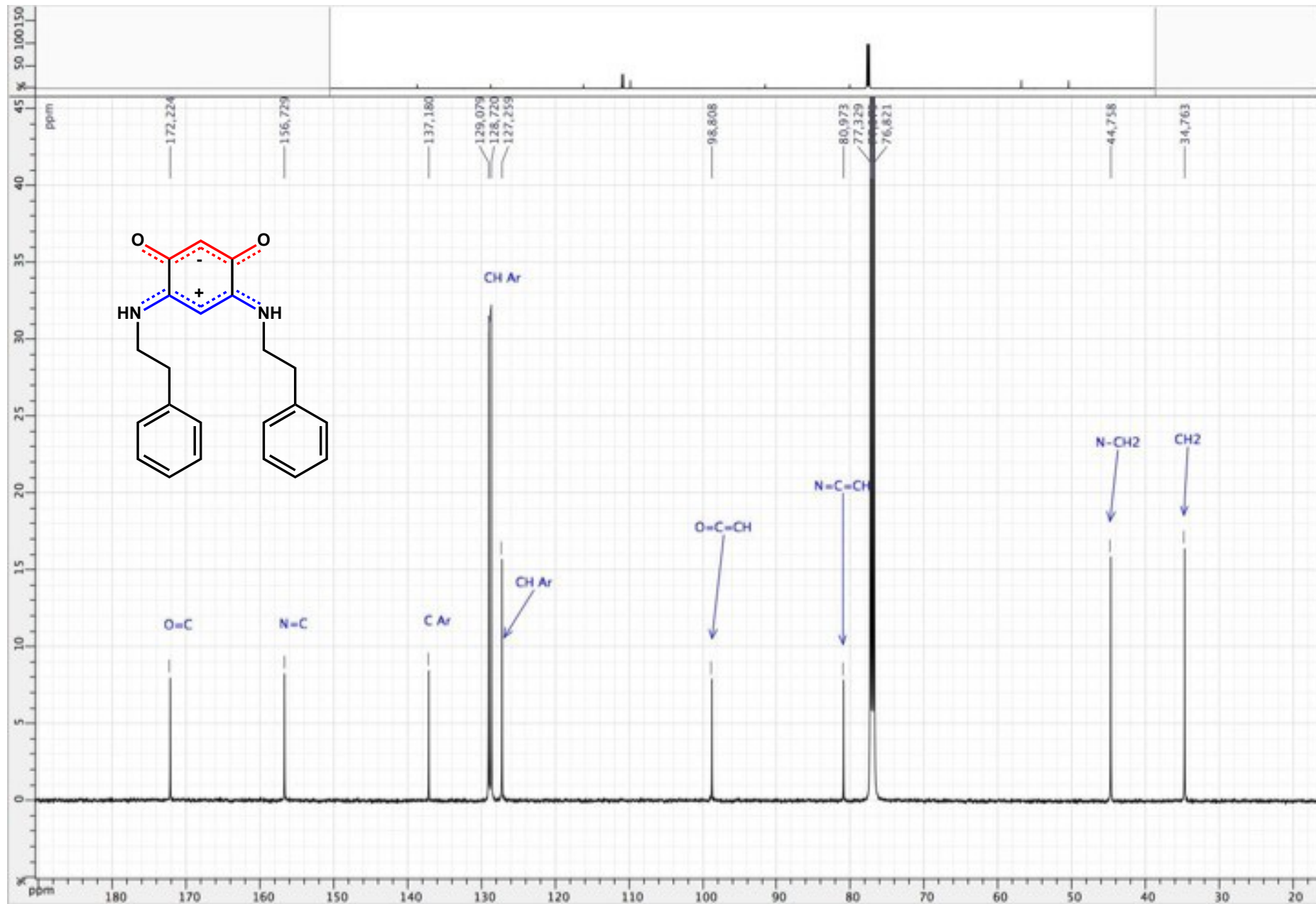


Figure S29. ^{13}C $\{^1\text{H}\}$ NMR spectrum of zwitterion **6** (CDCl_3 ; 125 MHz)

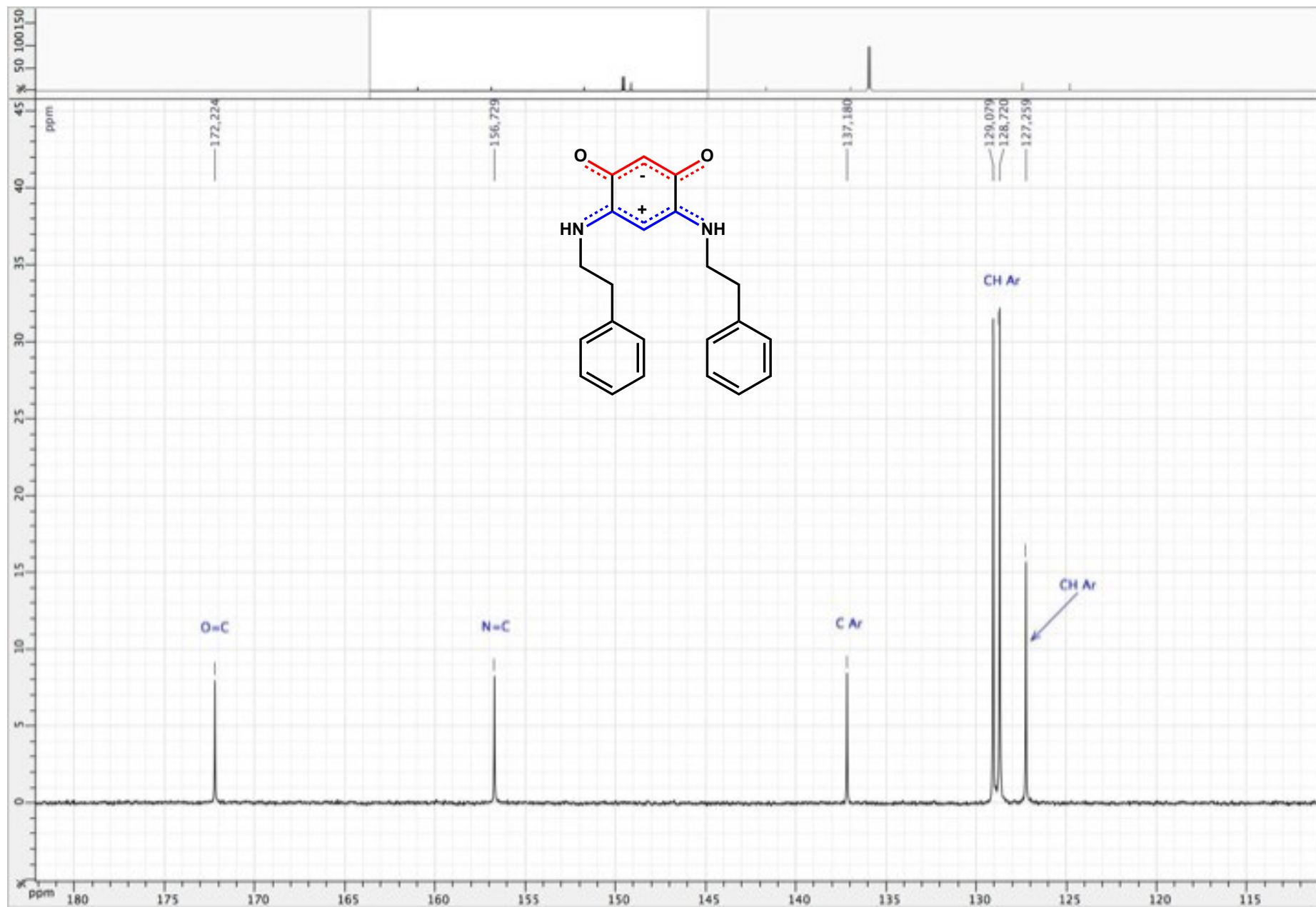


Figure S30. ^{13}C $\{^1\text{H}\}$ NMR spectrum of zwitterion 6 (CDCl_3 ; 125 MHz)

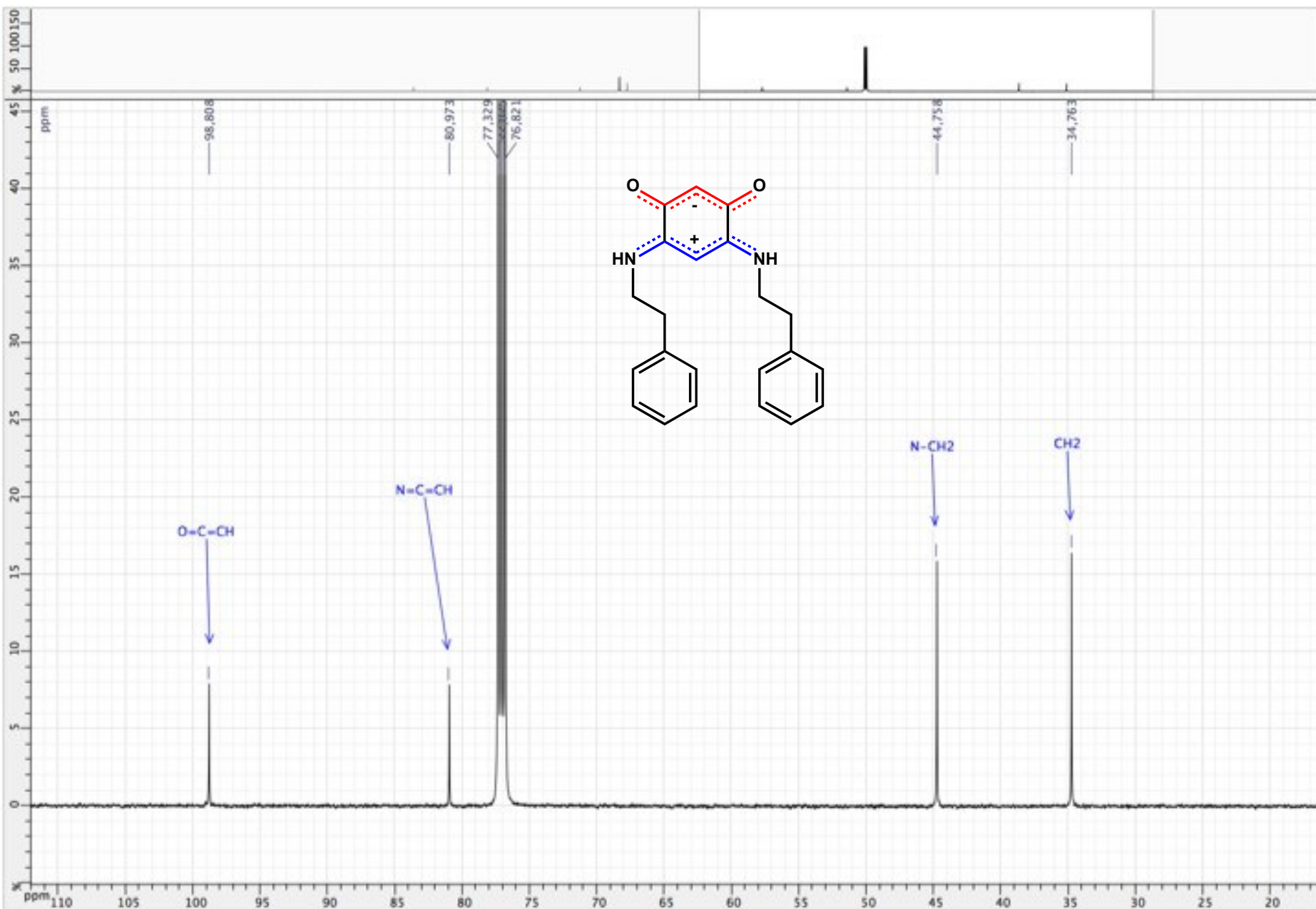


Figure S31. HSQC ($^1\text{H} / ^{13}\text{C} \{^1\text{H}\}$) spectrum of zwitterion **6** (CDCl_3 ; 500 / 125 MHz)

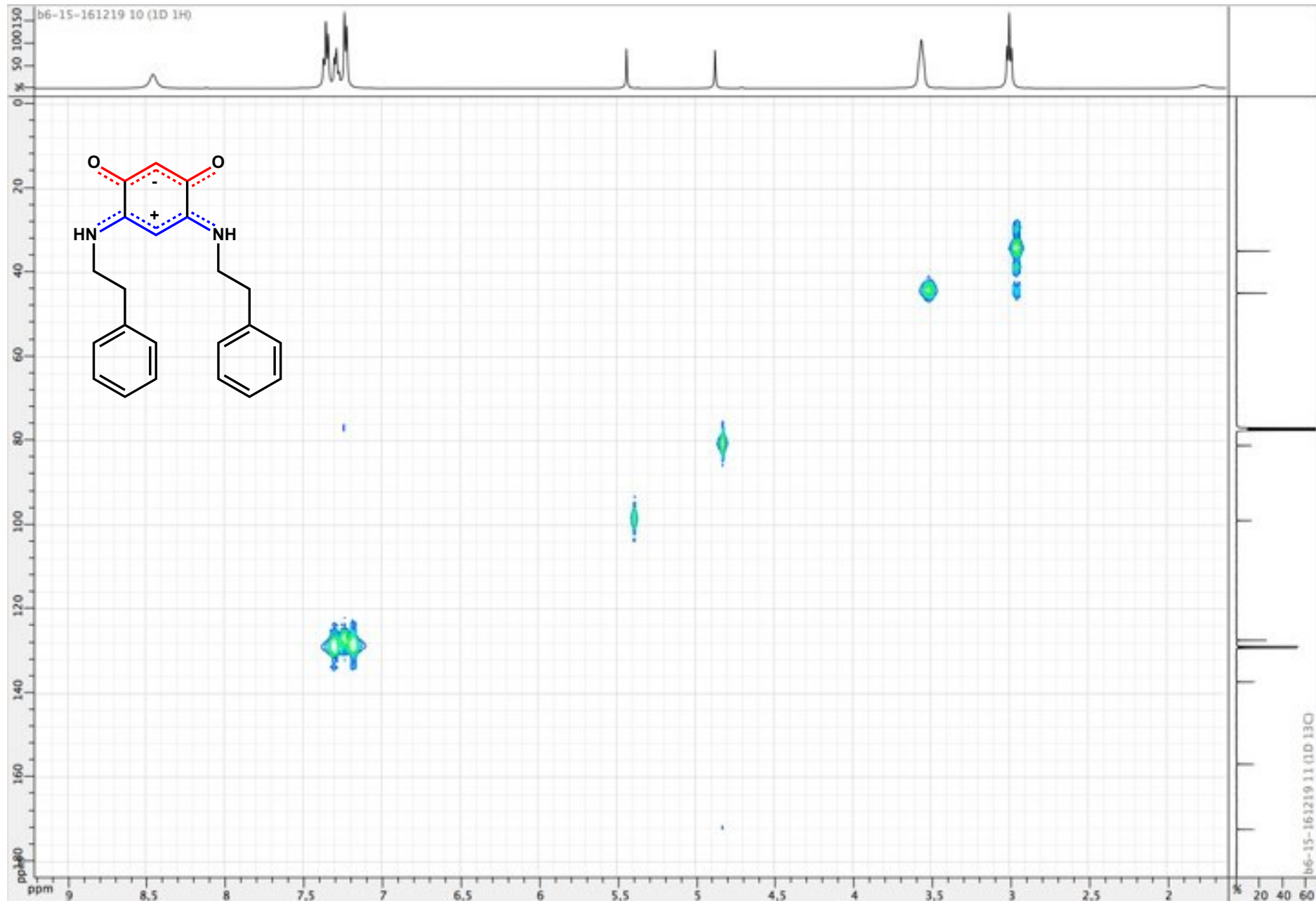


Figure S32. ^1H NMR spectrum of zwitterion **7** (CDCl_3 ; 500 MHz)

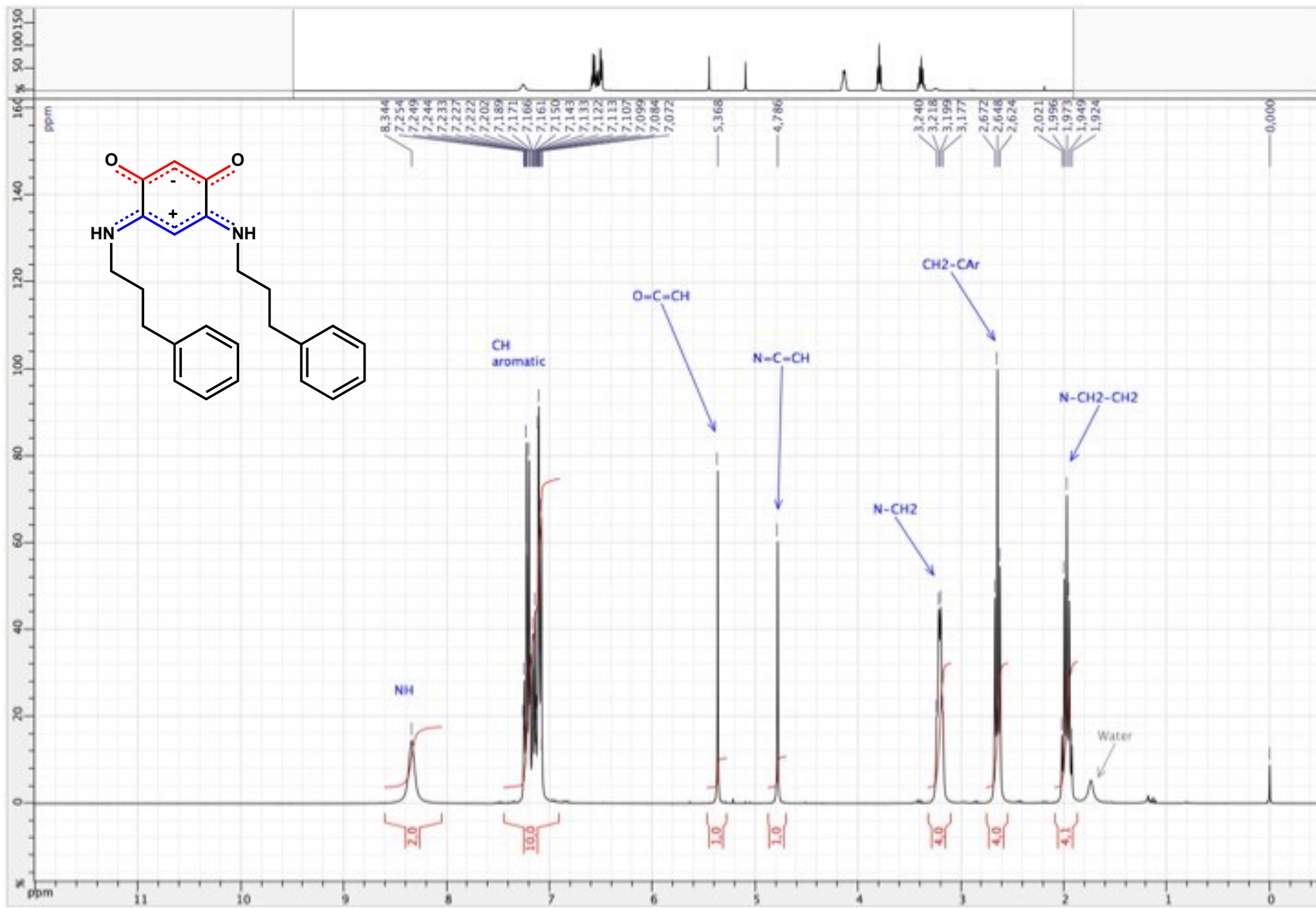


Figure S33. ^1H NMR spectrum of zwitterion **7** (CDCl_3 ; 500 MHz)

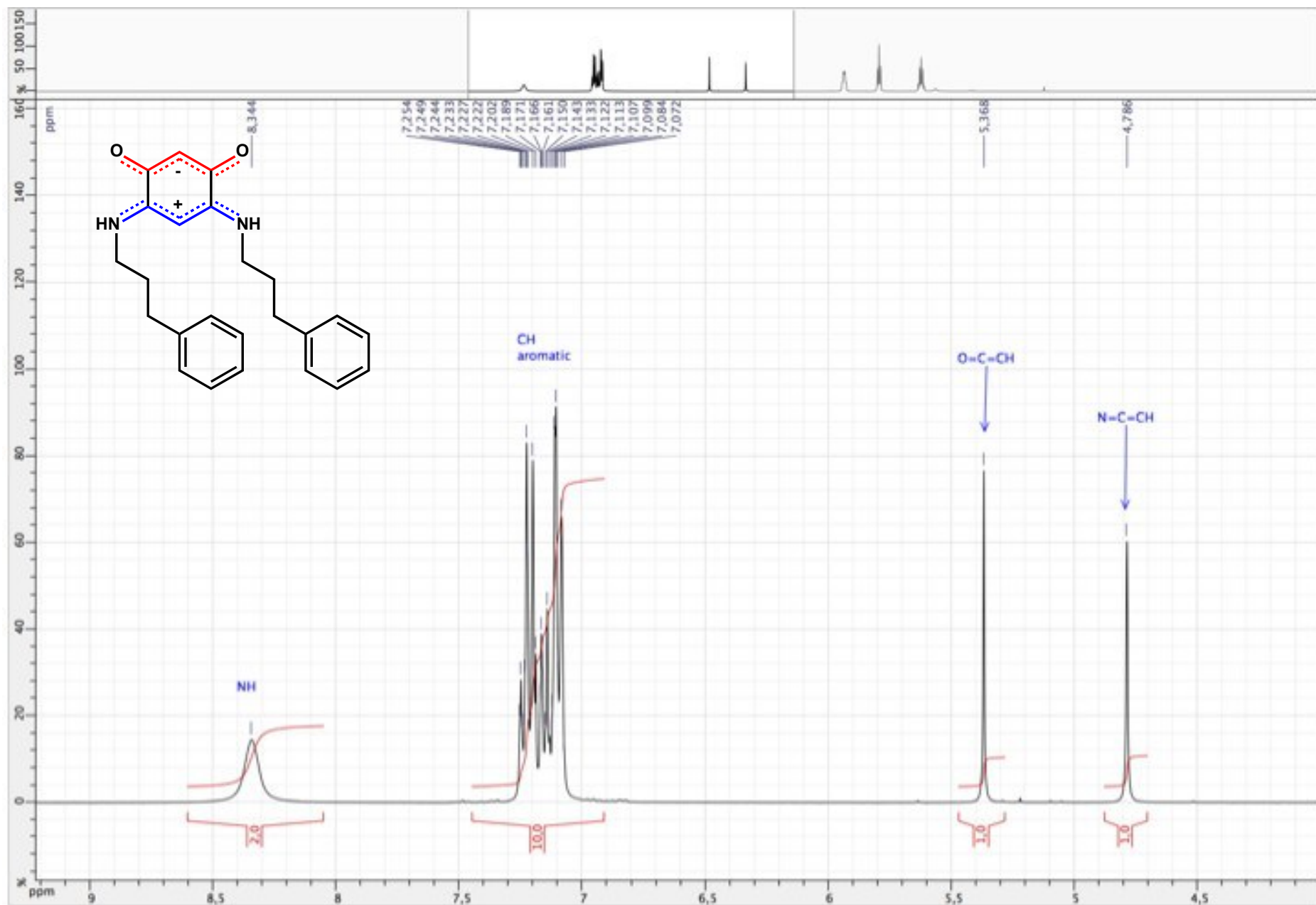


Figure S34. ^1H NMR spectrum of zwitterion **7** (CDCl_3 ; 500 MHz)

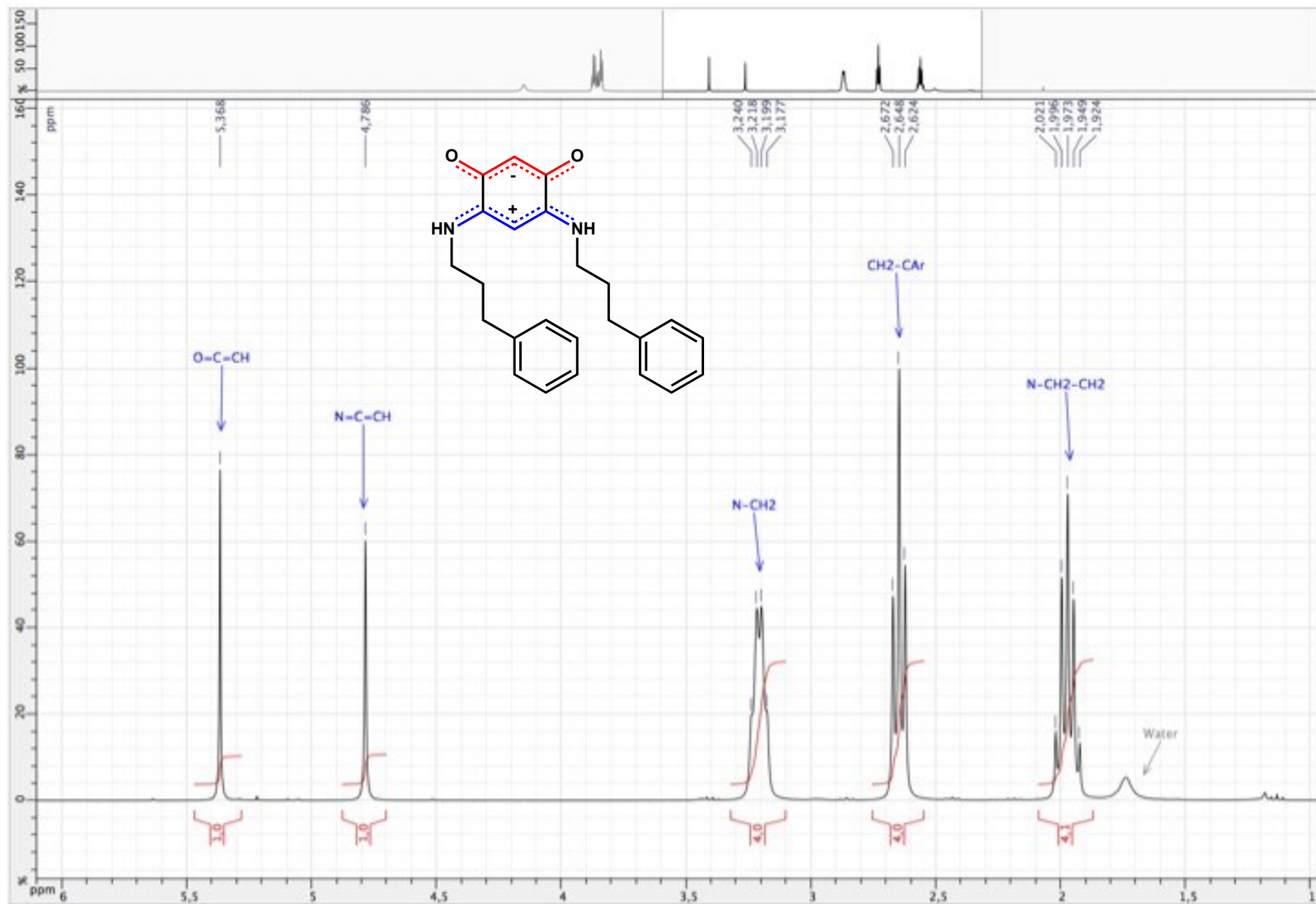


Figure S35. ^1H NMR spectrum of zwitterion **7** (CDCl_3 ; 500 MHz)

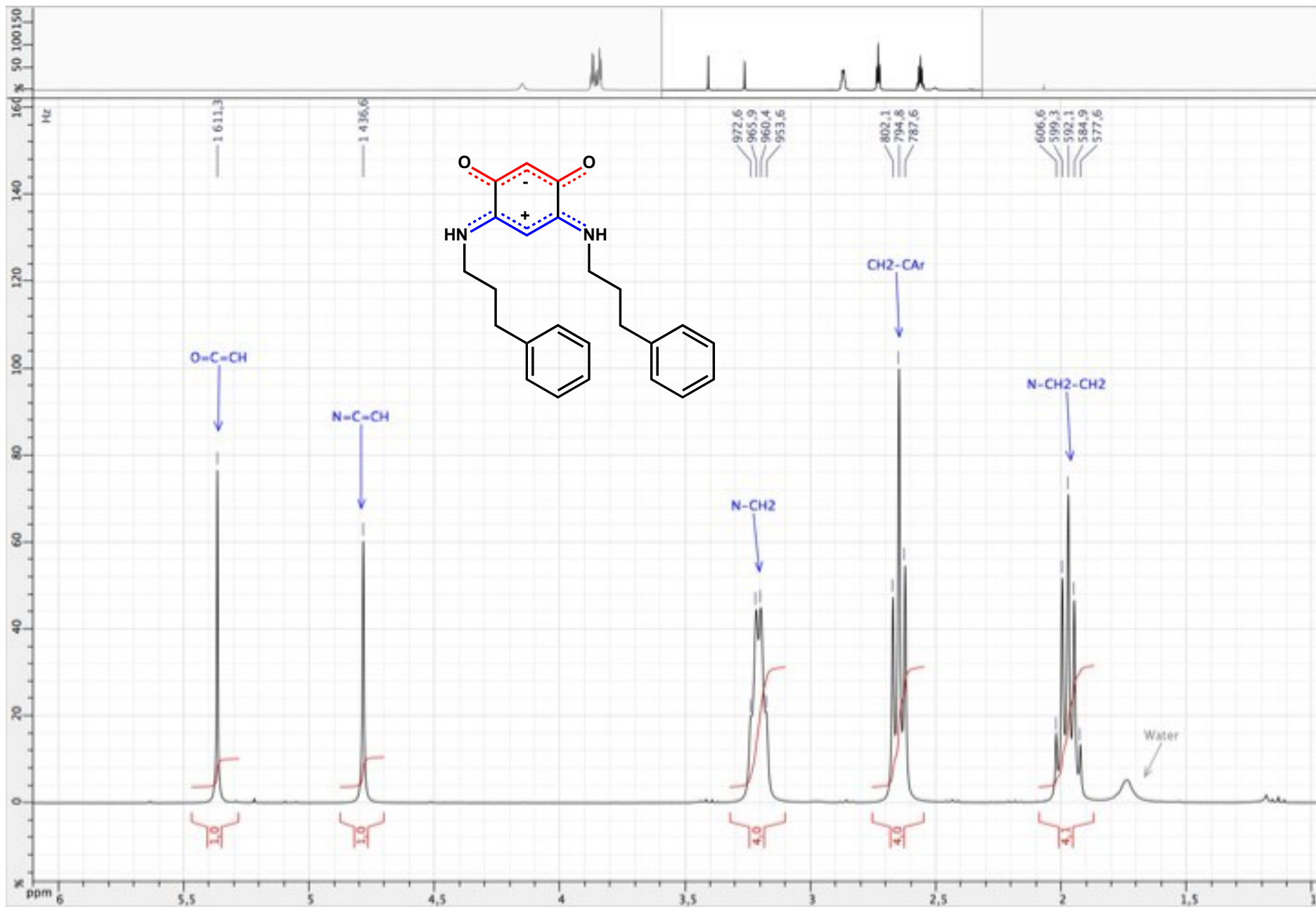


Figure S36. ^{13}C $\{^1\text{H}\}$ NMR spectrum of zwitterion 7 (CDCl_3 ; 125 MHz)

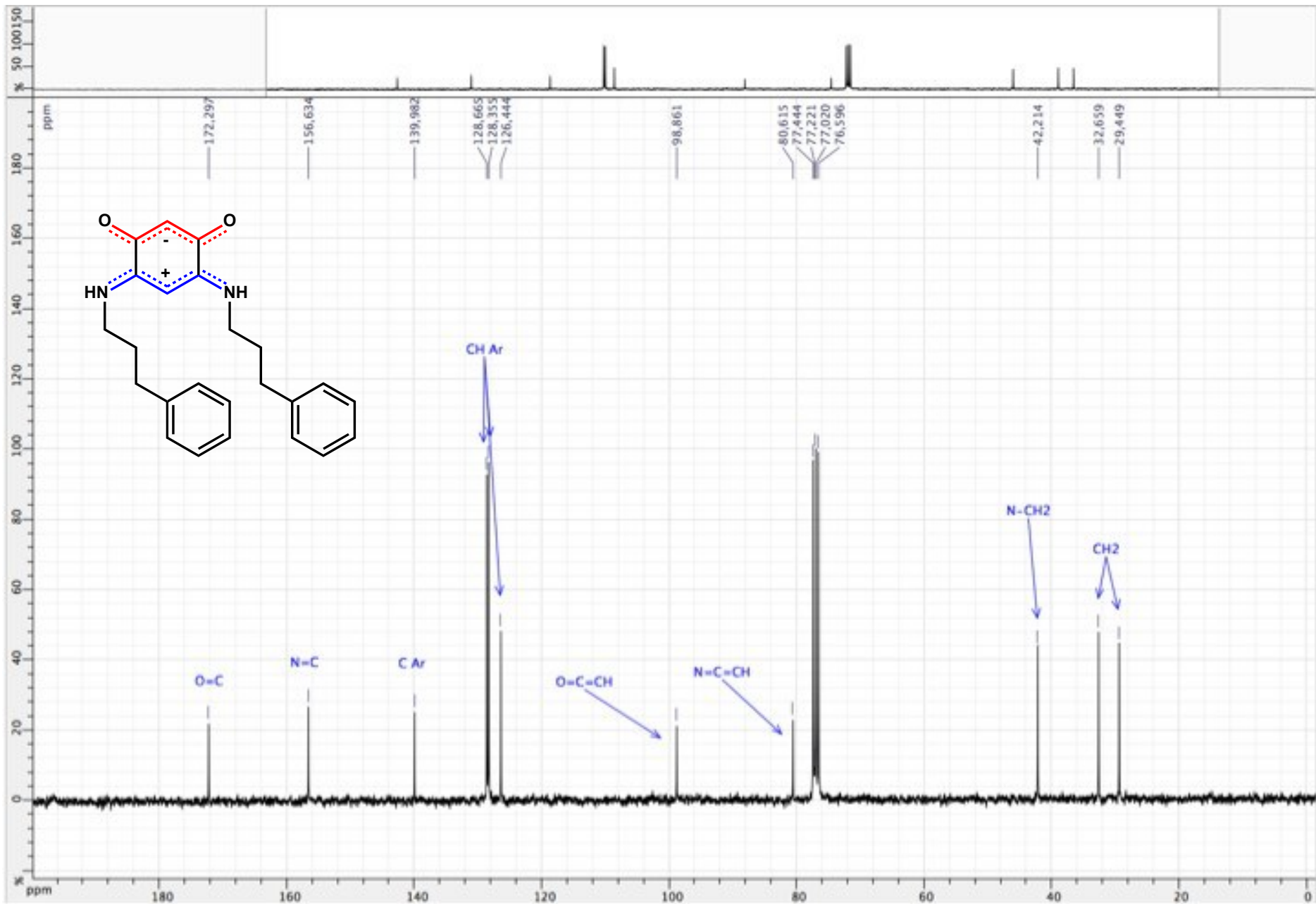


Figure S37. ^{13}C $\{^1\text{H}\}$ NMR spectrum of zwitterion 7 (CDCl_3 ; 125 MHz)

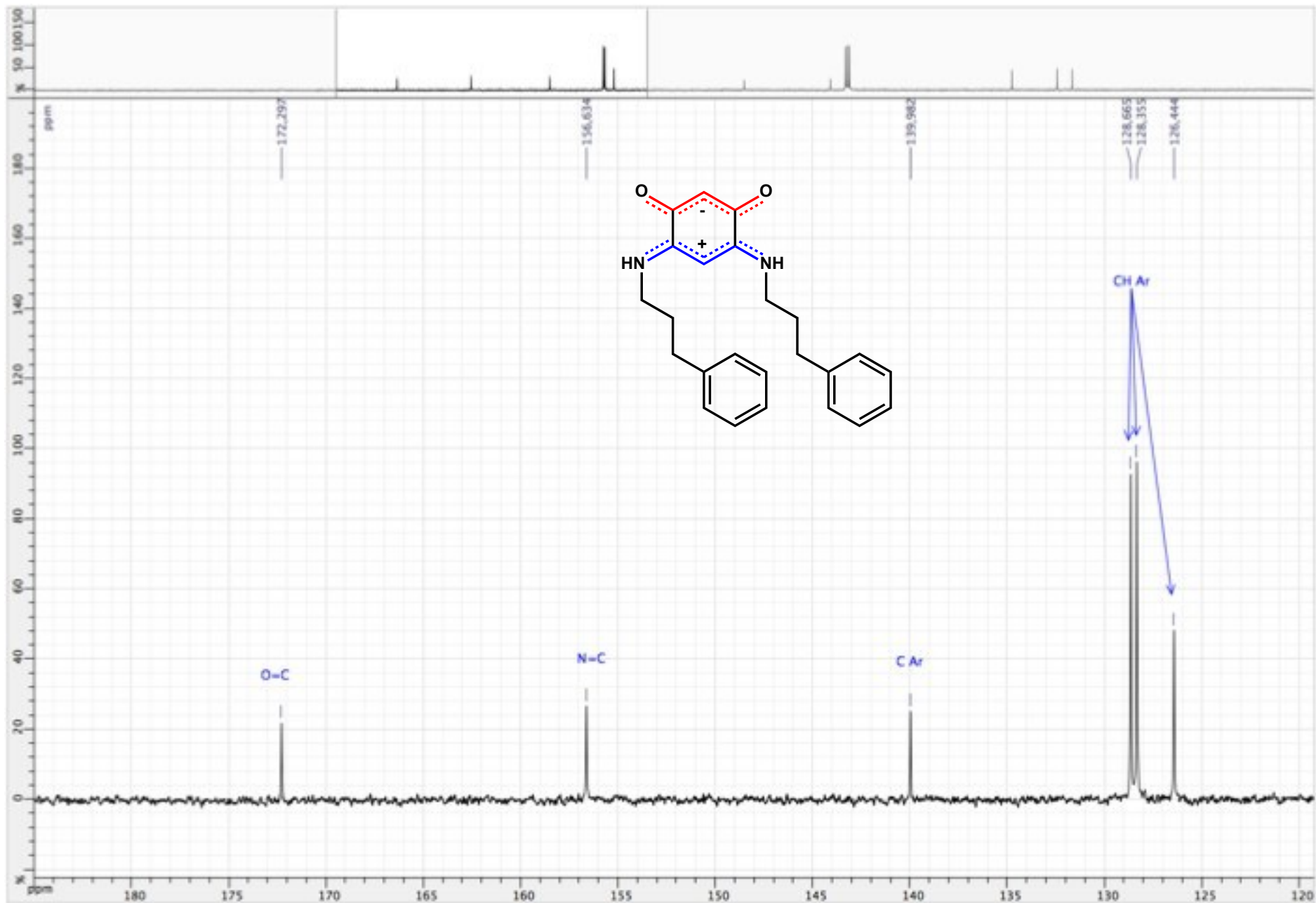


Figure S38. ^{13}C $\{^1\text{H}\}$ NMR spectrum of zwitterion 7 (CDCl_3 ; 125 MHz)

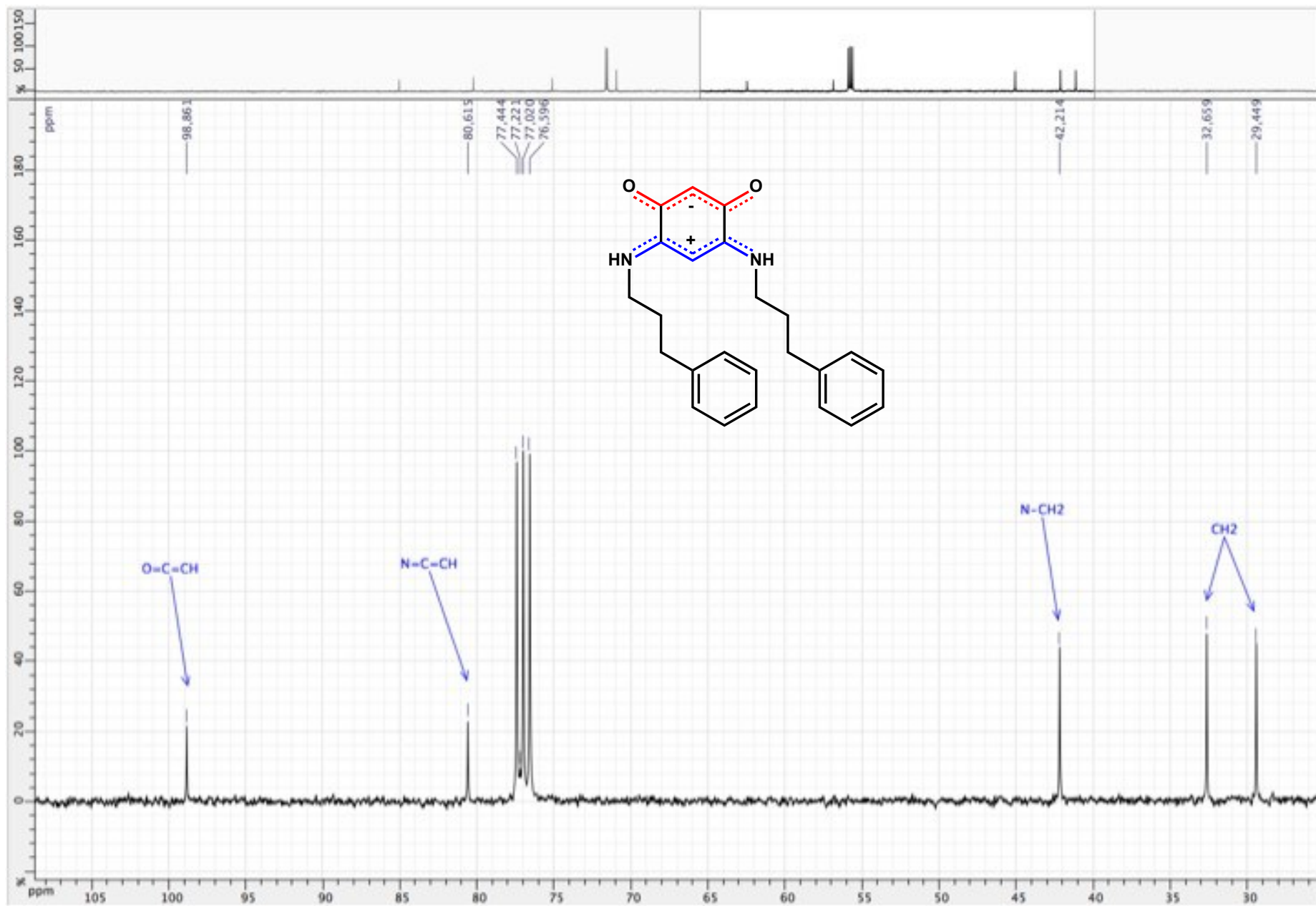


Figure S40. ^1H NMR spectrum of zwitterion **8** (CDCl_3 ; 500 MHz)

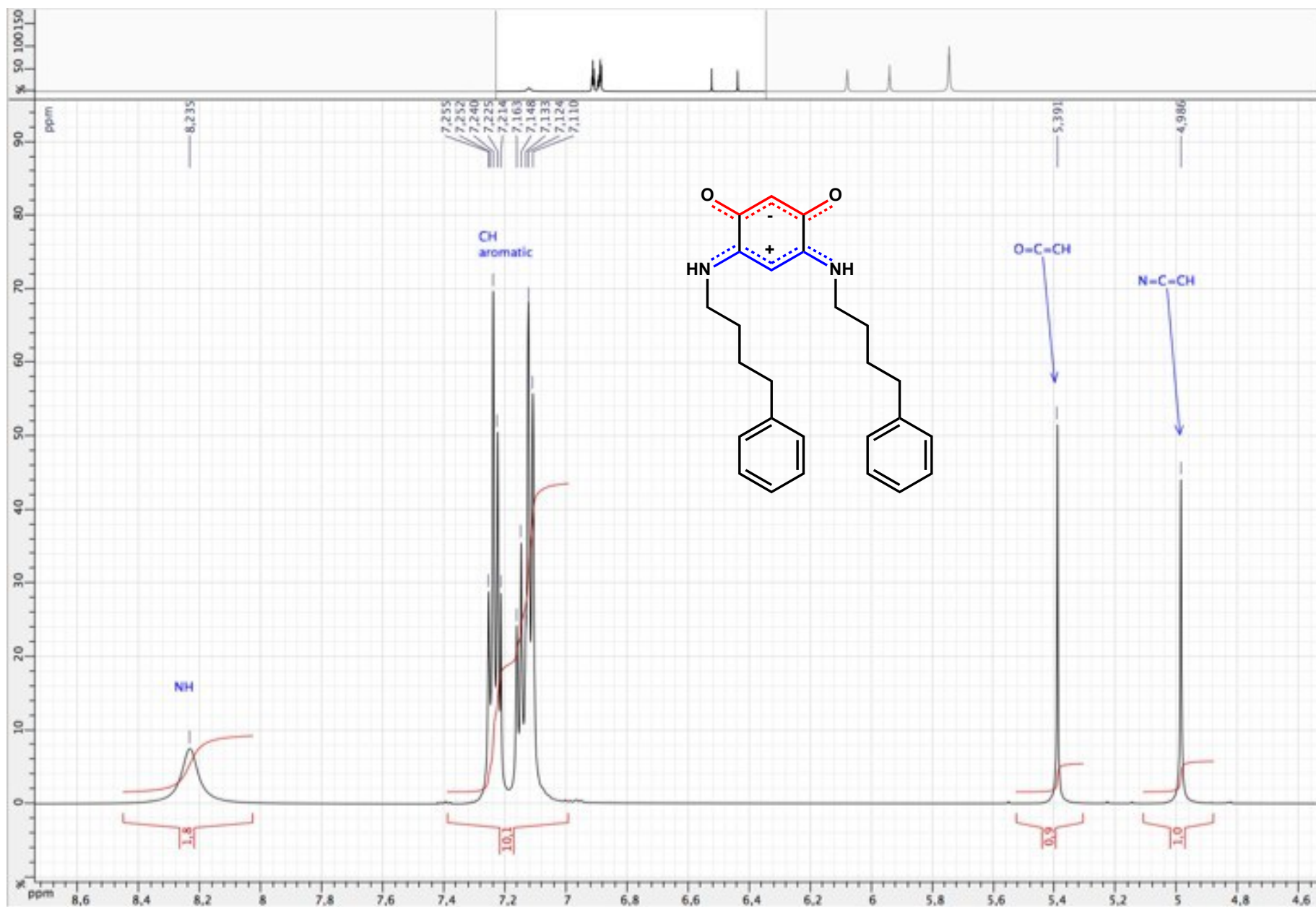


Figure S41. ^1H NMR spectrum of zwitterion **8** (CDCl_3 ; 500 MHz)

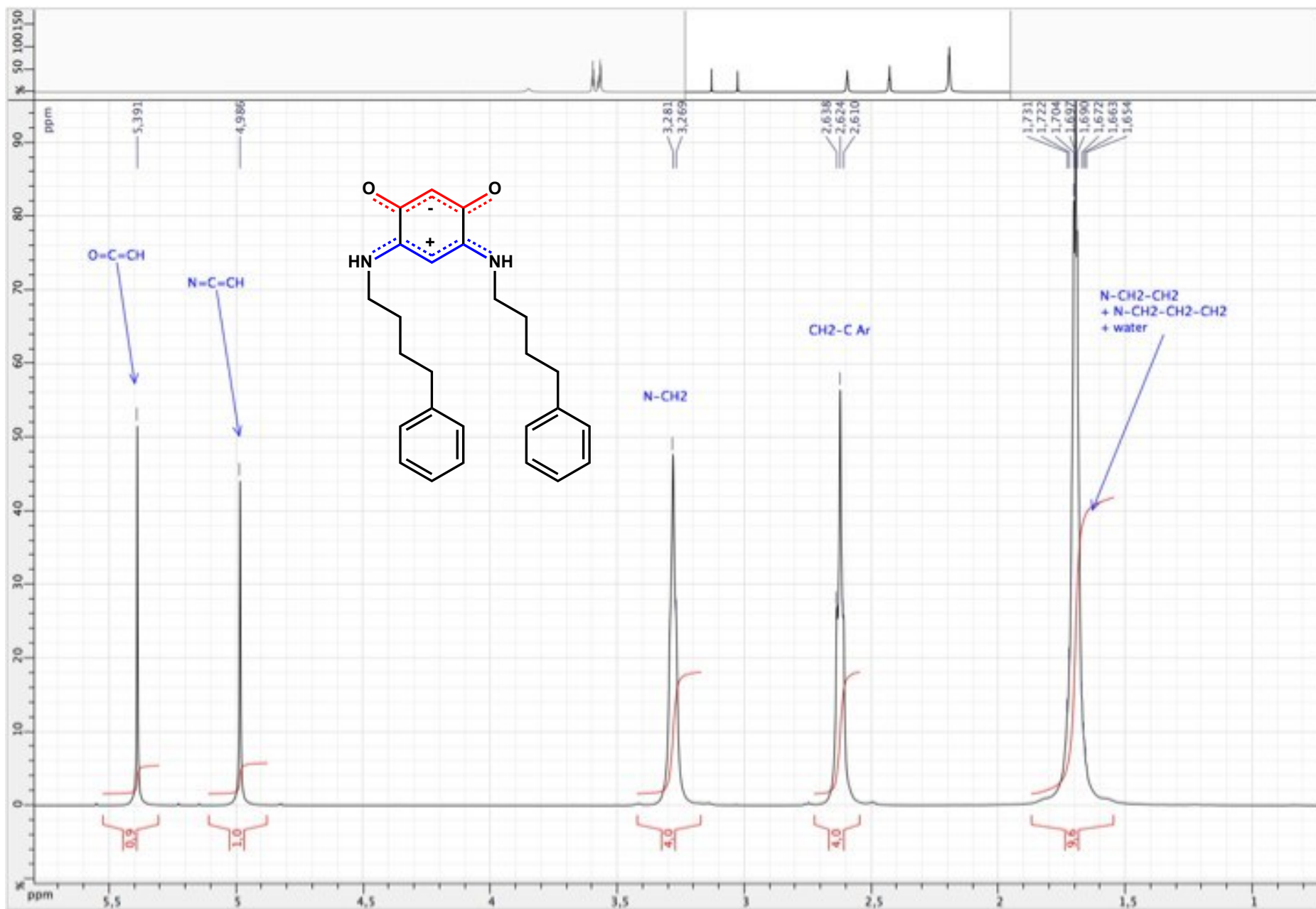


Figure S42. ^{13}C $\{^1\text{H}\}$ NMR spectrum of zwitterion **8** (CDCl_3 ; 125 MHz)

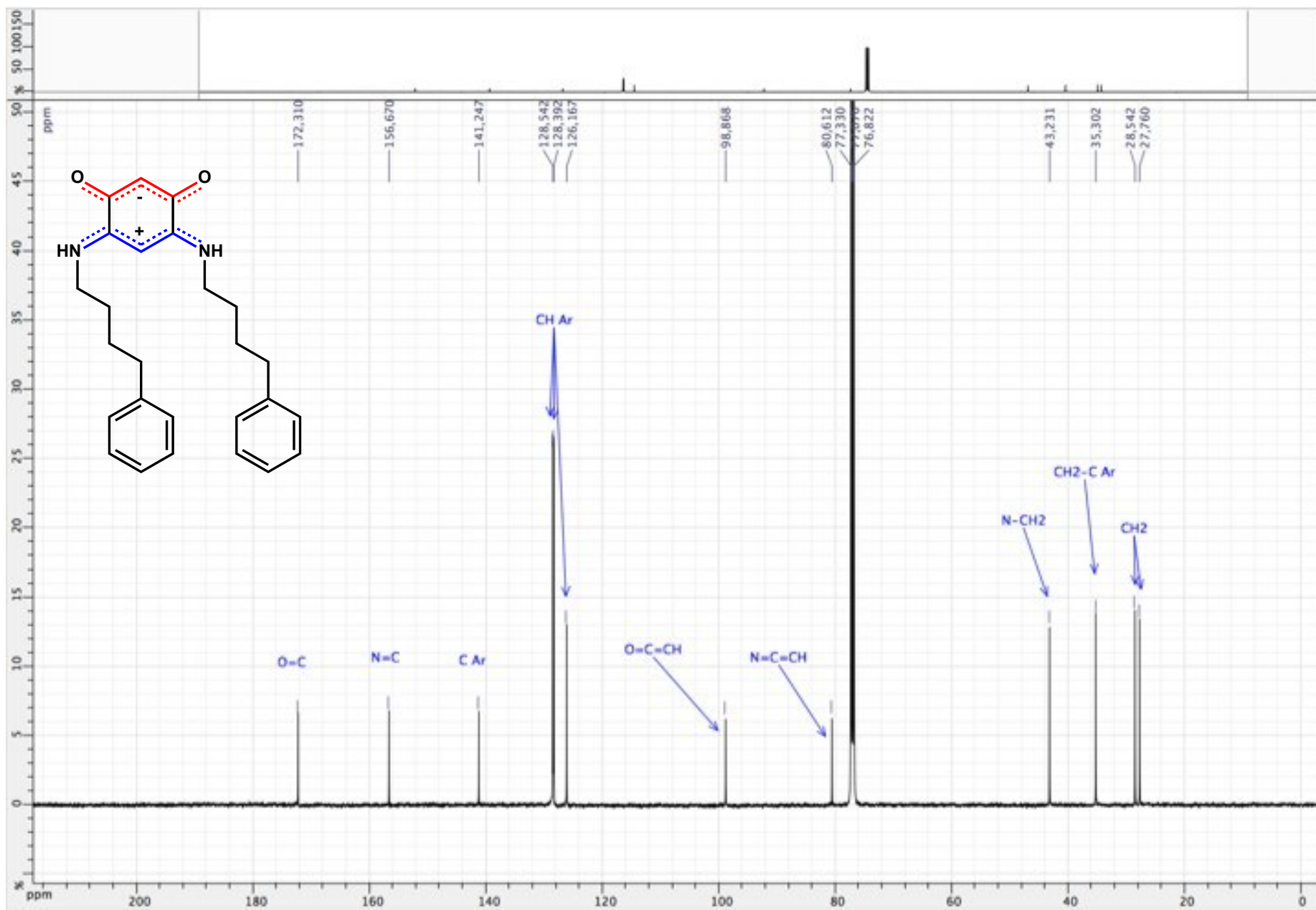


Figure S43. ^{13}C $\{^1\text{H}\}$ NMR spectrum of zwitterion **8** (CDCl_3 ; 125 MHz)

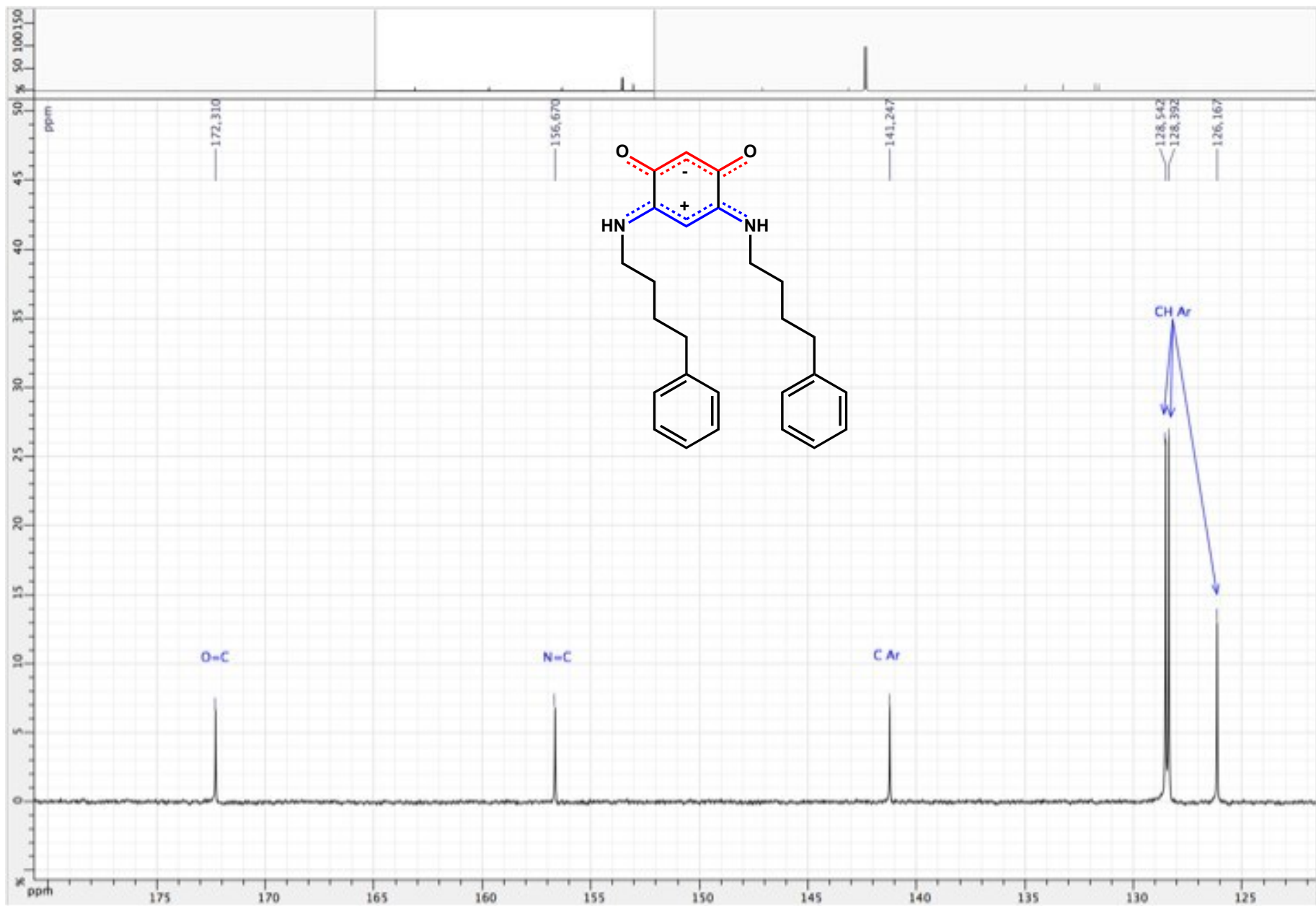


Figure S44. ^{13}C $\{^1\text{H}\}$ NMR spectrum of zwitterion **8** (CDCl_3 ; 125 MHz)

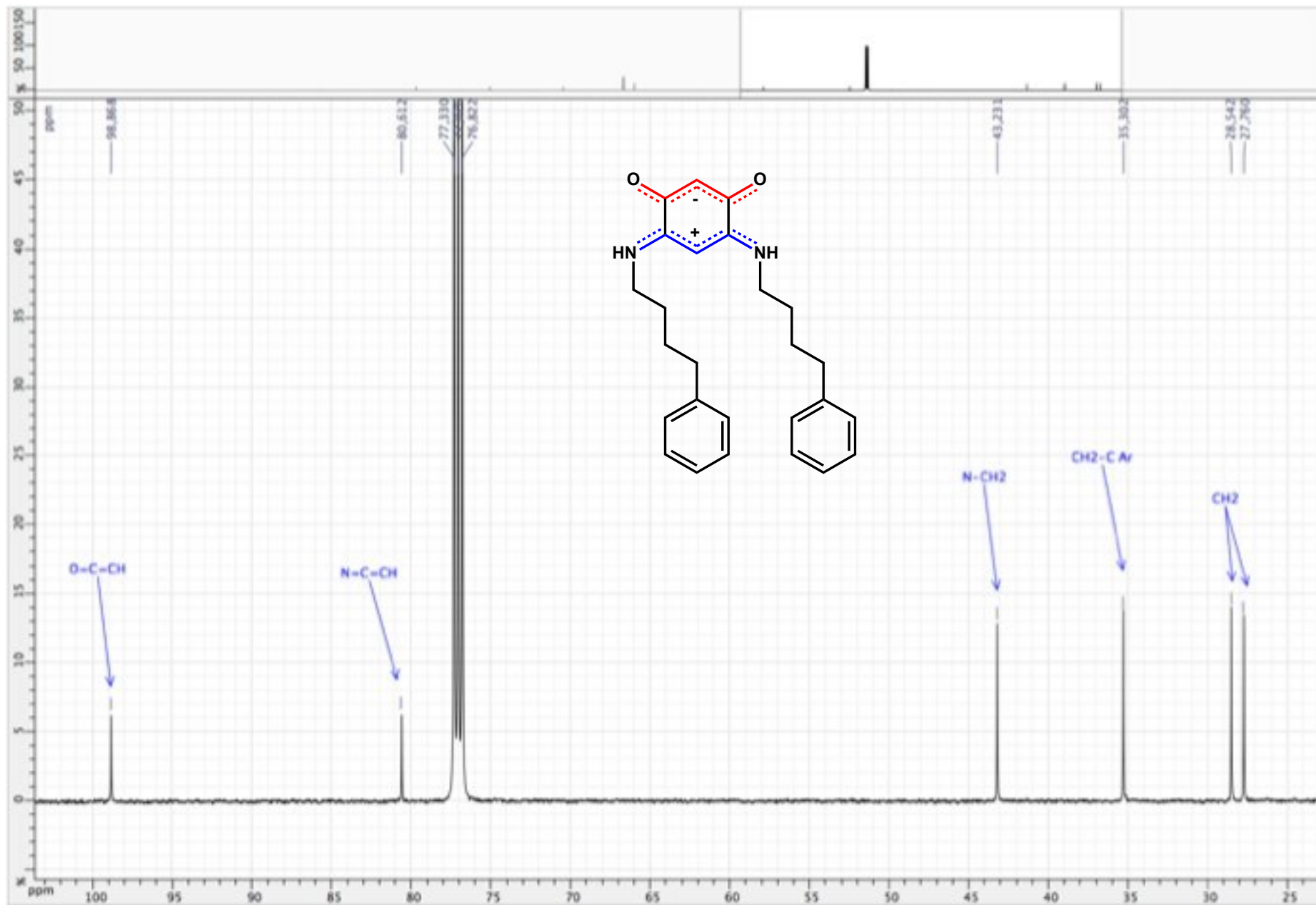


Figure S45. HSQC ($^1\text{H} / ^{13}\text{C} \{^1\text{H}\}$) spectrum of zwitterion **8** (CDCl_3 ; 500 / 125 MHz)

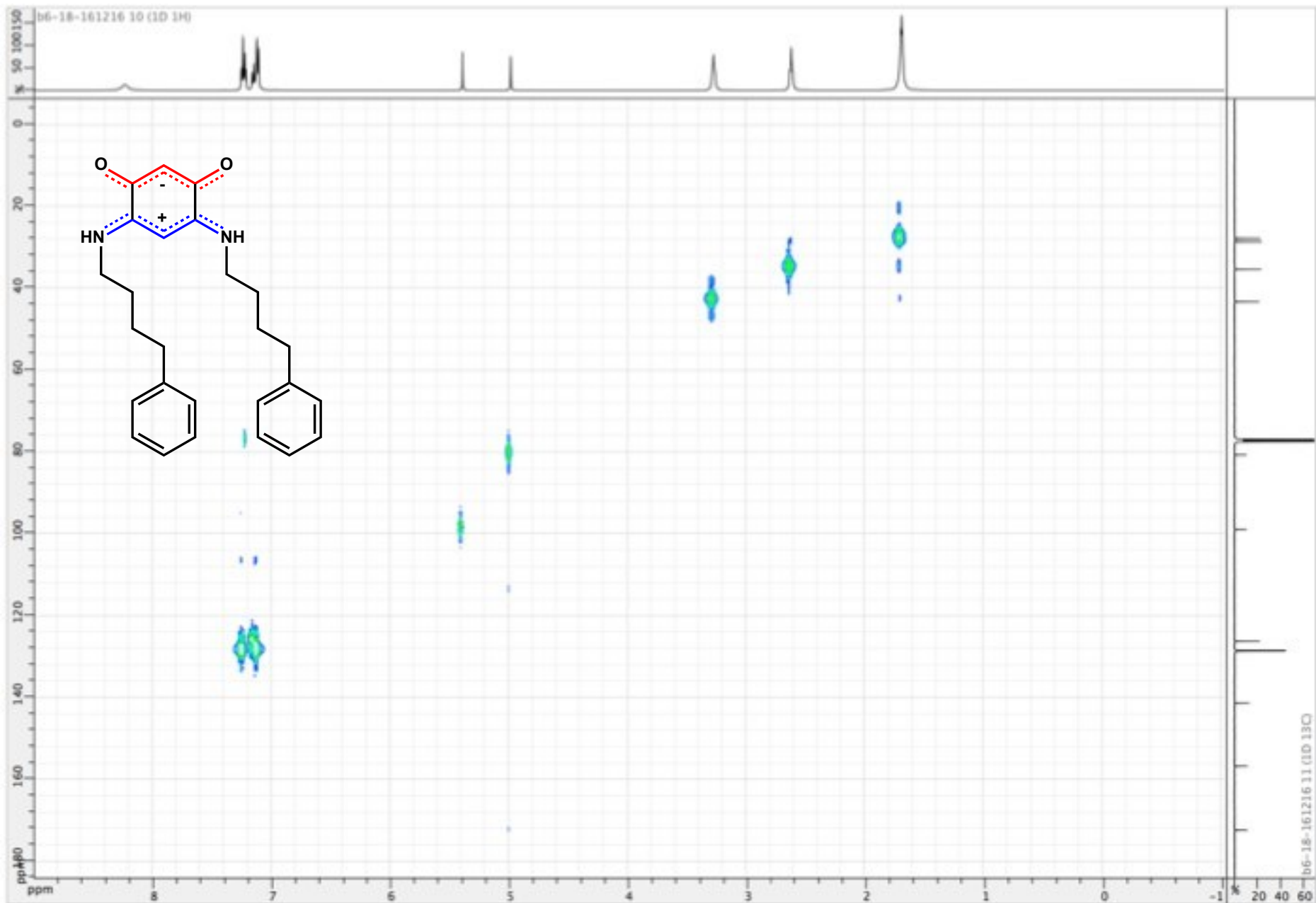


Figure S46. COSY ($^1\text{H} / ^1\text{H}$) spectrum of zwitterion **8** (CDCl_3 ; 500 MHz)

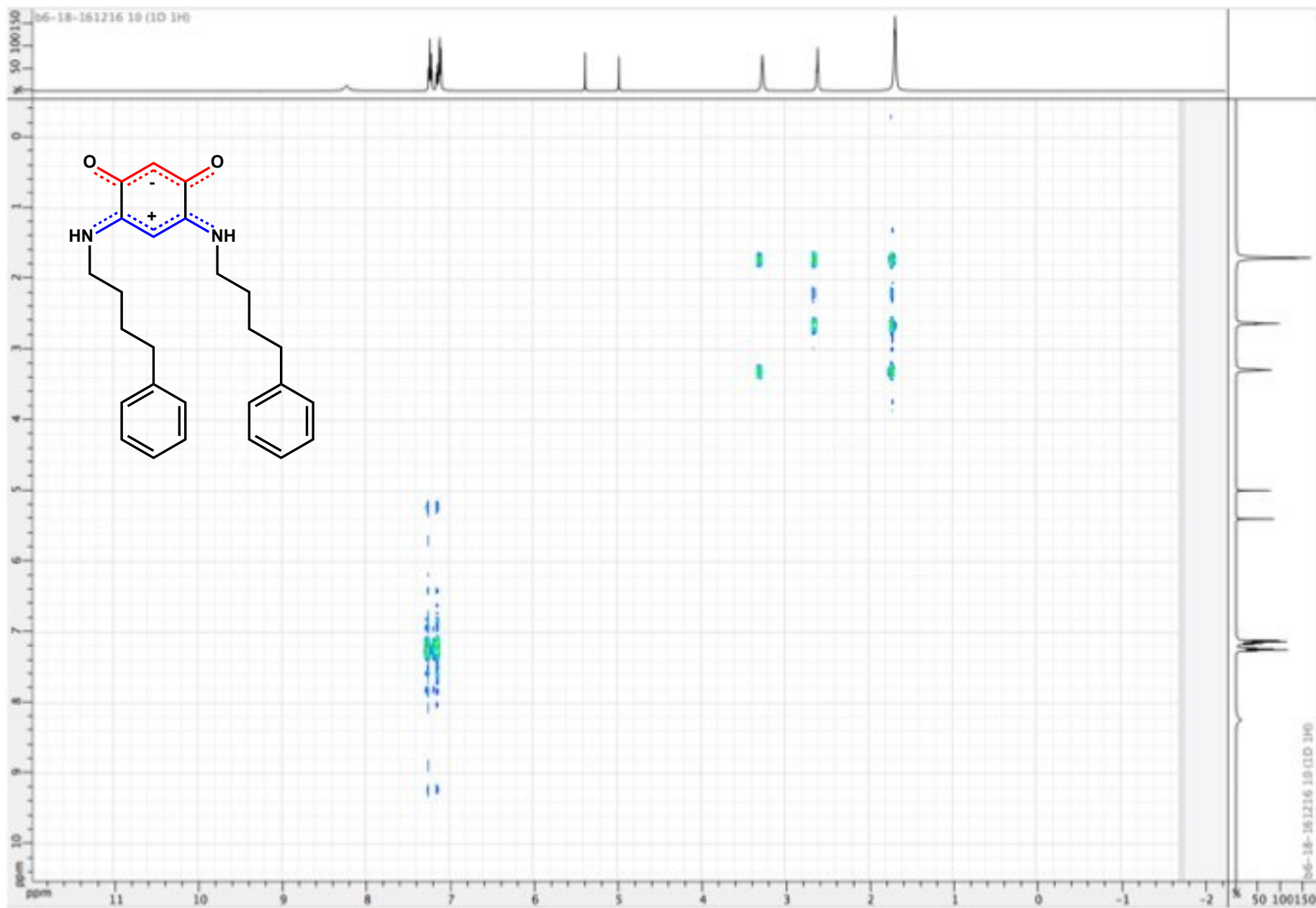


Figure S47. ^1H NMR spectrum of zwitterion **9** (CDCl_3 ; 500 MHz)

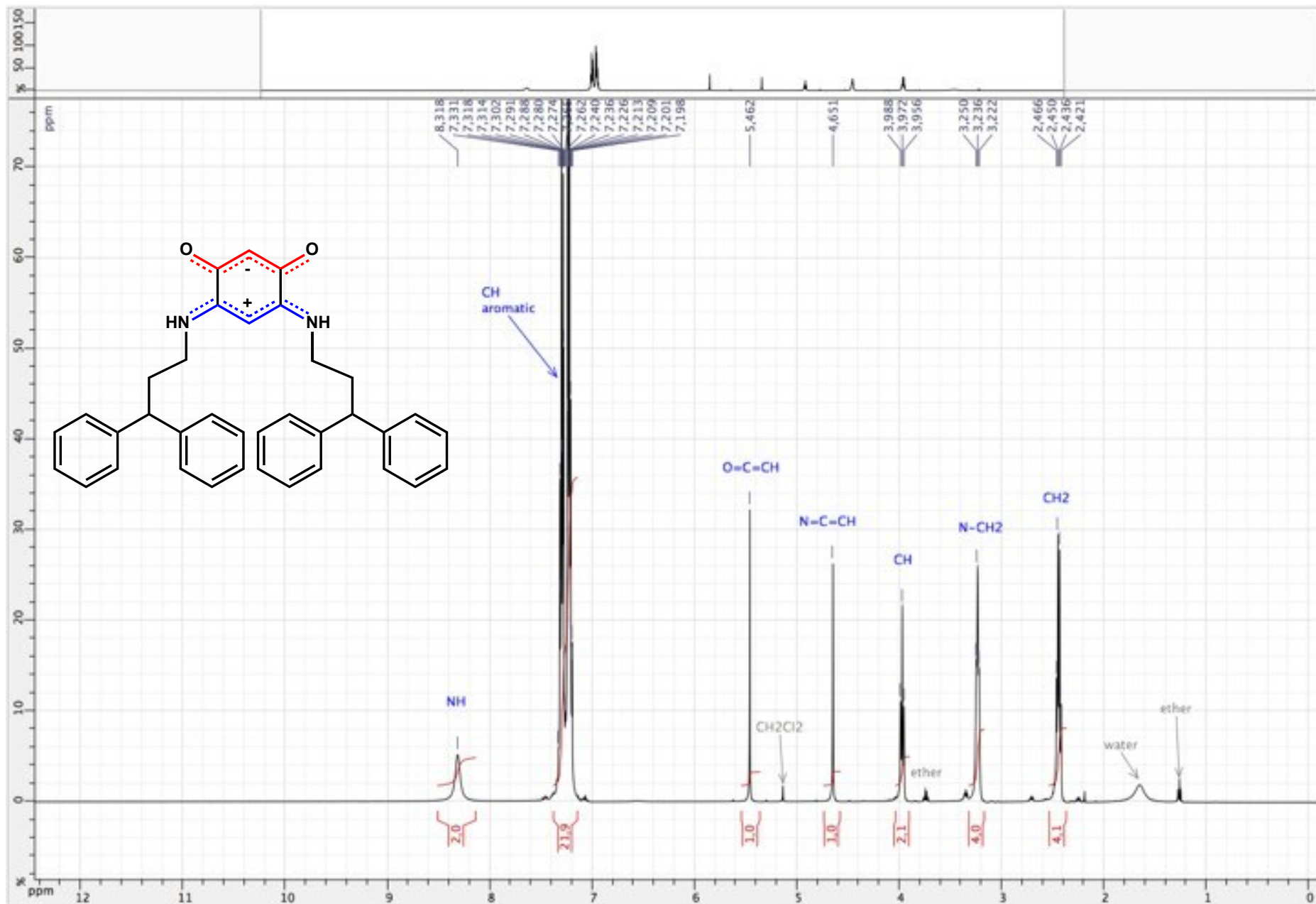


Figure S48. ^1H NMR spectrum of zwitterion **9** (CDCl_3 ; 500 MHz)

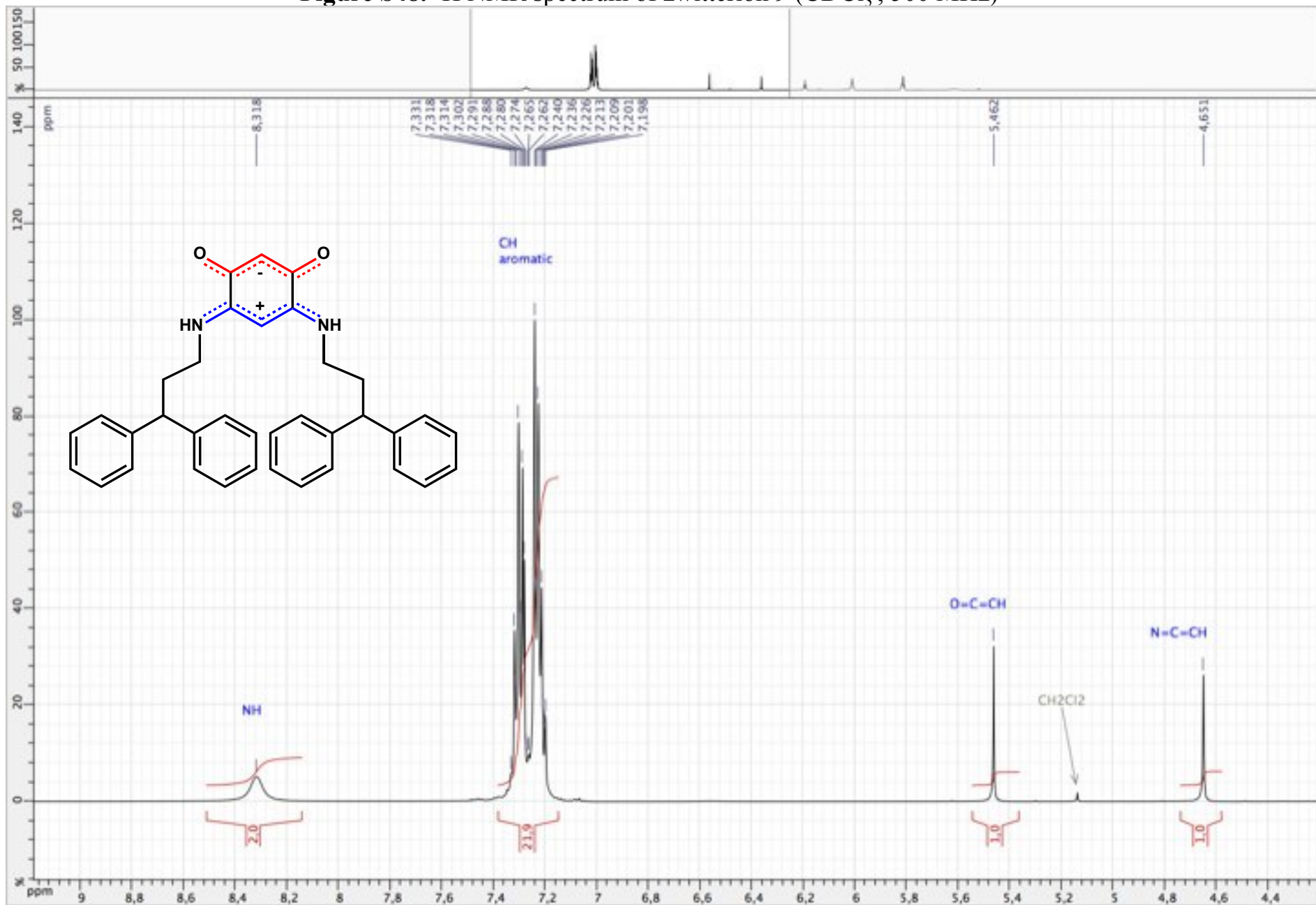


Figure S49. ^1H NMR spectrum of zwitterion **9** (CDCl_3 ; 500 MHz)

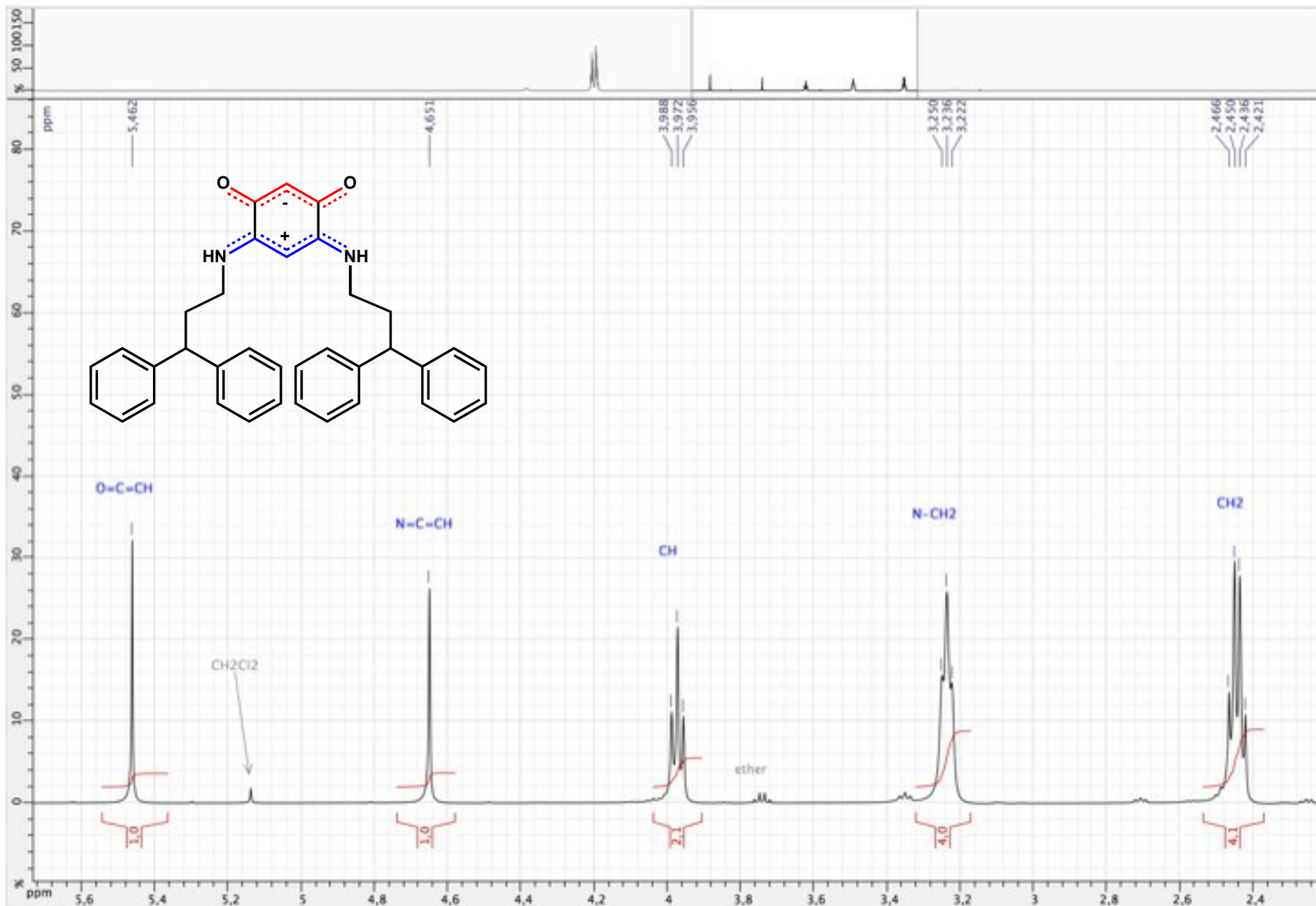


Figure S50. ^1H NMR spectrum of zwitterion **9** (CDCl_3 ; 500 MHz)

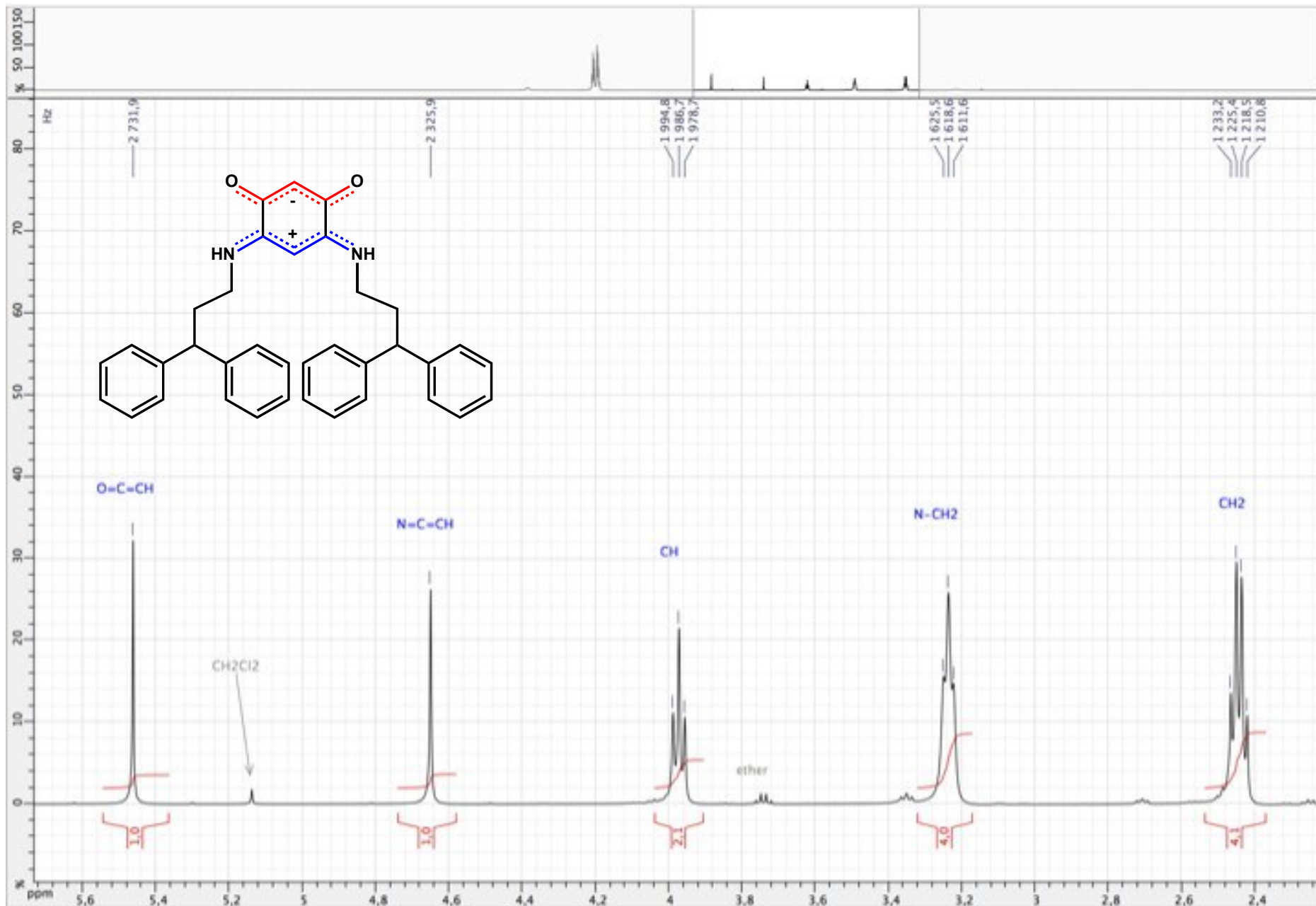


Figure S51. ^{13}C $\{^1\text{H}\}$ NMR spectrum of zwitterion **9** (CDCl_3 ; 125 MHz)

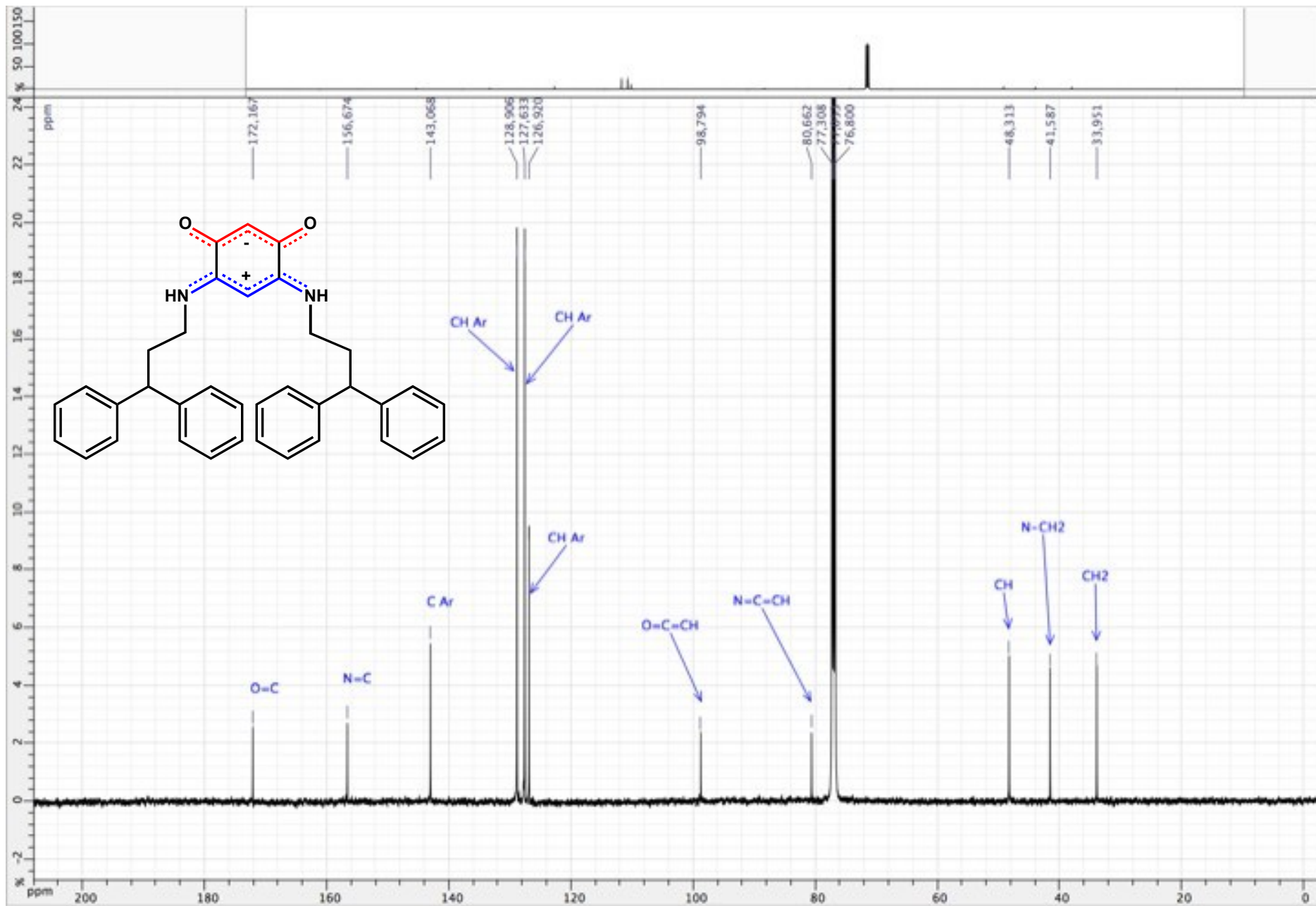


Figure S52. ^{13}C $\{^1\text{H}\}$ NMR spectrum of zwitterion **9** (CDCl_3 ; 125 MHz)

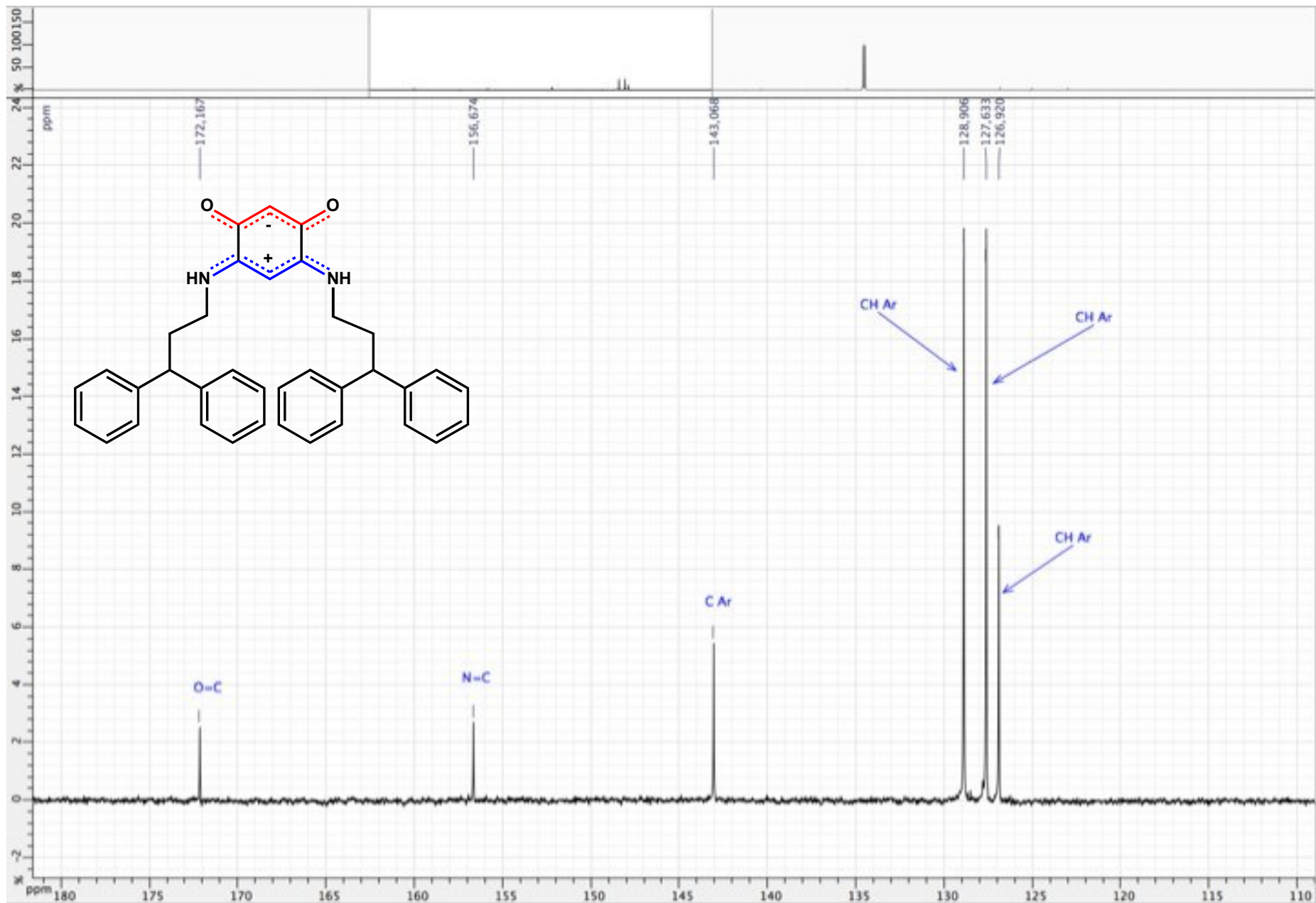


Figure S53. ^{13}C $\{^1\text{H}\}$ NMR spectrum of zwitterion **9** (CDCl_3 ; 125 MHz)

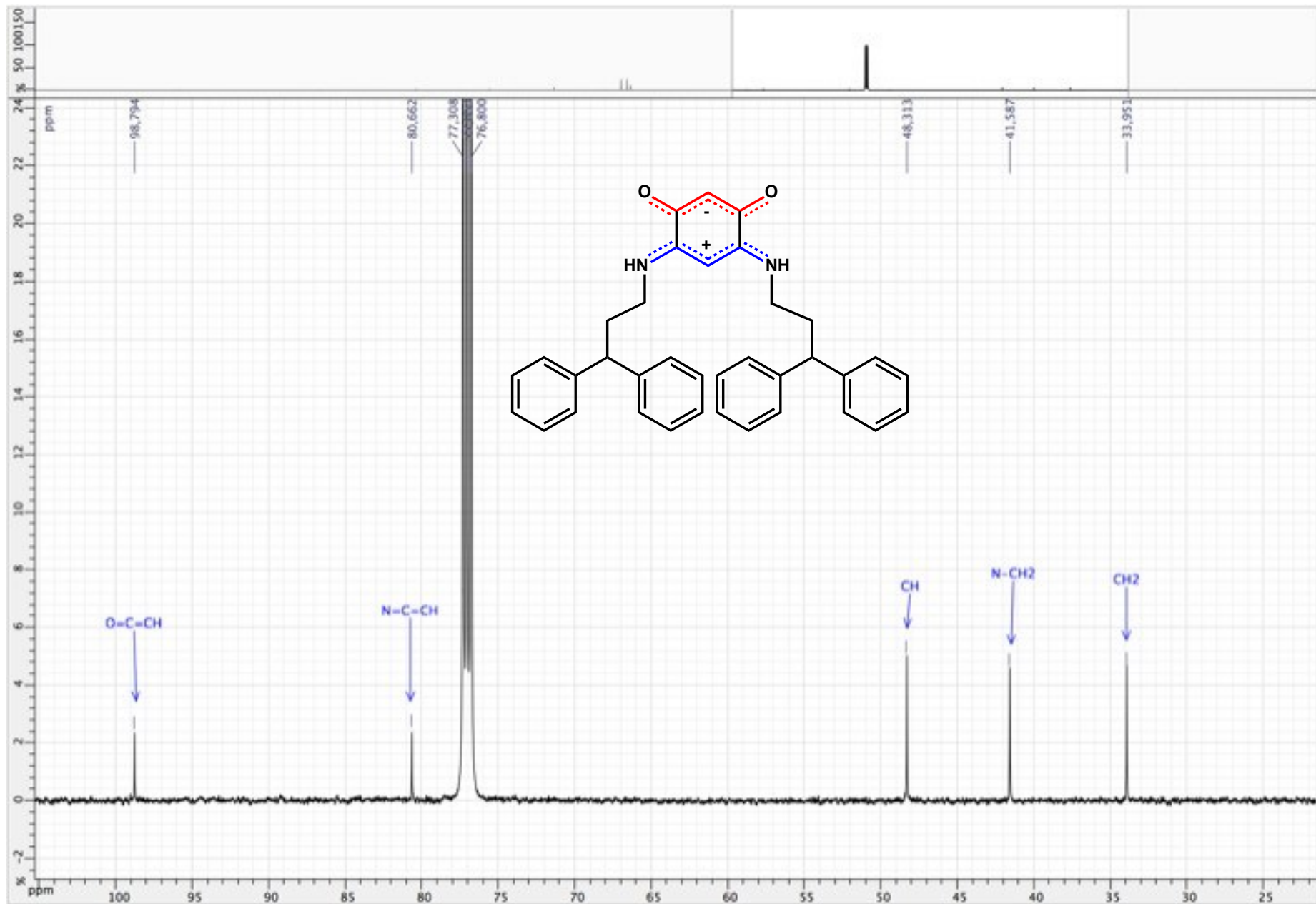


Figure S54. HSQC ($^1\text{H} / ^{13}\text{C} \{^1\text{H}\}$) spectrum of zwitterion **9** (CDCl_3 ; 500 / 125 MHz)

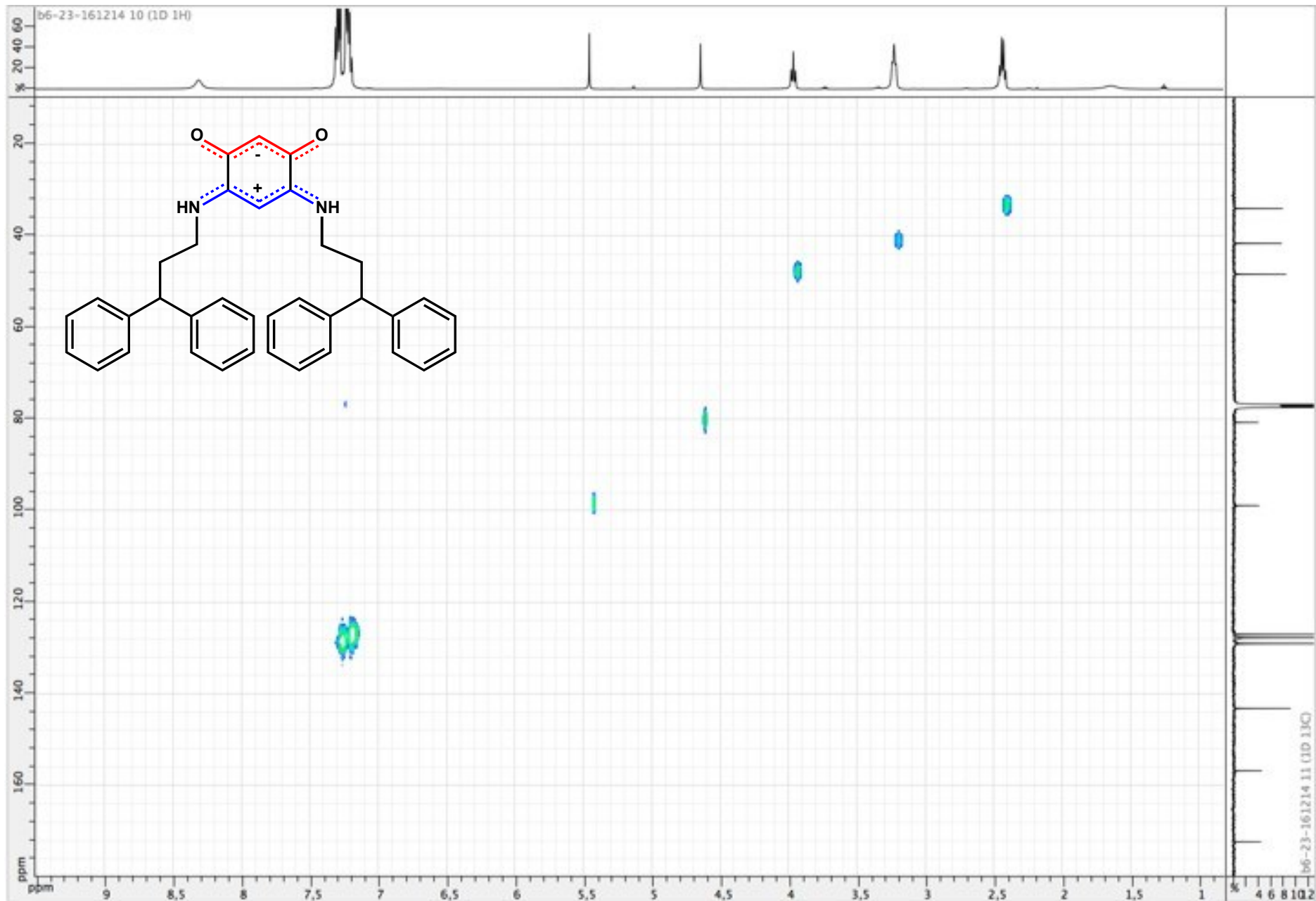


Figure S55. COSY ($^1\text{H} / ^1\text{H}$) spectrum of zwitterion **9** (CDCl_3 ; 500 MHz)

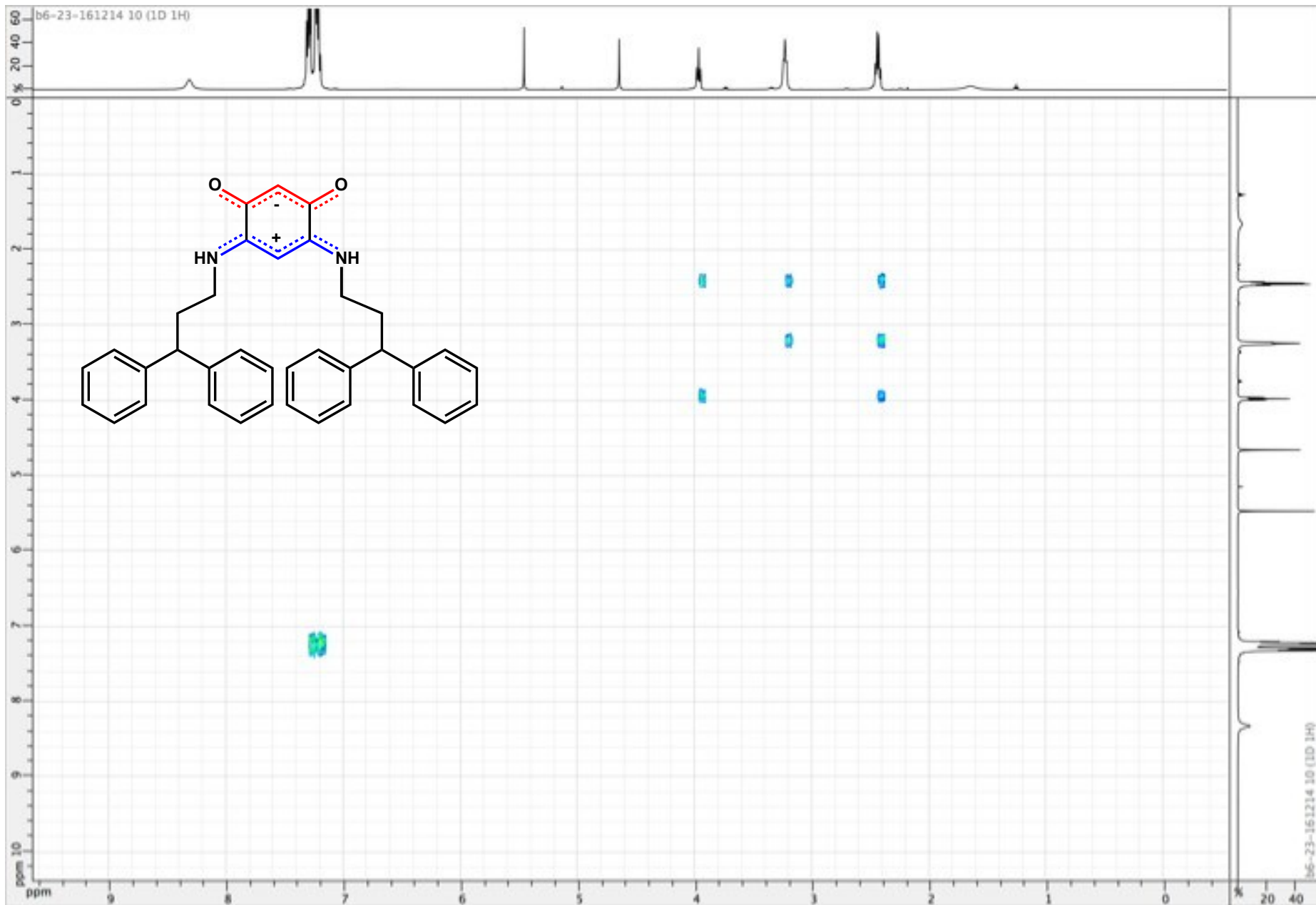


Figure S56. ^1H NMR spectrum of zwitterion **10** (CDCl_3 ; 500 MHz)

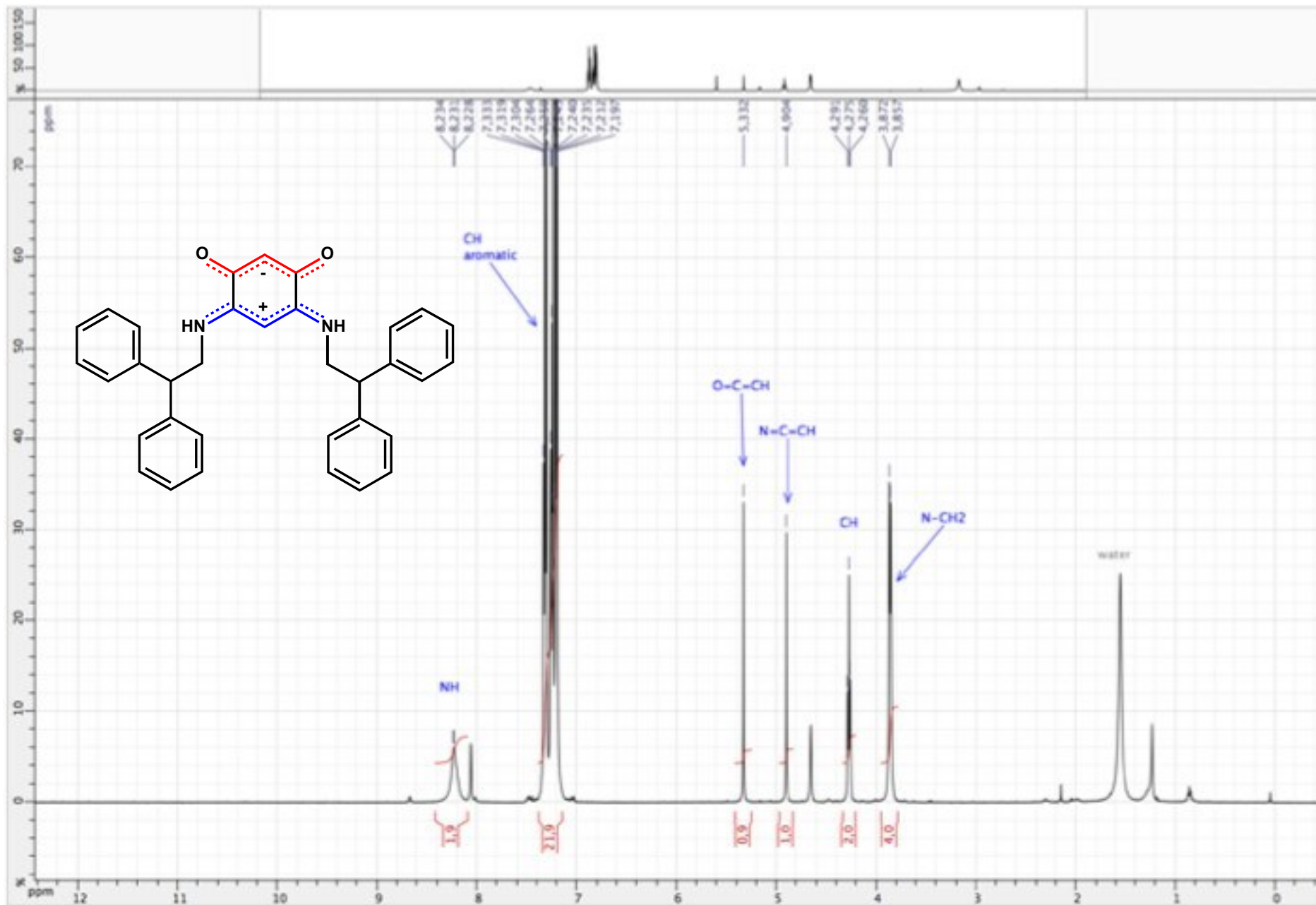


Figure S57. ^1H NMR spectrum of zwitterion **10** (CDCl_3 ; 500 MHz)

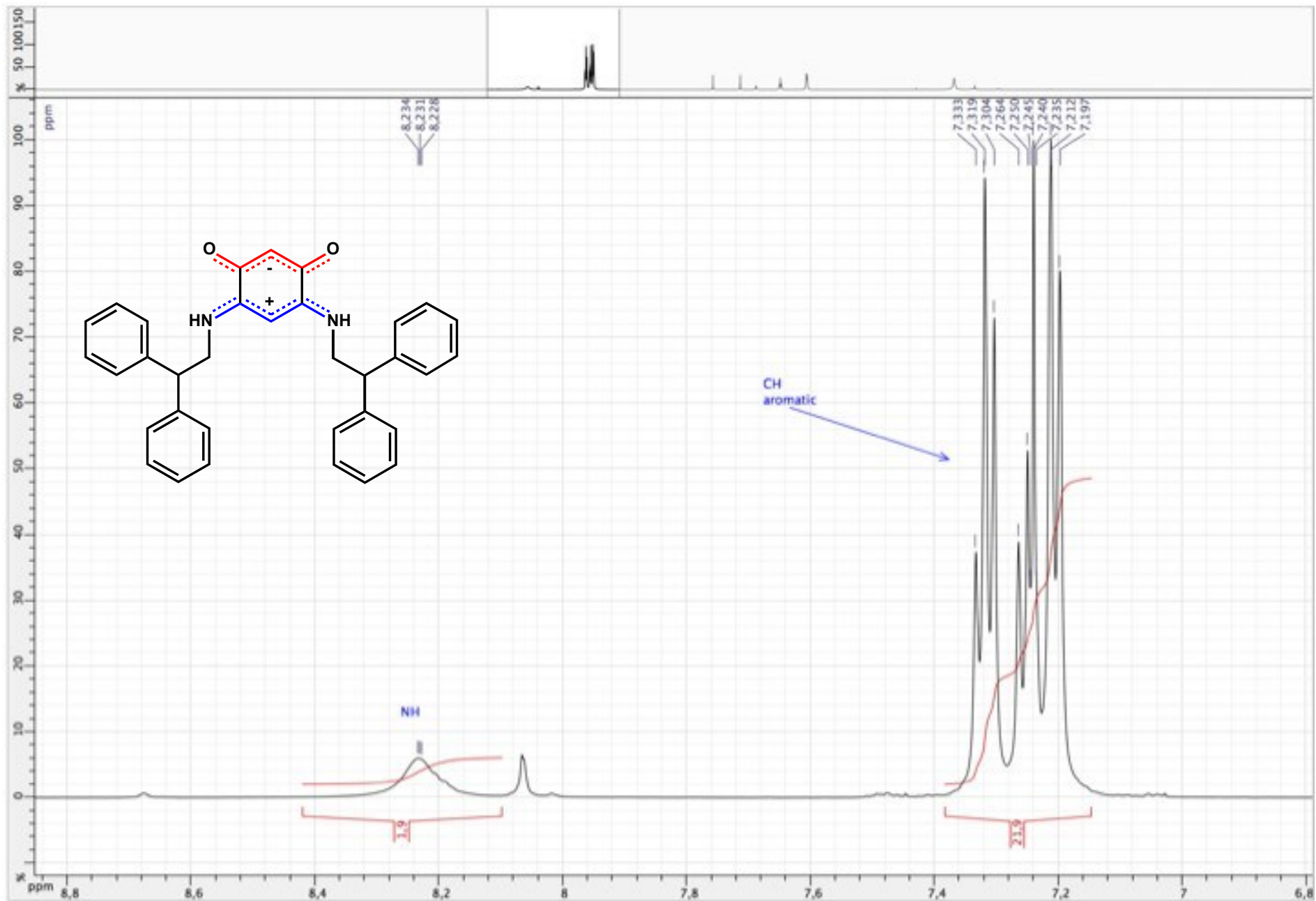


Figure S58. ^1H NMR spectrum of zwitterion **10** (CDCl_3 ; 500 MHz)

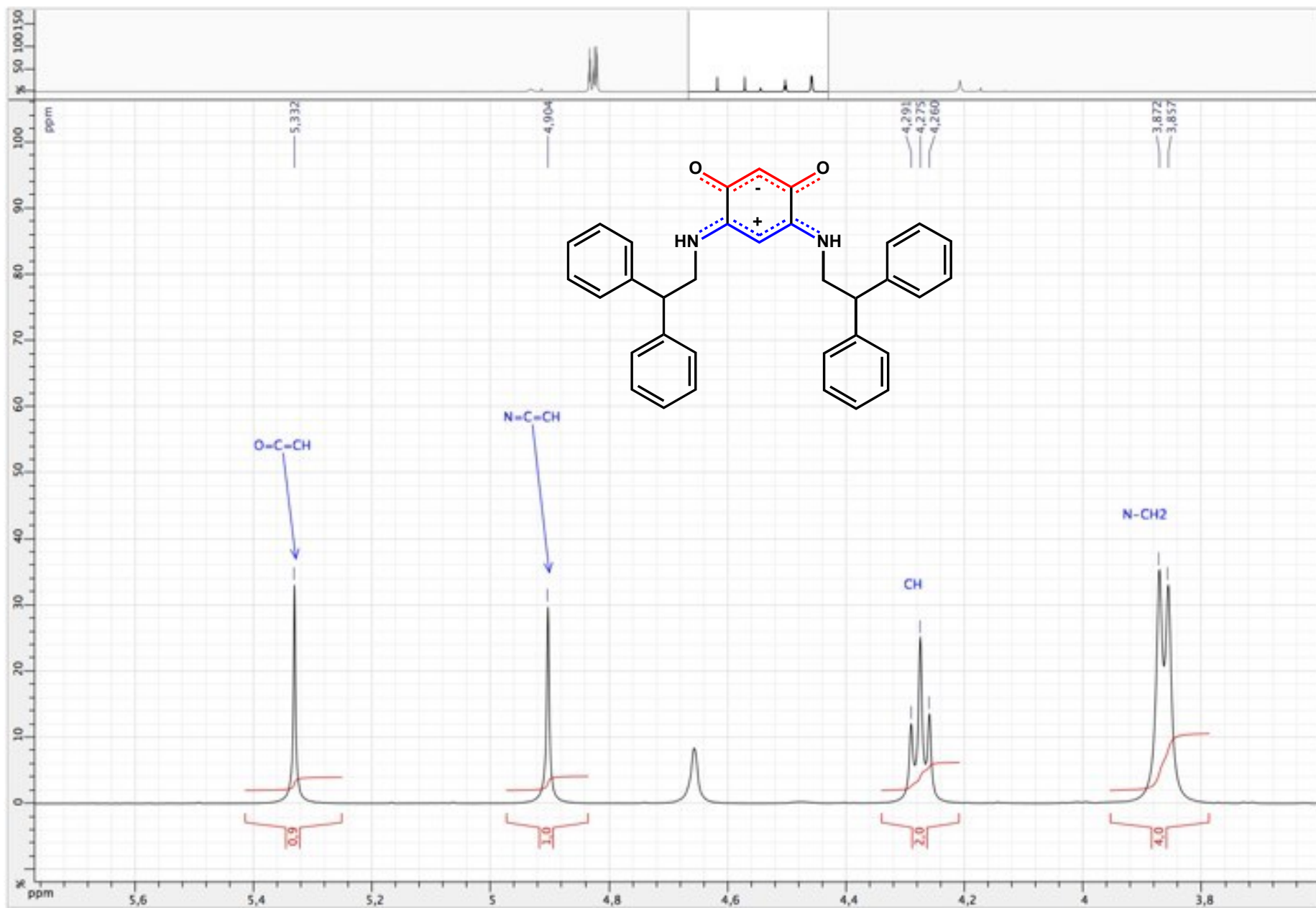


Figure S59. ^1H NMR spectrum of zwitterion **10** (CDCl_3 ; 500 MHz)

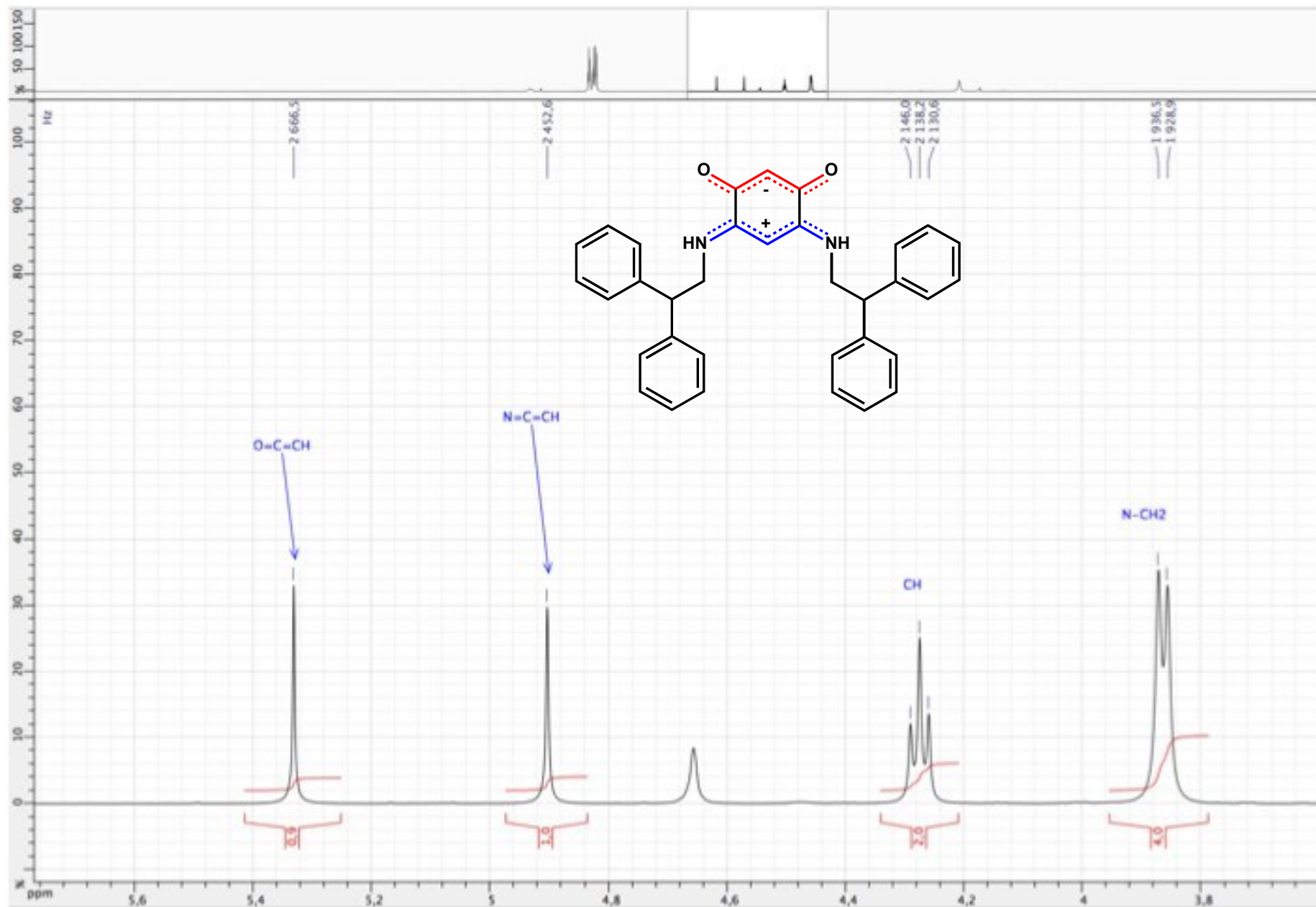


Figure S60. ^{13}C $\{^1\text{H}\}$ NMR spectrum of zwitterion **10** (CDCl_3 ; 125 MHz)

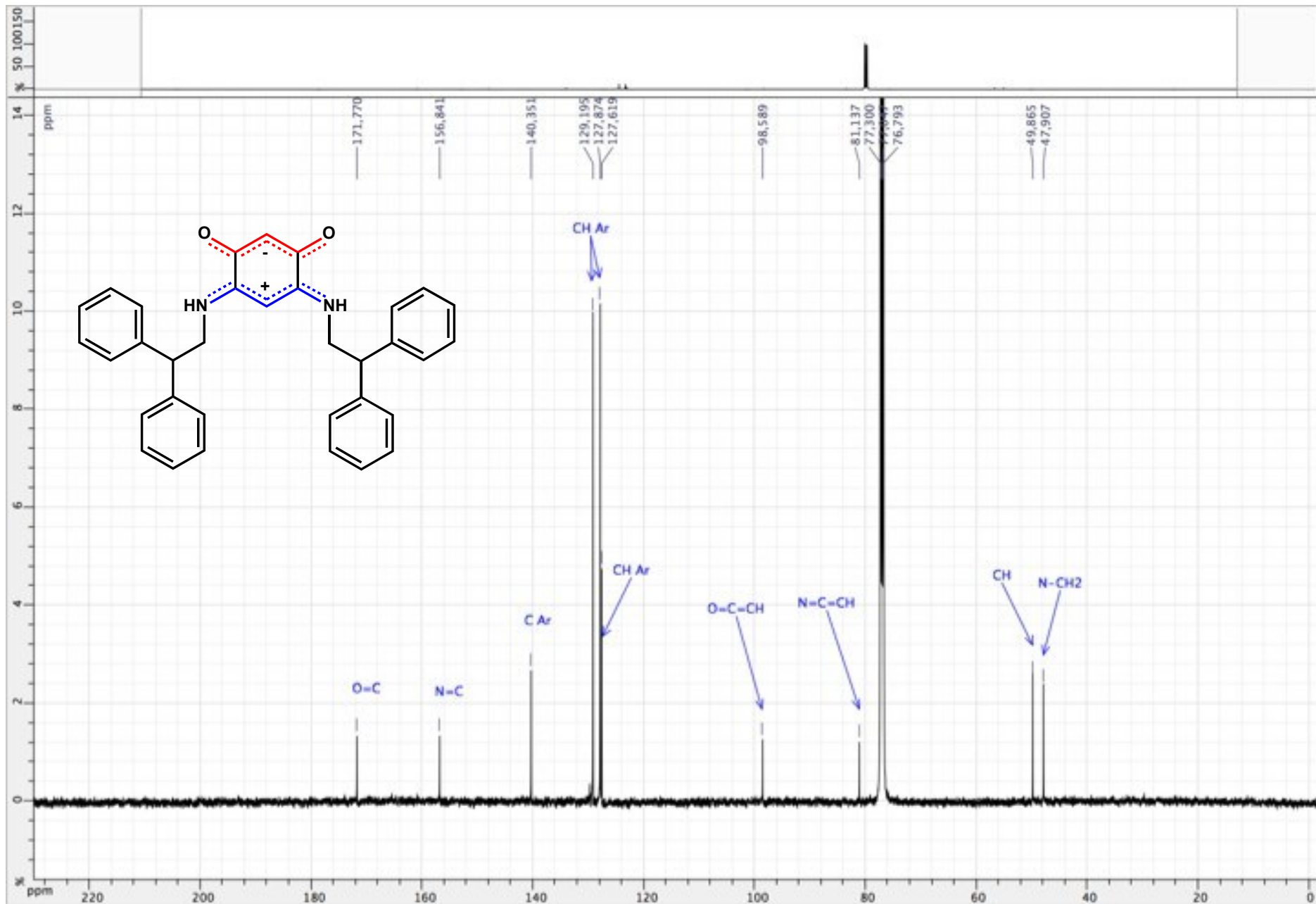


Figure S61. ^{13}C $\{^1\text{H}\}$ NMR spectrum of zwitterion **10** (CDCl_3 ; 125 MHz)

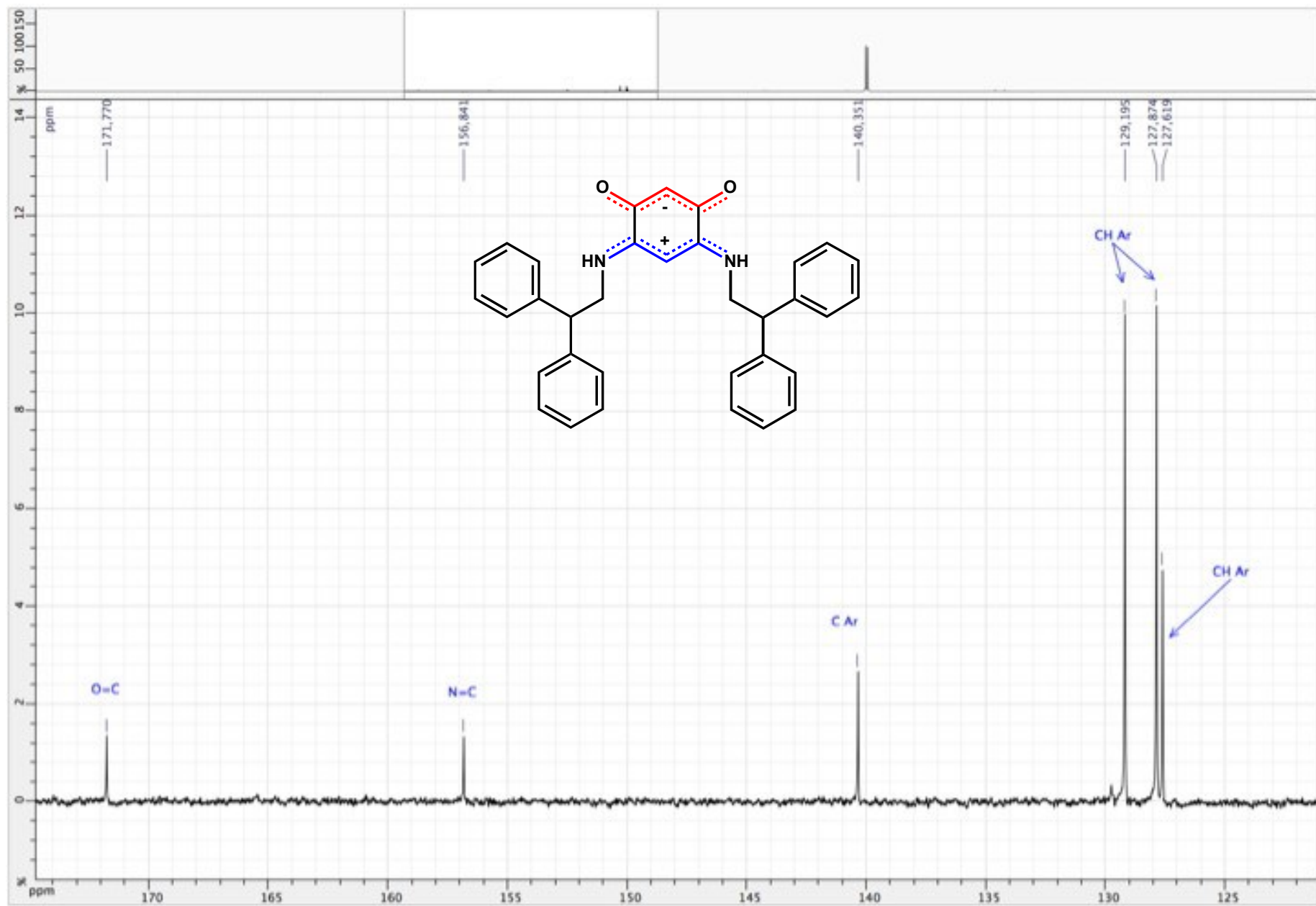


Figure S62. ^{13}C $\{^1\text{H}\}$ NMR spectrum of zwitterion **10** (CDCl_3 ; 125 MHz)

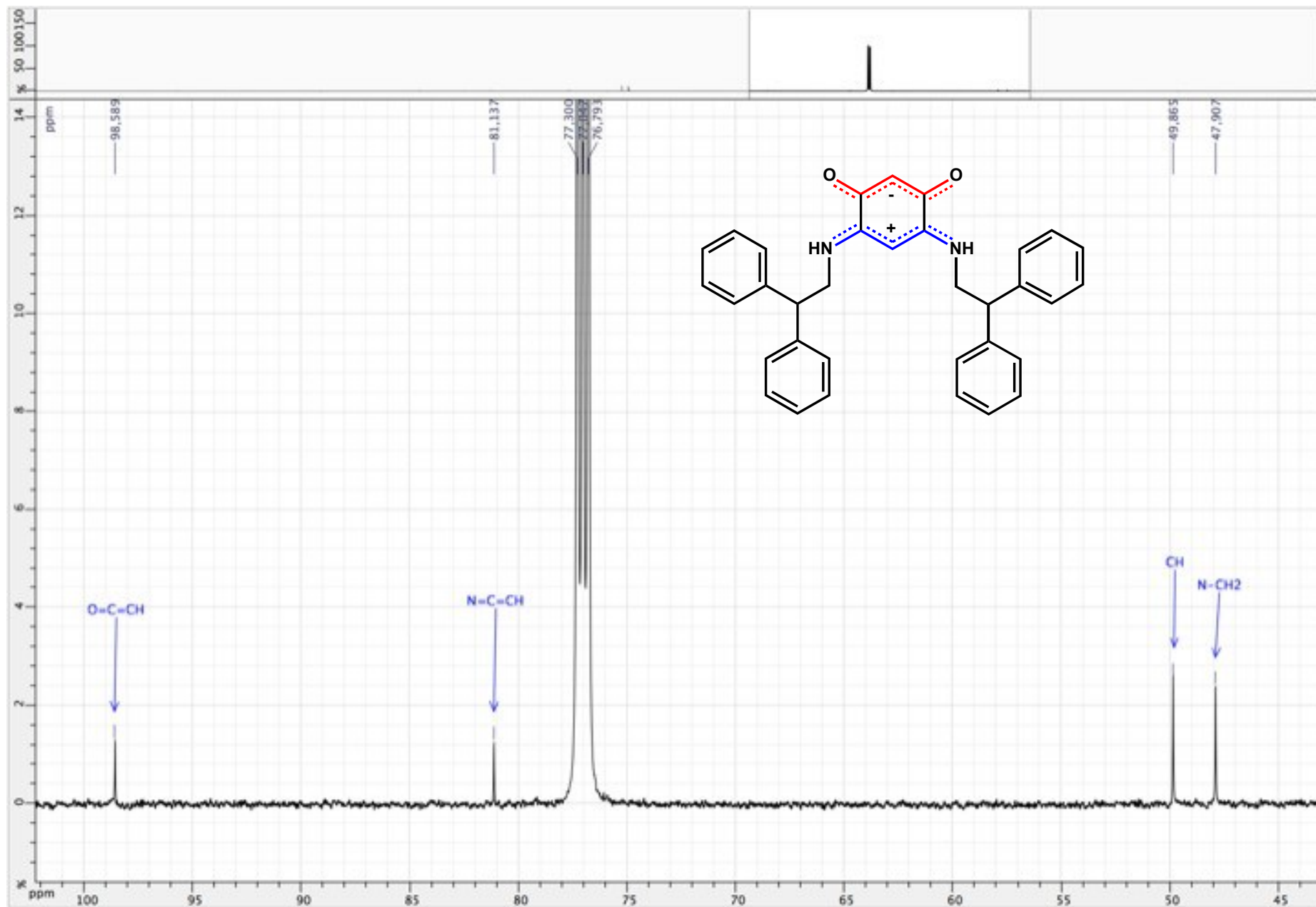


Figure S63. HSQC ($^1\text{H} / ^{13}\text{C} \{^1\text{H}\}$) spectrum of zwitterion **10** (CDCl_3 ; 500 / 125 MHz)

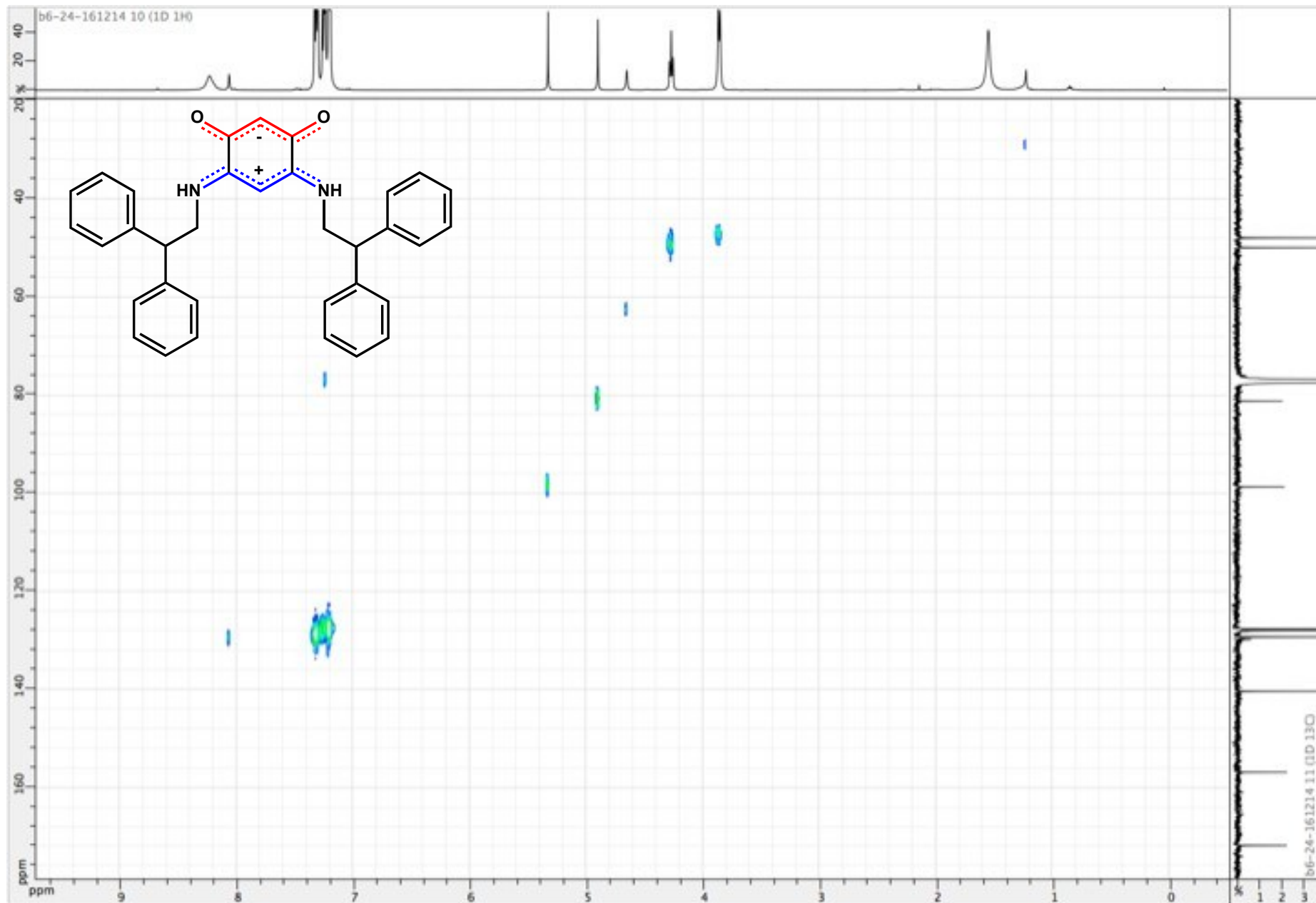


Figure S64. ^1H NMR spectrum of zwitterion **11** (CDCl_3 ; 500 MHz)

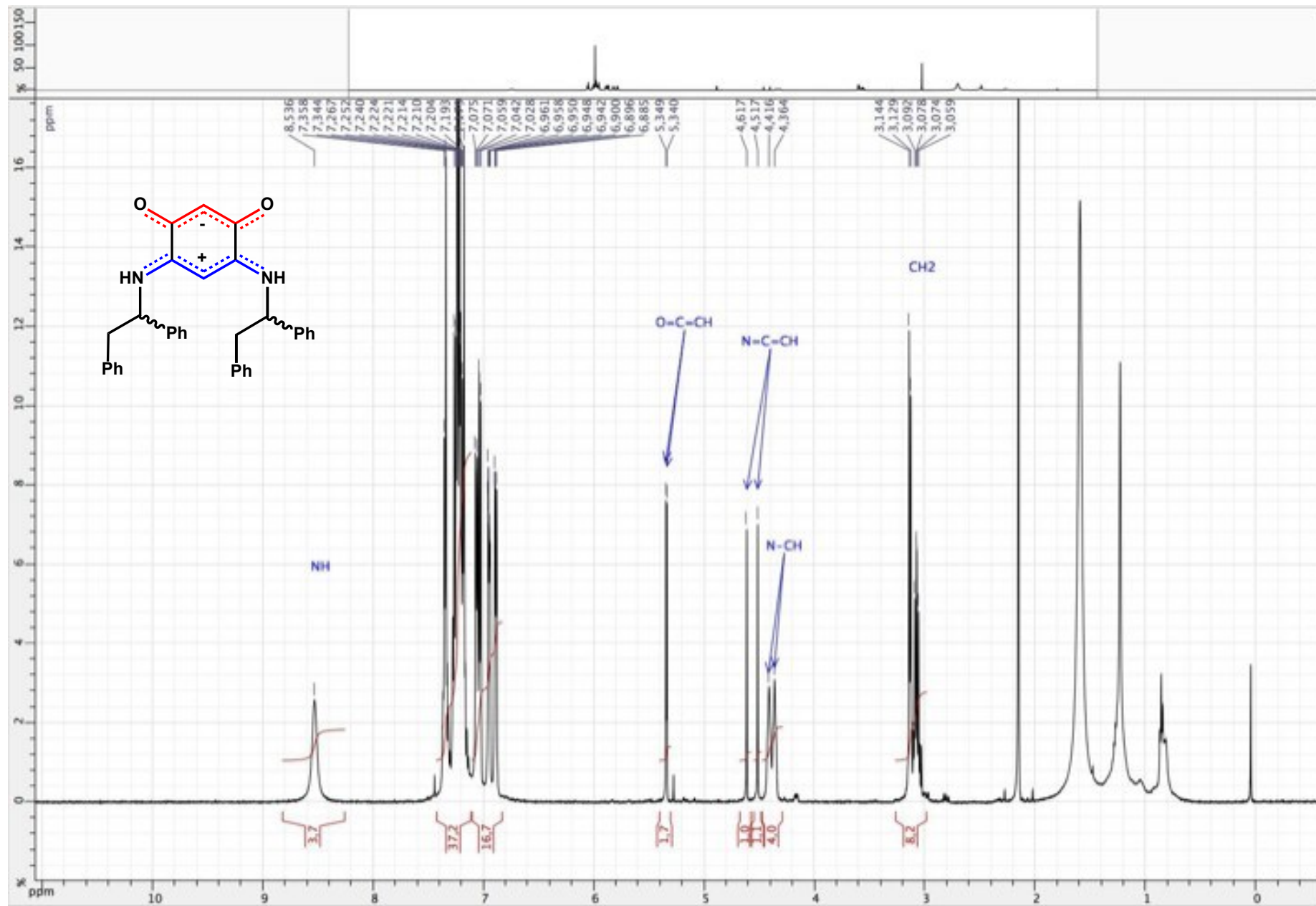


Figure S65. ^1H NMR spectrum of zwitterion **11** (CDCl_3 ; 500 MHz)

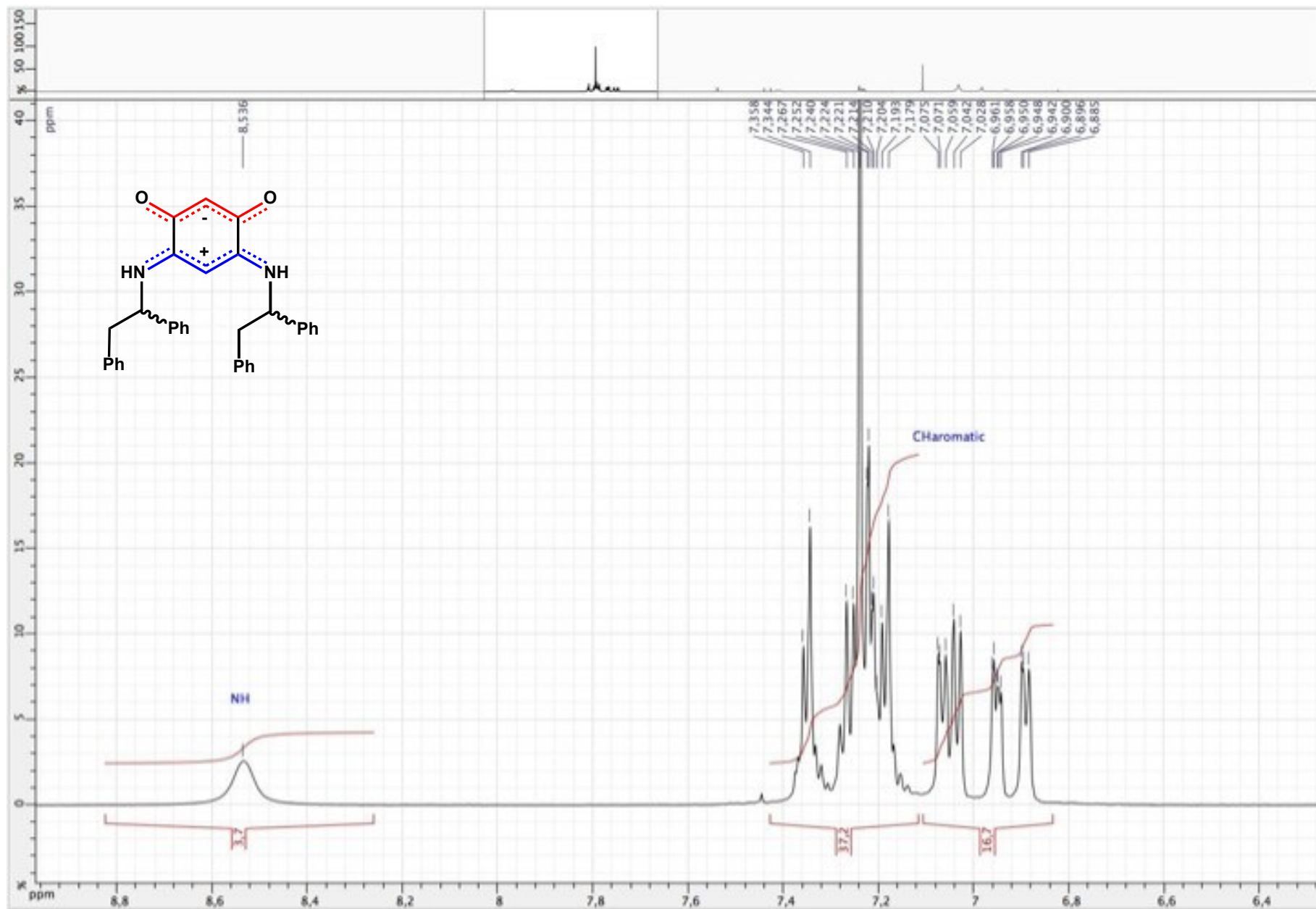


Figure S66. ^1H NMR spectrum of zwitterion **11** (CDCl_3 ; 500 MHz)

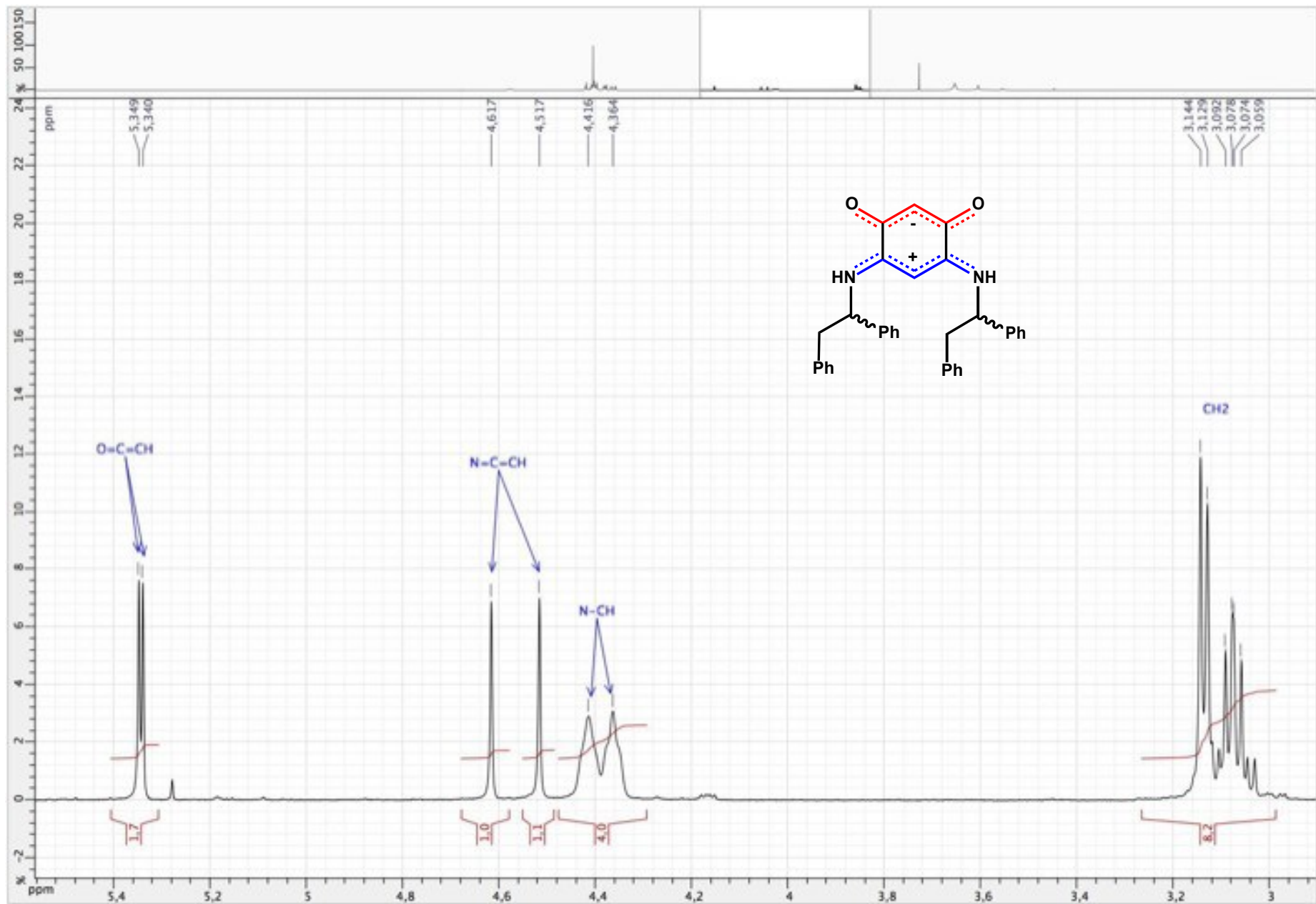


Figure S67. ^{13}C $\{^1\text{H}\}$ NMR spectrum of zwitterion **11** (CDCl_3 ; 125 MHz)

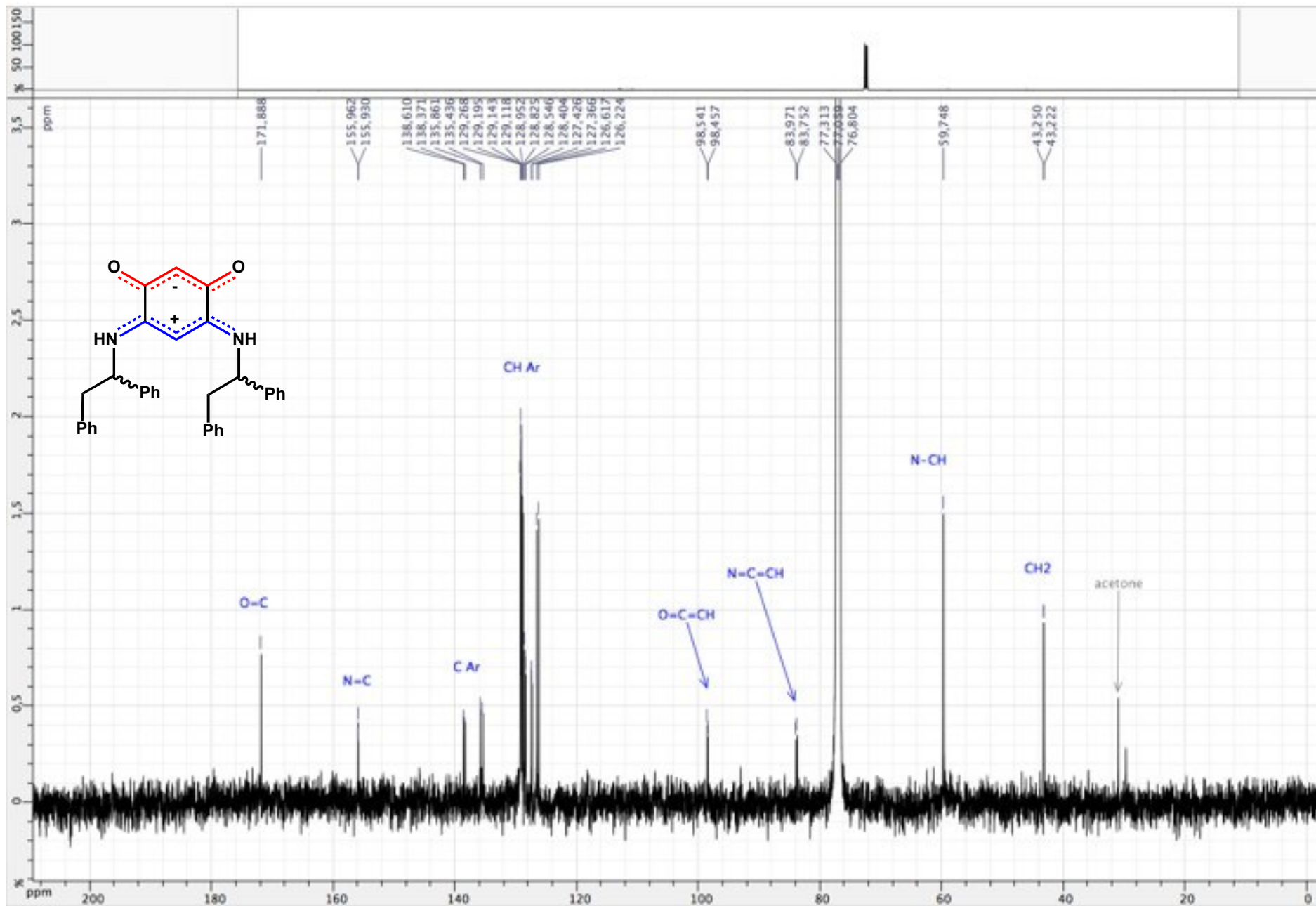


Figure S68. ^{13}C $\{^1\text{H}\}$ NMR spectrum of zwitterion **11** (CDCl_3 ; 125 MHz)

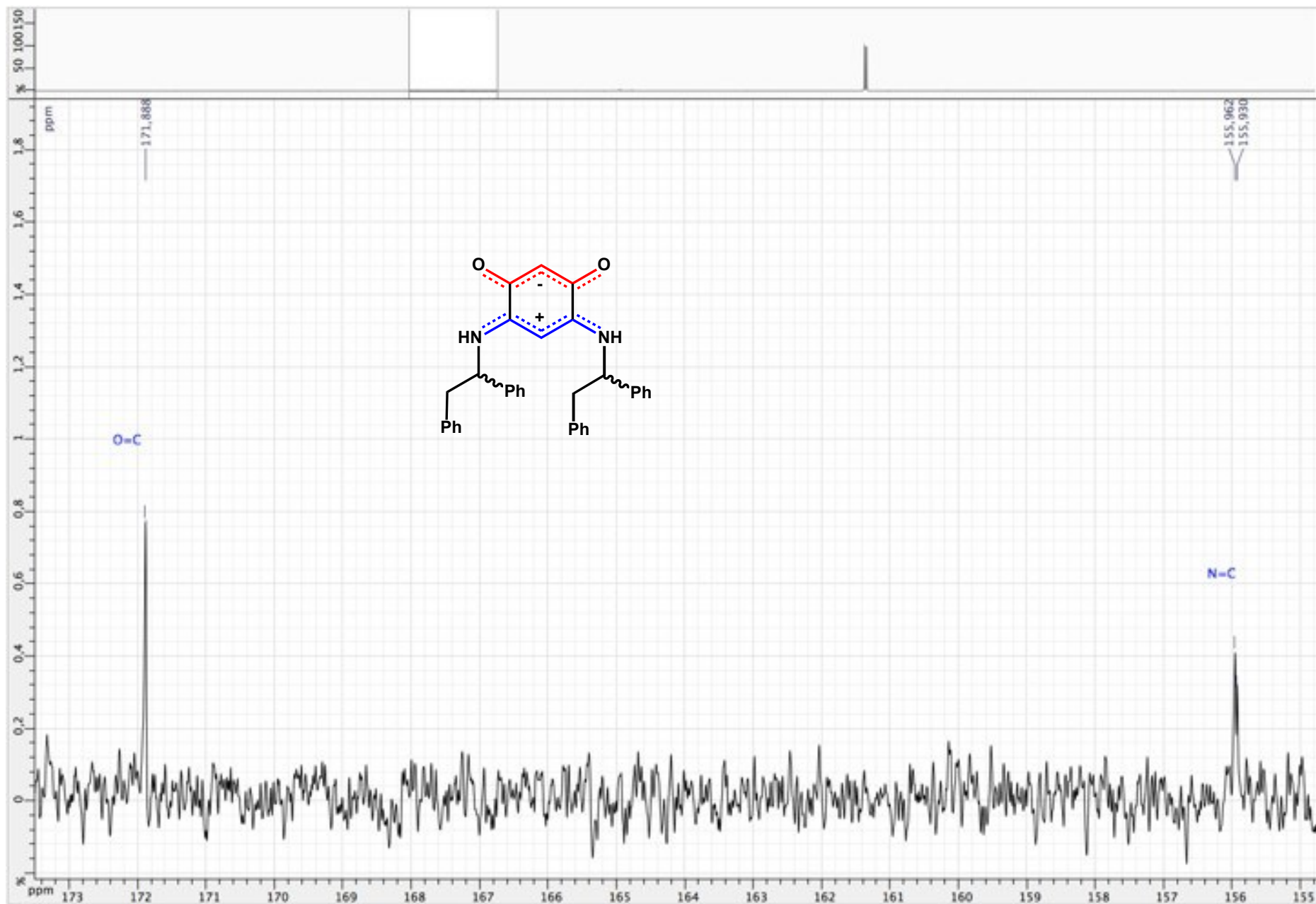


Figure S69. ^{13}C $\{^1\text{H}\}$ NMR spectrum of zwitterion **11** (CDCl_3 ; 125 MHz)

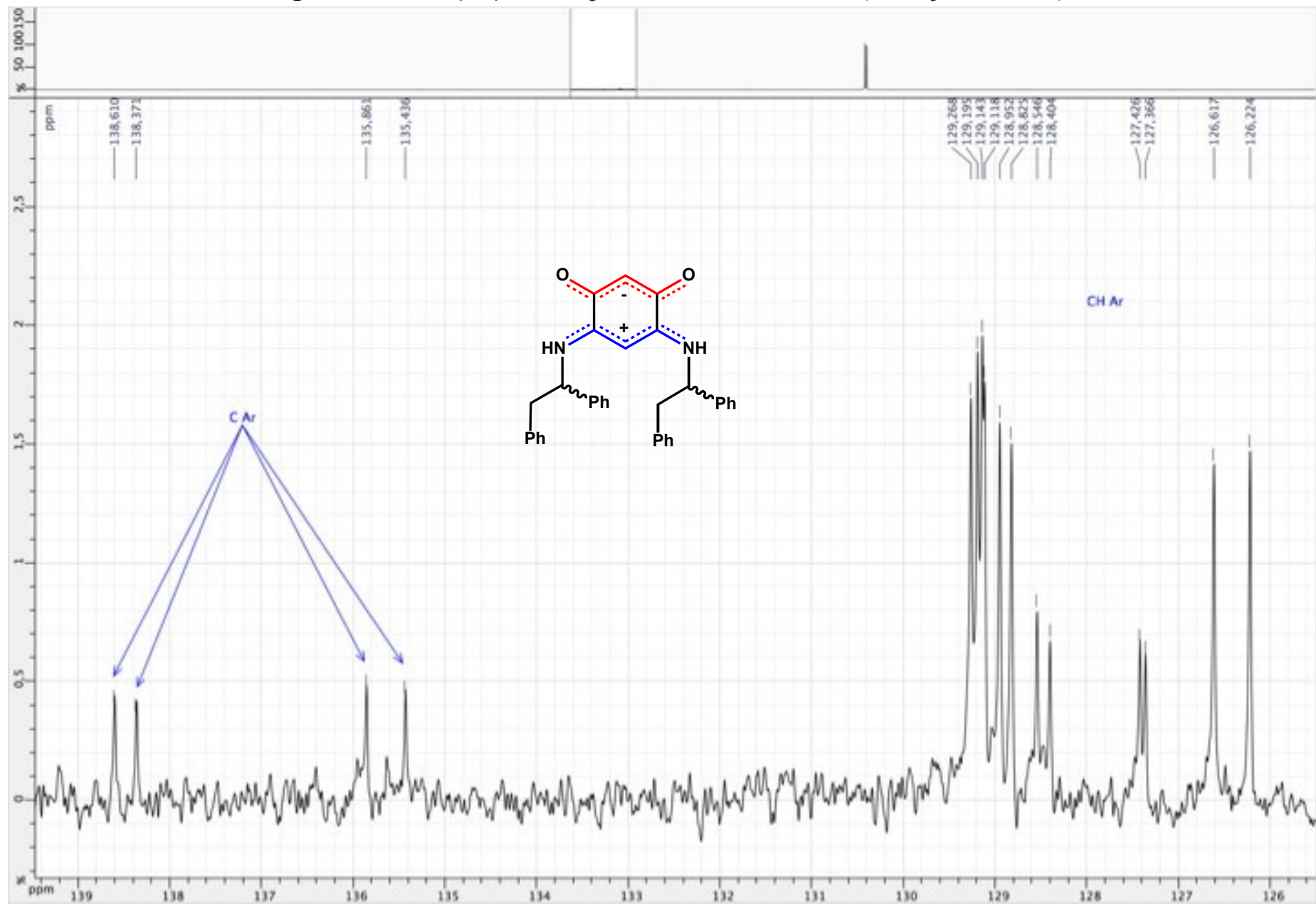


Figure S70. ^{13}C $\{^1\text{H}\}$ NMR spectrum of zwitterion **11** (CDCl_3 ; 125 MHz)

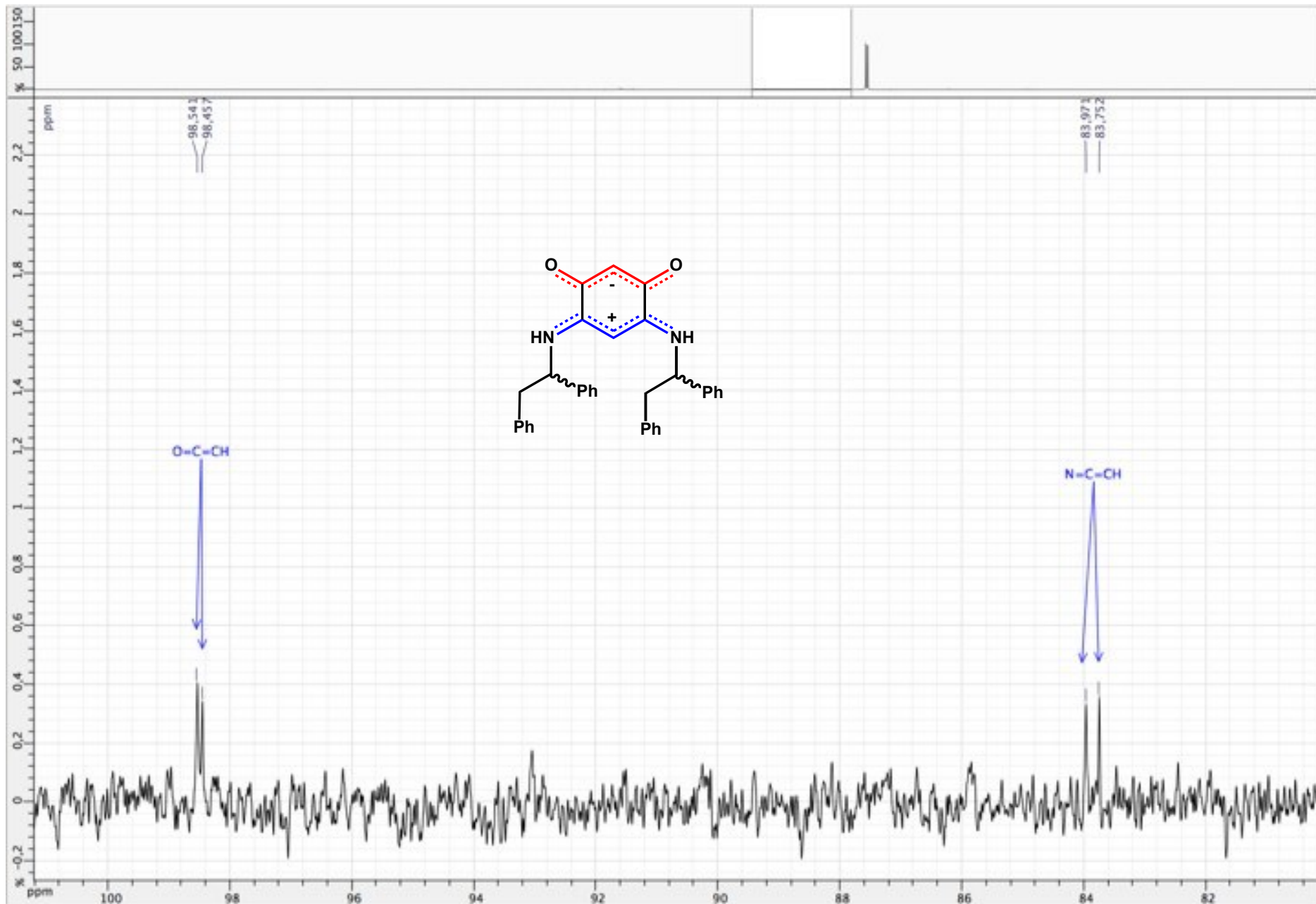


Figure S71. ^{13}C $\{^1\text{H}\}$ NMR spectrum of zwitterion **11** (CDCl_3 ; 125 MHz)

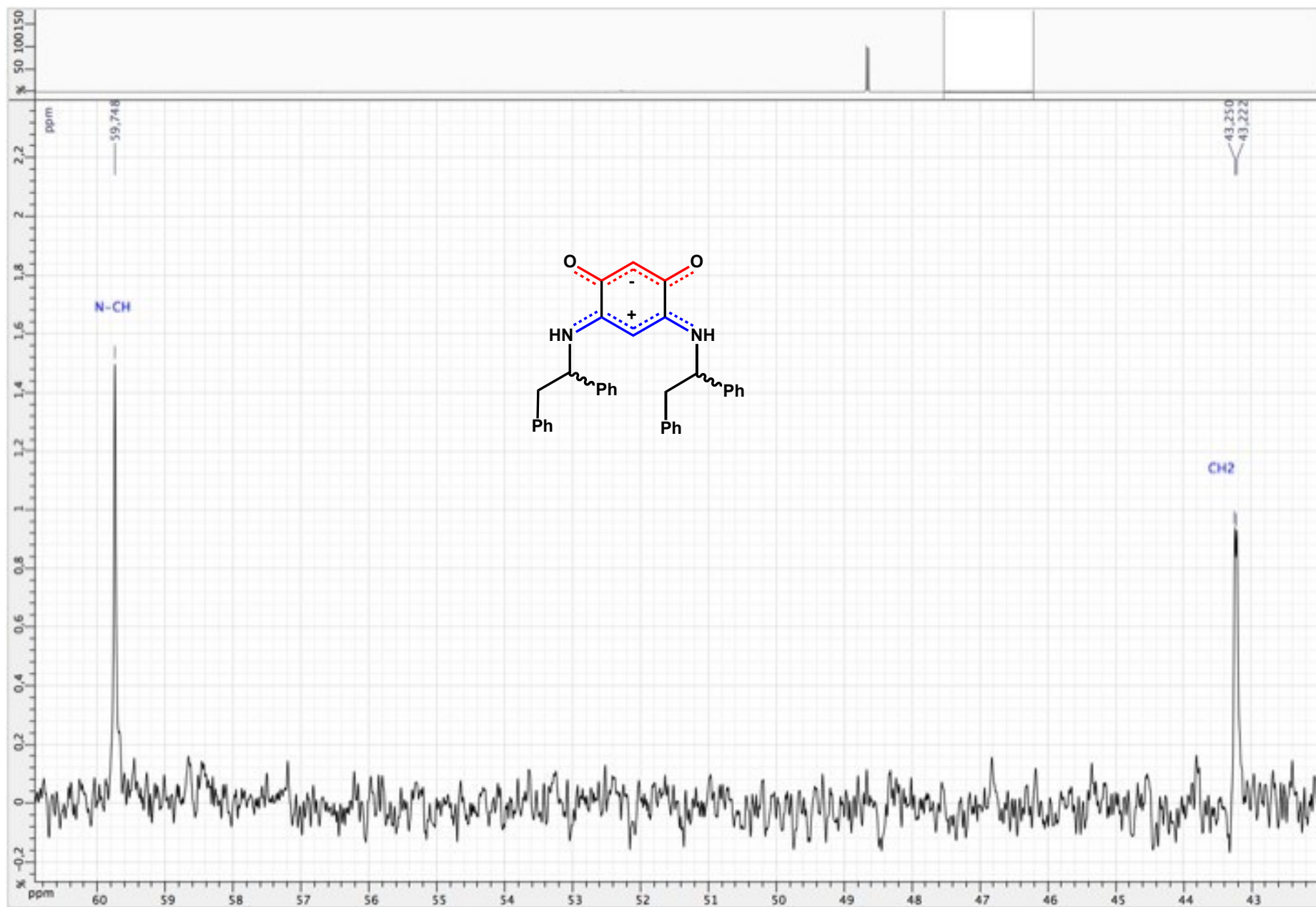


Figure S72. HSQC ($^1\text{H} / ^{13}\text{C} \{^1\text{H}\}$) spectrum of zwitterion **11** (CDCl_3 ; 500 / 125 MHz)

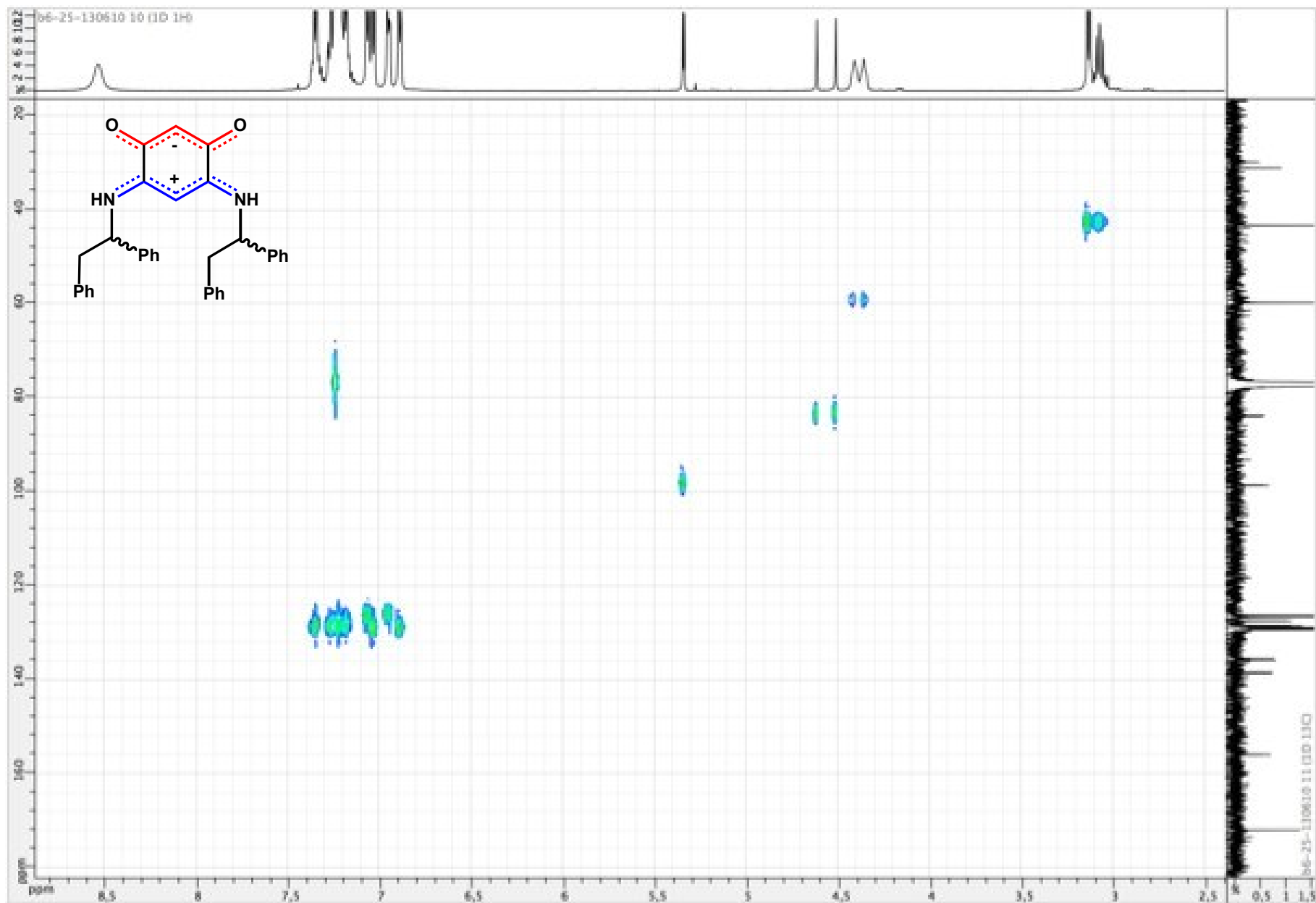


Figure S73. COSY ($^1\text{H} / ^1\text{H}$) spectrum of zwitterion **11** (CDCl_3 ; 500 MHz)

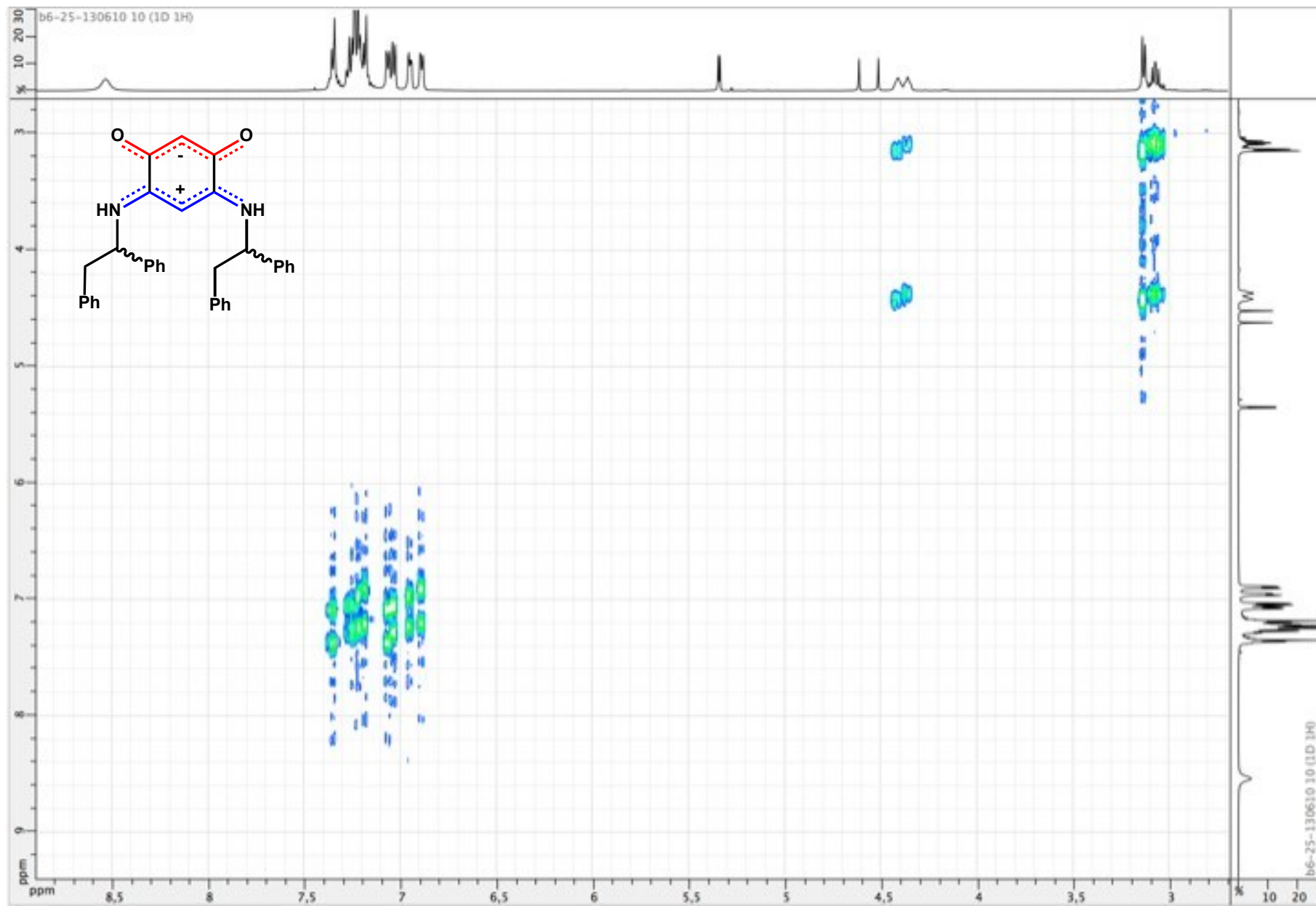


Figure S74. ^1H NMR spectrum of zwitterion **12** (CDCl_3 ; 500 MHz)

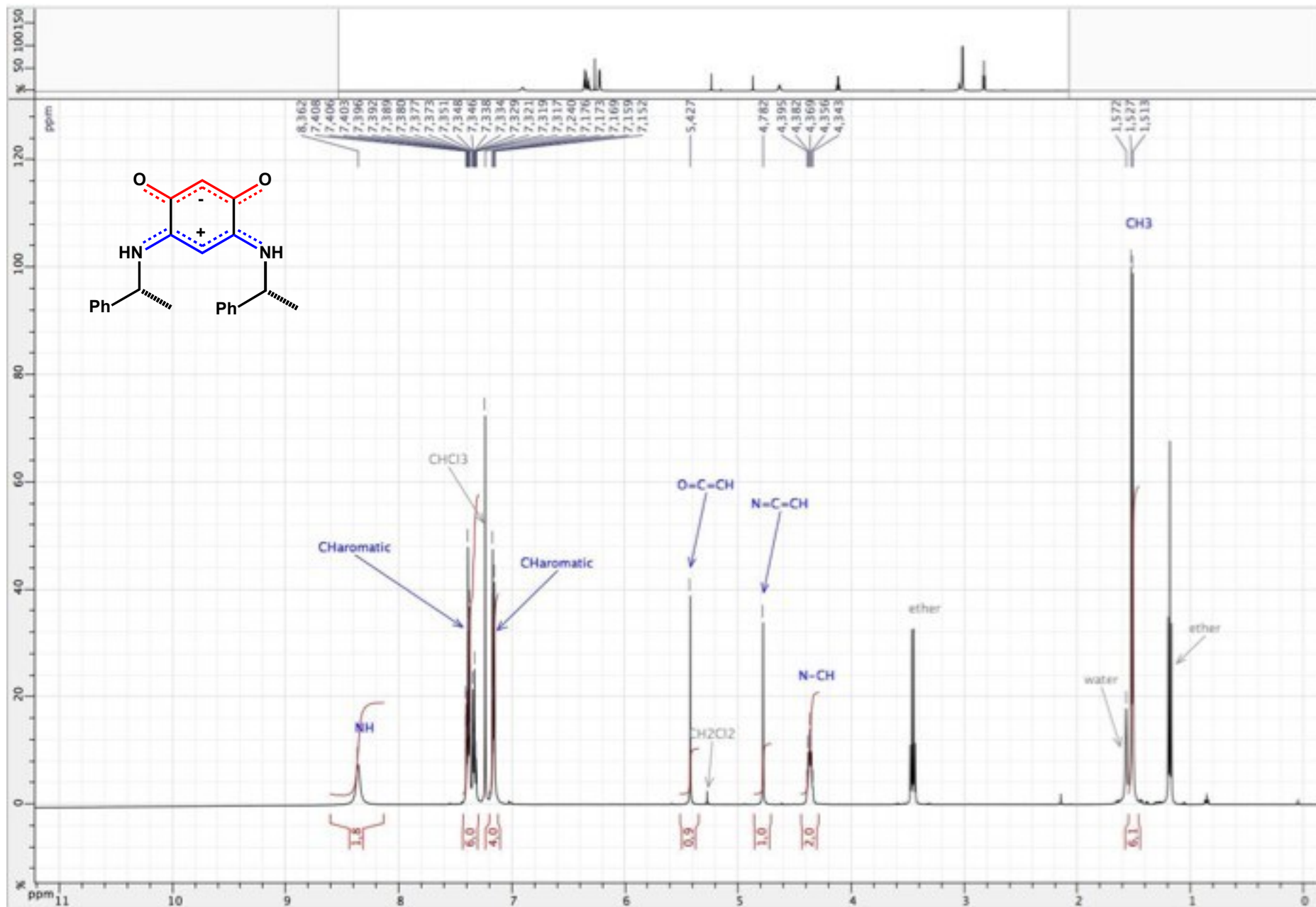


Figure S75. ^1H NMR spectrum of zwitterion **12** (CDCl_3 ; 500 MHz)

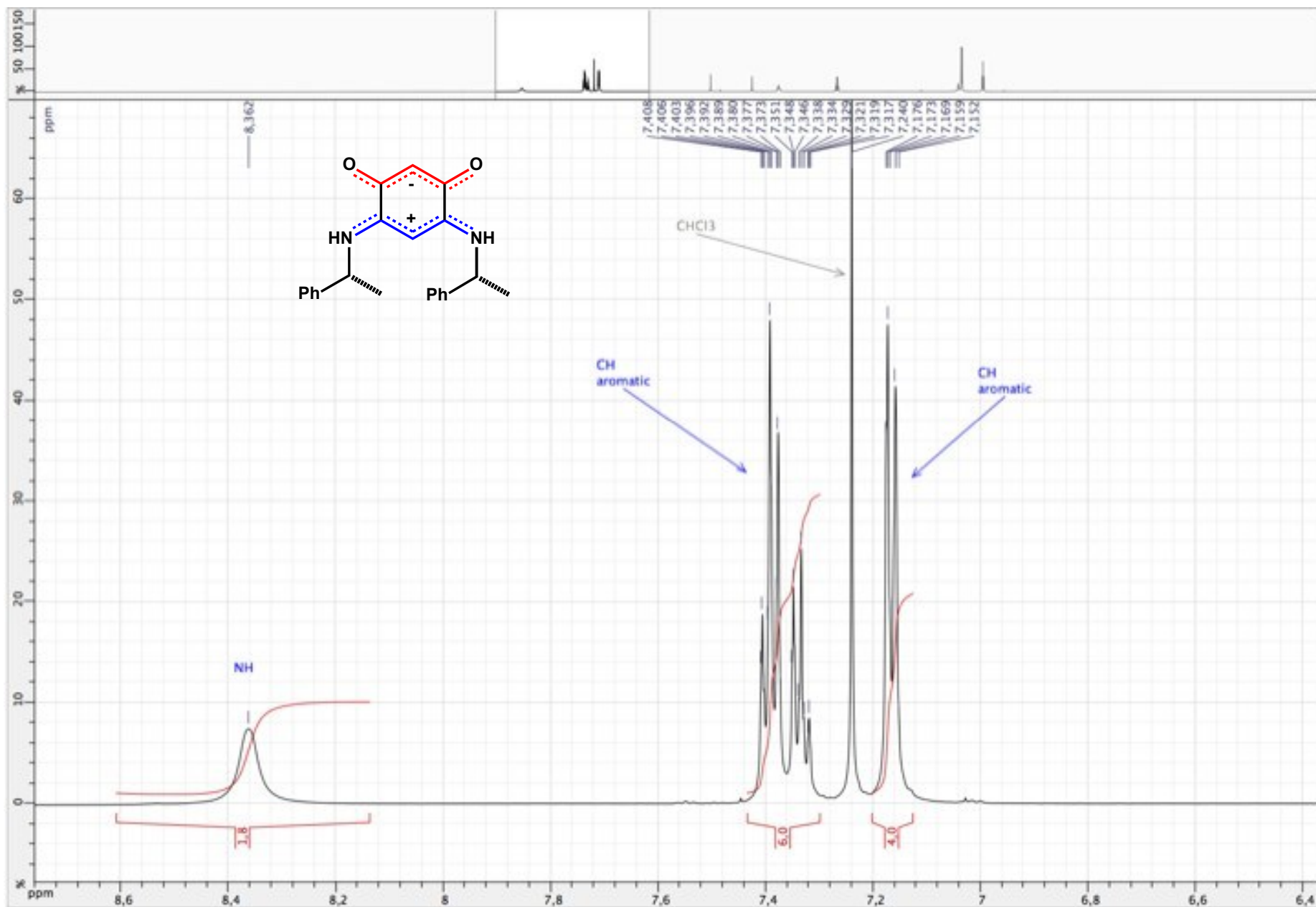


Figure S76. ^1H NMR spectrum of zwitterion **12** (CDCl_3 ; 500 MHz)

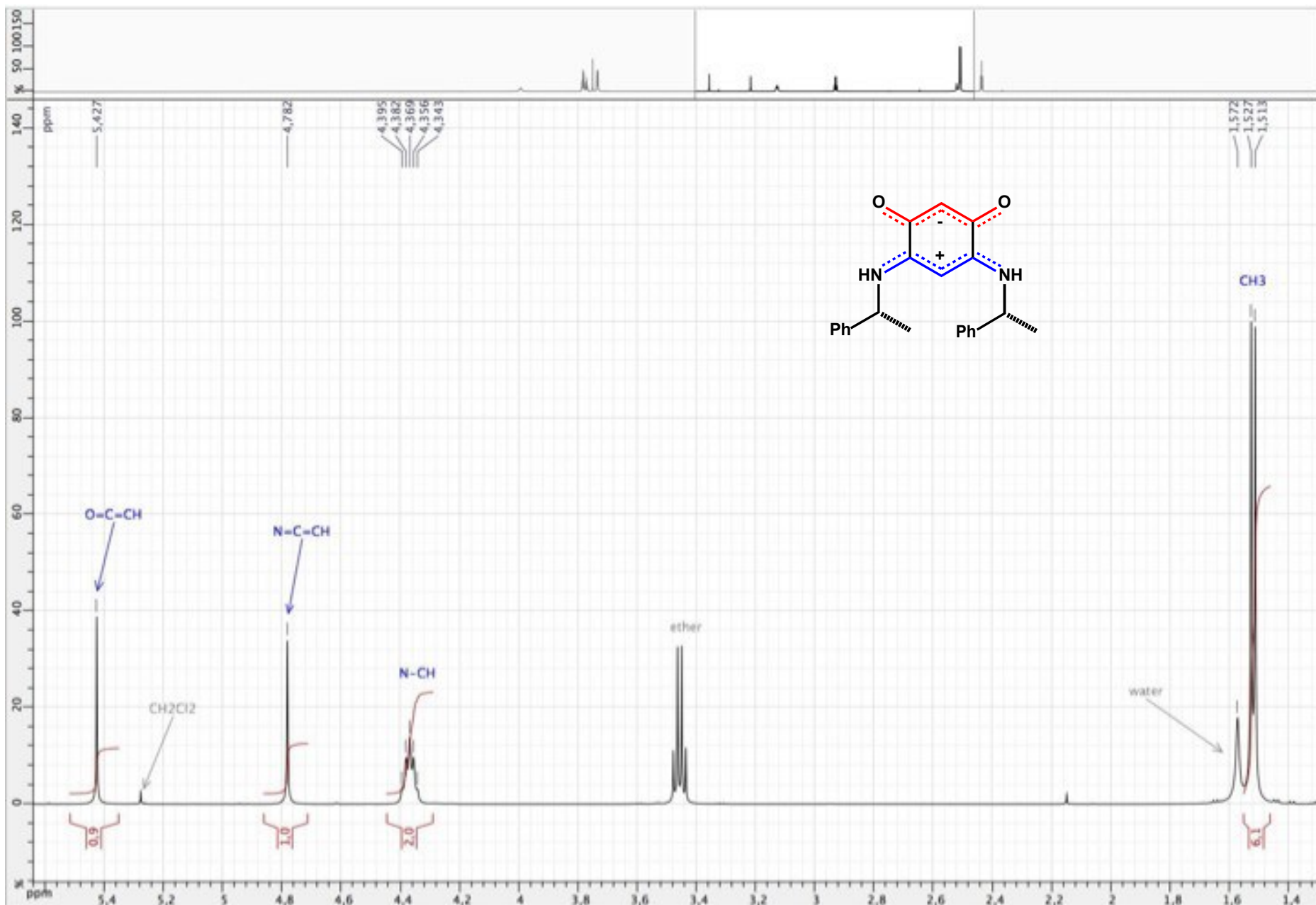


Figure S77. ^1H NMR spectrum of zwitterion **12** (CDCl_3 ; 500 MHz)

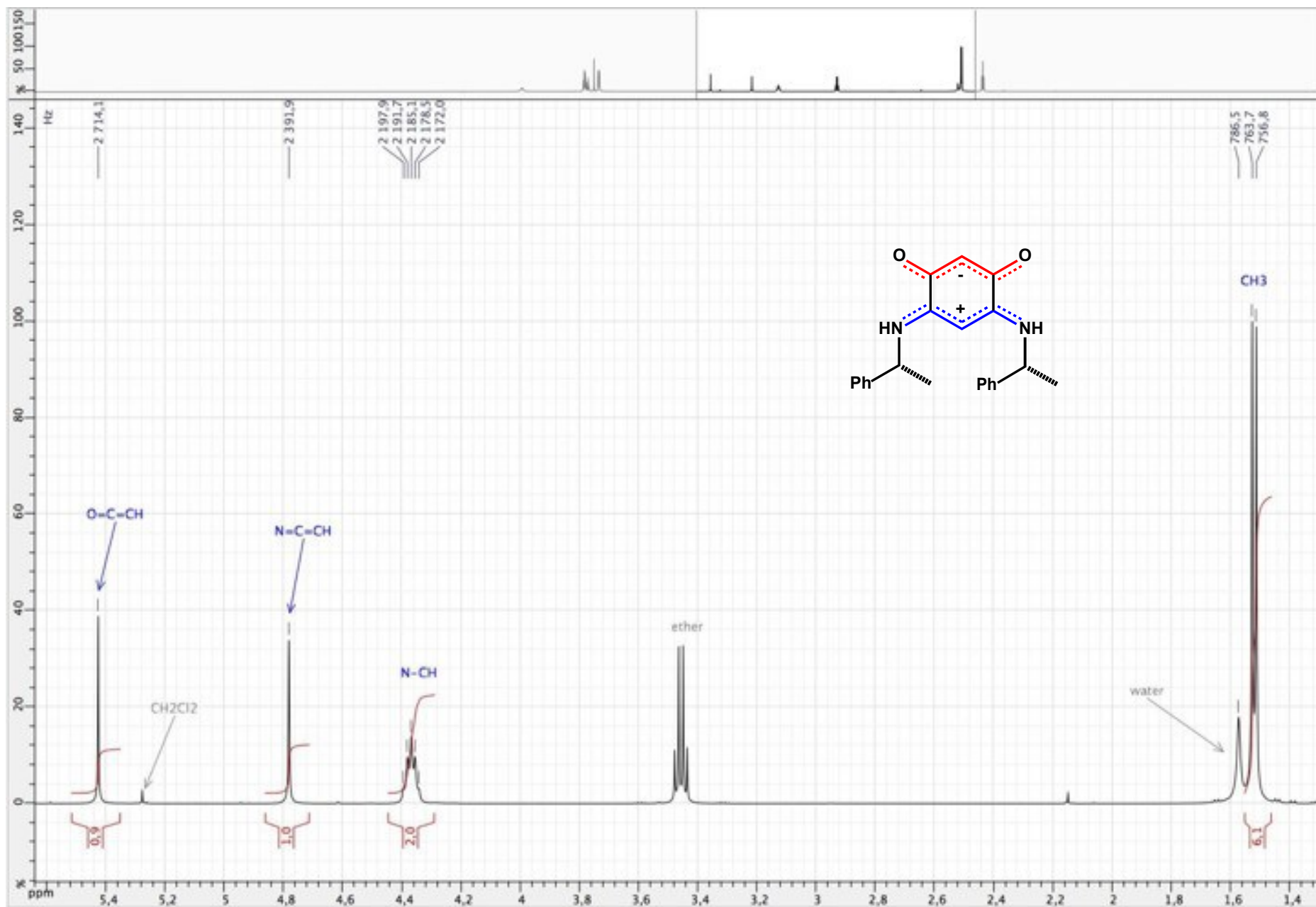


Figure S78. ^{13}C $\{^1\text{H}\}$ NMR spectrum of zwitterion **12** (CDCl_3 ; 125 MHz)

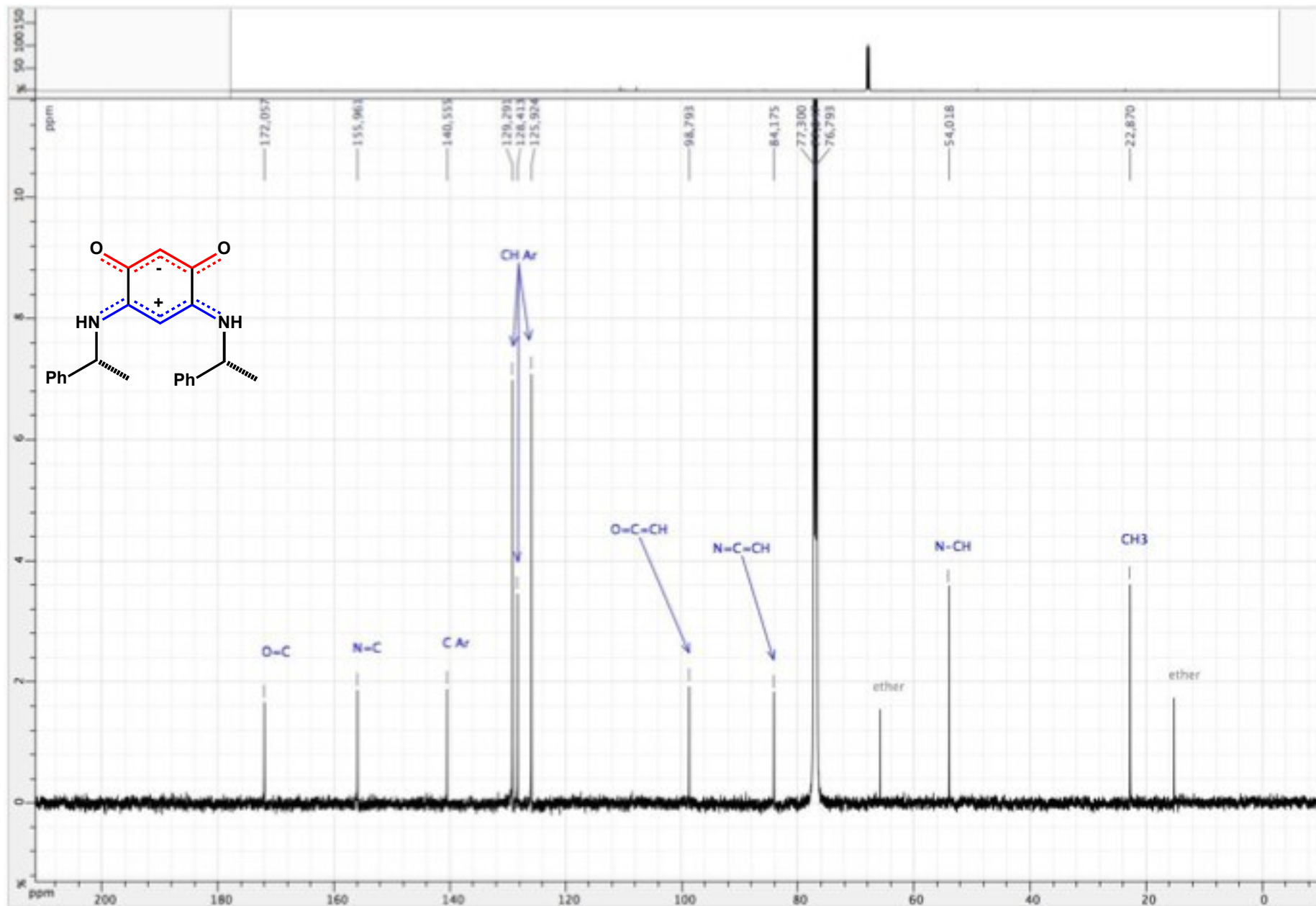


Figure S79. ^{13}C $\{^1\text{H}\}$ NMR spectrum of zwitterion **12** (CDCl_3 ; 125 MHz)

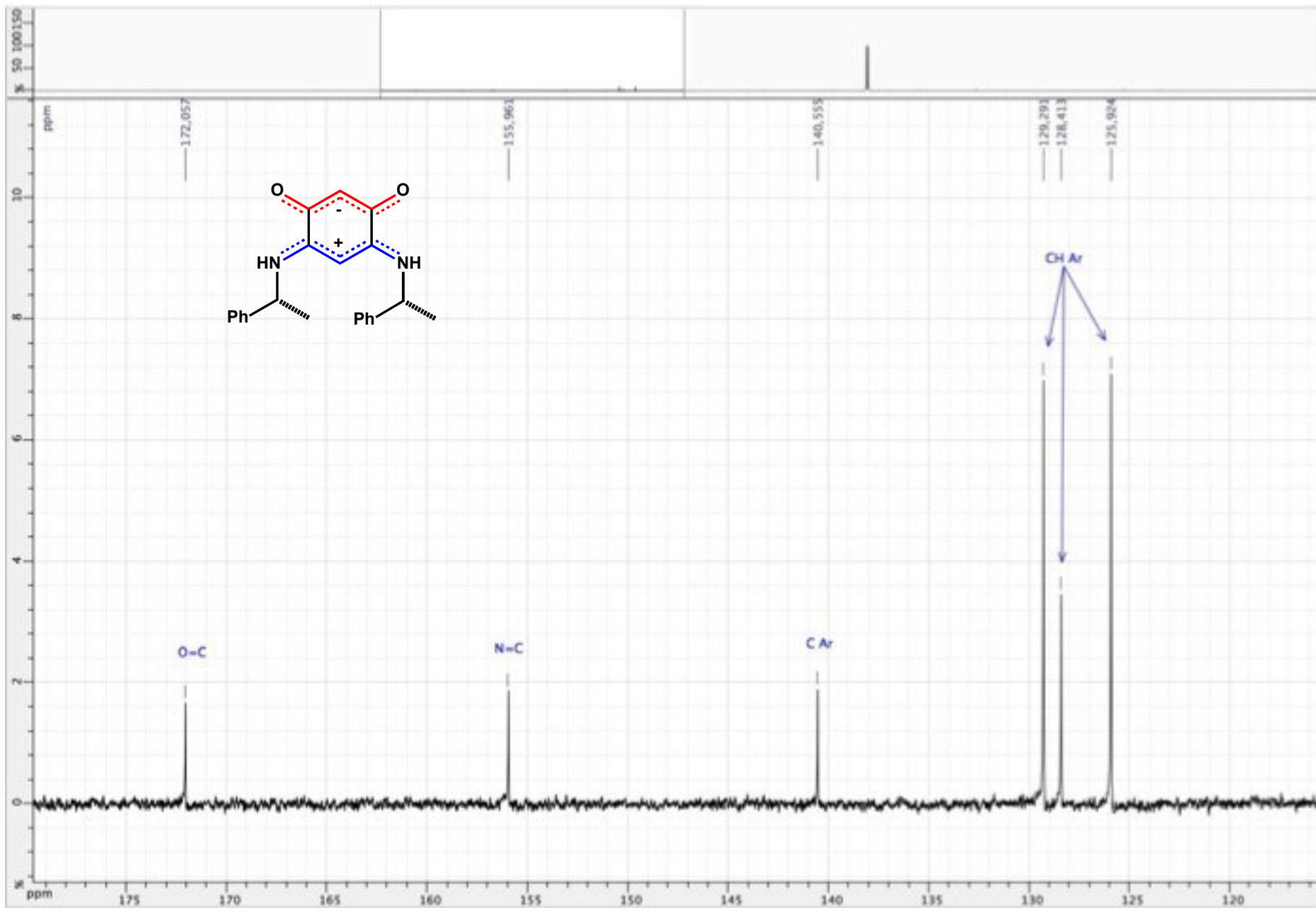


Figure S80. ^{13}C $\{^1\text{H}\}$ NMR spectrum of zwitterion **12** (CDCl_3 ; 125 MHz)

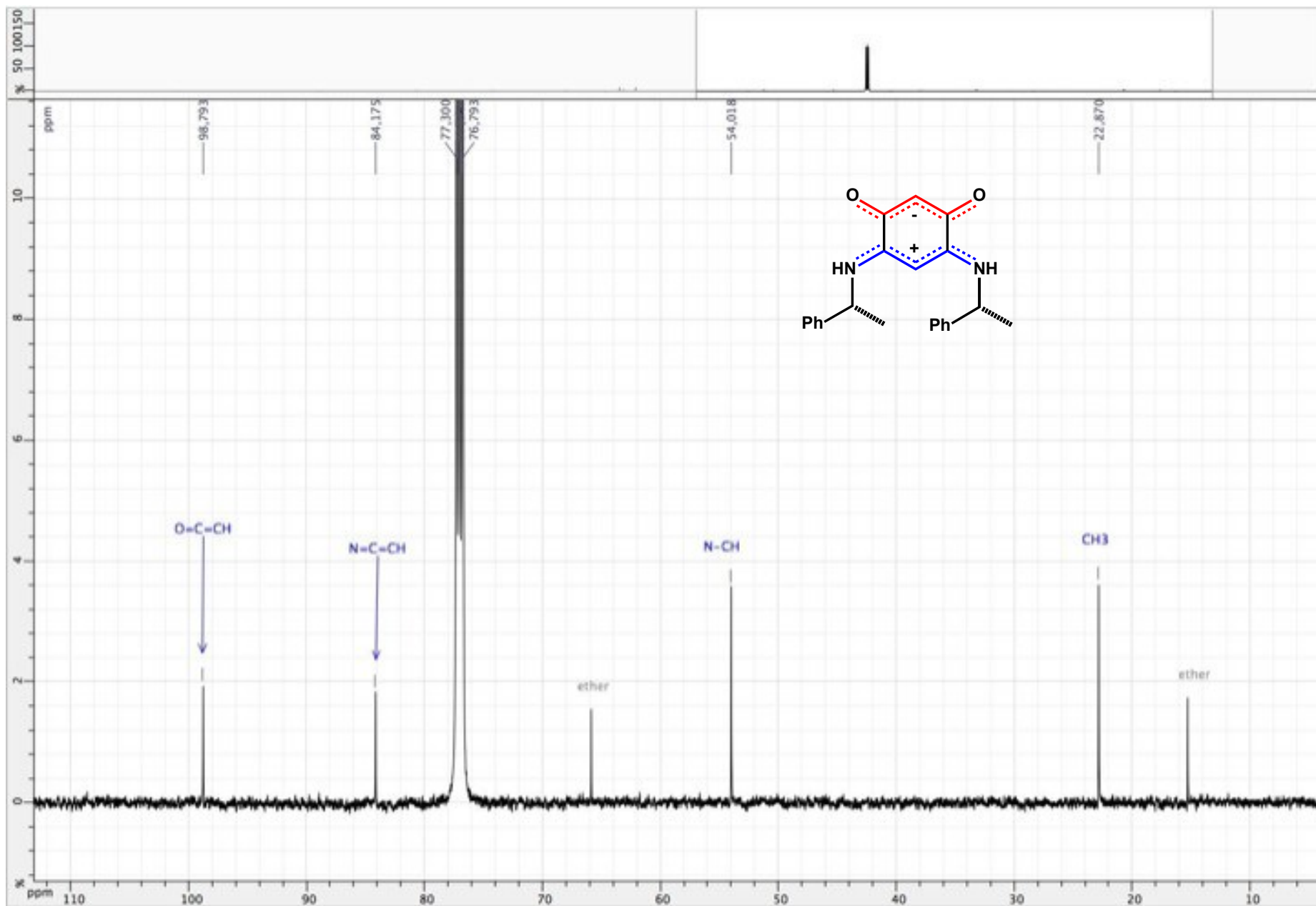


Figure S81. HSQC ($^1\text{H} / ^{13}\text{C} \{^1\text{H}\}$) spectrum of zwitterion **12** (CDCl_3 ; 500 / 125 MHz)

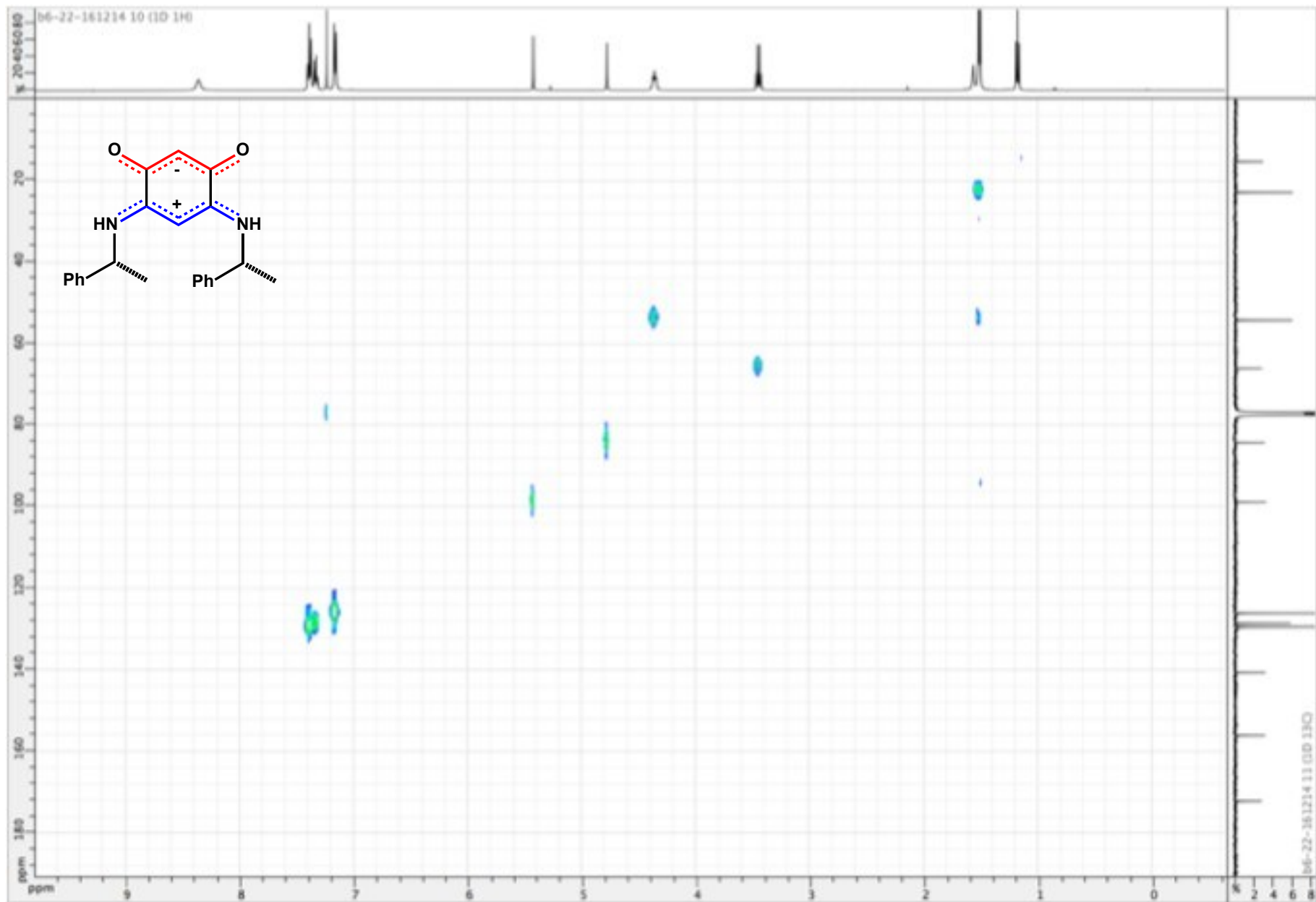


Figure S82. COSY ($^1\text{H} / ^1\text{H}$) spectrum of zwitterion **12** (CDCl_3 ; 500 MHz)

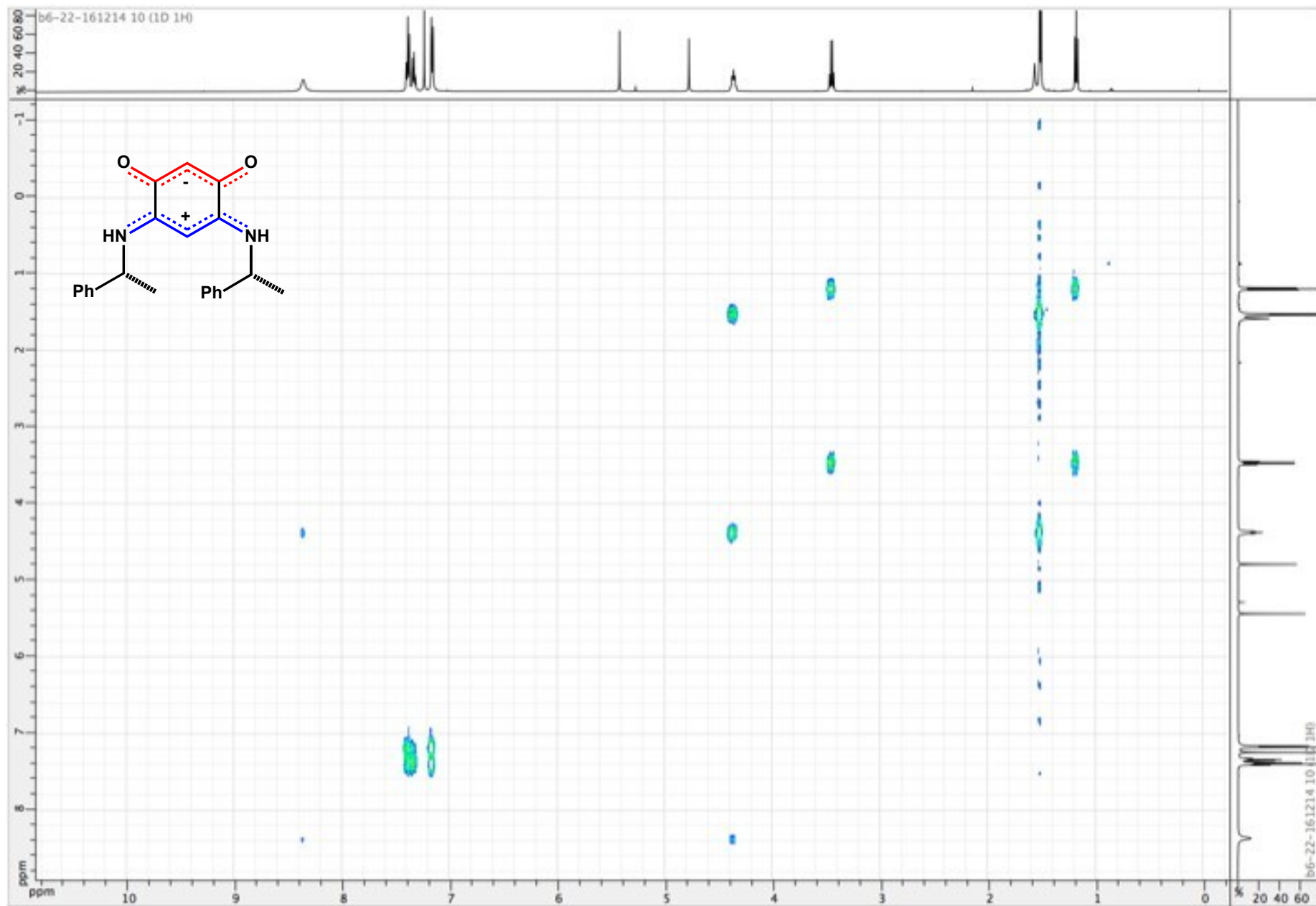


Figure S83. ^1H NMR spectrum of zwitterion **13** (CDCl_3 ; 500 MHz)

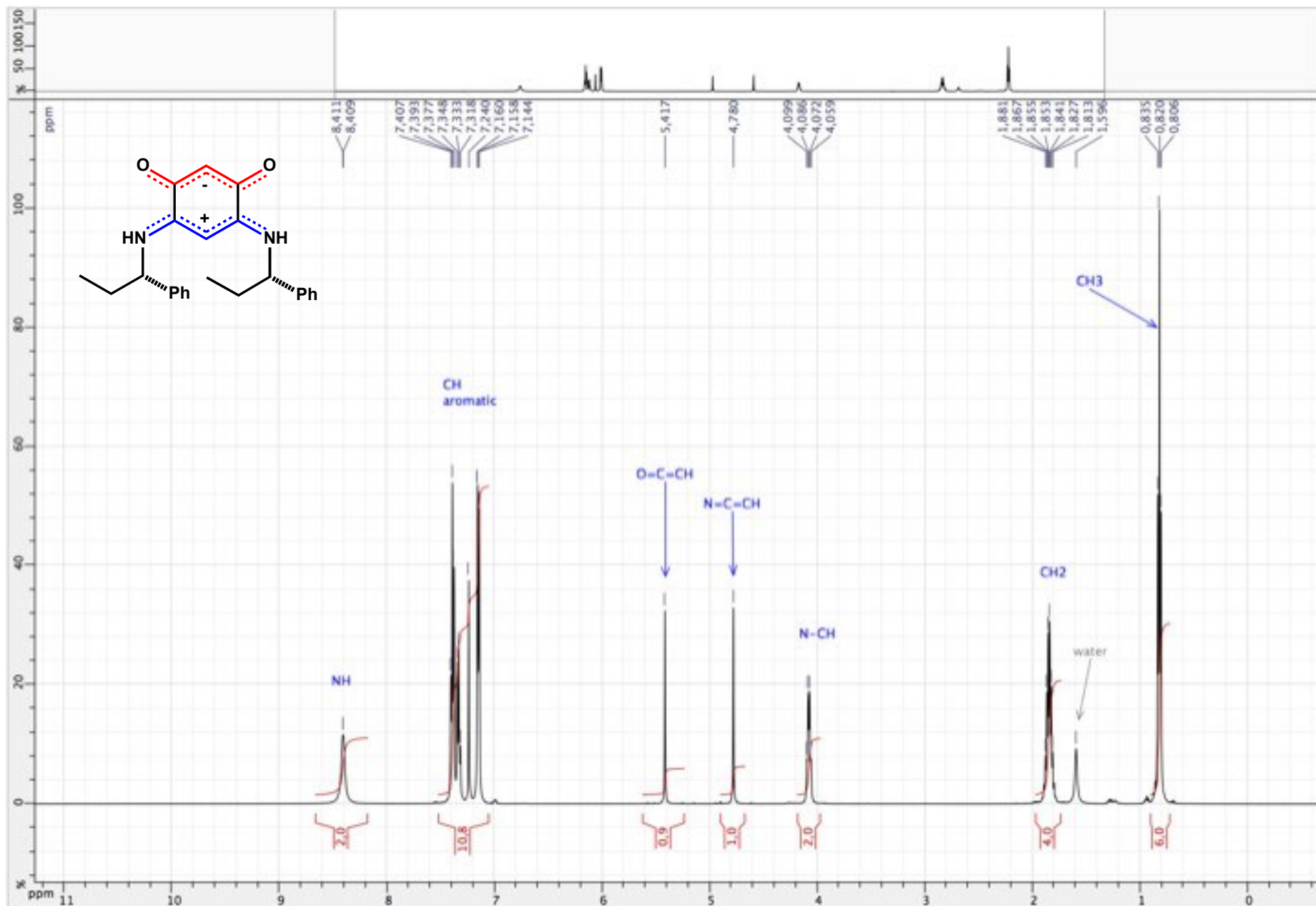


Figure S84. ^1H NMR spectrum of zwitterion **13** (CDCl_3 ; 500 MHz)

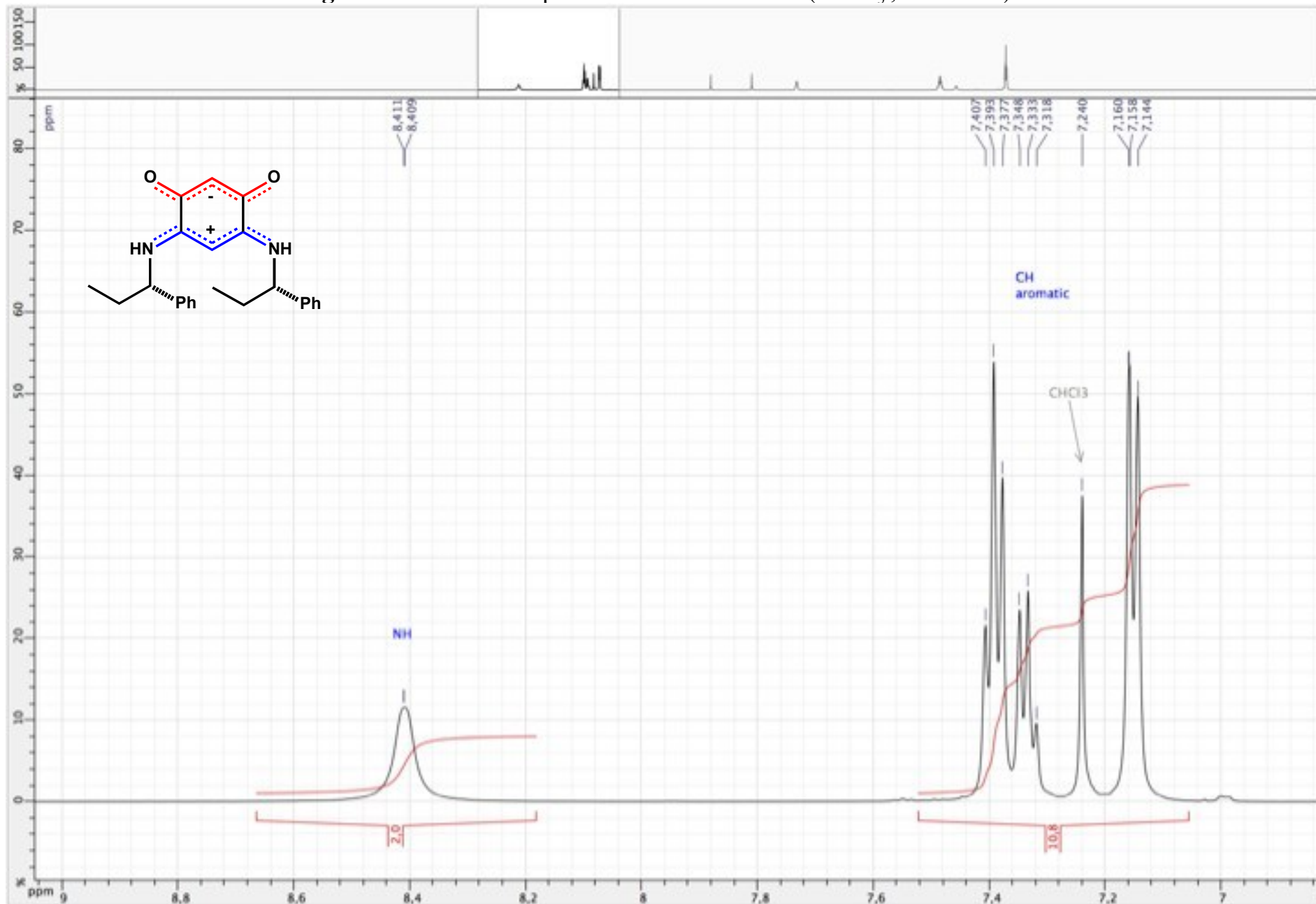


Figure S85. ^1H NMR spectrum of zwitterion **13** (CDCl_3 ; 500 MHz)

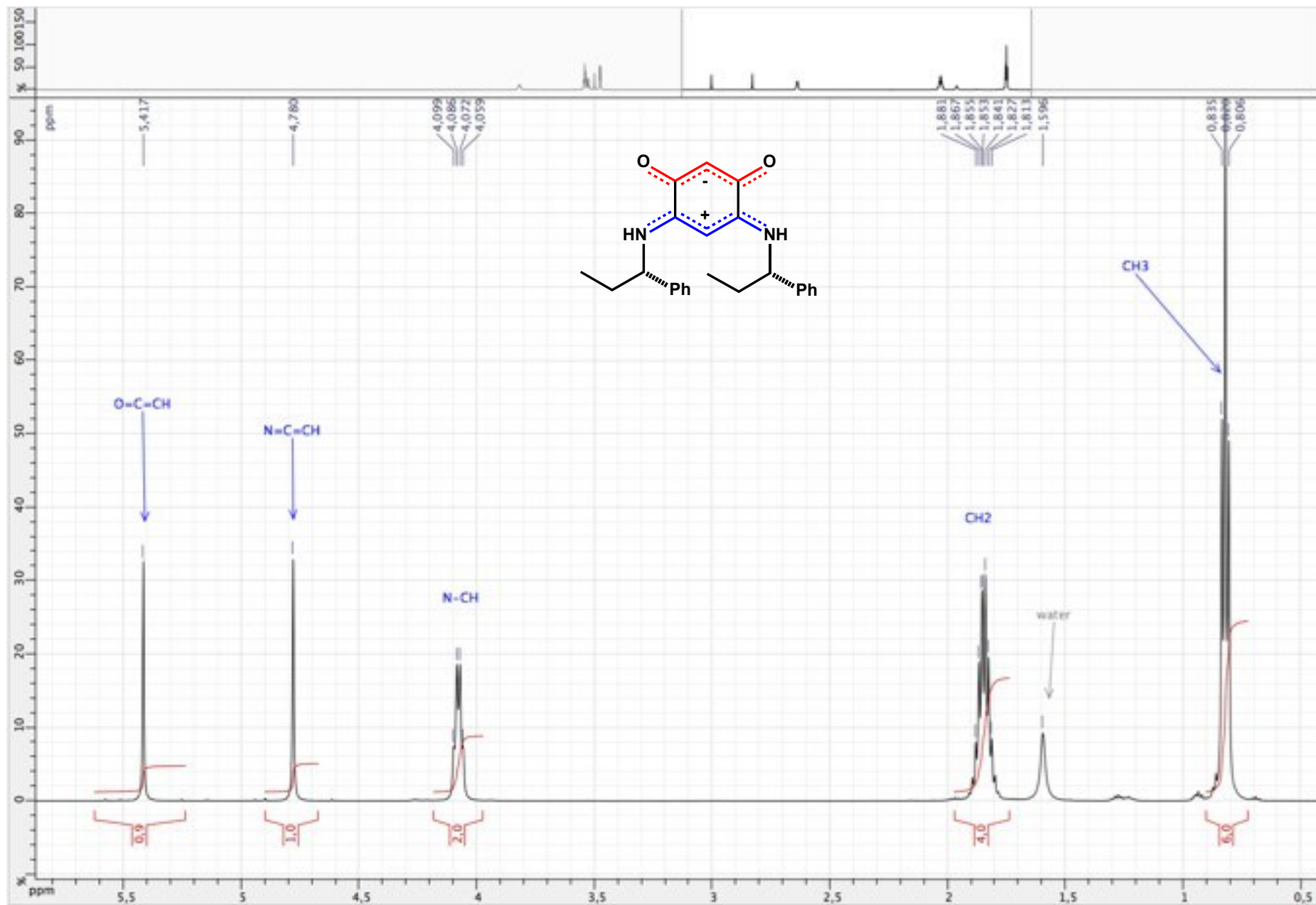


Figure S86. ¹H NMR spectrum of zwitterion **13** (CDCl₃; 500 MHz)

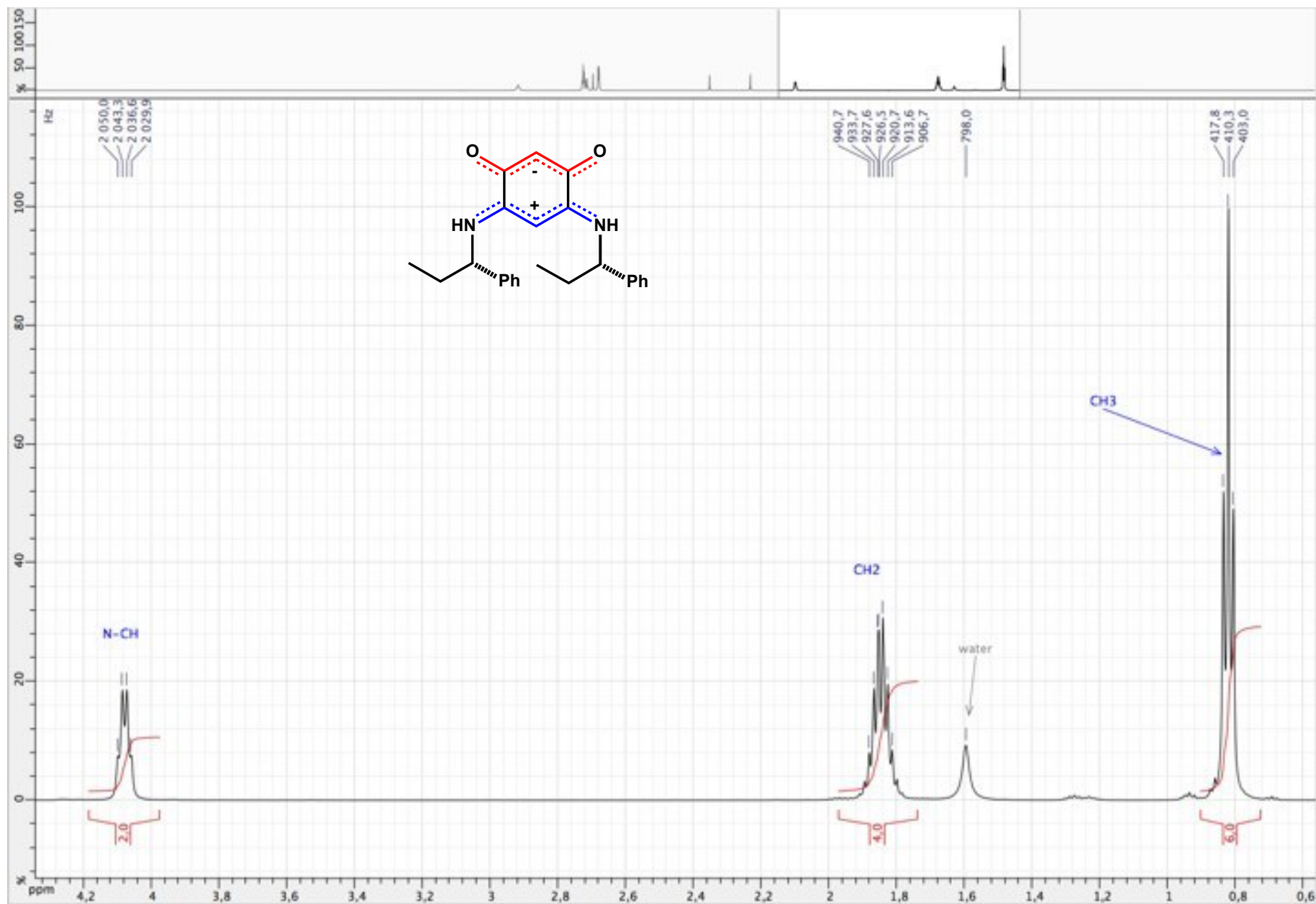


Figure S87. ^{13}C $\{^1\text{H}\}$ NMR spectrum of zwitterion **13** (CDCl_3 ; 125 MHz)

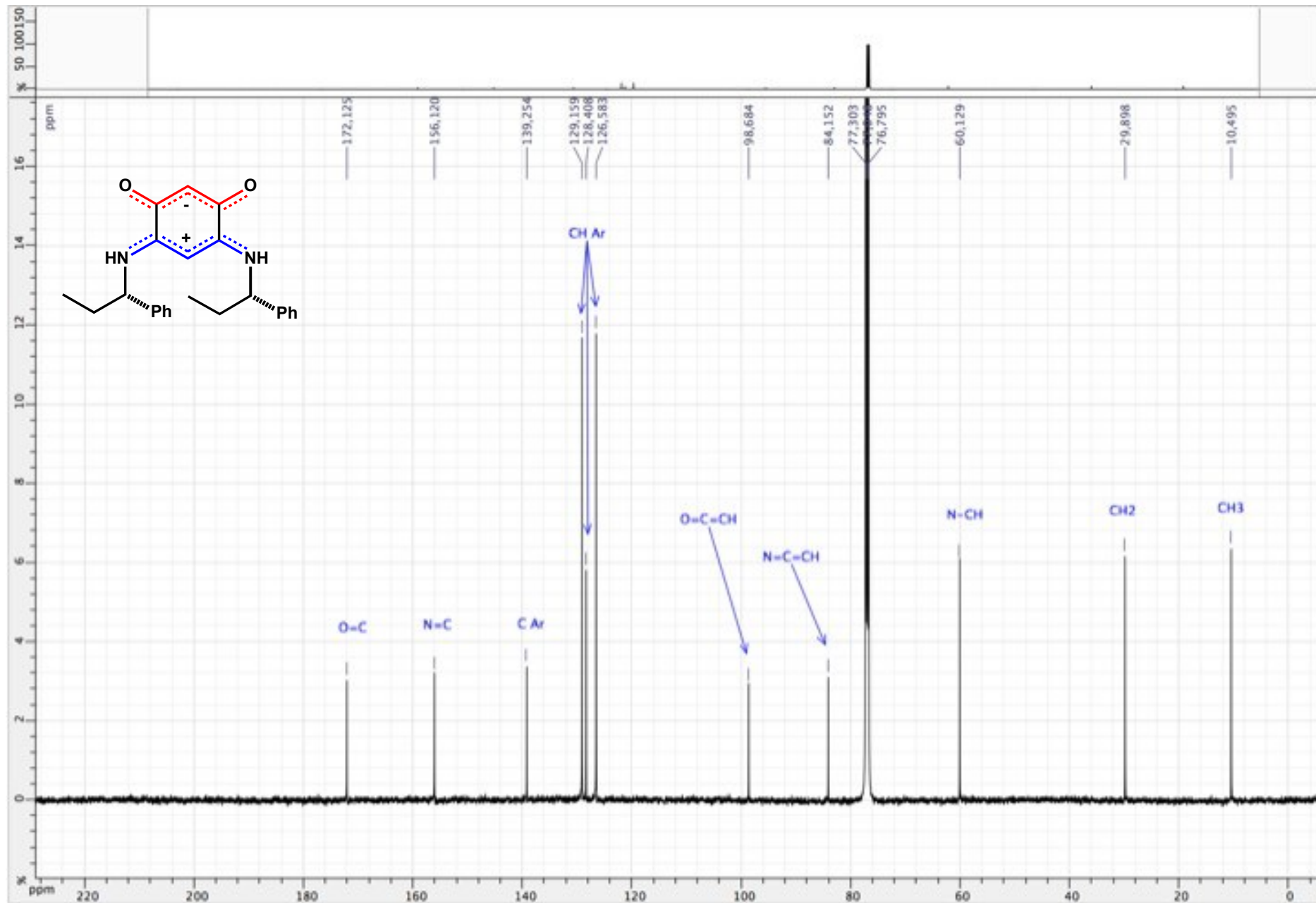


Figure S88. ^{13}C $\{^1\text{H}\}$ NMR spectrum of zwitterion **13** (CDCl_3 ; 125 MHz)

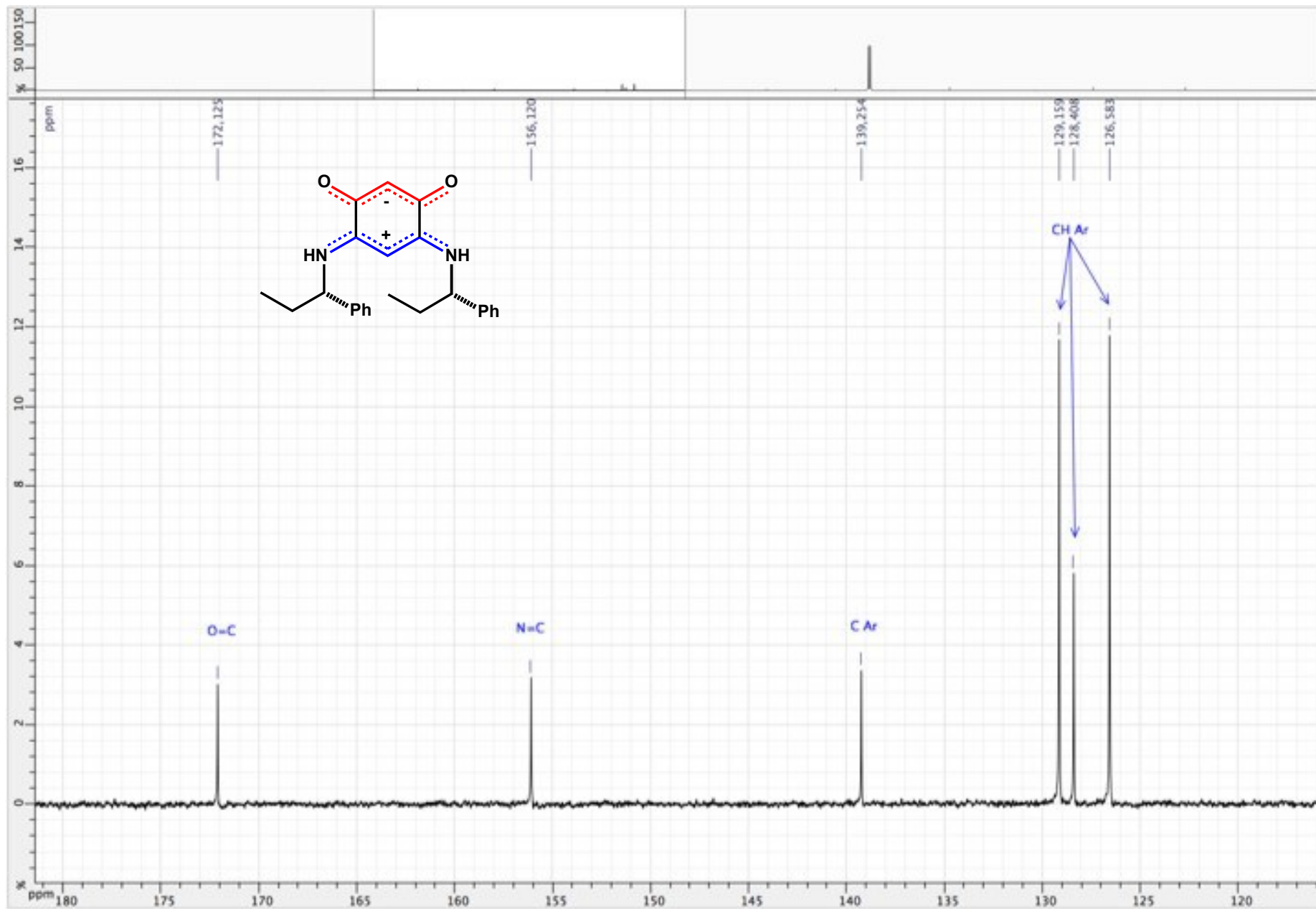


Figure S89. ^{13}C $\{^1\text{H}\}$ NMR spectrum of zwitterion **13** (CDCl_3 ; 125 MHz)

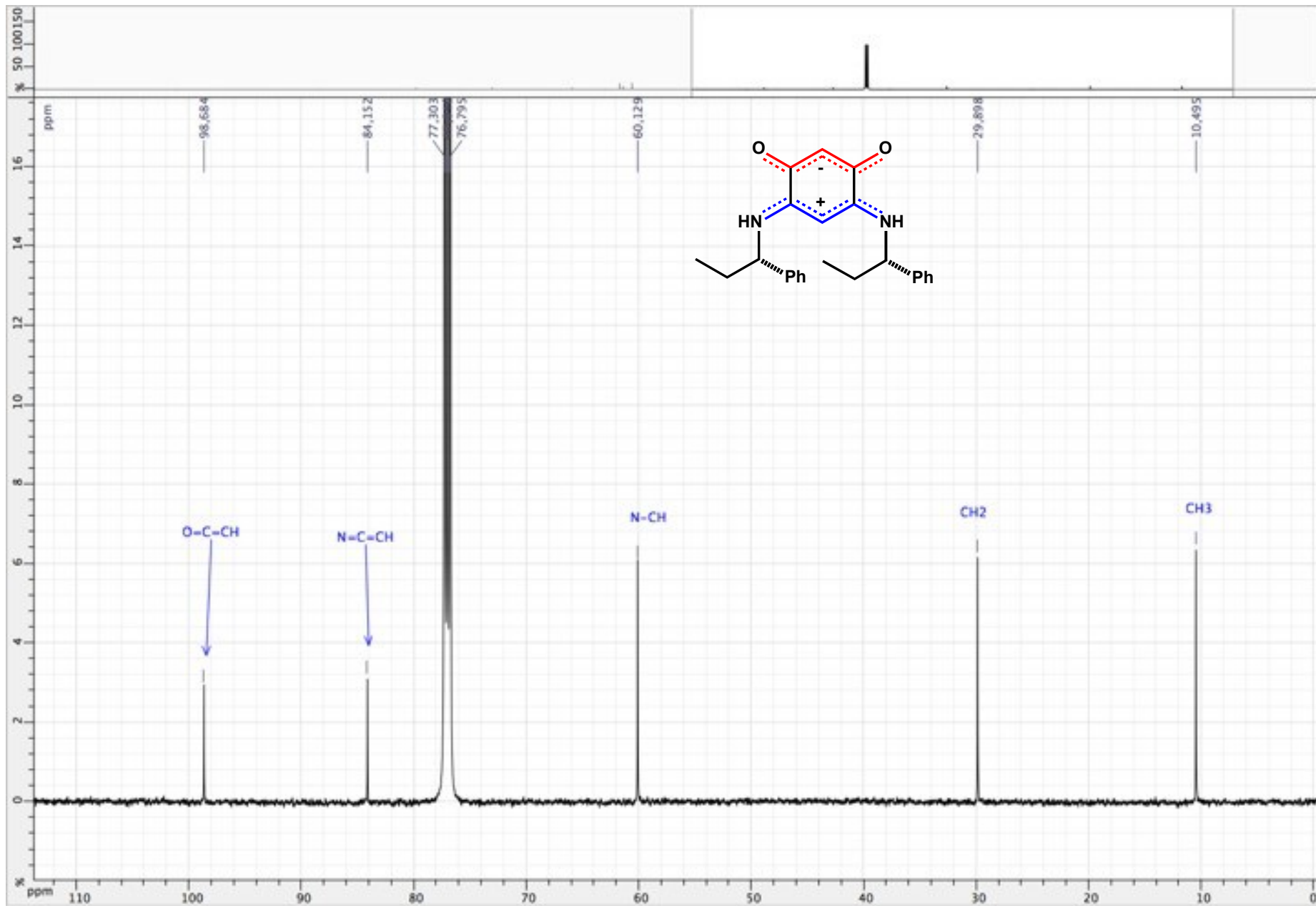


Figure S90. HSQC ($^1\text{H} / ^{13}\text{C} \{^1\text{H}\}$) spectrum of zwitterion **13** (CDCl_3 ; 500 / 125 MHz)

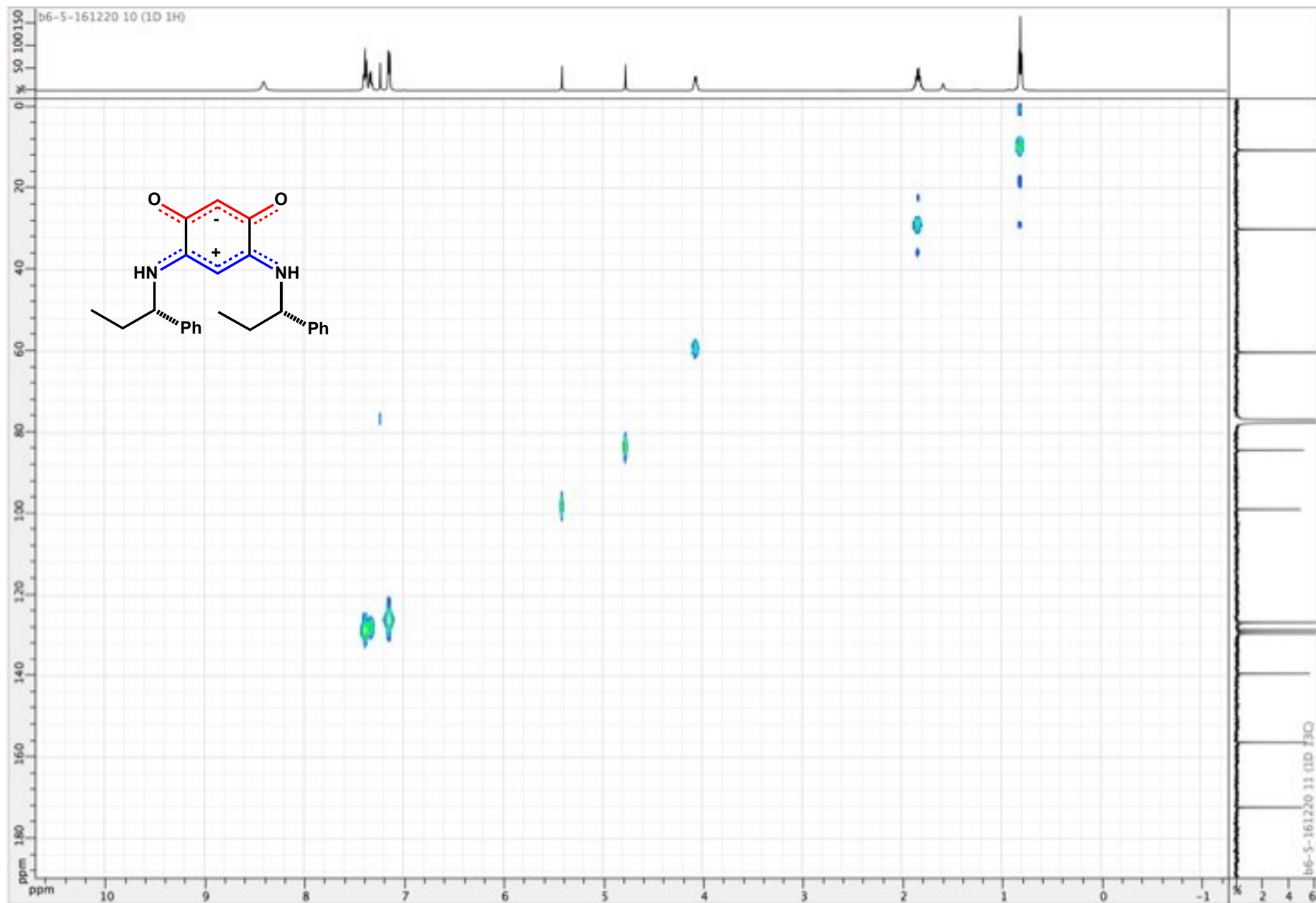


Figure S91. IR spectra of zwitterion **13**. a) IR spectrum of **13** in the solid state; b) IR spectrum of the gold surface functionalized by **13**.

Zwitterion **13**

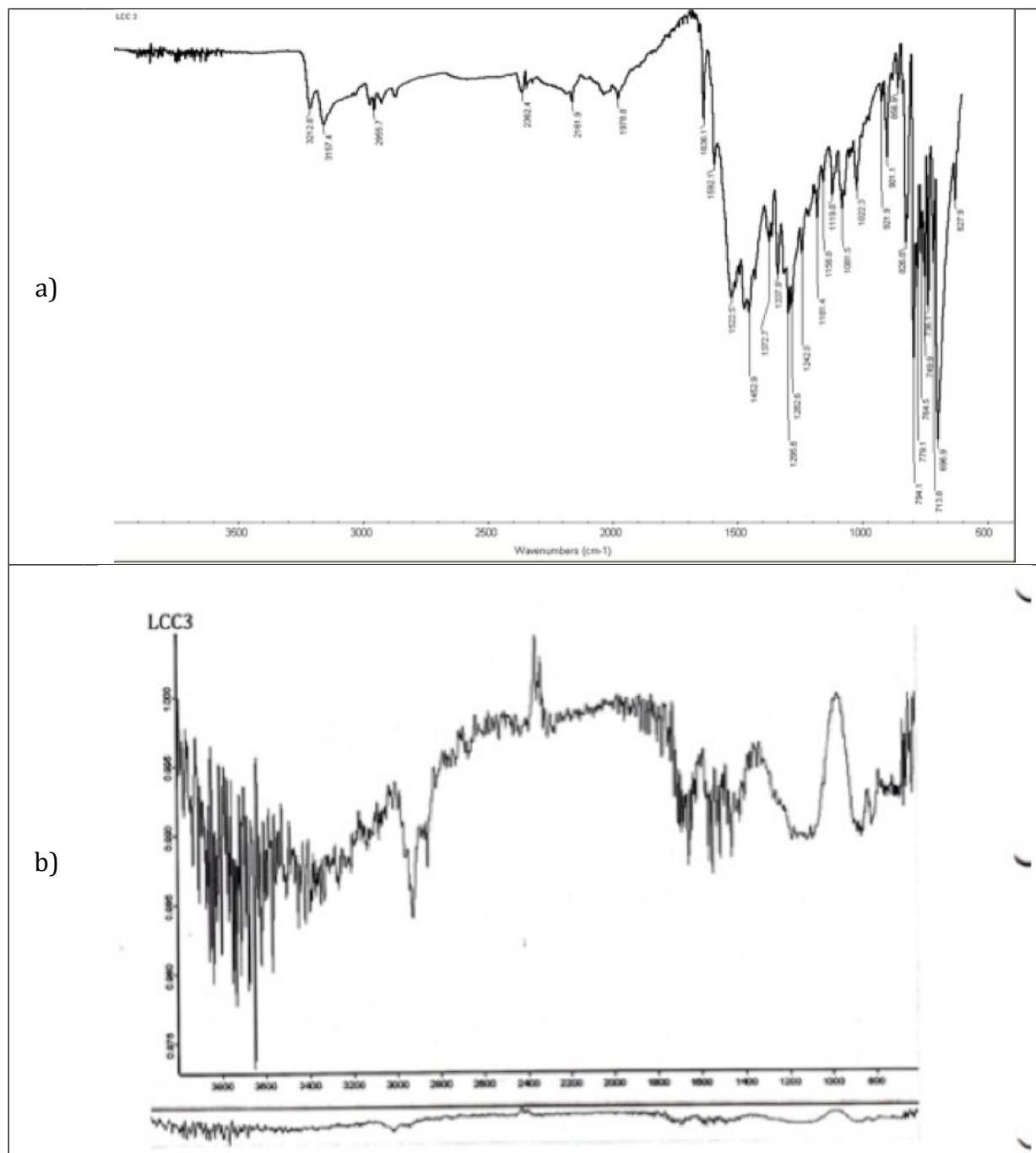
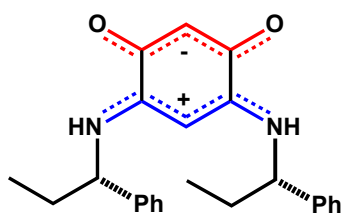


Figure S92. ¹H NMR spectrum of zwitterion 14 (DMSO d6 ; 500 MHz)

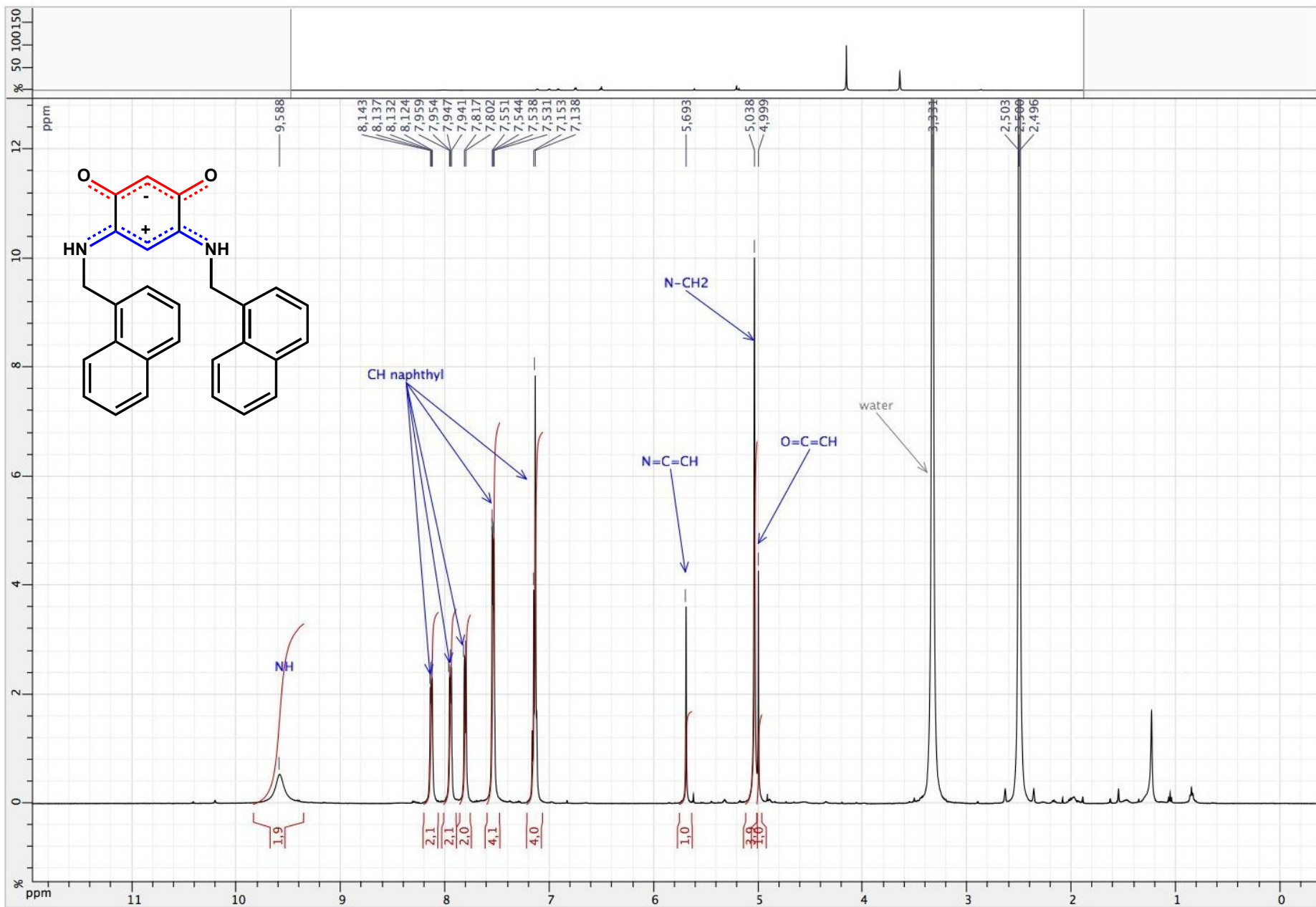


Figure S93. ^1H NMR spectrum of zwitterion **14** (DMSO d_6 ; 500 MHz)

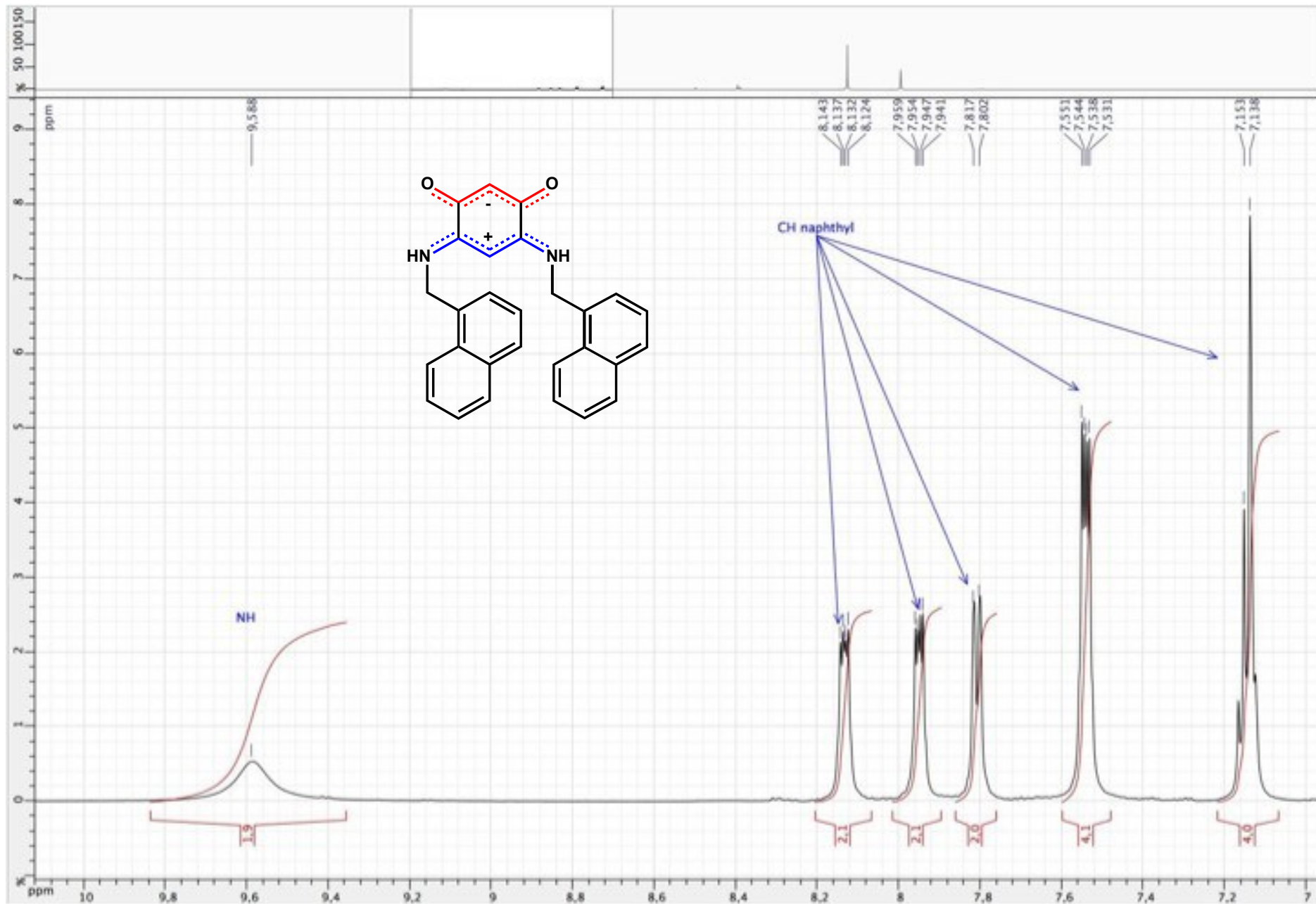


Figure S94. ¹H NMR spectrum of zwitterion **14** (DMSO d₆ ; 500 MHz)

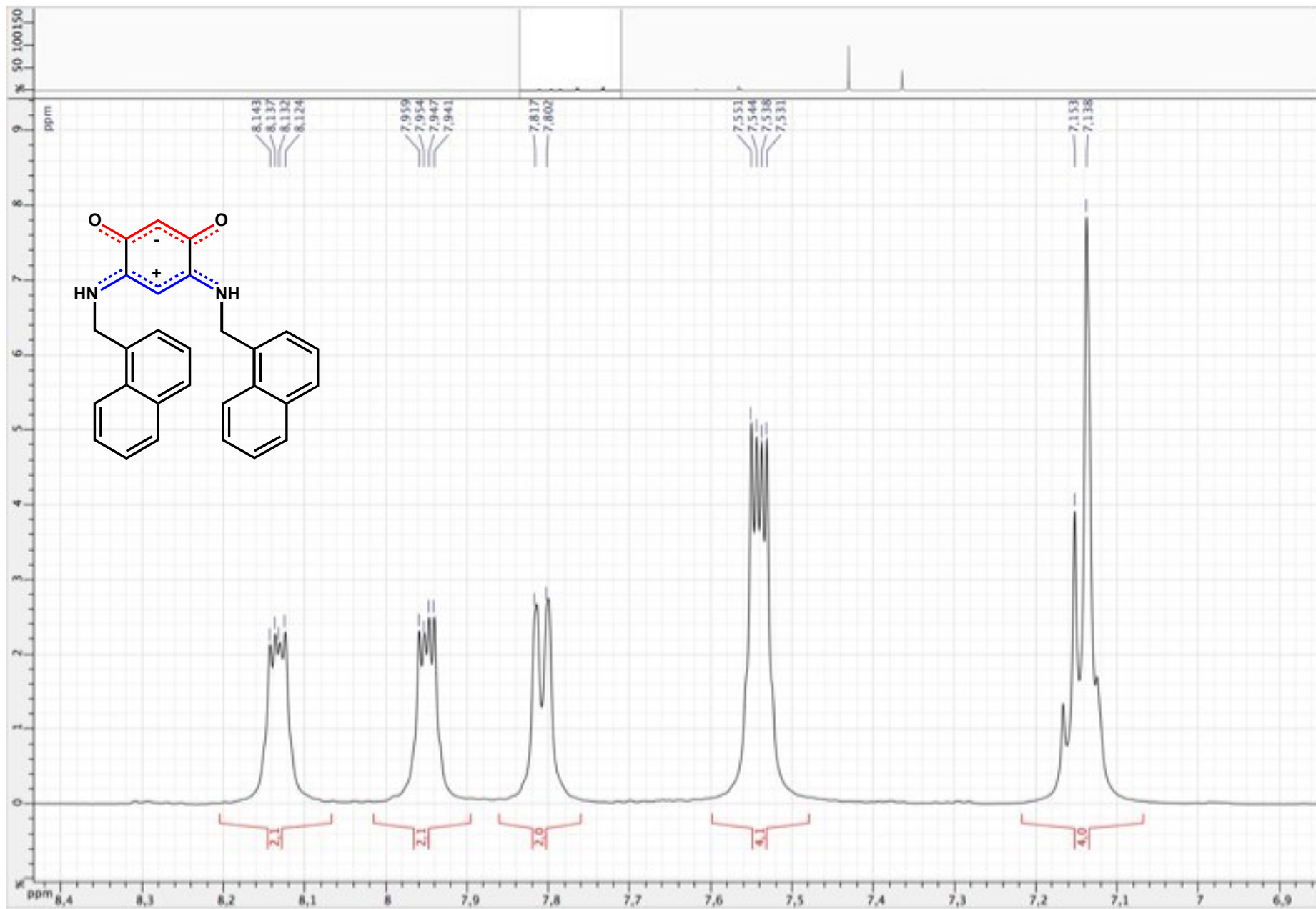


Figure S95. ^1H NMR spectrum of zwitterion **14** (DMSO d_6 ; 500 MHz)

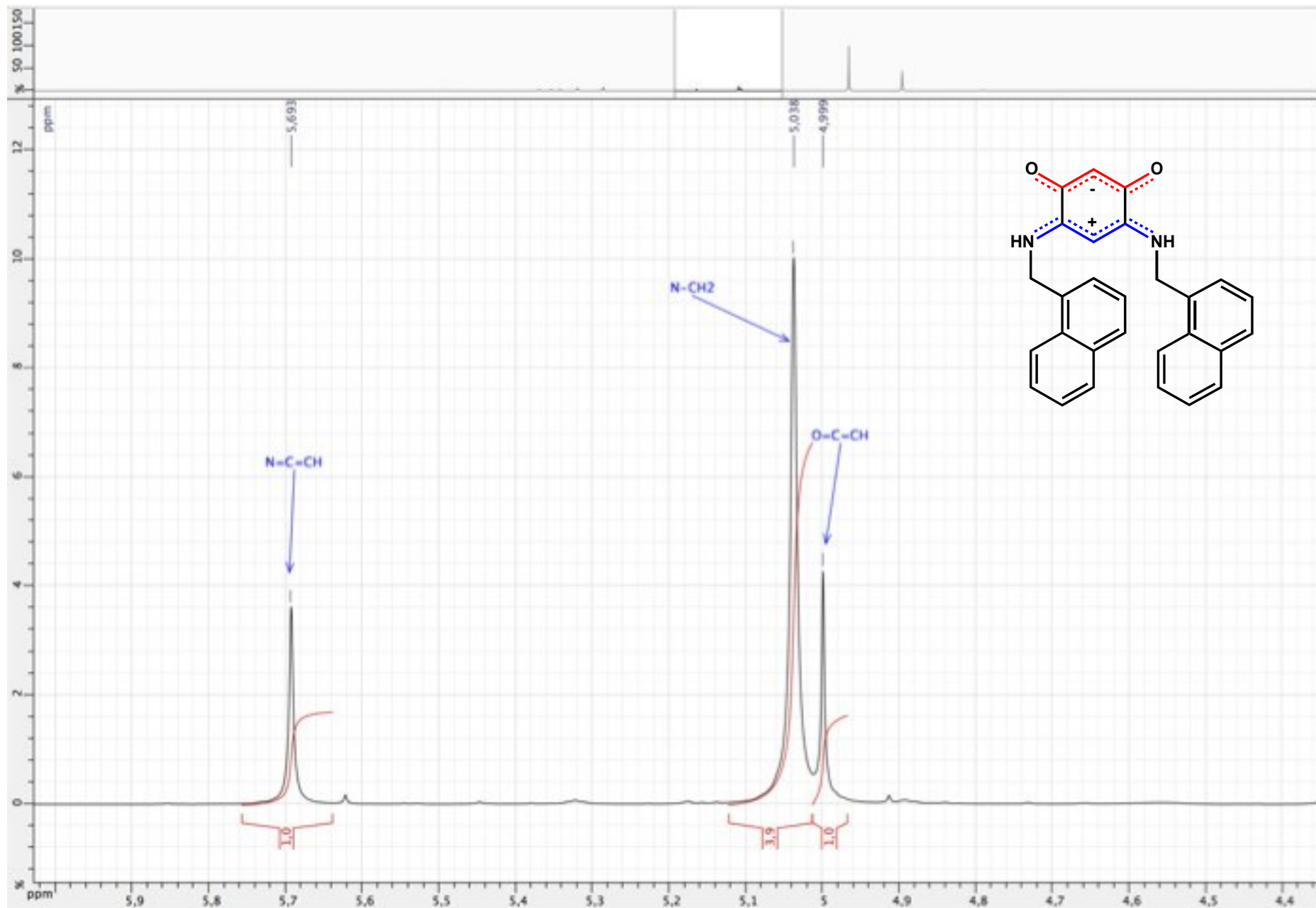


Figure S96. ^{13}C $\{^1\text{H}\}$ NMR spectrum of zwitterion **14** (DMSO d_6 ; 125 MHz)

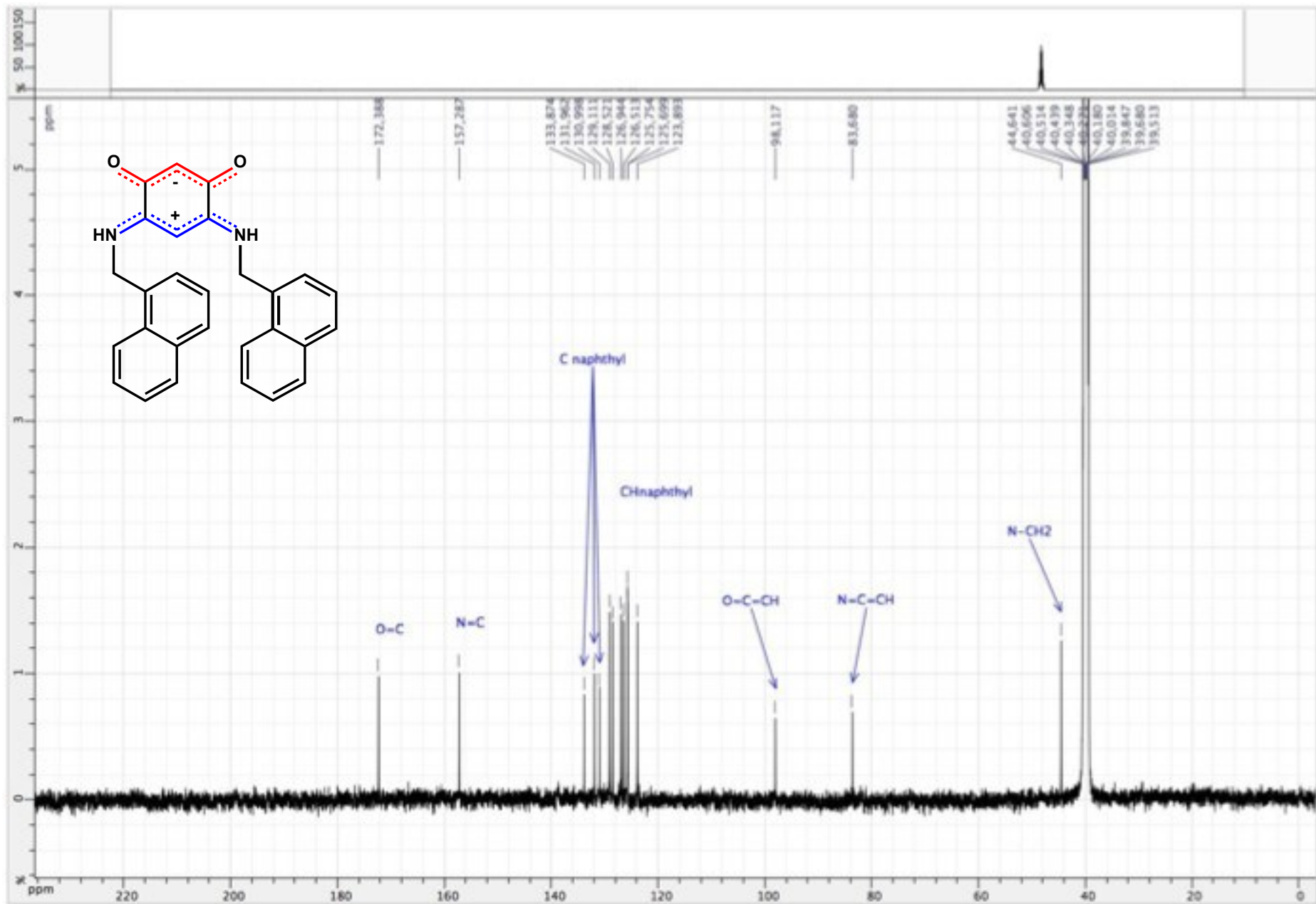


Figure S97. ^{13}C $\{^1\text{H}\}$ NMR spectrum of zwitterion **14** (DMSO d_6 ; 125 MHz)

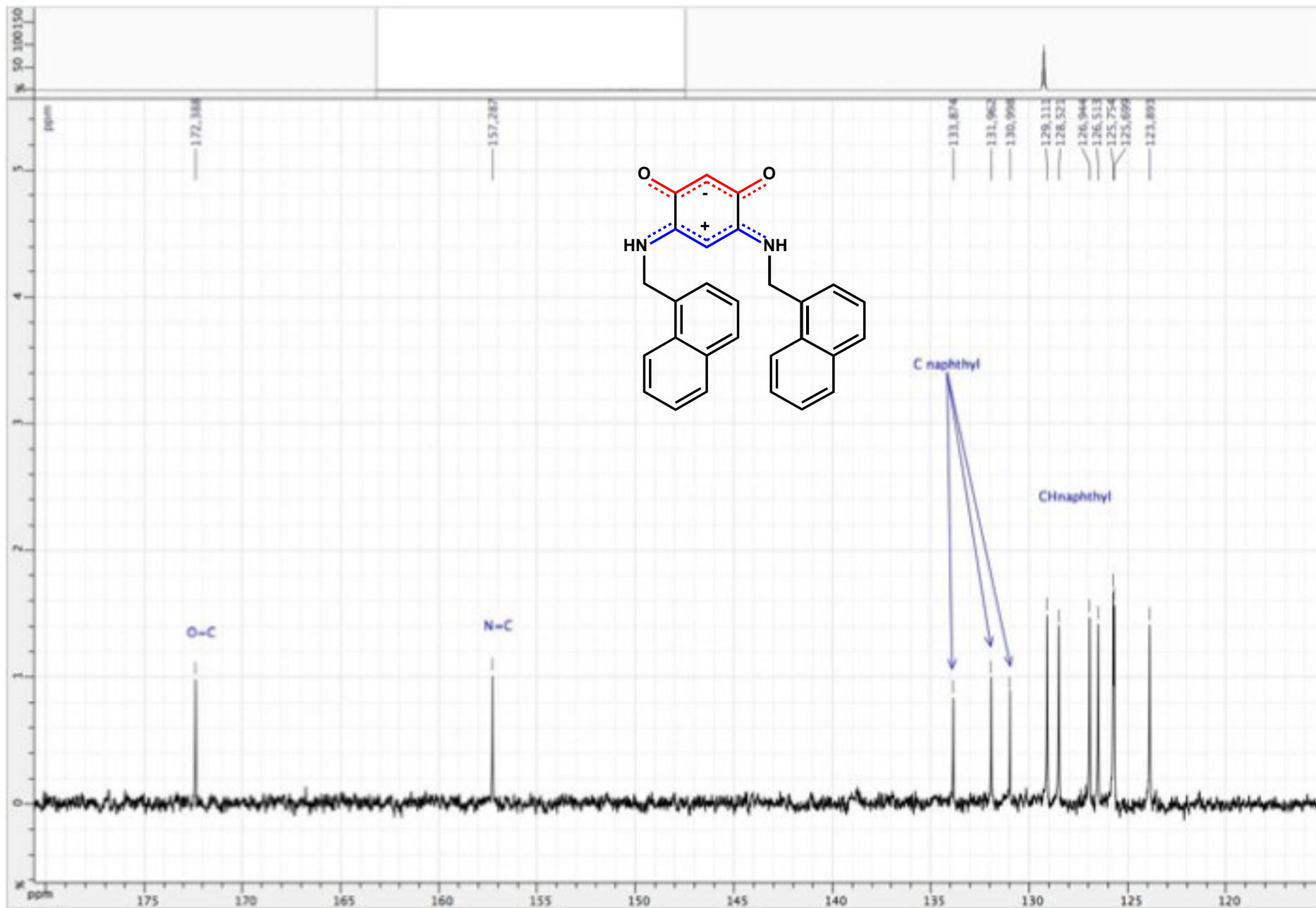


Figure S98. ^{13}C $\{^1\text{H}\}$ NMR spectrum of zwitterion **14** (DMSO d_6 ; 125 MHz)

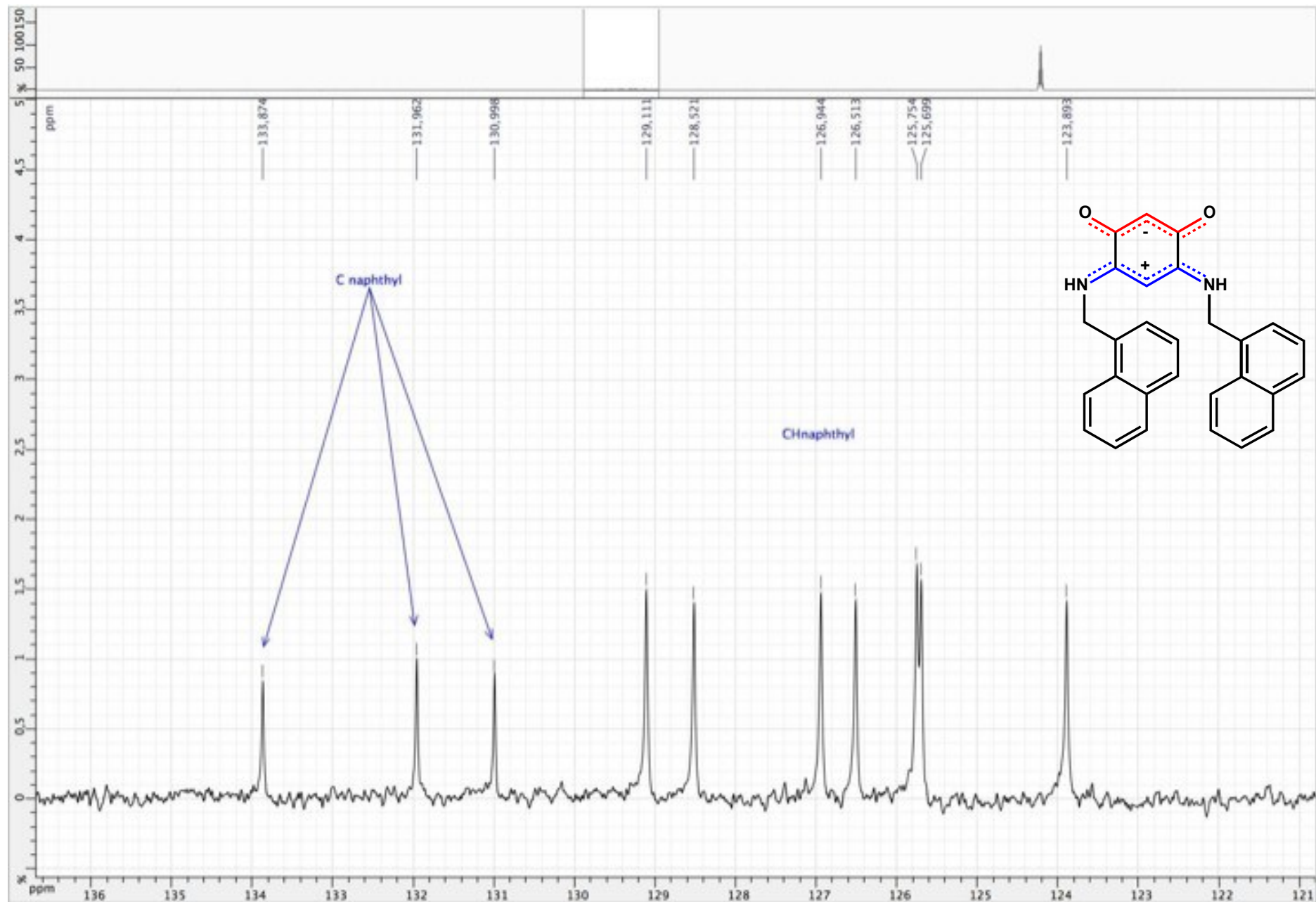


Figure S99. ^{13}C $\{^1\text{H}\}$ NMR spectrum of zwitterion **14** (DMSO d_6 ; 125 MHz)

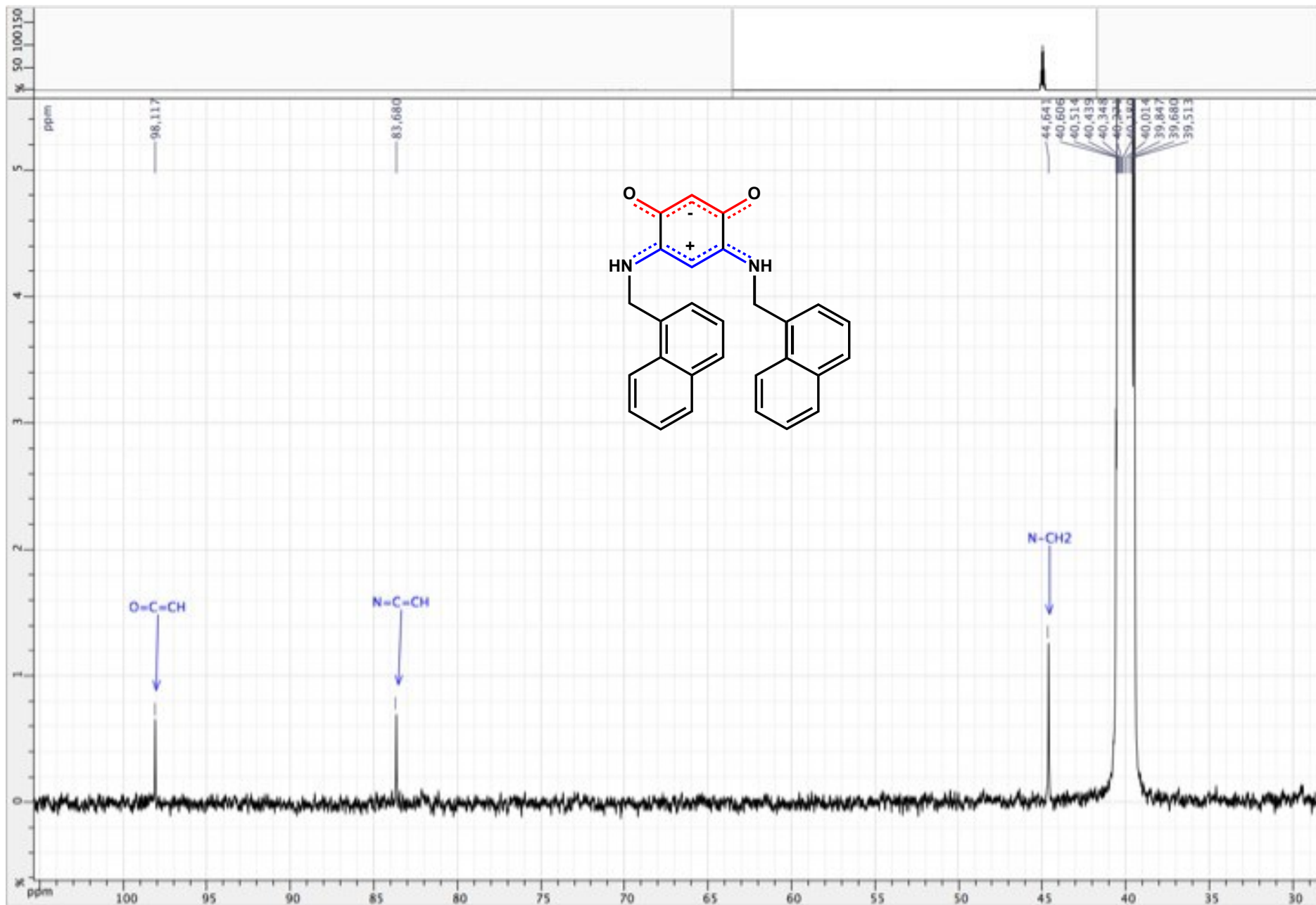


Figure S100. HSQC ($^1\text{H} / ^{13}\text{C} \{^1\text{H}\}$) spectrum of zwitterion **14** (DMSO d_6 ; 500 / 125 MHz)

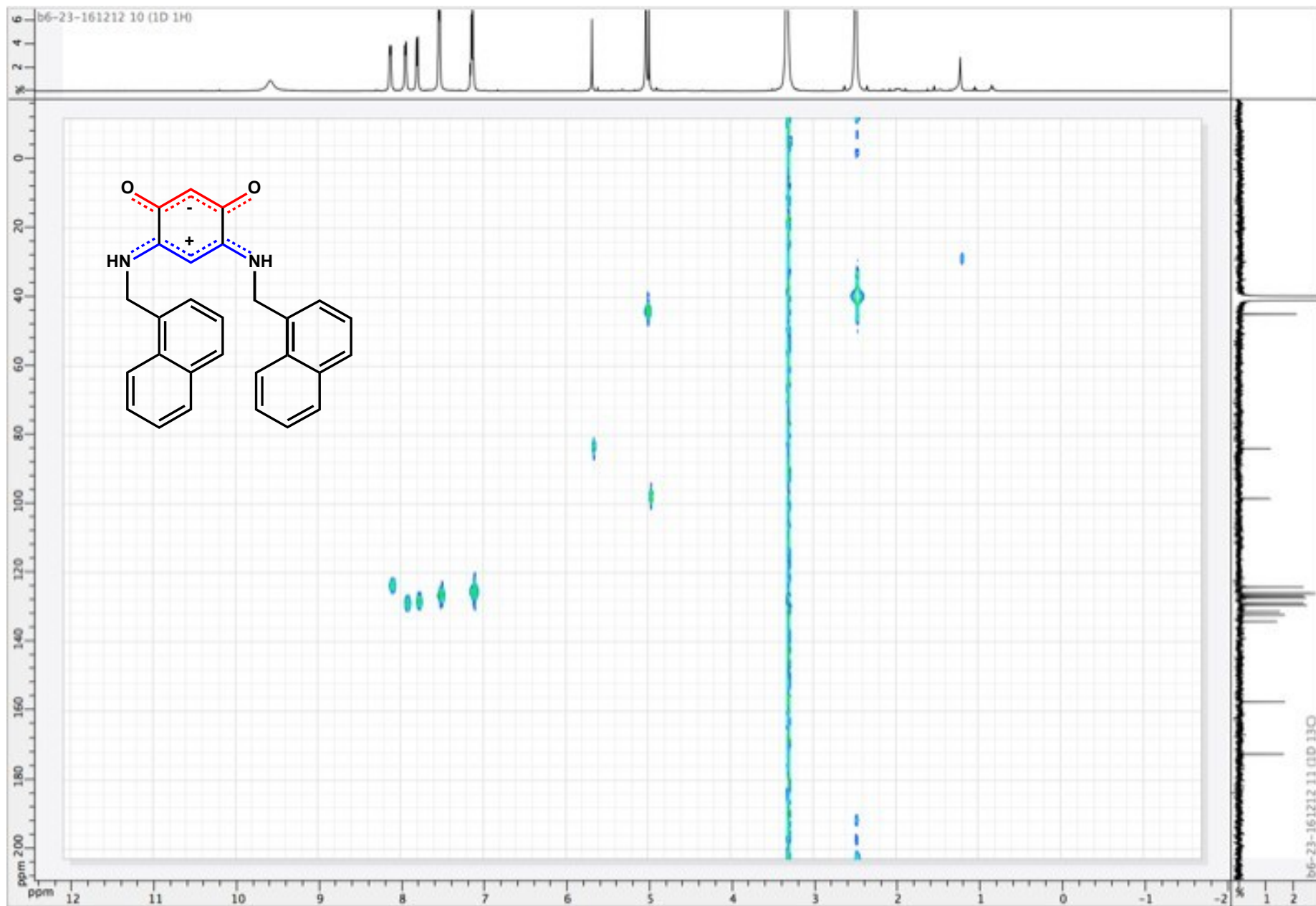


Figure S102. COSY ($^1\text{H} / ^1\text{H}$) spectrum of zwitterion **14** (DMSO d_6 ; 500 MHz)

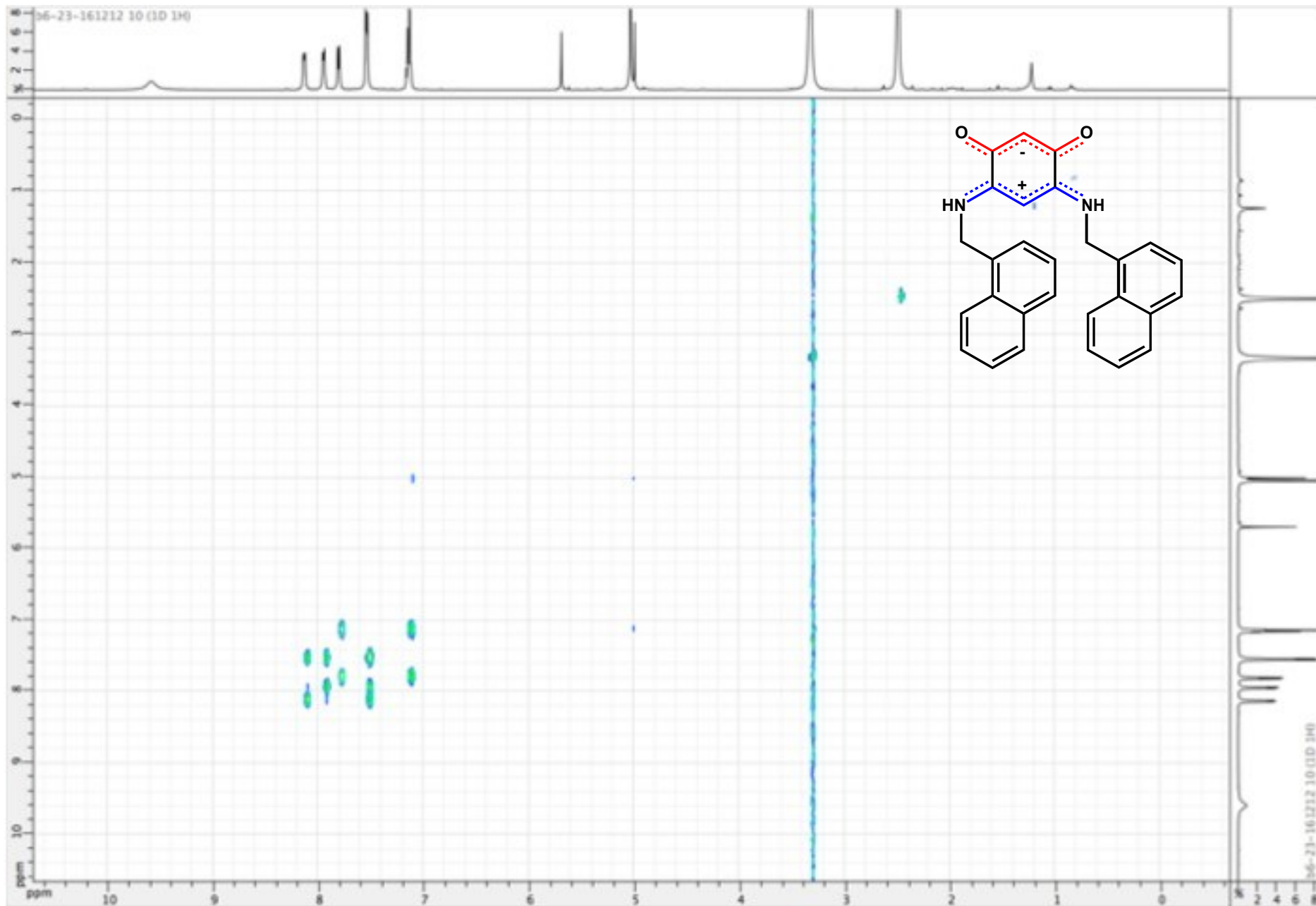


Figure S103. COSY ($^1\text{H} / ^1\text{H}$) spectrum of zwitterion **14** (DMSO d_6 ; 500 MHz)

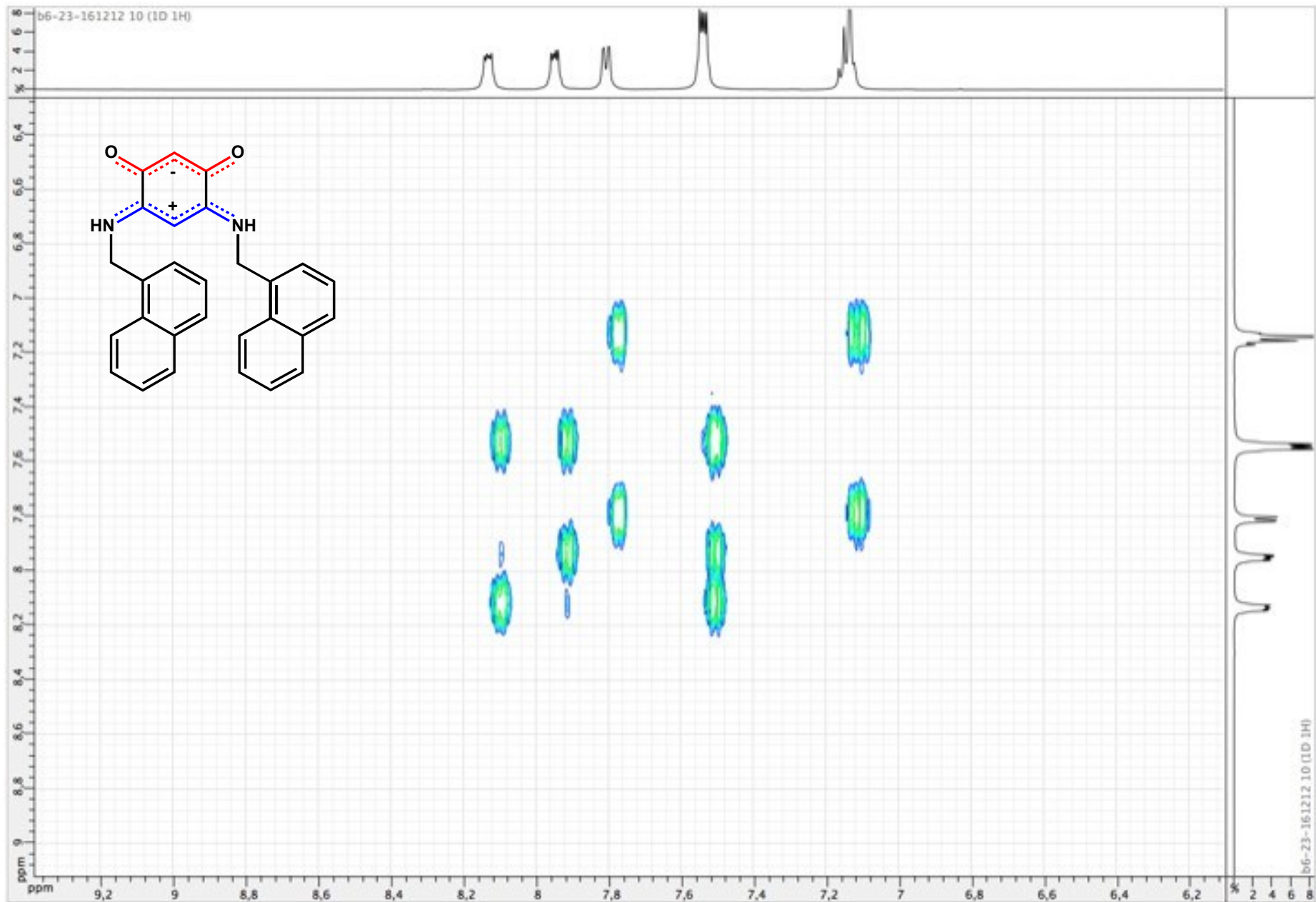


Figure S104. ^1H NMR spectrum of zwitterion **15** (CDCl_3 ; 500 MHz)

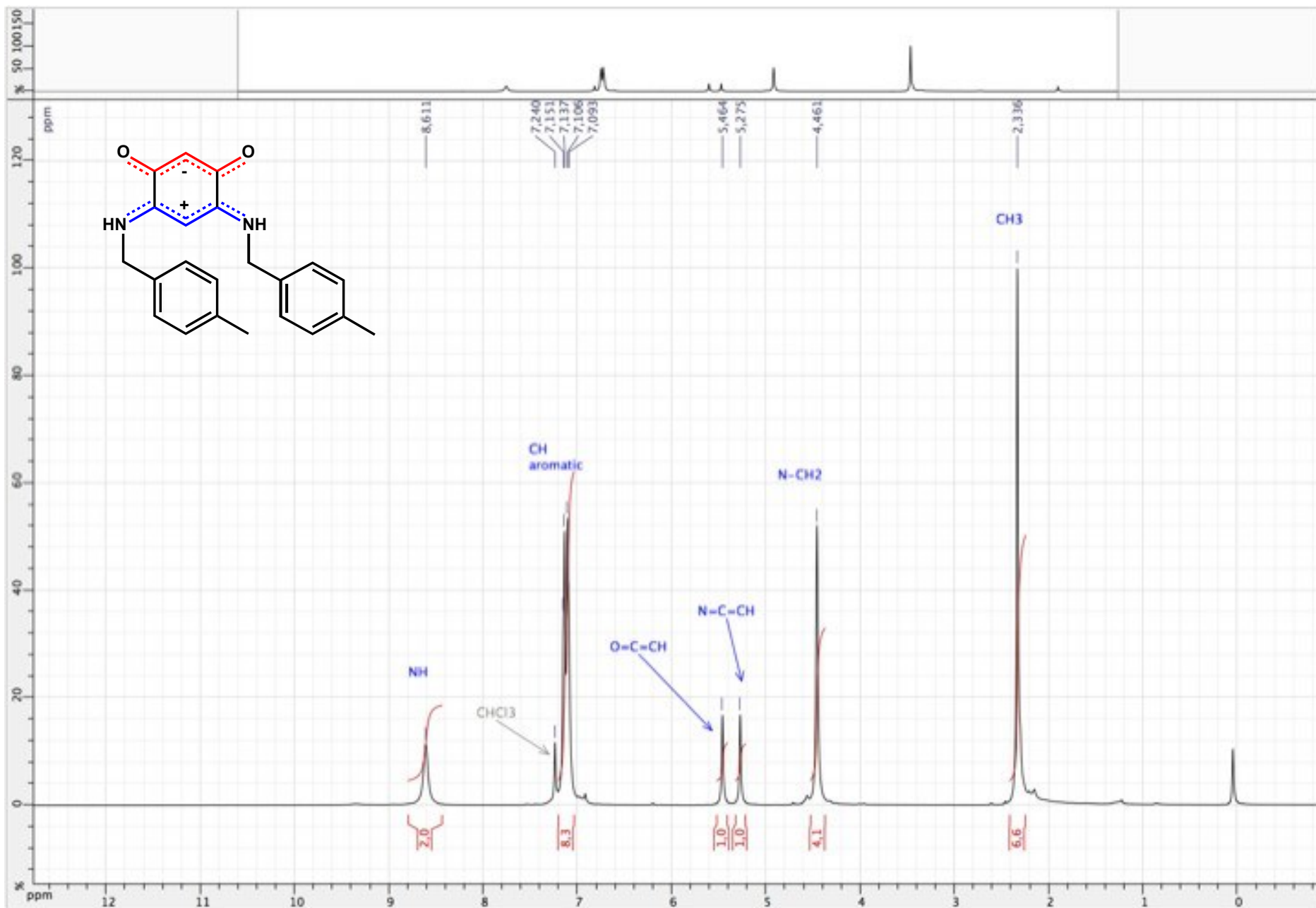


Figure S105. ^1H NMR spectrum of zwitterion **15** (CDCl_3 ; 500 MHz)

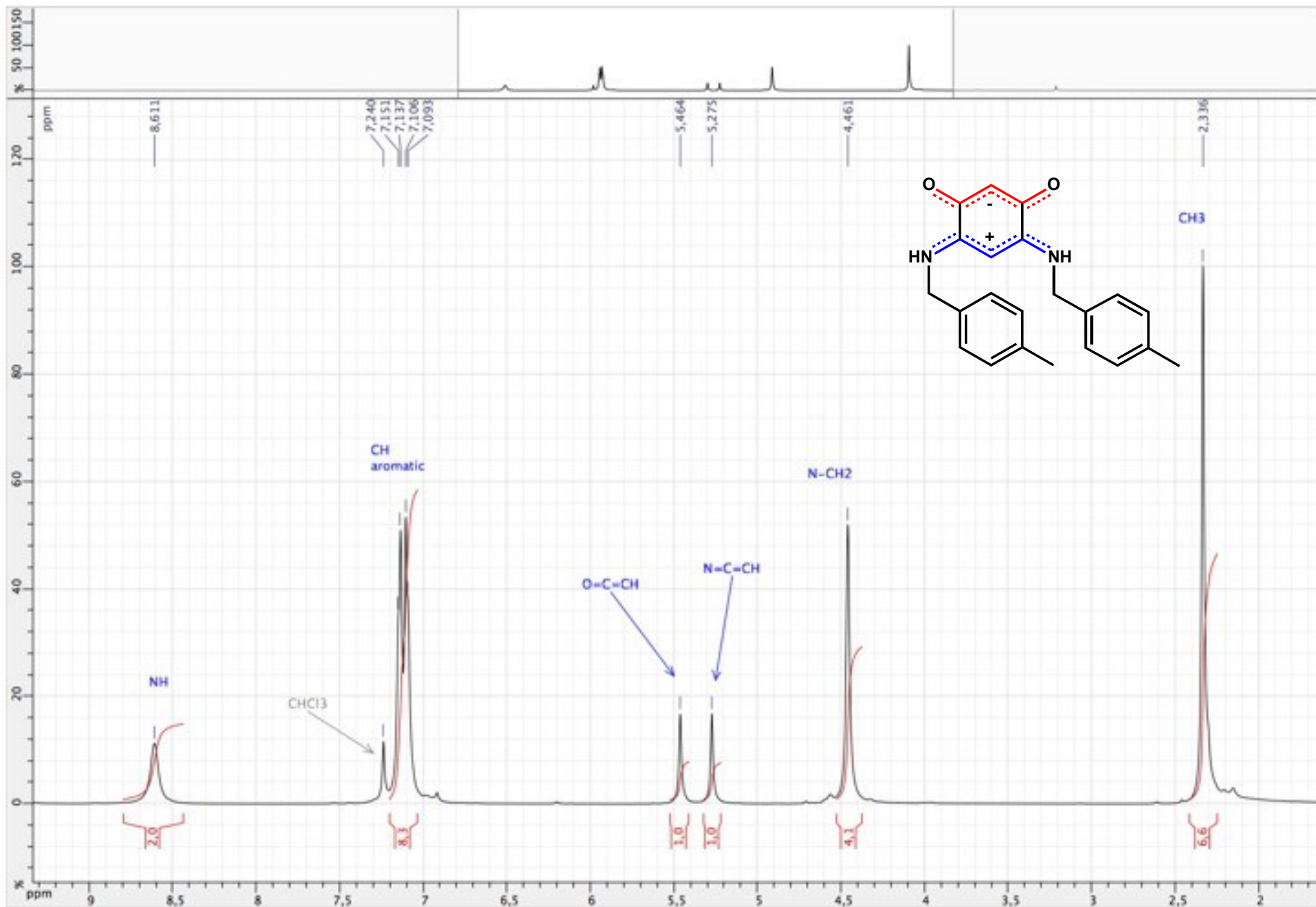


Figure S106. ^{13}C $\{^1\text{H}\}$ NMR spectrum of zwitterion **15** (CDCl_3 ; 125 MHz)

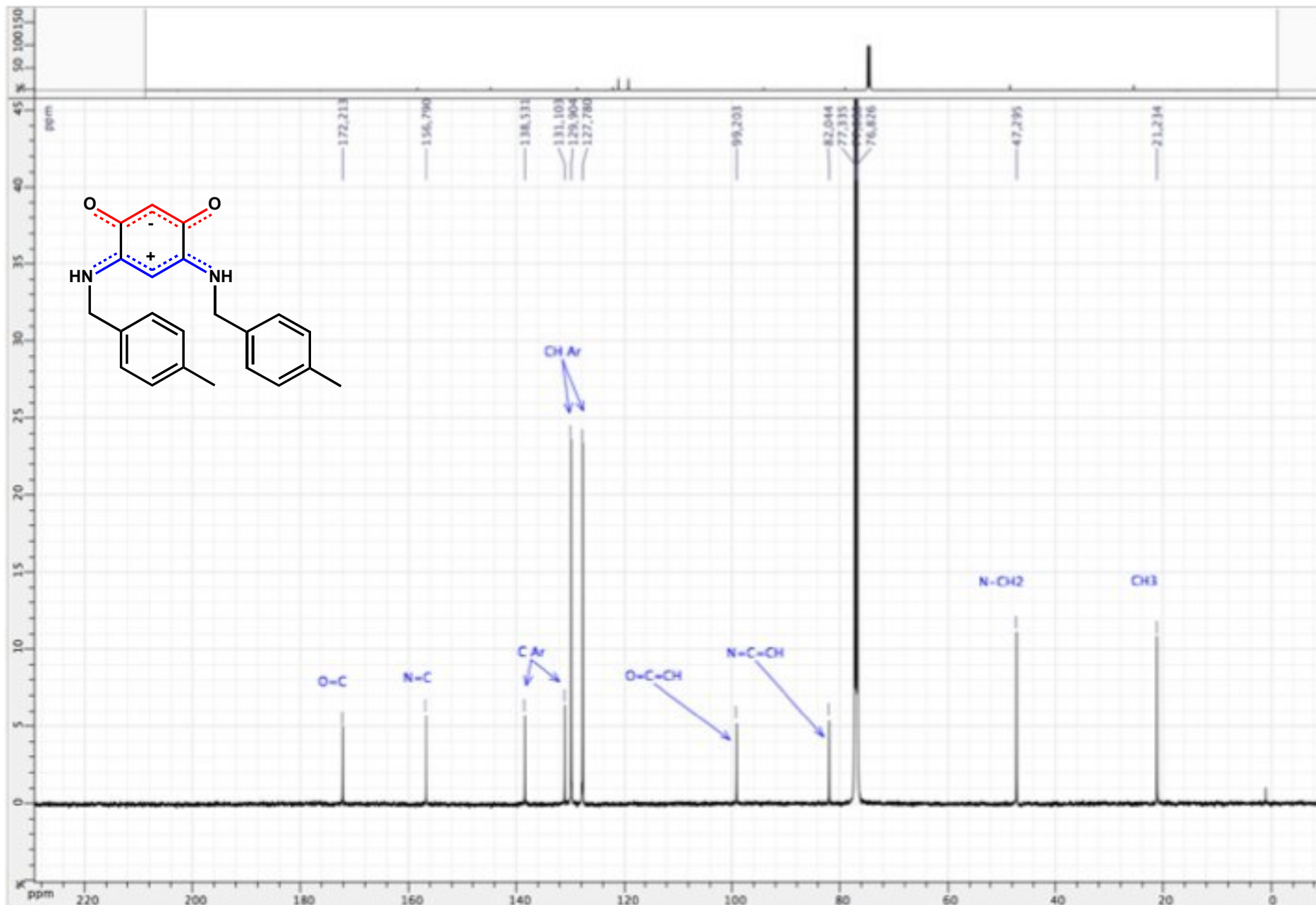


Figure S107. ^{13}C $\{^1\text{H}\}$ NMR spectrum of zwitterion **15** (CDCl_3 ; 125 MHz)

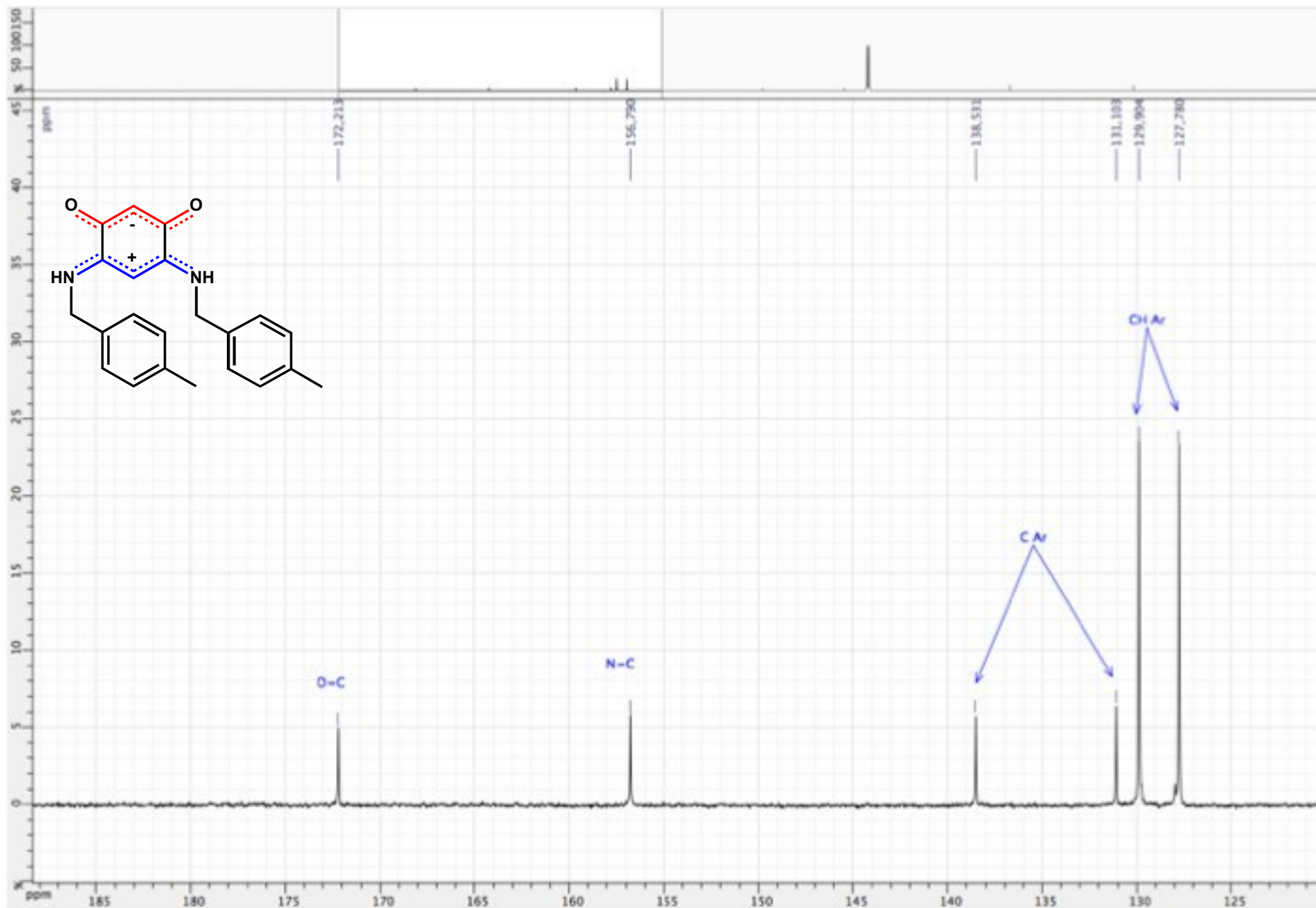


Figure S108. ^{13}C $\{^1\text{H}\}$ NMR spectrum of zwitterion **15** (CDCl_3 ; 125 MHz)

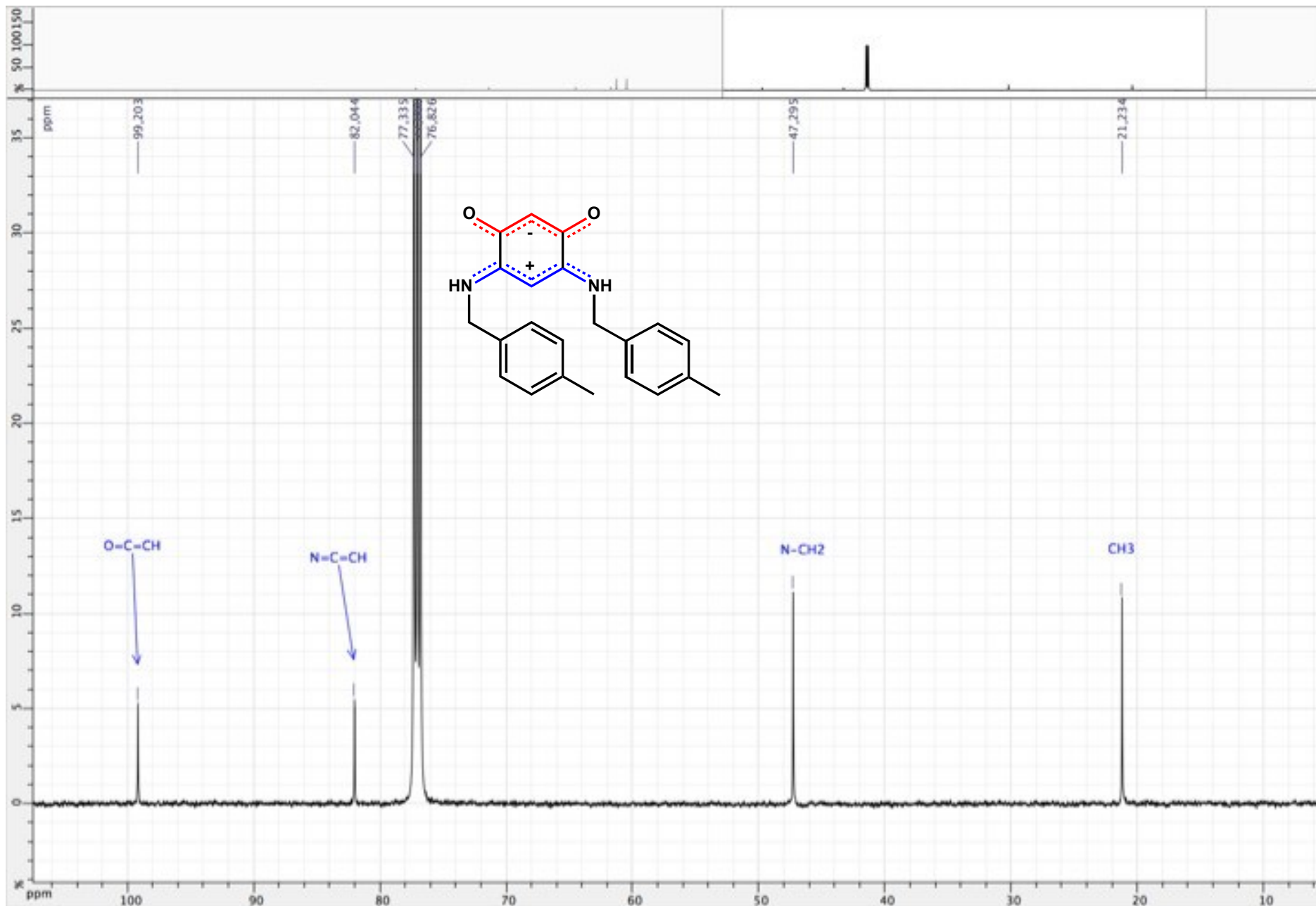


Figure S109. ¹H NMR spectrum of zwitterion 16 (DMSO d6 ; 500 MHz)

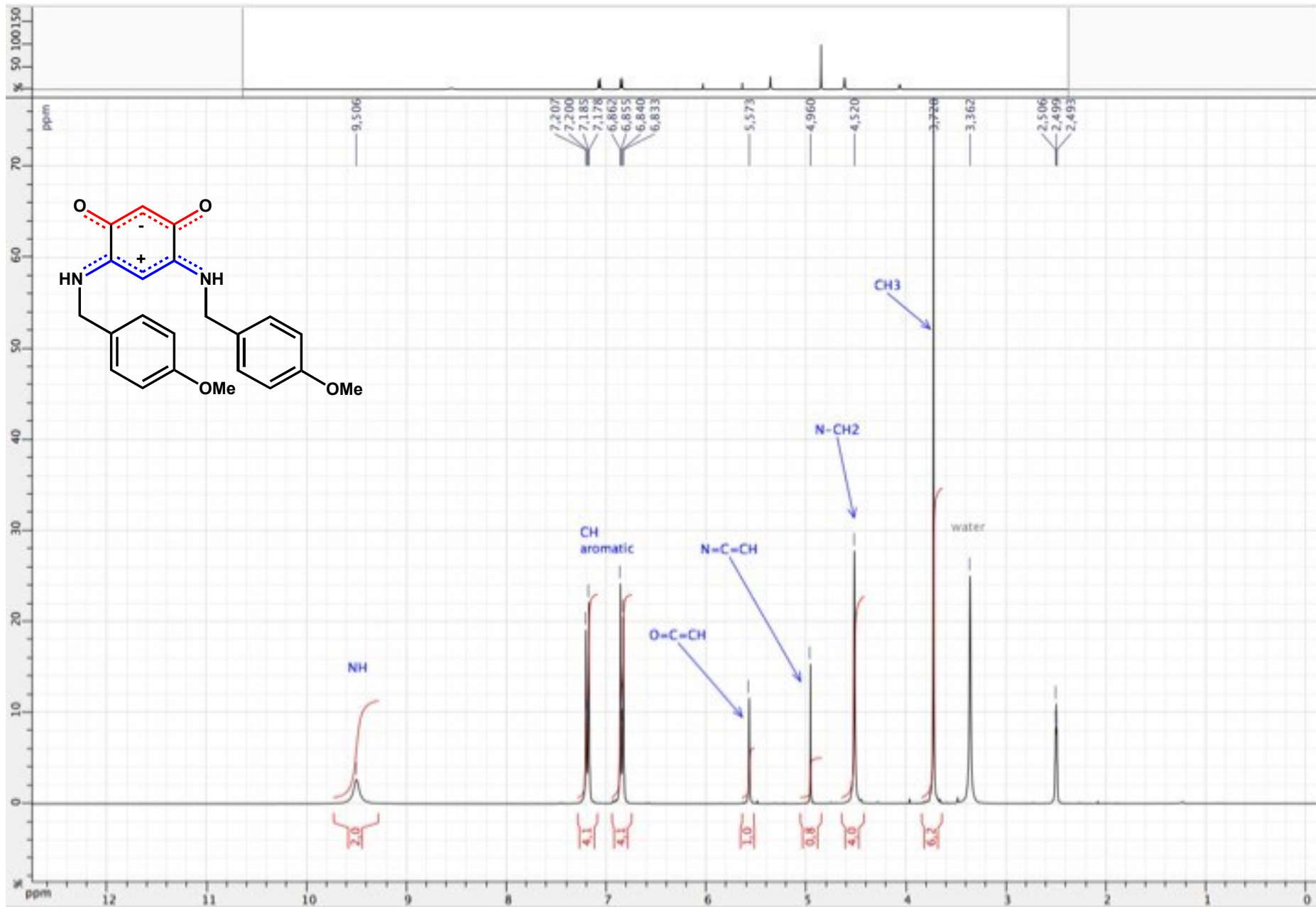


Figure S110. ¹H NMR spectrum of zwitterion **16** (DMSO d₆ ; 500 MHz)

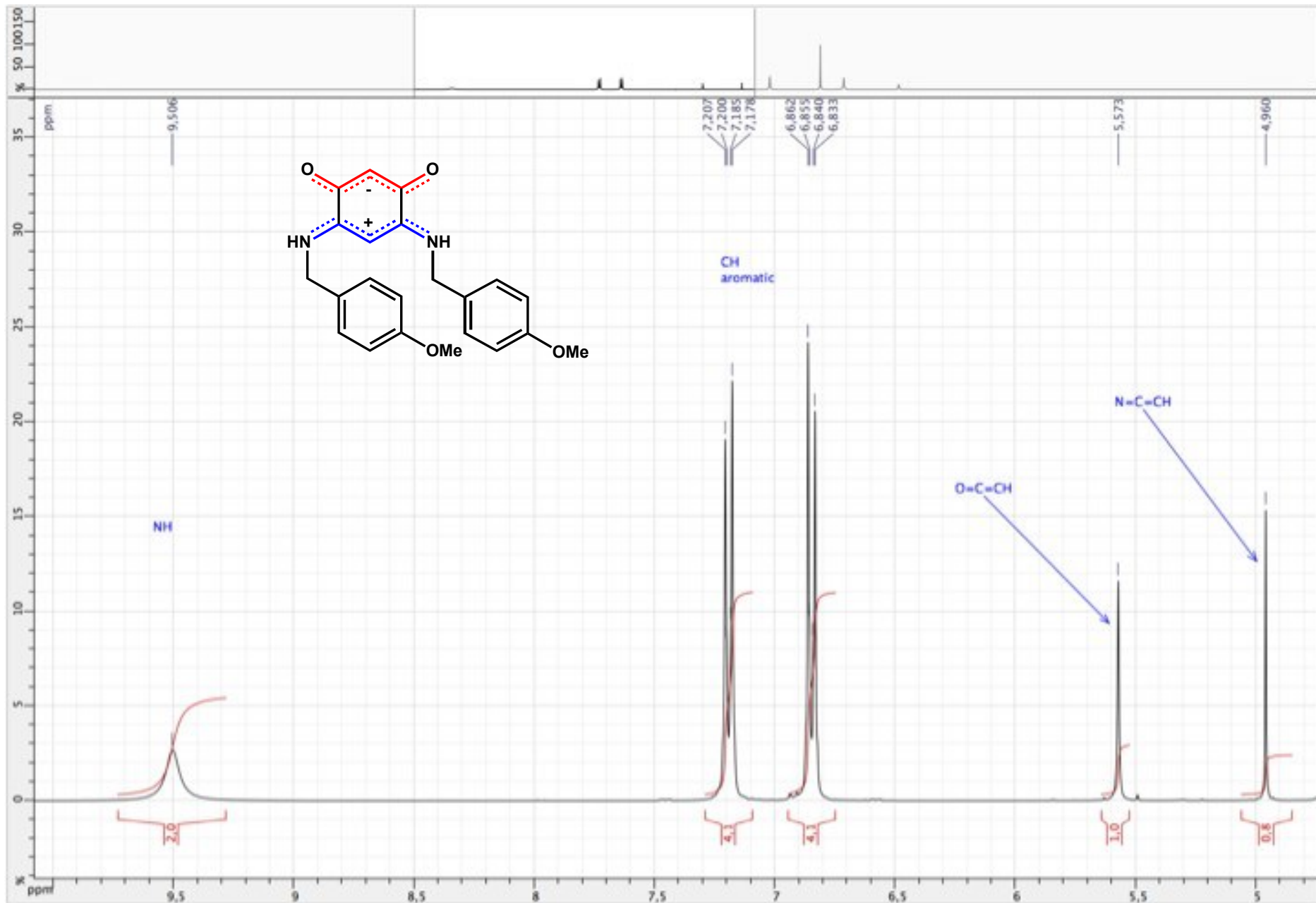


Figure S111. ¹H NMR spectrum of zwitterion 16 (DMSO d₆ ; 500 MHz)

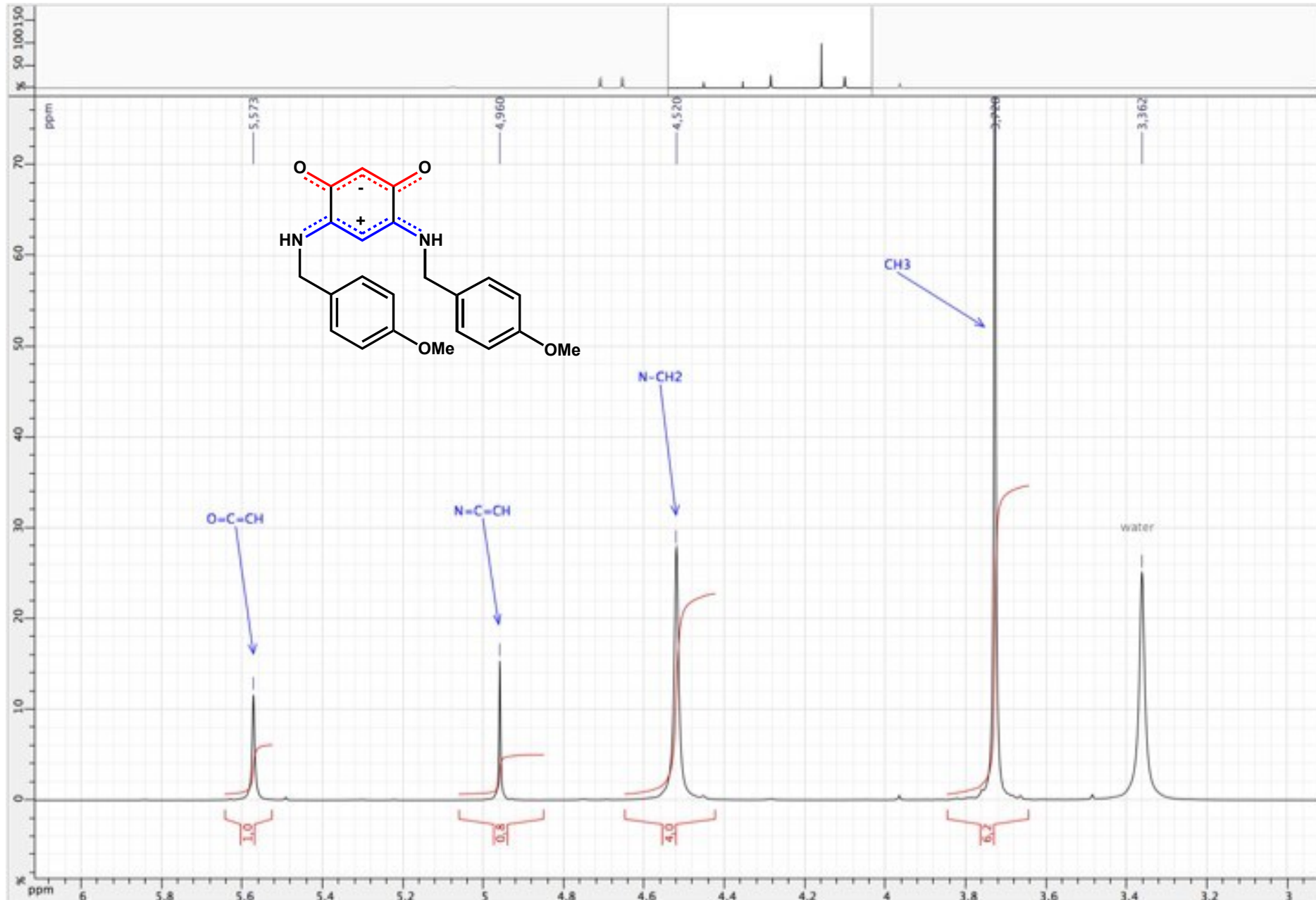


Figure S112. ^{13}C $\{^1\text{H}\}$ NMR spectrum of zwitterion **16** (DMSO d_6 ; 125 MHz)

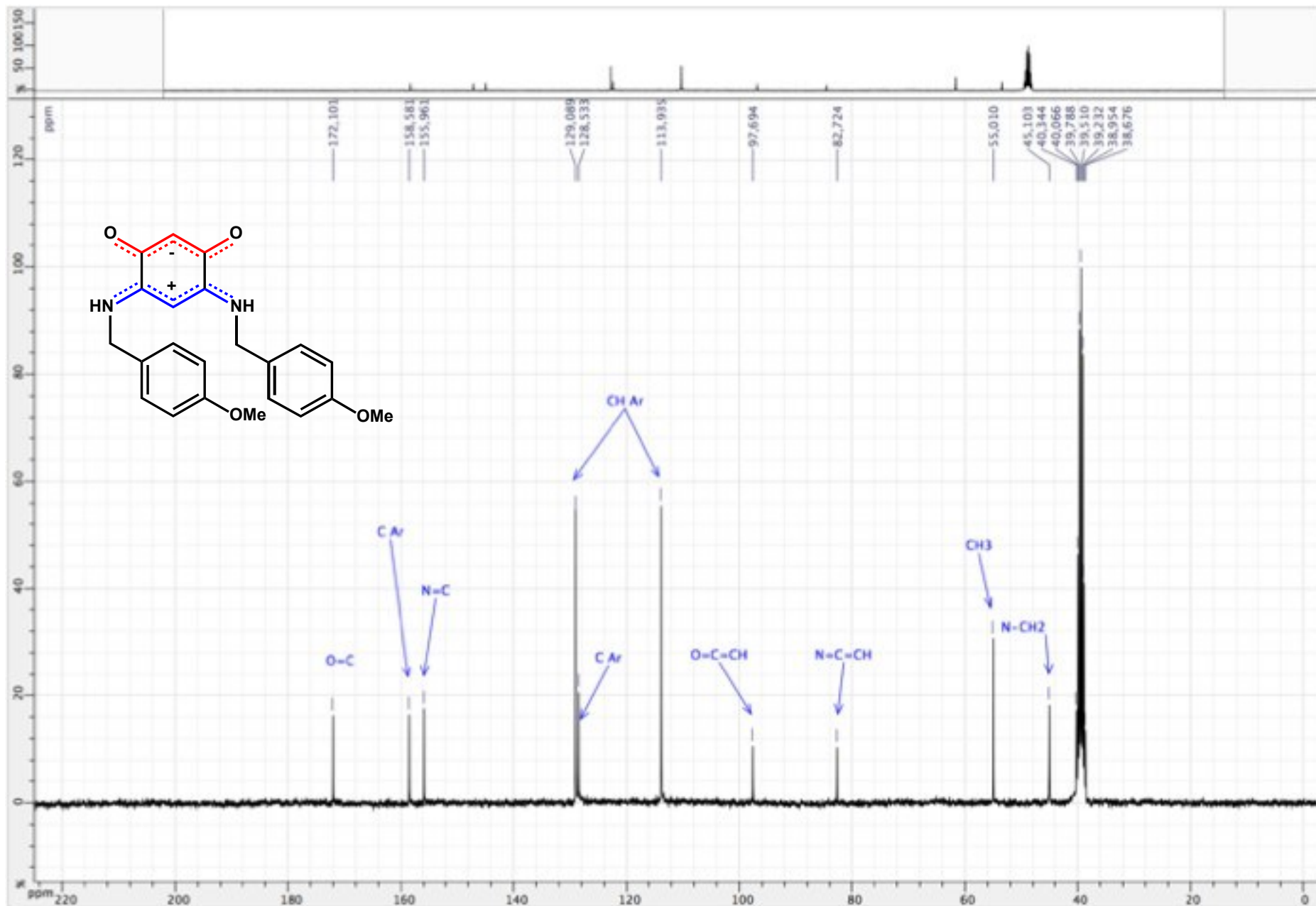


Figure S113. ^{13}C $\{^1\text{H}\}$ NMR spectrum of zwitterion **16** (DMSO d_6 ; 125 MHz)

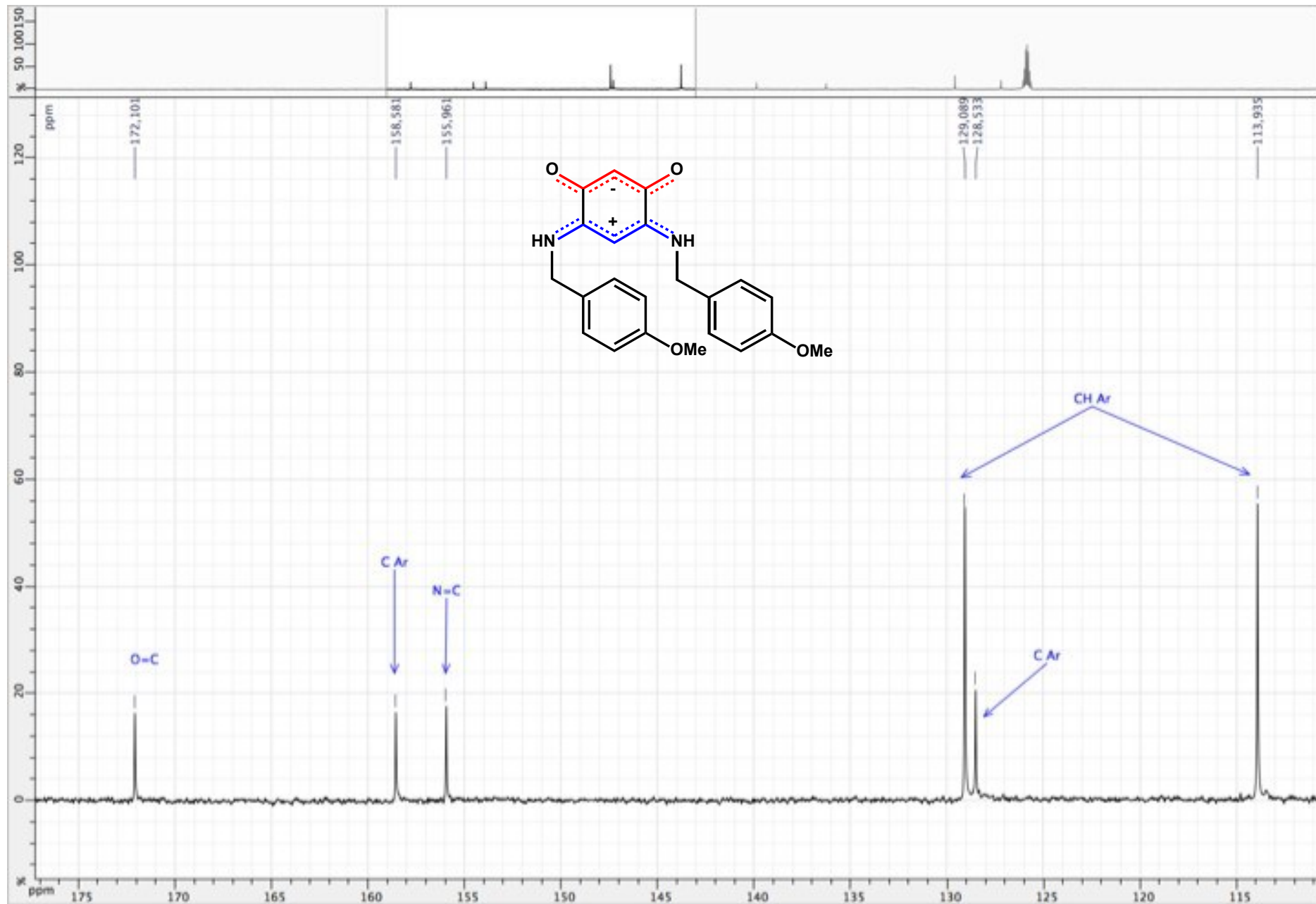


Figure S114. ^{13}C $\{^1\text{H}\}$ NMR spectrum of zwitterion **16** (DMSO d_6 ; 125 MHz)

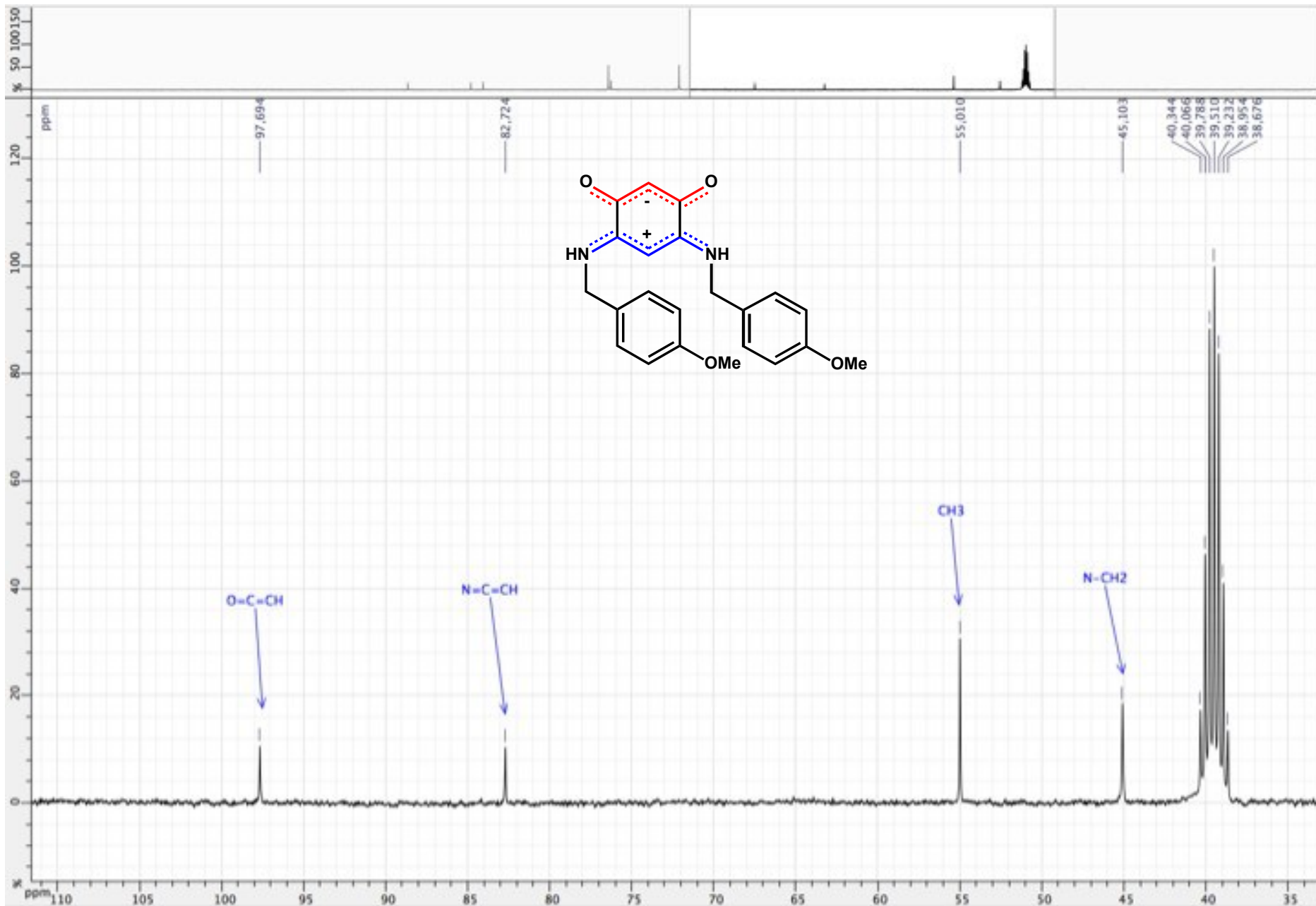


Figure S115. ¹H NMR spectrum of zwitterion 17 (DMSO d₆ ; 500 MHz)

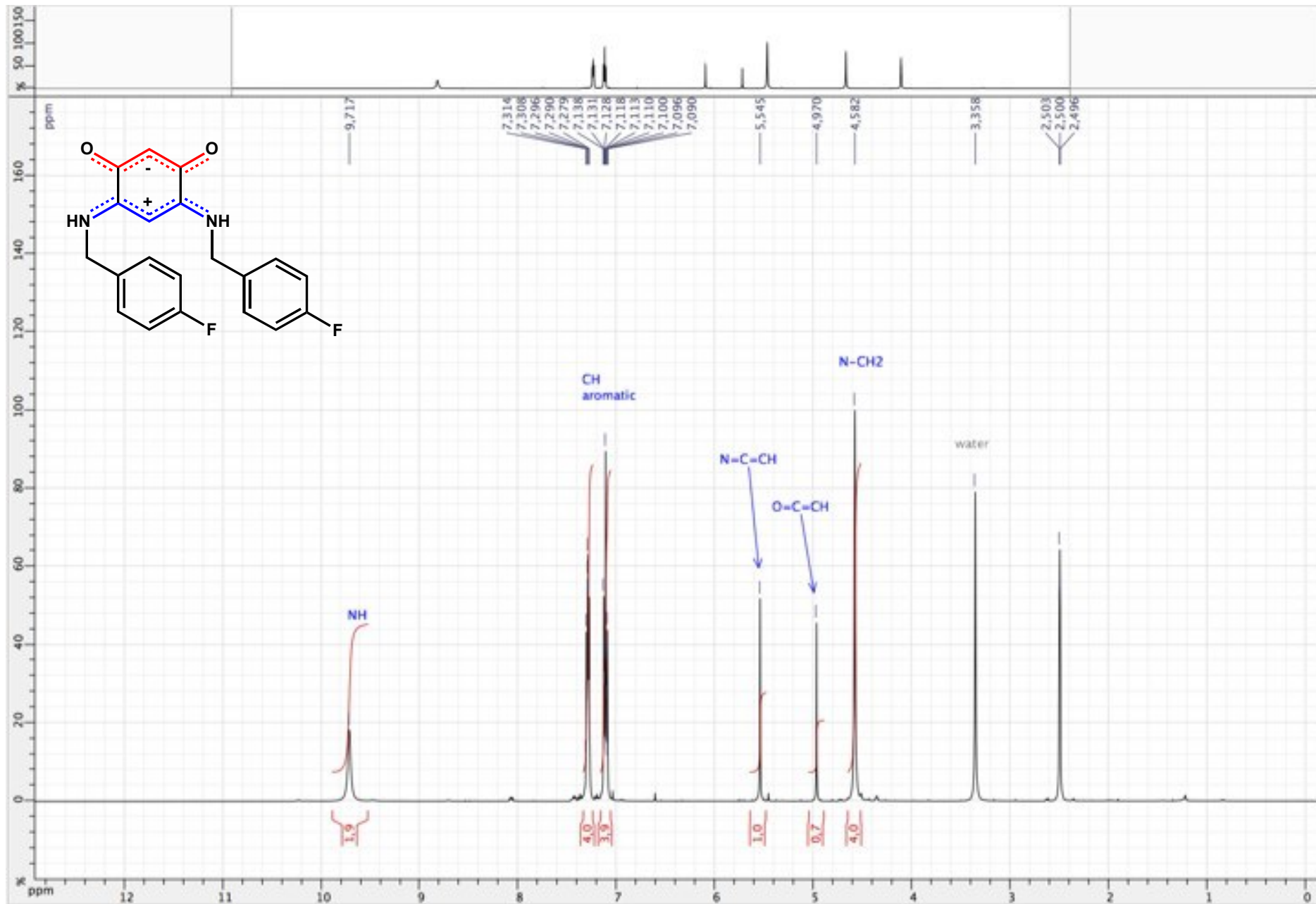


Figure S116. ¹H NMR spectrum of zwitterion 17 (DMSO d6 ; 500 MHz)

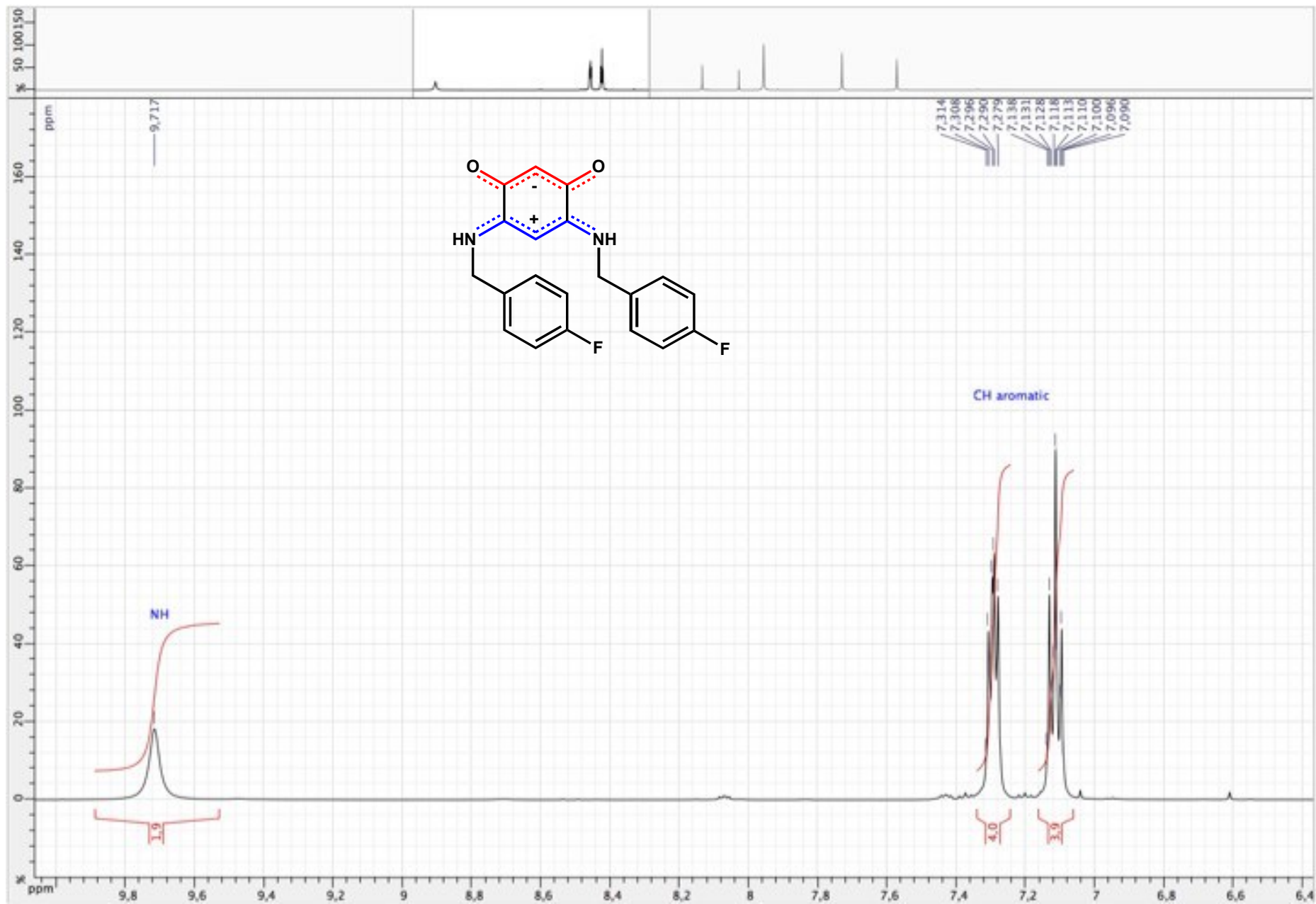


Figure S117. ^1H NMR spectrum of zwitterion **17** (DMSO d_6 ; 500 MHz)

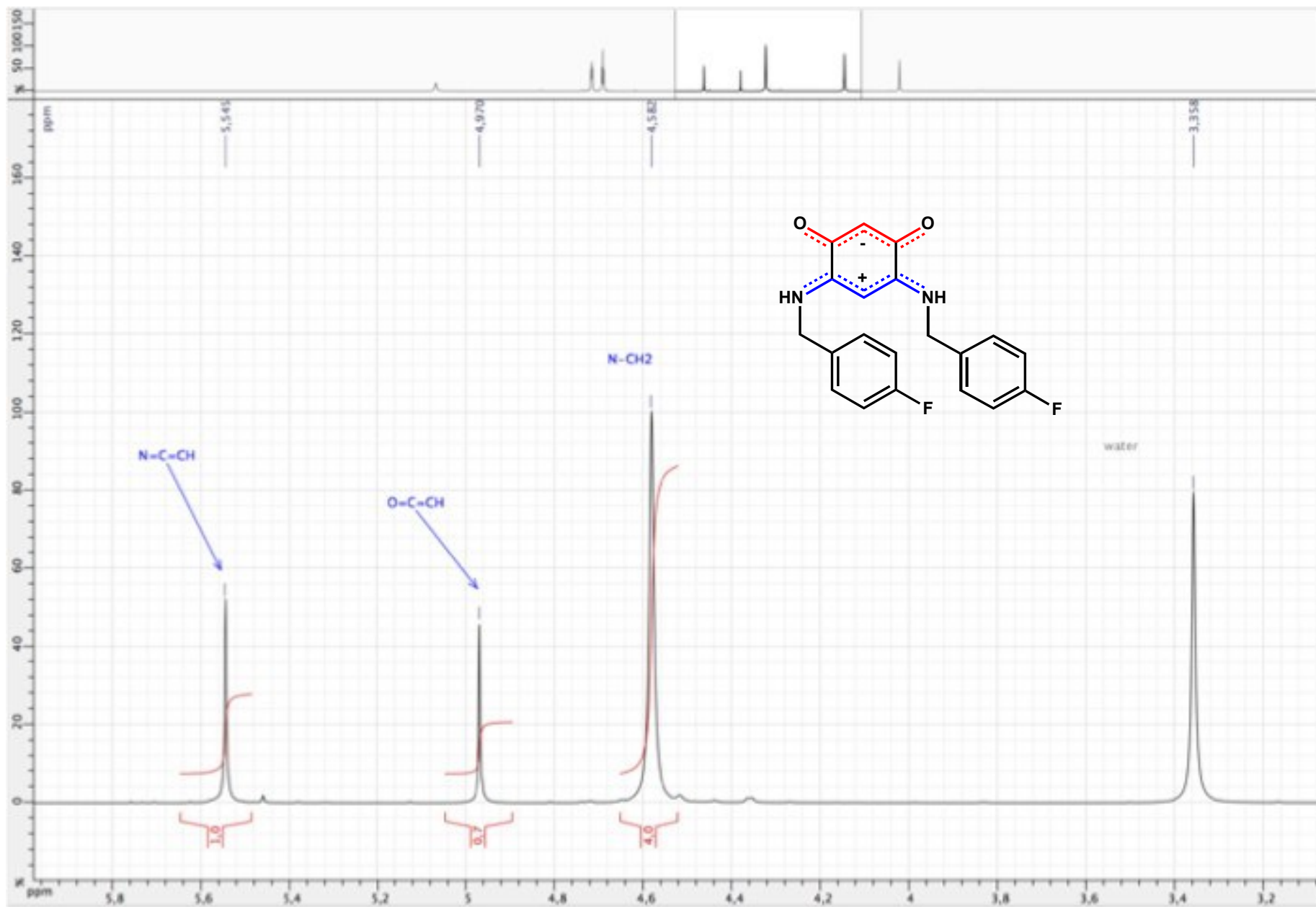


Figure S118. ^{13}C $\{^1\text{H}\}$ NMR spectrum of zwitterion **17** (DMSO d_6 ; 125 MHz)

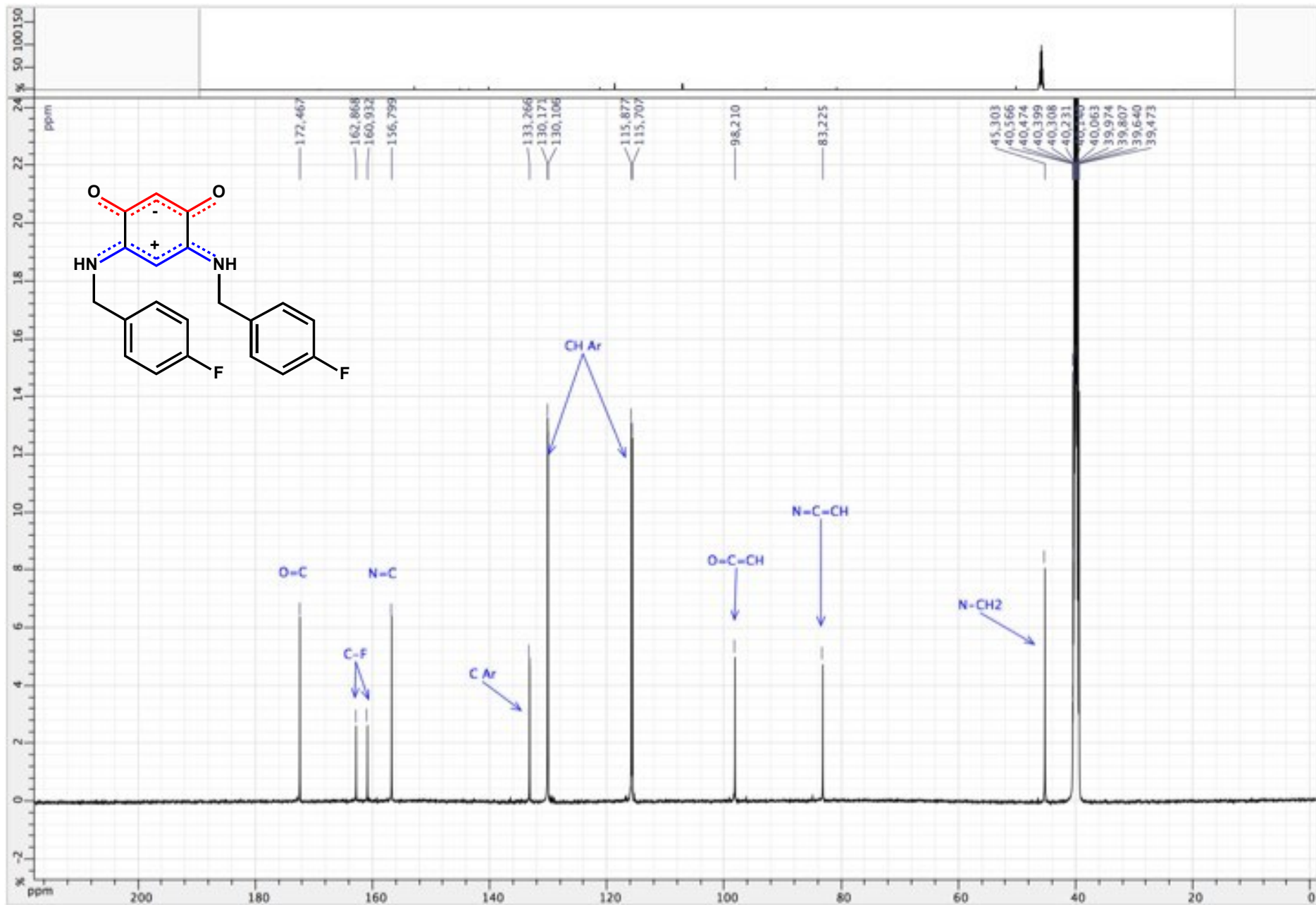


Figure S119. ^{13}C $\{^1\text{H}\}$ NMR spectrum of zwitterion **17** (DMSO d_6 ; 125 MHz)

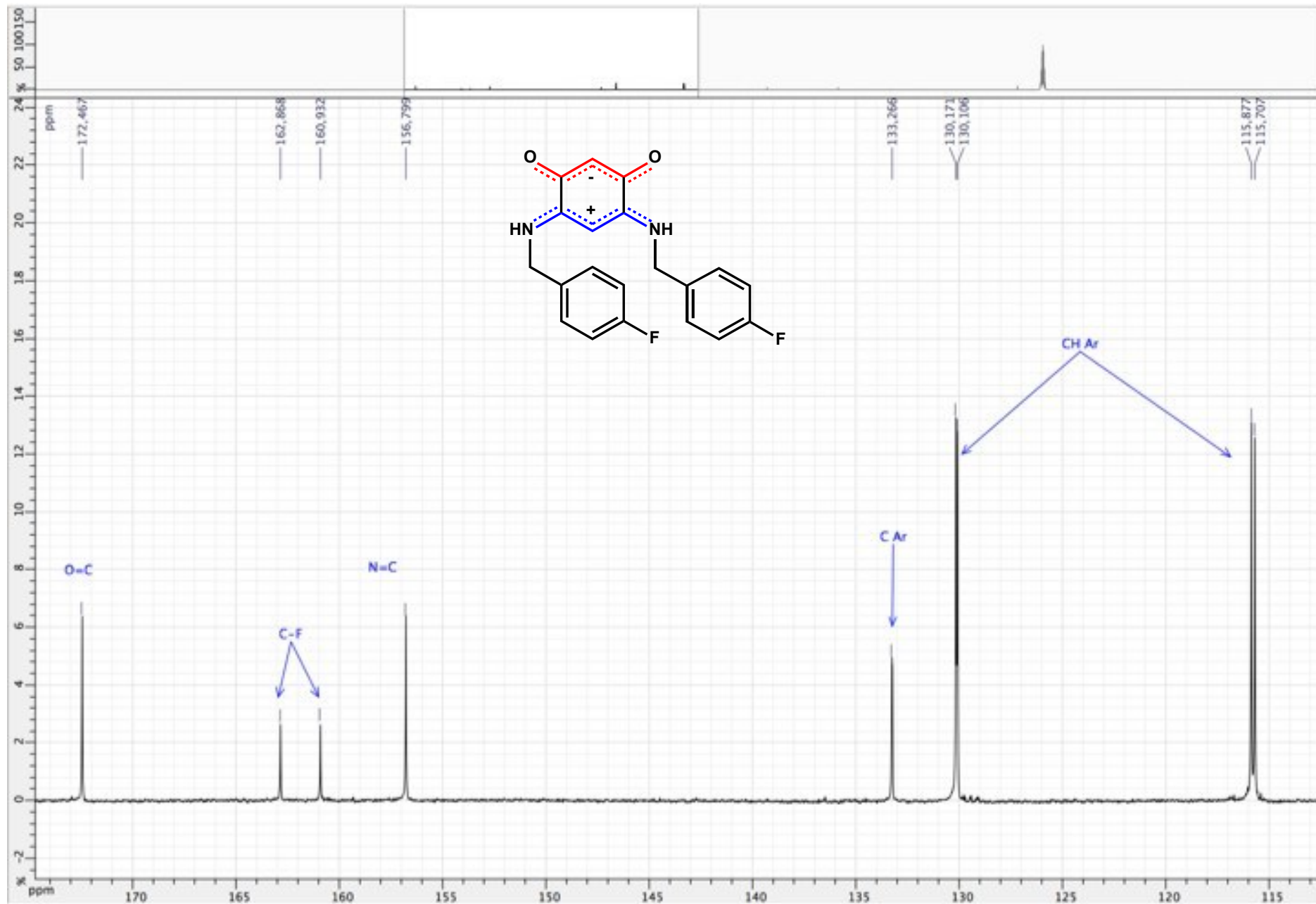


Figure S120. ^{13}C $\{^1\text{H}\}$ NMR spectrum of zwitterion **17** (DMSO d_6 ; 125 MHz)

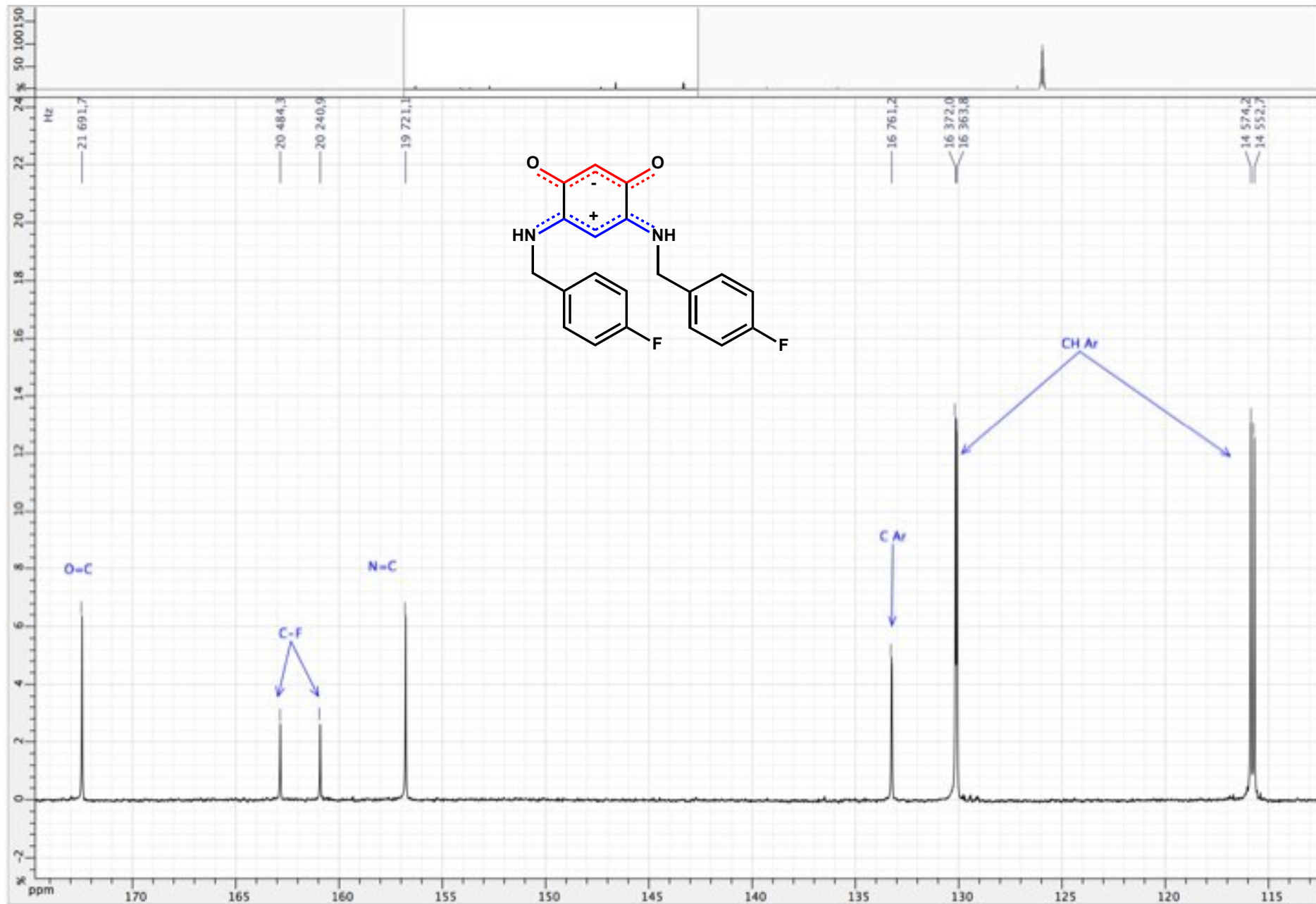


Figure S121. ^{13}C $\{^1\text{H}\}$ NMR spectrum of zwitterion **17** (DMSO d_6 ; 125 MHz)

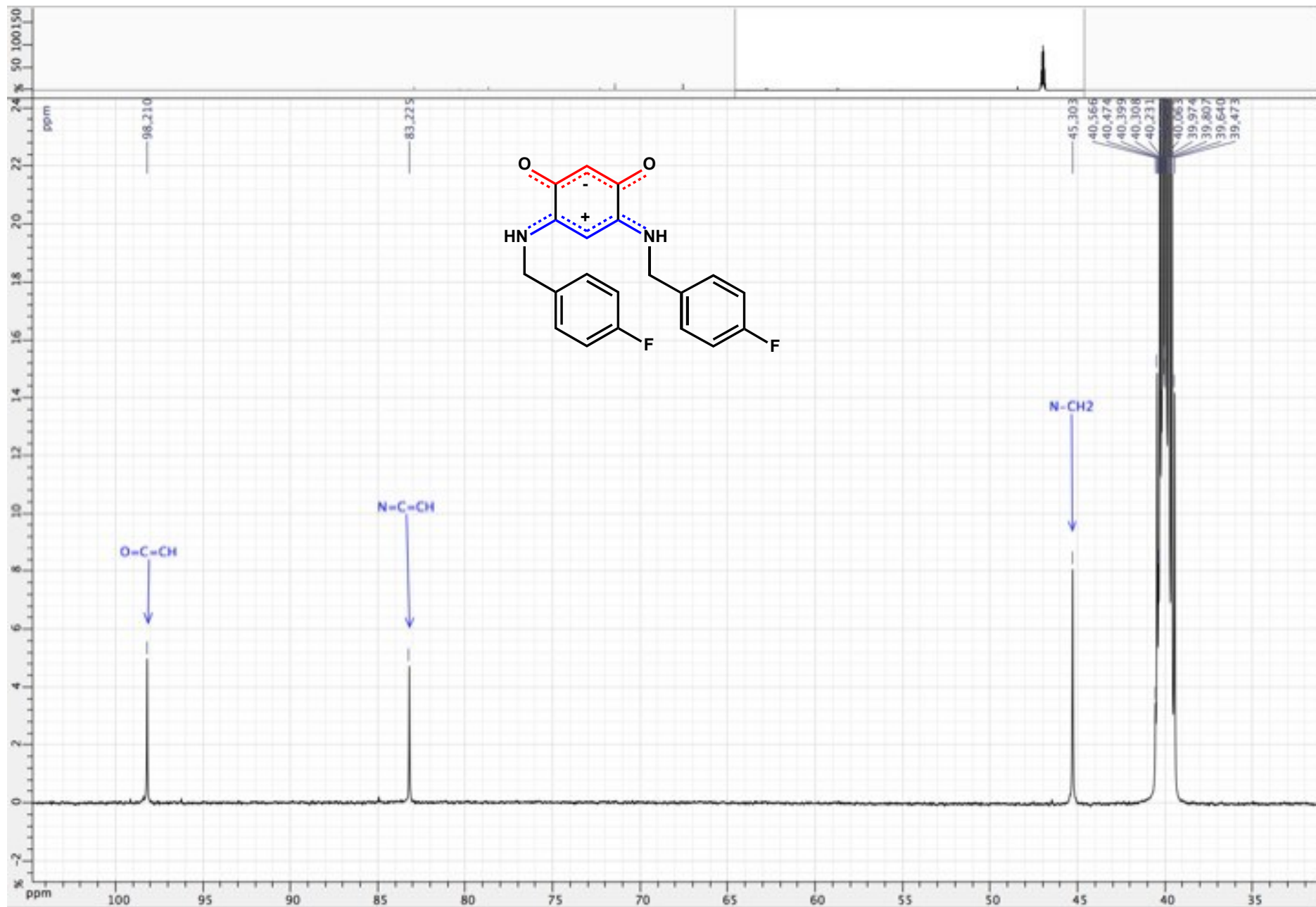


Figure S122. ^{19}F $\{^1\text{H}\}$ NMR spectrum of zwitterion **17** (DMSO d_6 ; 282 MHz)

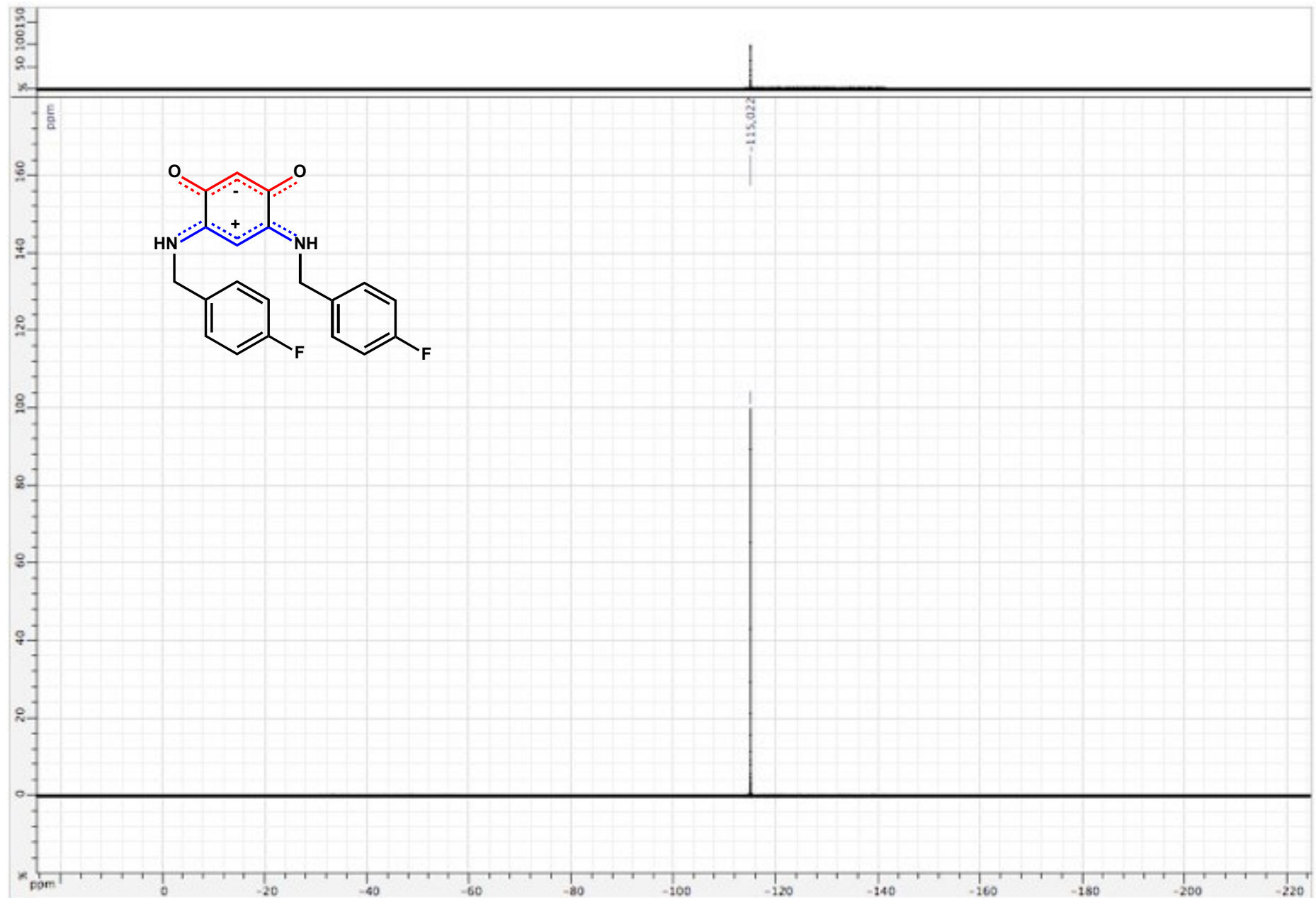


Figure S123. ¹H NMR spectrum of zwitterion **18** (DMSO d₆ ; 500 MHz)

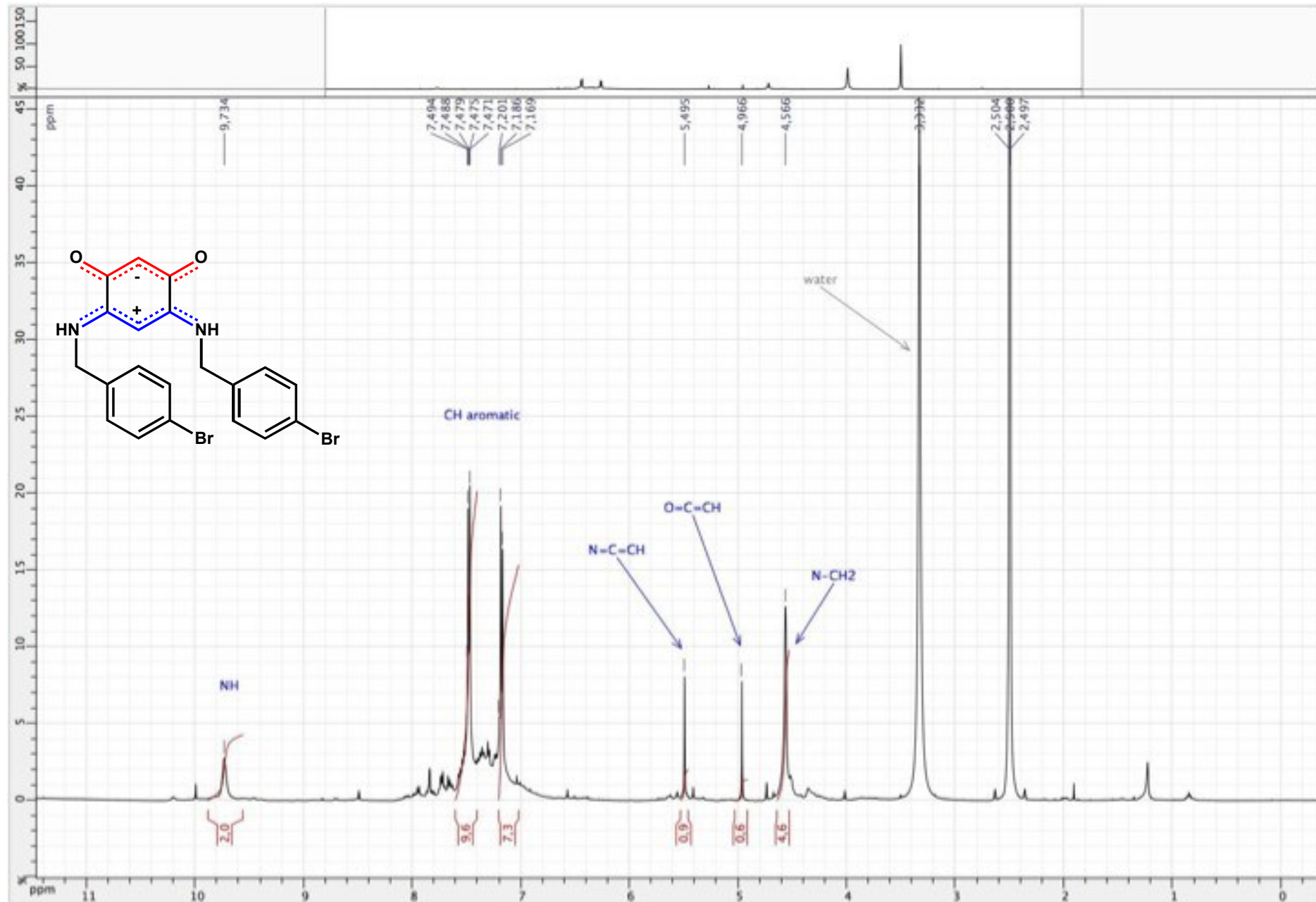


Figure S124. ^{13}C $\{^1\text{H}\}$ NMR spectrum of zwitterion **18** (DMSO d_6 ; 125 MHz)

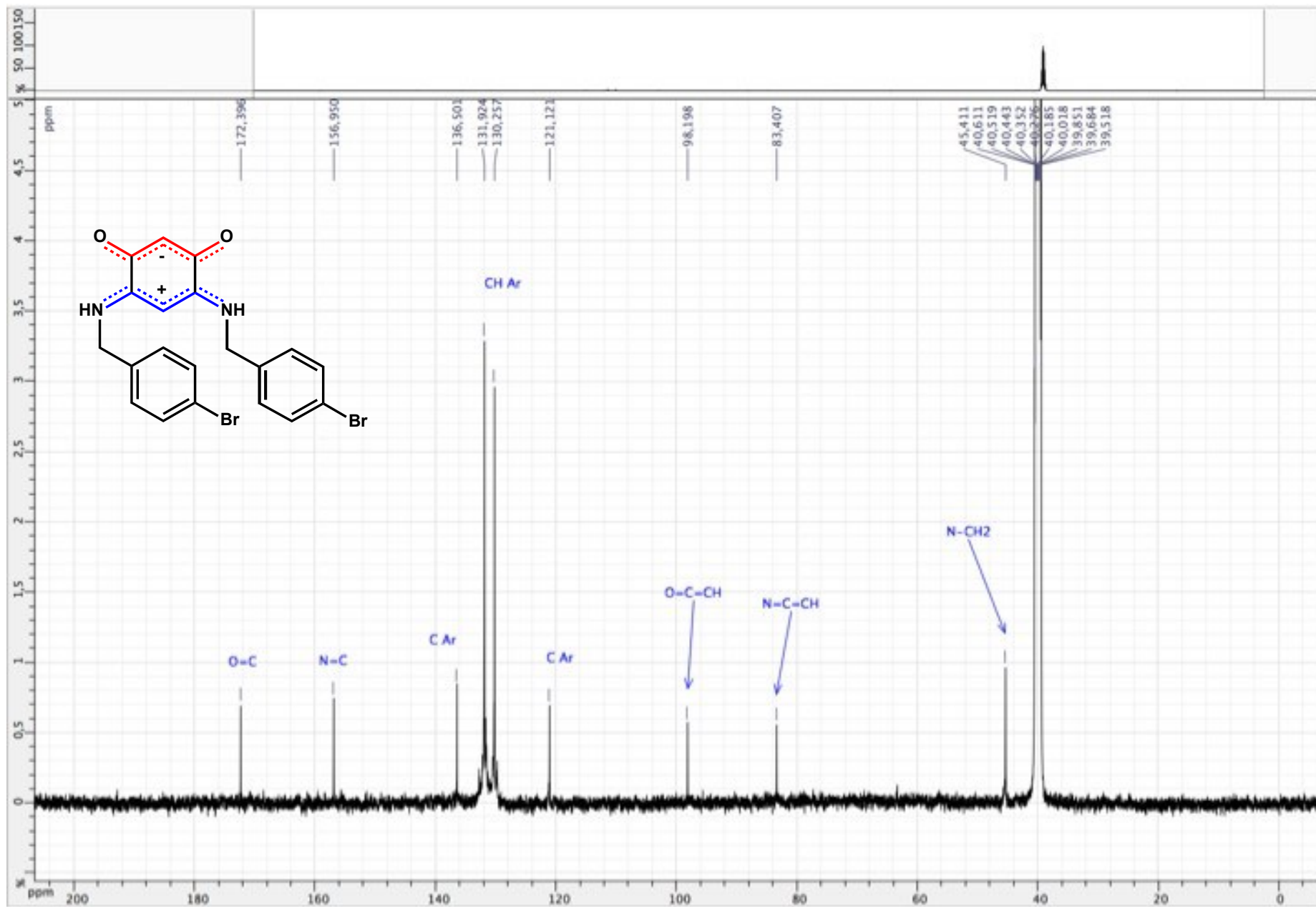


Figure S125. ^{13}C $\{^1\text{H}\}$ NMR spectrum of zwitterion **18** (DMSO d_6 ; 125 MHz)

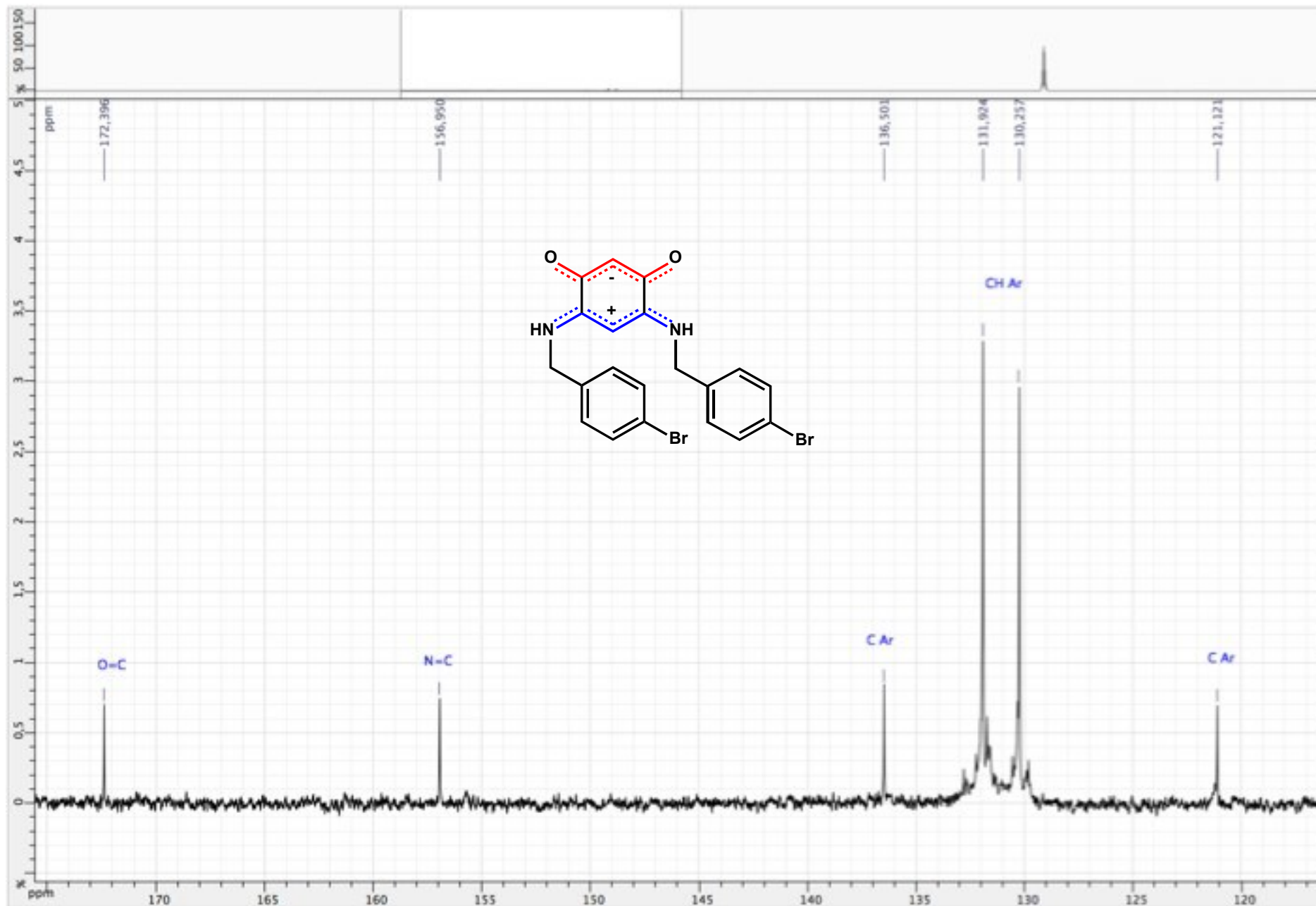


Figure S126. ^{13}C $\{^1\text{H}\}$ NMR spectrum of zwitterion **18** (DMSO d_6 ; 125 MHz)

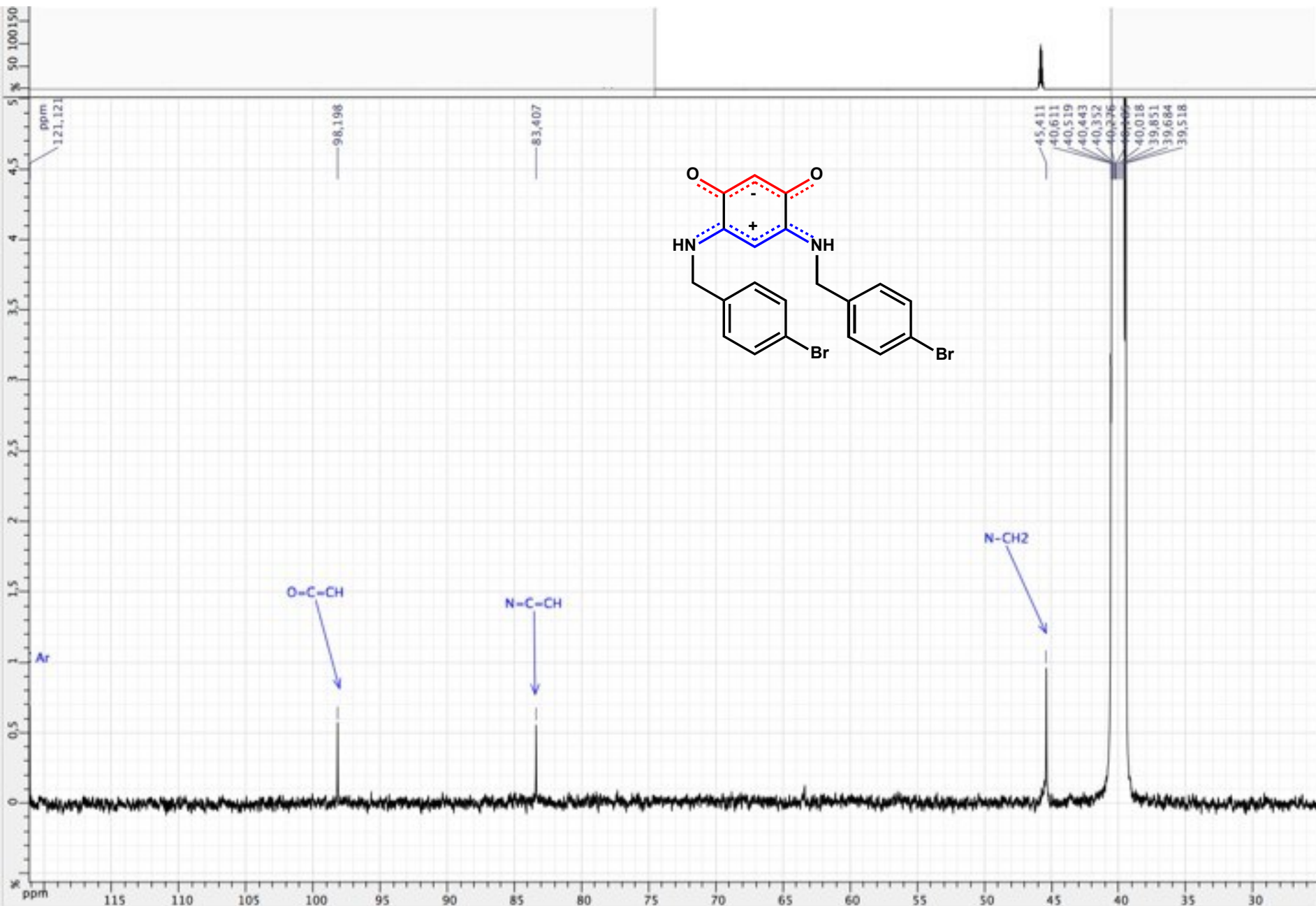


Figure S127. ¹H NMR spectrum of zwitterion **19** (DMSO d₆ ; 500 MHz)

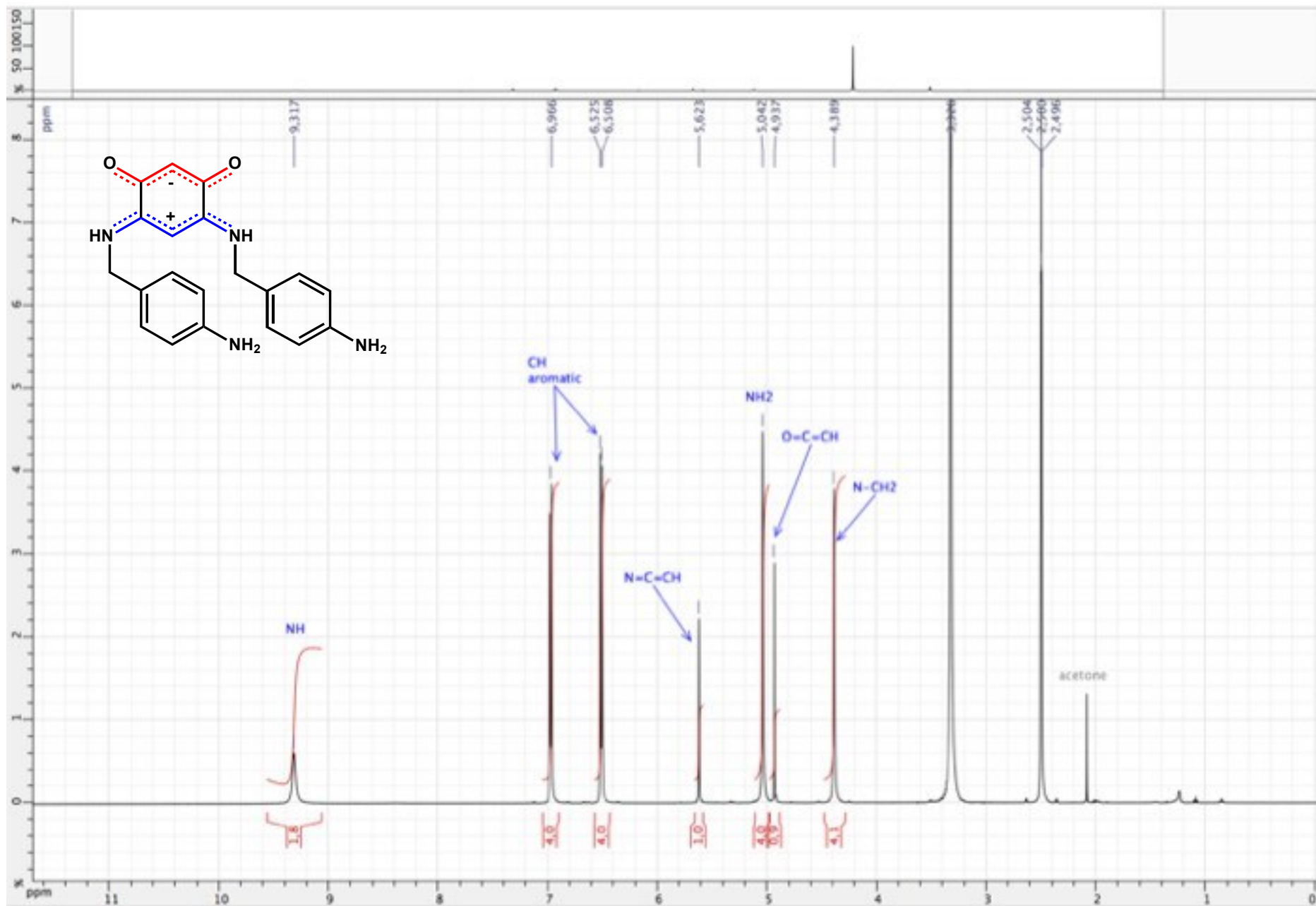


Figure S128. ^1H NMR spectrum of zwitterion **19** (DMSO d_6 ; 500 MHz)

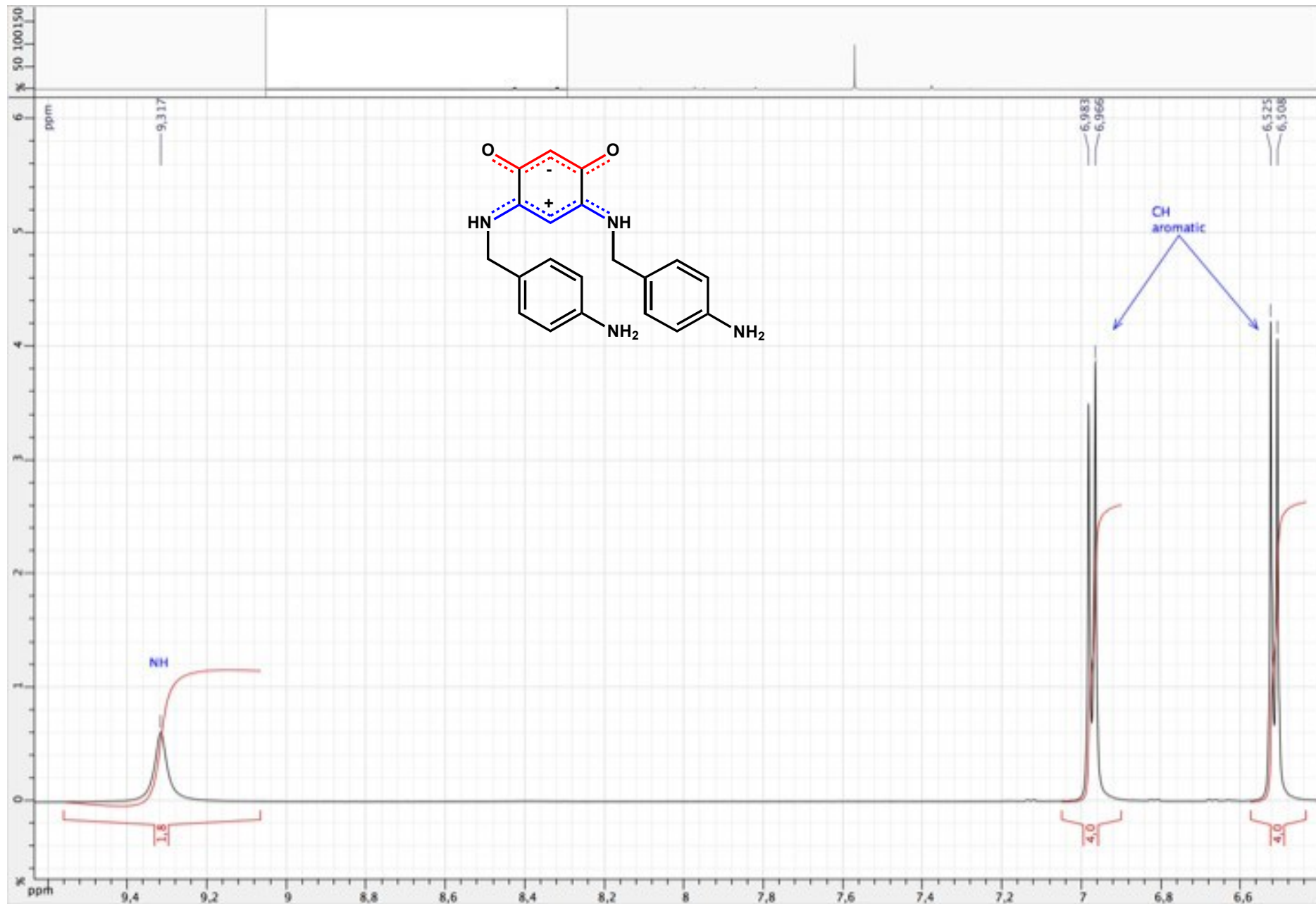


Figure S129. ^1H NMR spectrum of zwitterion **19** (DMSO d_6 ; 500 MHz)

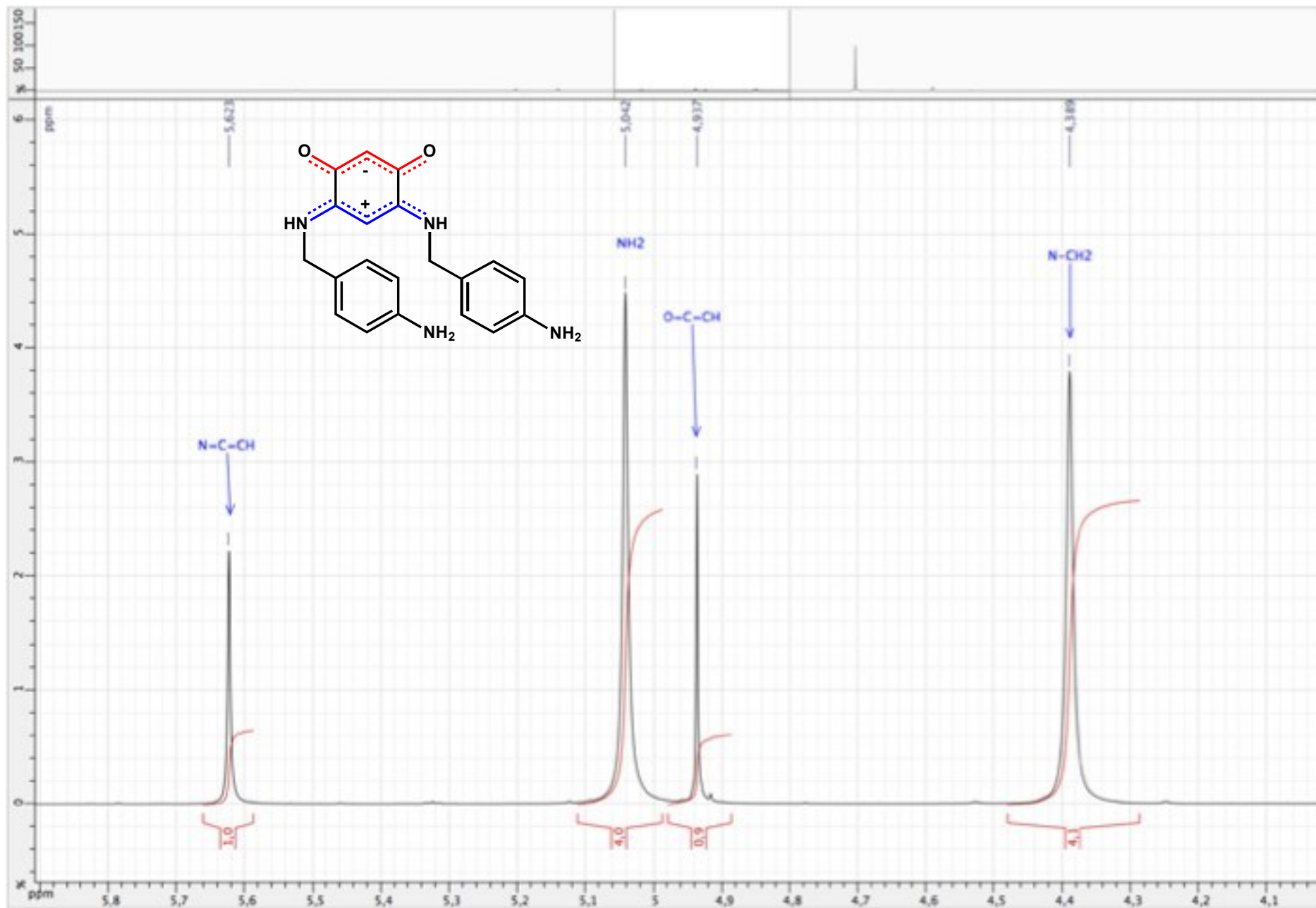


Figure S130. ^{13}C $\{^1\text{H}\}$ NMR spectrum of zwitterion **19** (DMSO d_6 ; 125 MHz)

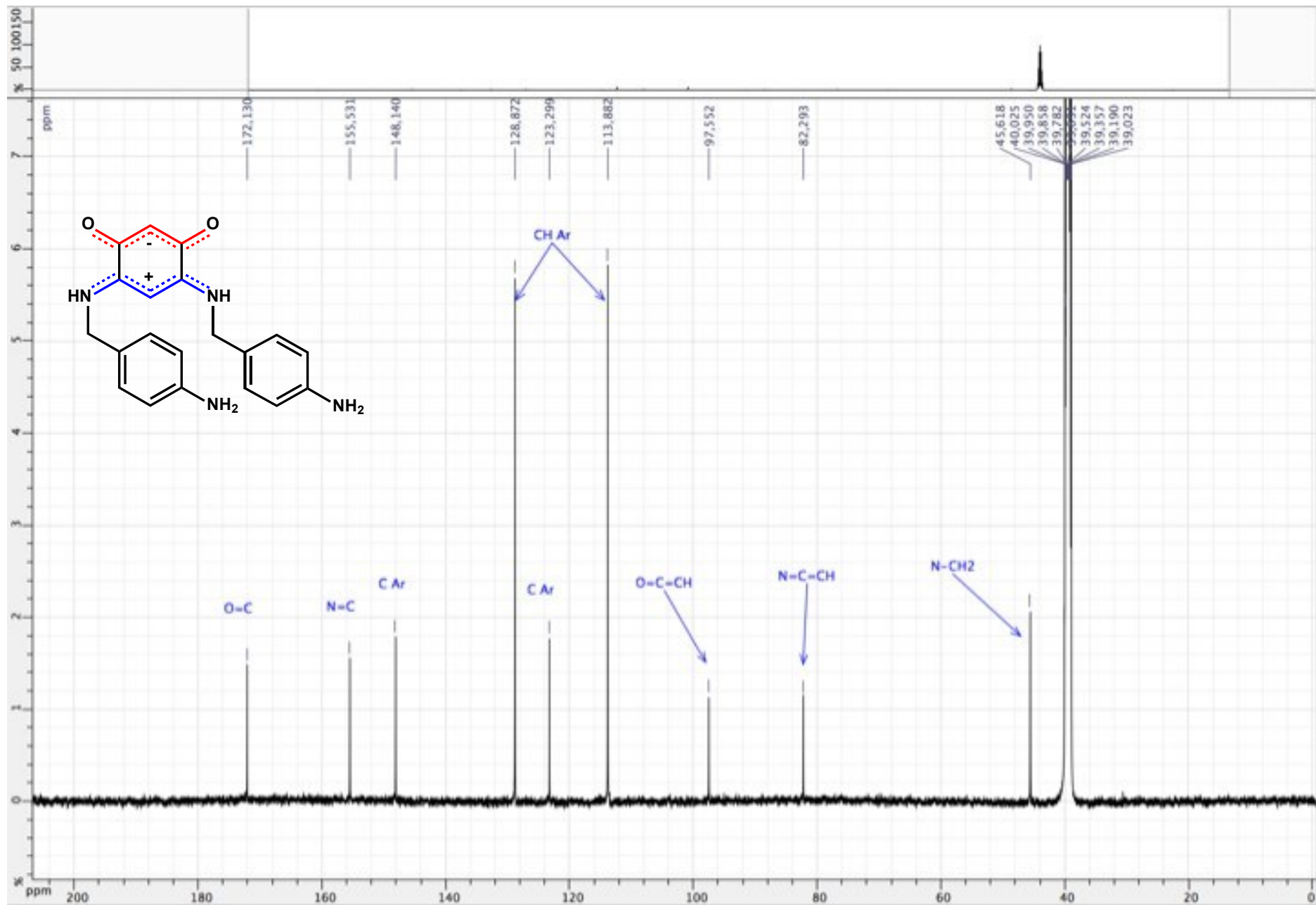


Figure S131. ^{13}C $\{^1\text{H}\}$ NMR spectrum of zwitterion **19** (DMSO d_6 ; 125 MHz)

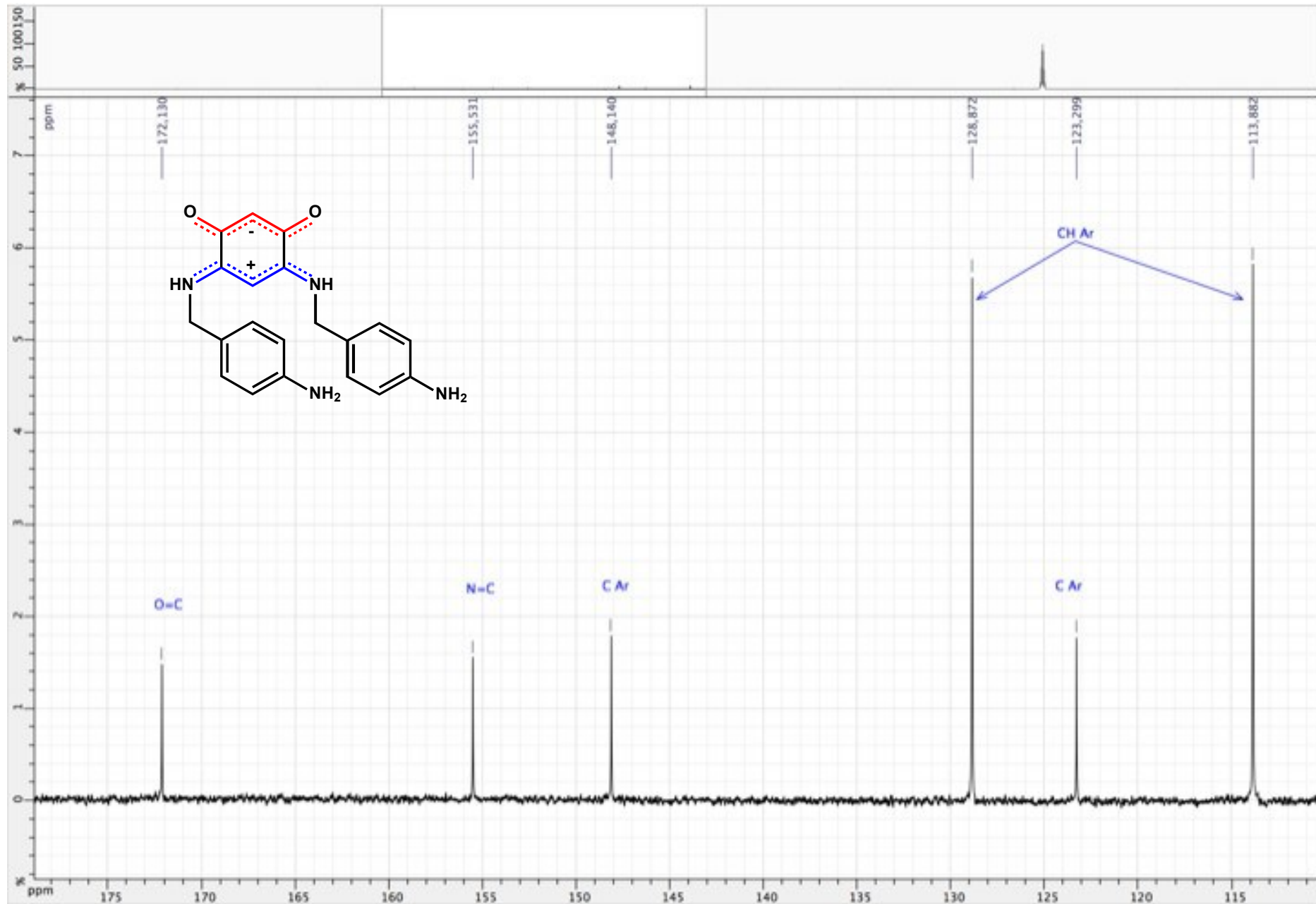


Figure S132. ^{13}C $\{^1\text{H}\}$ NMR spectrum of zwitterion **19** (DMSO d_6 ; 125 MHz)

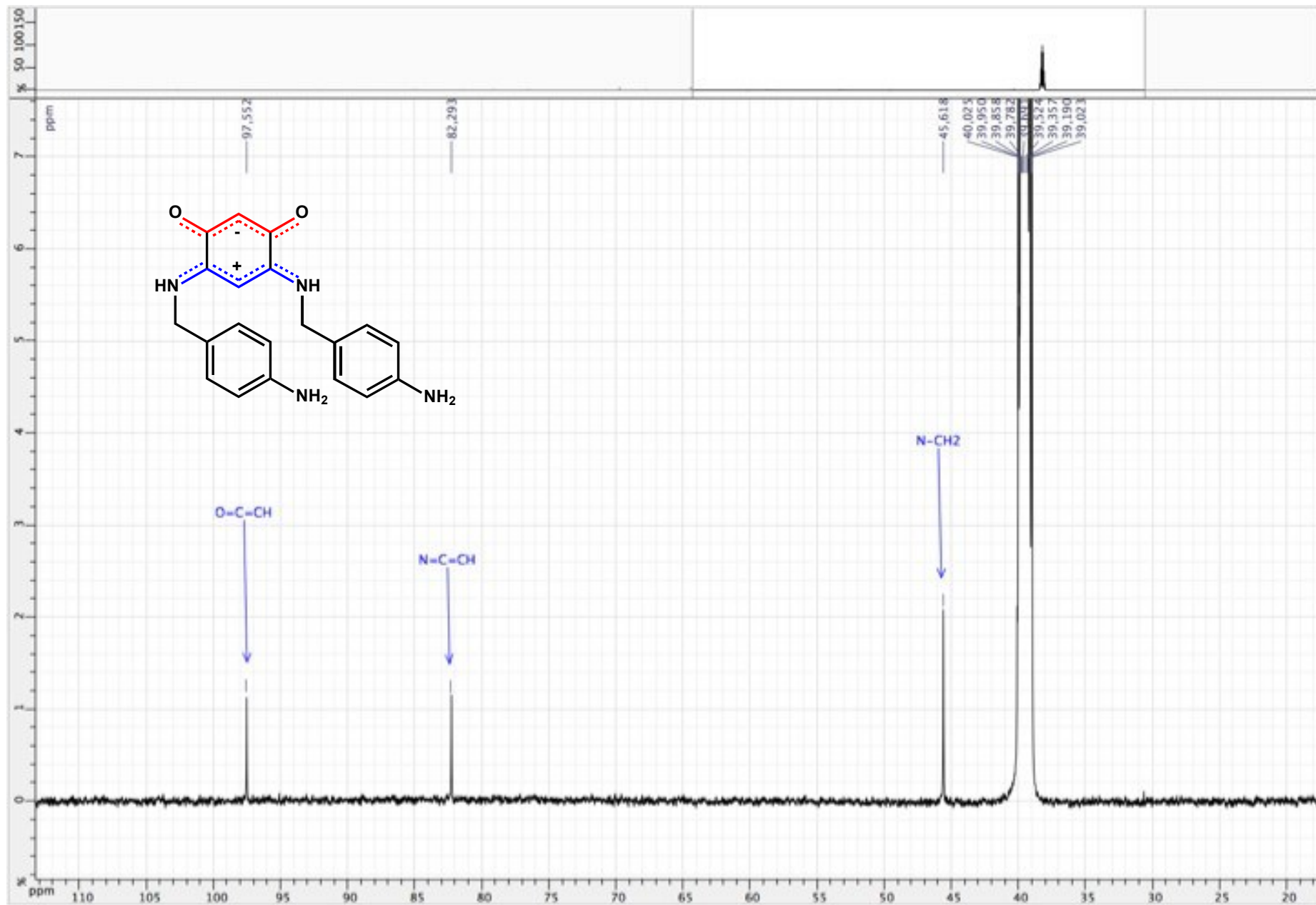


Figure S133. HSQC ($^1\text{H} / ^{13}\text{C} \{^1\text{H}\}$) spectrum of zwitterion **19** (DMSO d_6 ; 500 / 125 MHz)

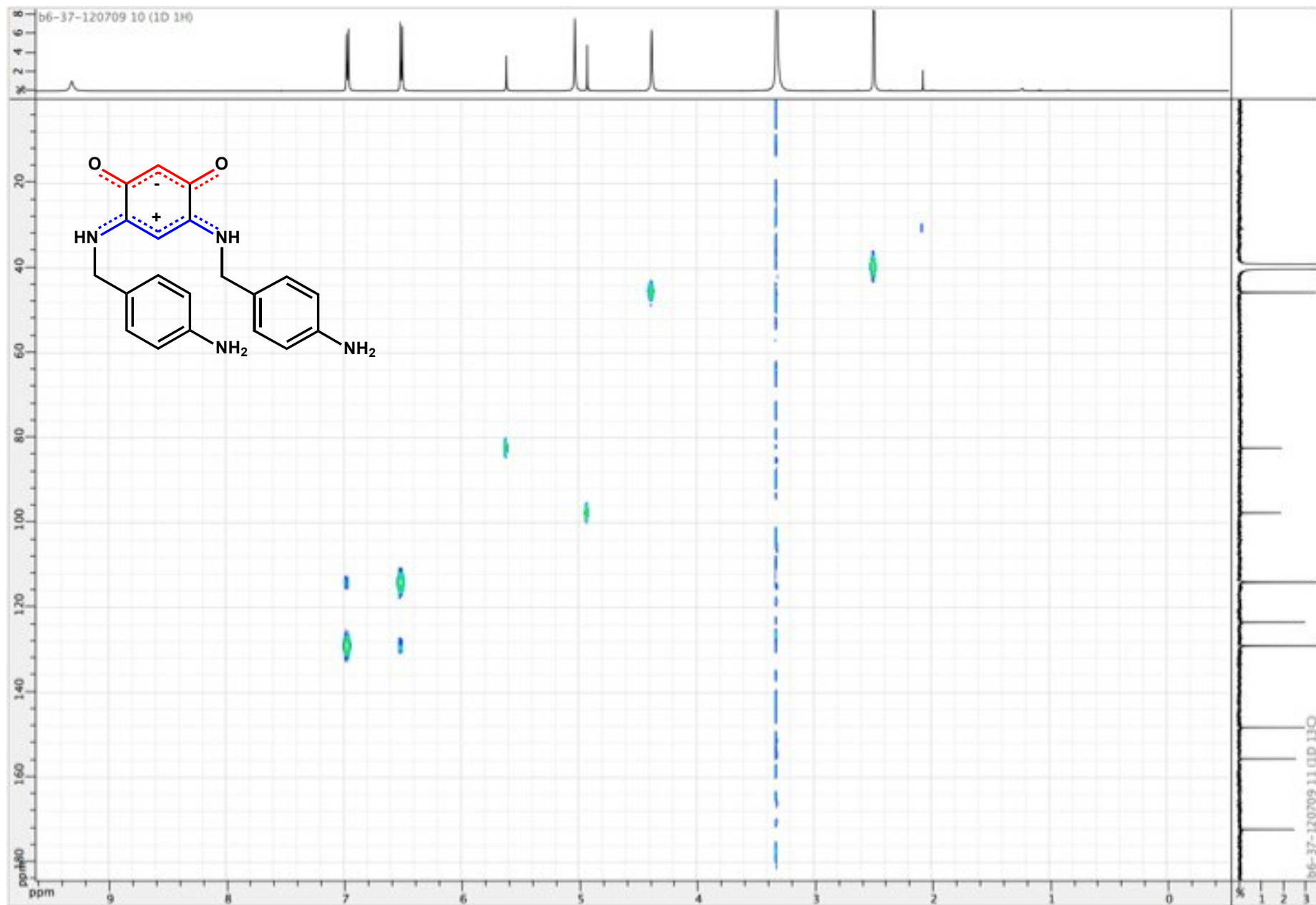


Figure S134. ¹H NMR spectrum of zwitterion **20** (DMSO d₆ ; 500 MHz)

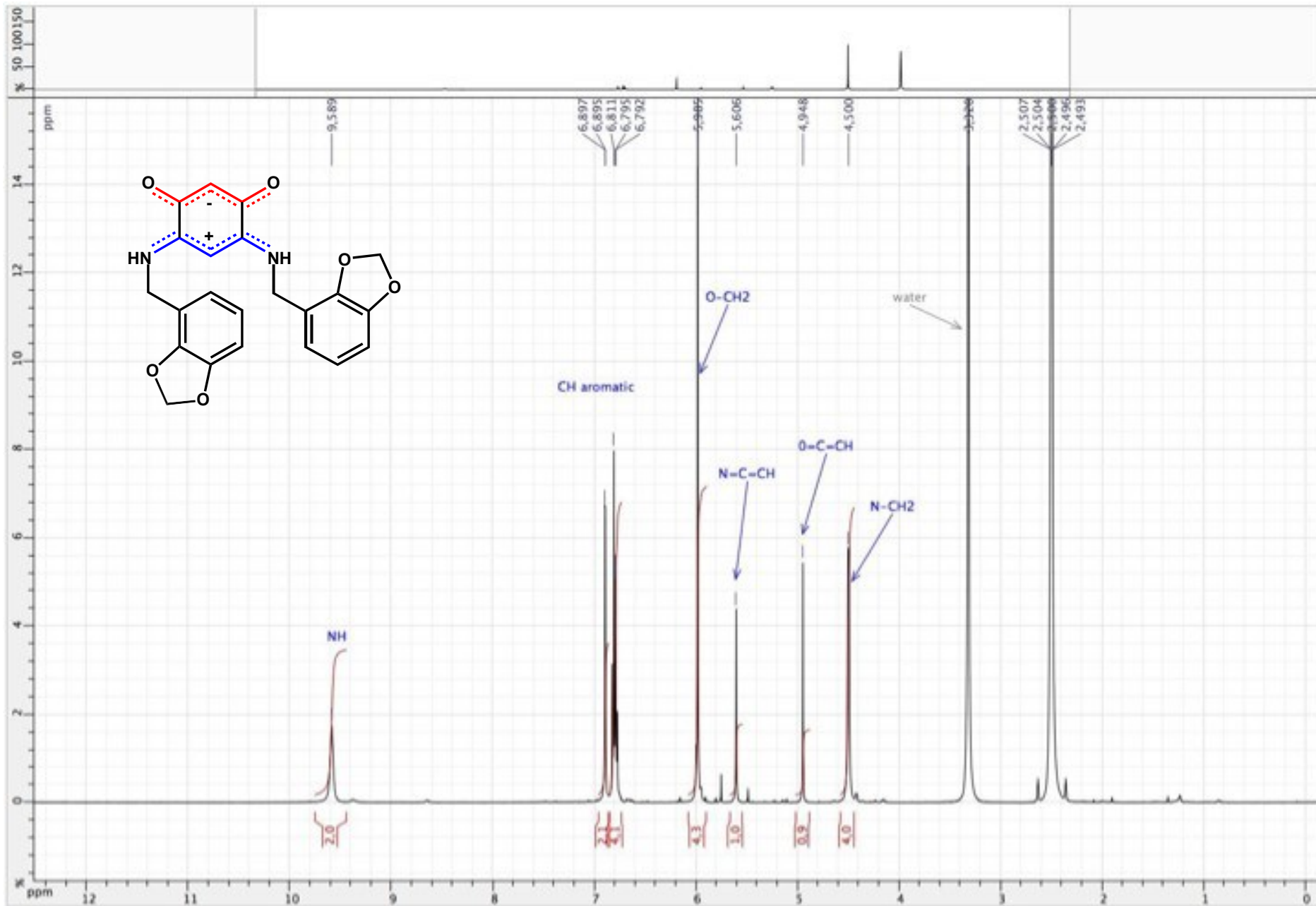


Figure S135. ¹H NMR spectrum of zwitterion **20** (DMSO d₆ ; 500 MHz)

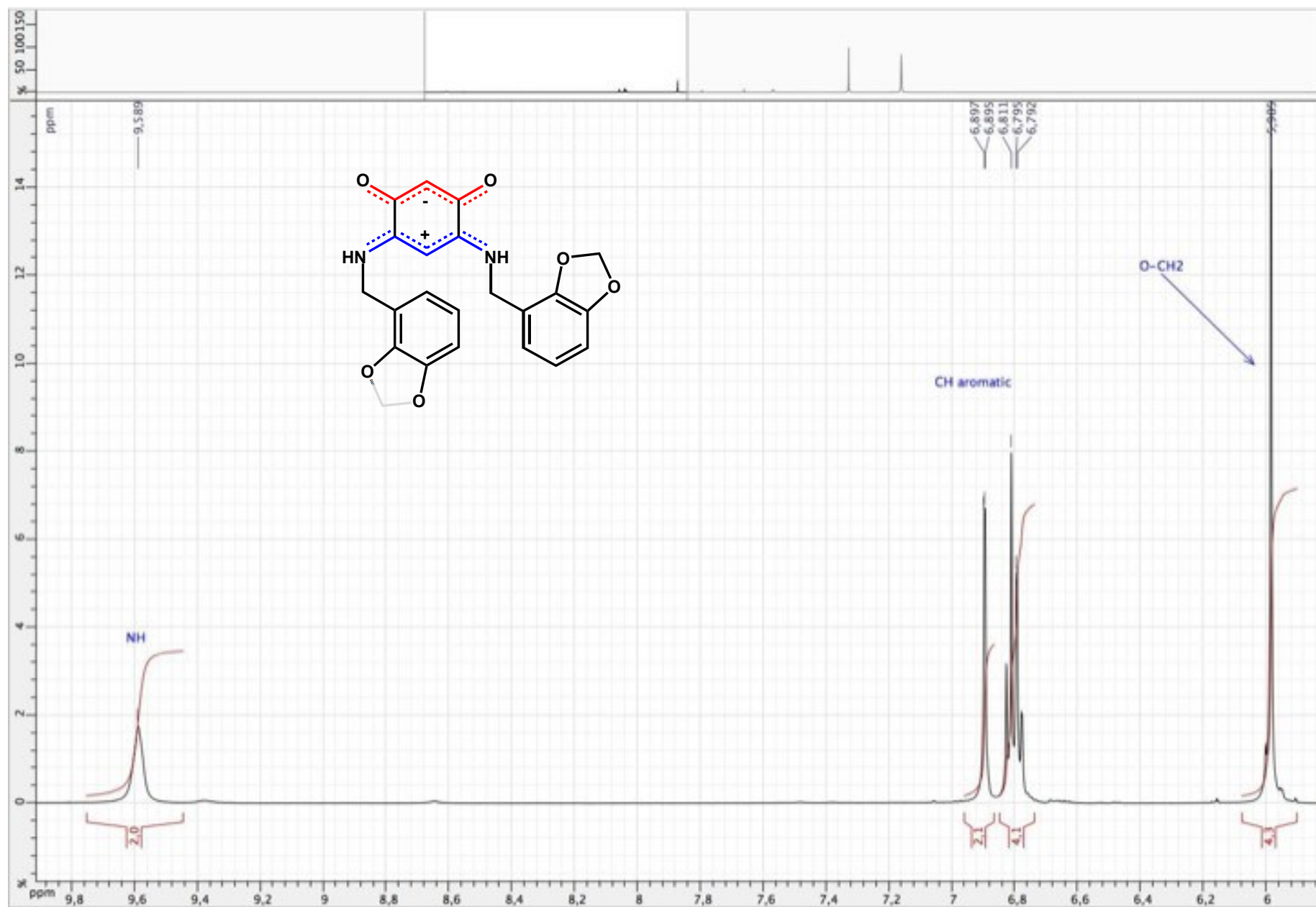


Figure S136. ^1H NMR spectrum of zwitterion **20** (DMSO d_6 ; 500 MHz)

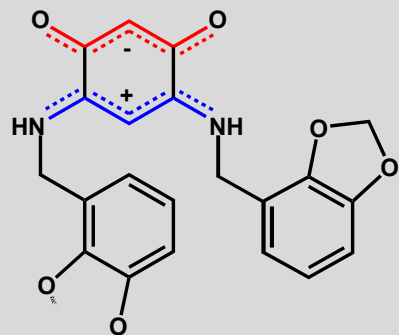


Figure S137. ^1H NMR spectrum of zwitterion **20** (DMSO d_6 ; 500 MHz)

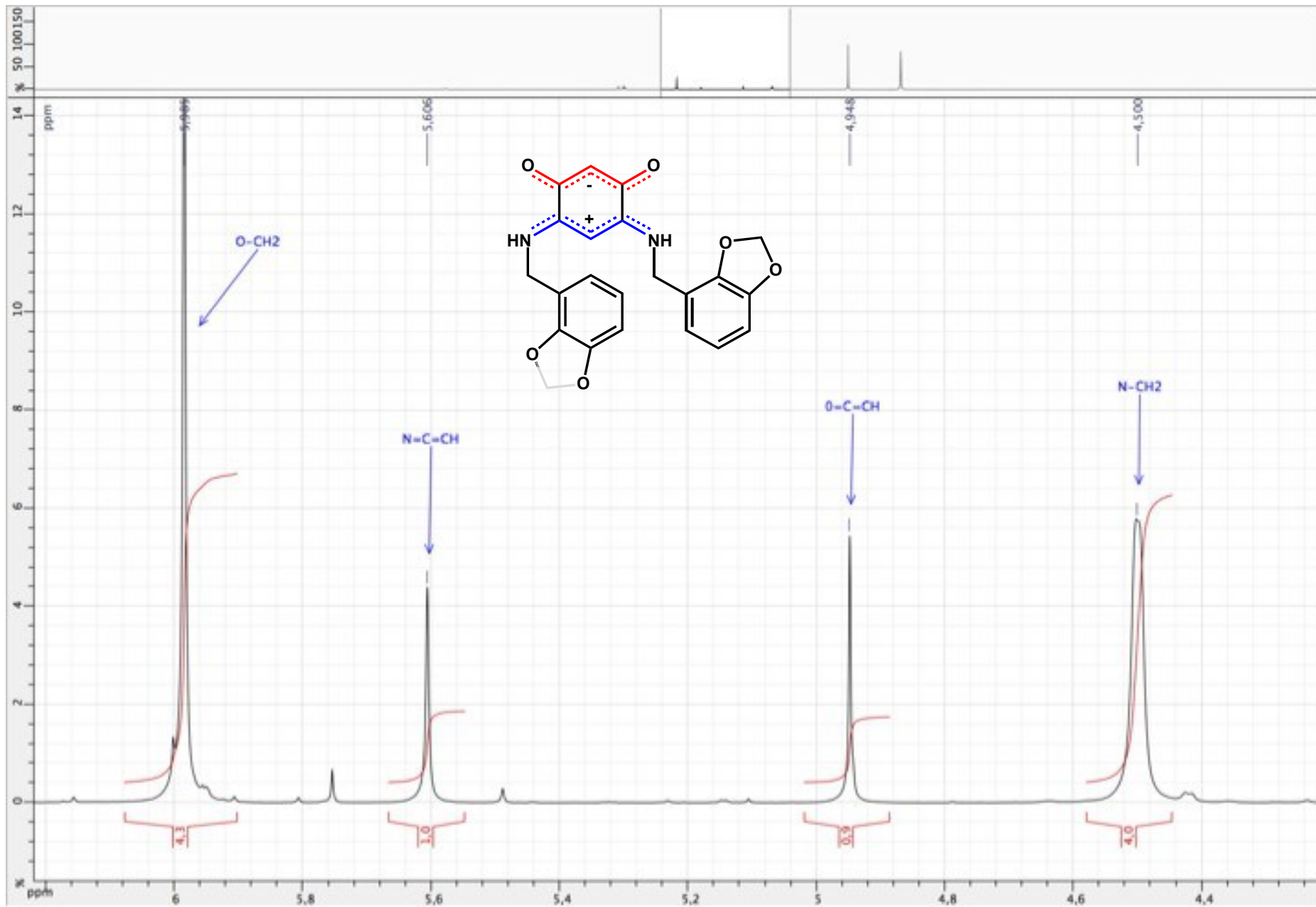


Figure S138. ^{13}C $\{^1\text{H}\}$ NMR spectrum of zwitterion **20** (DMSO d_6 ; 125 MHz)

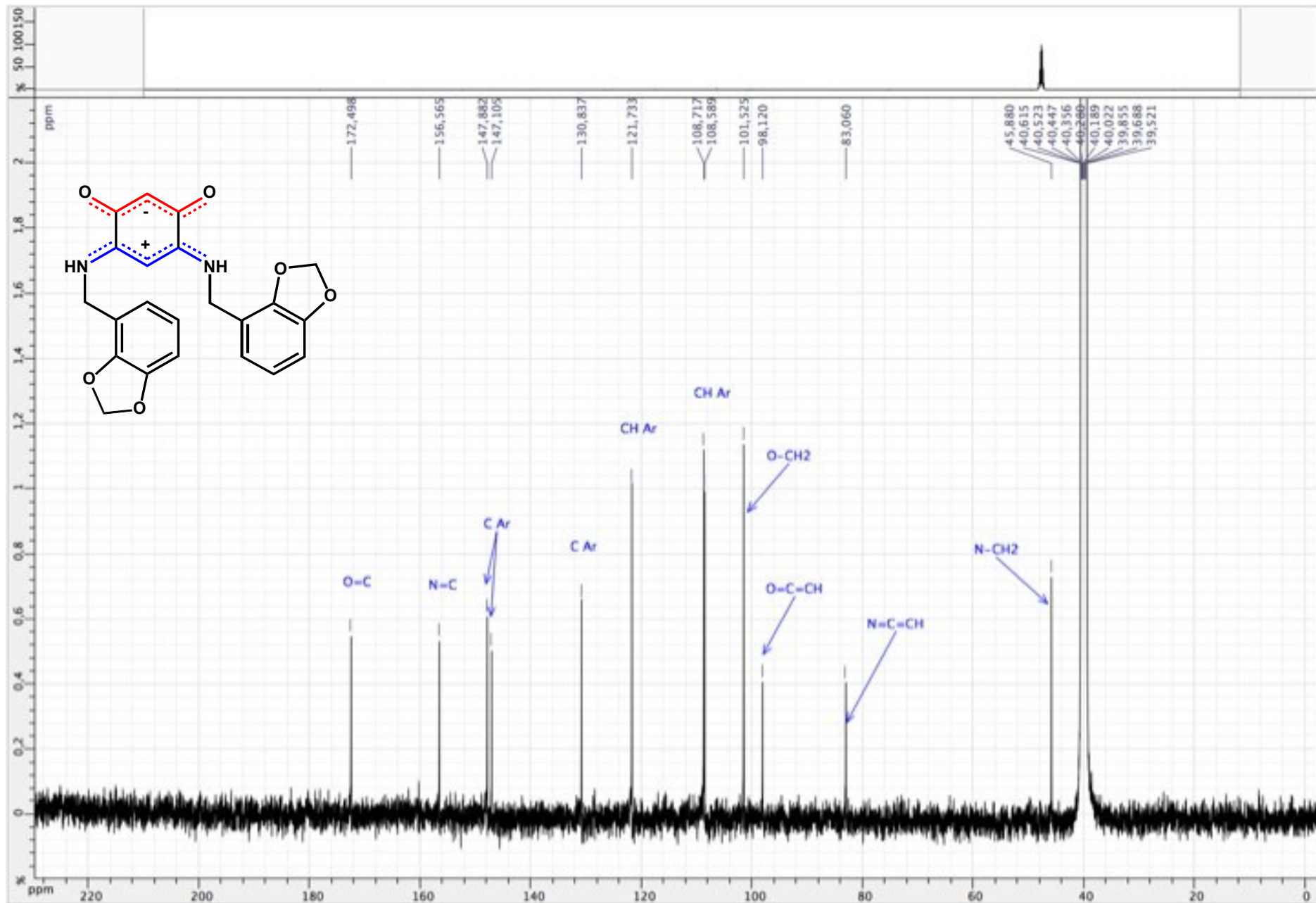


Figure S139. ^{13}C $\{^1\text{H}\}$ NMR spectrum of zwitterion **20** (DMSO d_6 ; 125 MHz)

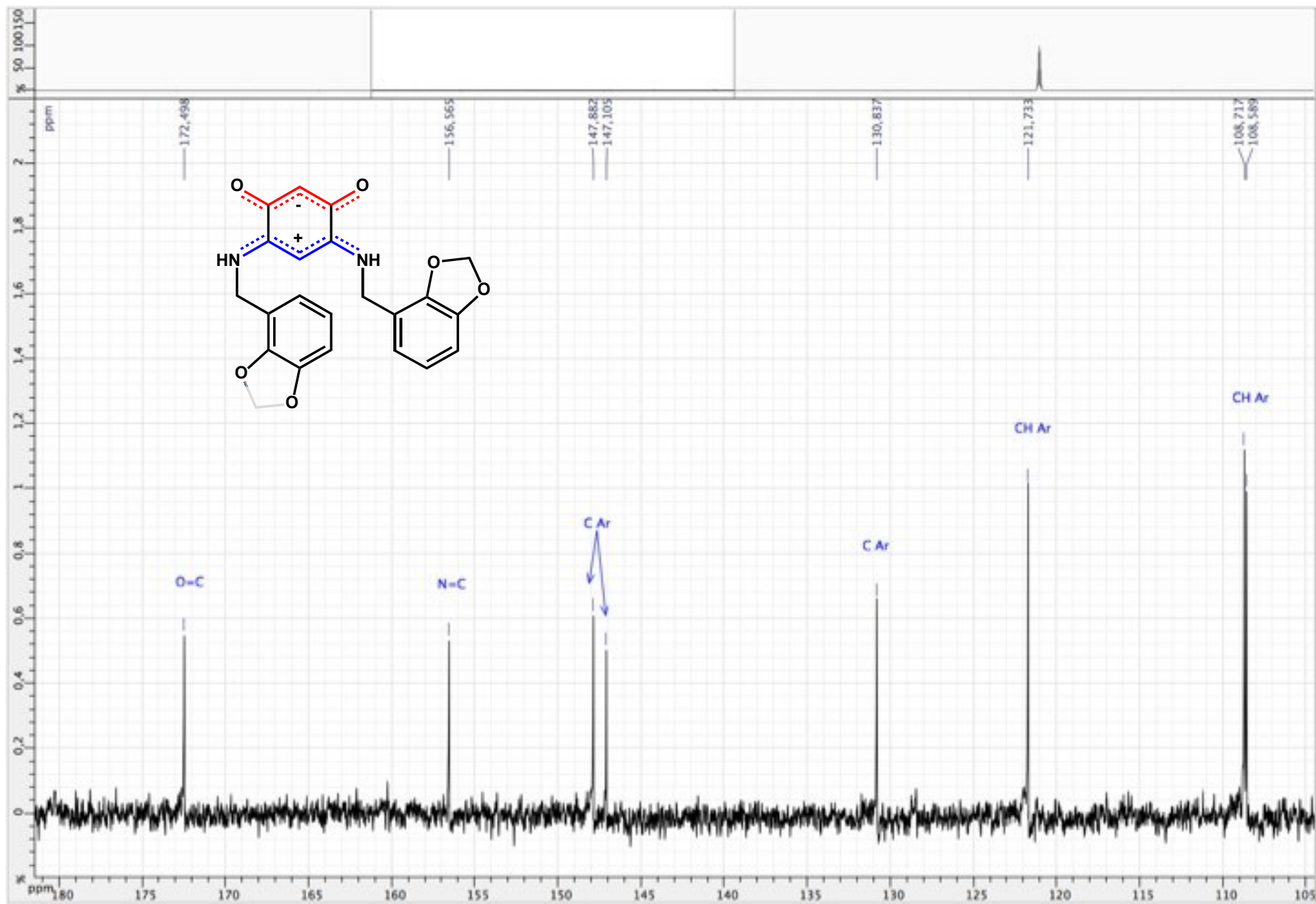


Figure S140. ^{13}C $\{^1\text{H}\}$ NMR spectrum of zwitterion **20** (DMSO d_6 ; 125 MHz)

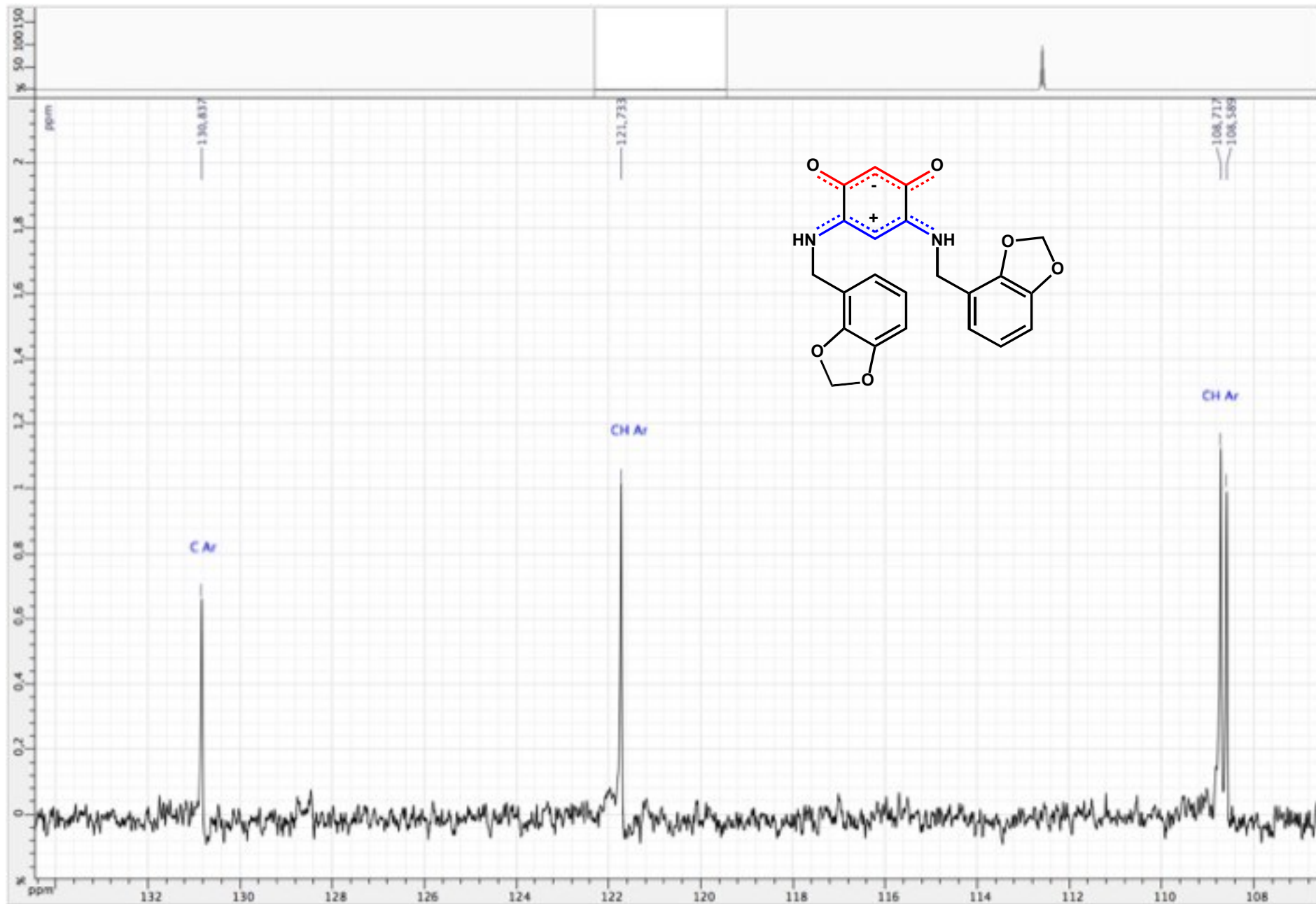


Figure S141. ^{13}C $\{^1\text{H}\}$ NMR spectrum of zwitterion **20** (DMSO d_6 ; 125 MHz)

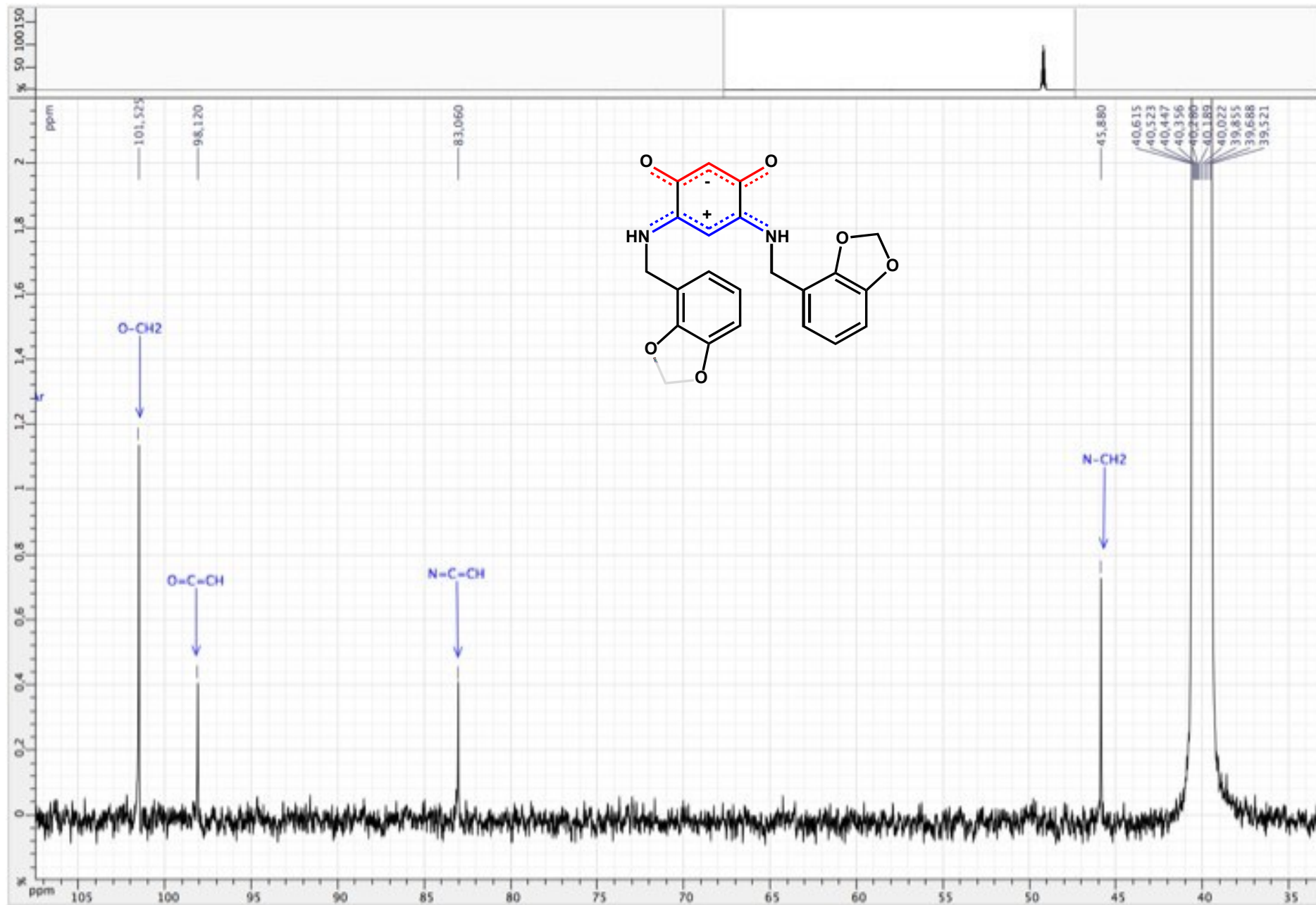


Figure S142. HSQC ($^1\text{H} / ^{13}\text{C} \{^1\text{H}\}$) spectrum of zwitterion **20** (DMSO d_6 ; 500 / 125 MHz)

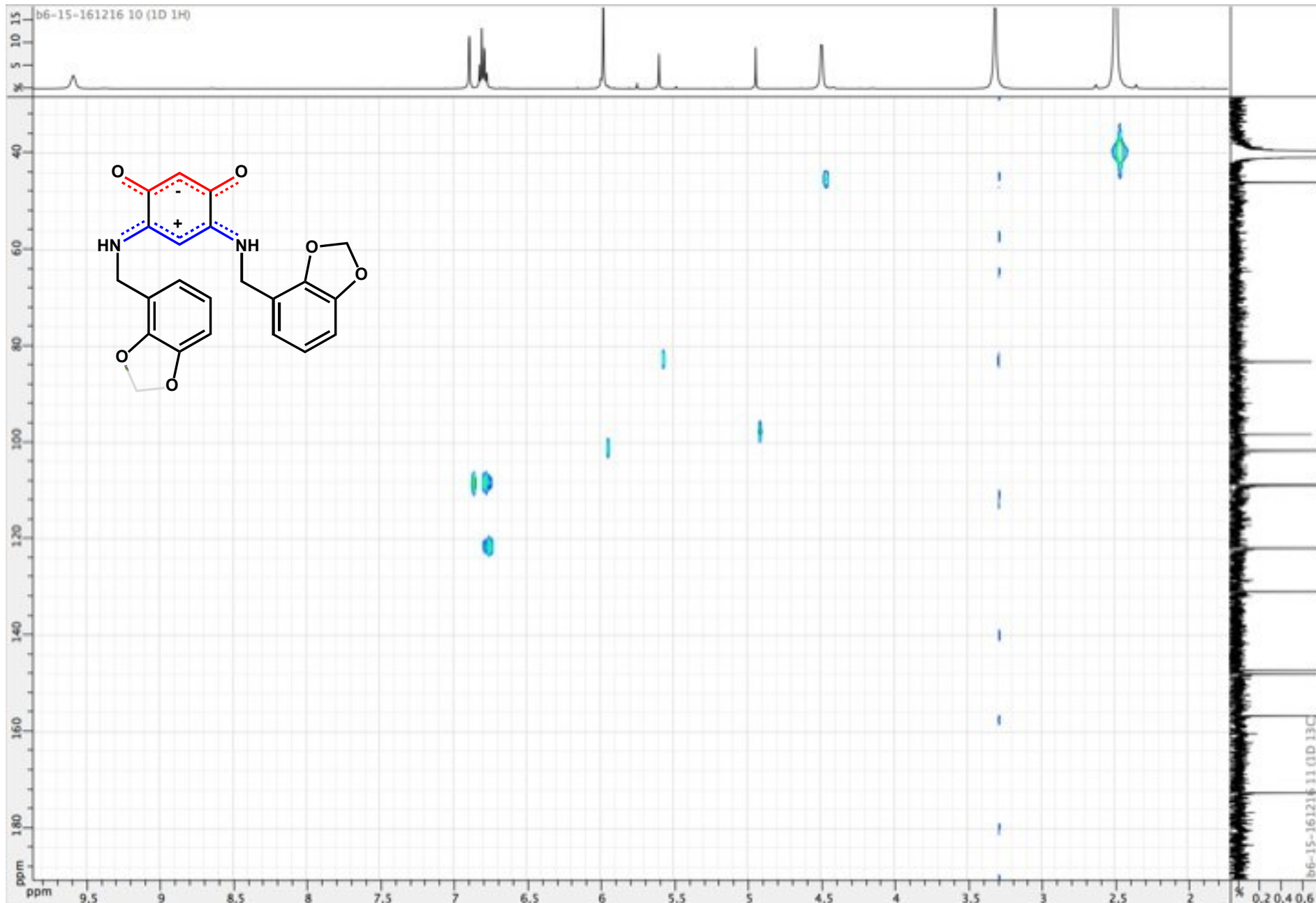


Figure S143. HSQC ($^1\text{H} / ^{13}\text{C} \{^1\text{H}\}$) spectrum of zwitterion **20** (DMSO d_6 ; 500 / 125 MHz)

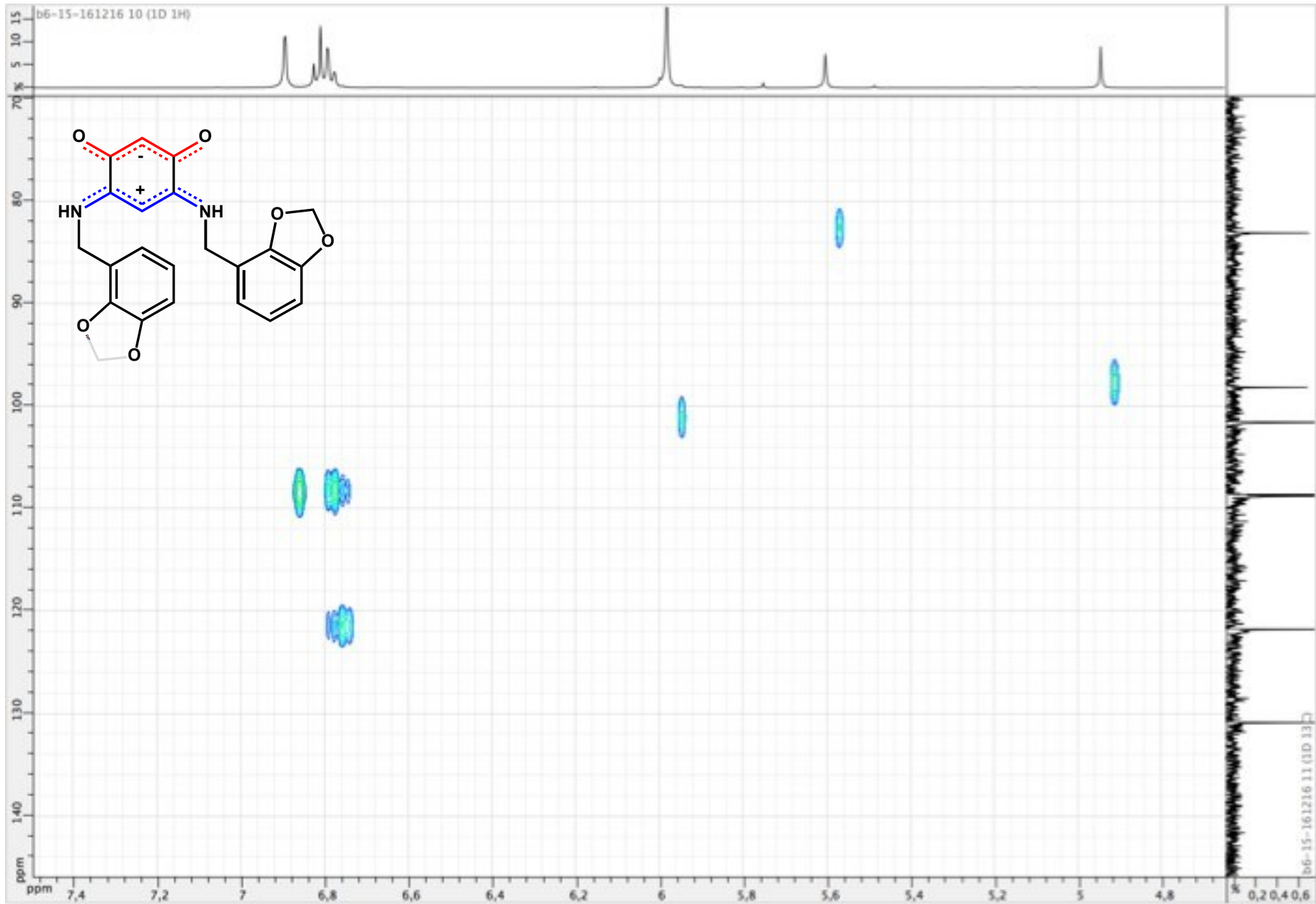


Figure S144. COSY ($^1\text{H} / ^1\text{H}$) spectrum of zwitterion **20** (DMSO d_6 ; 500 MHz)

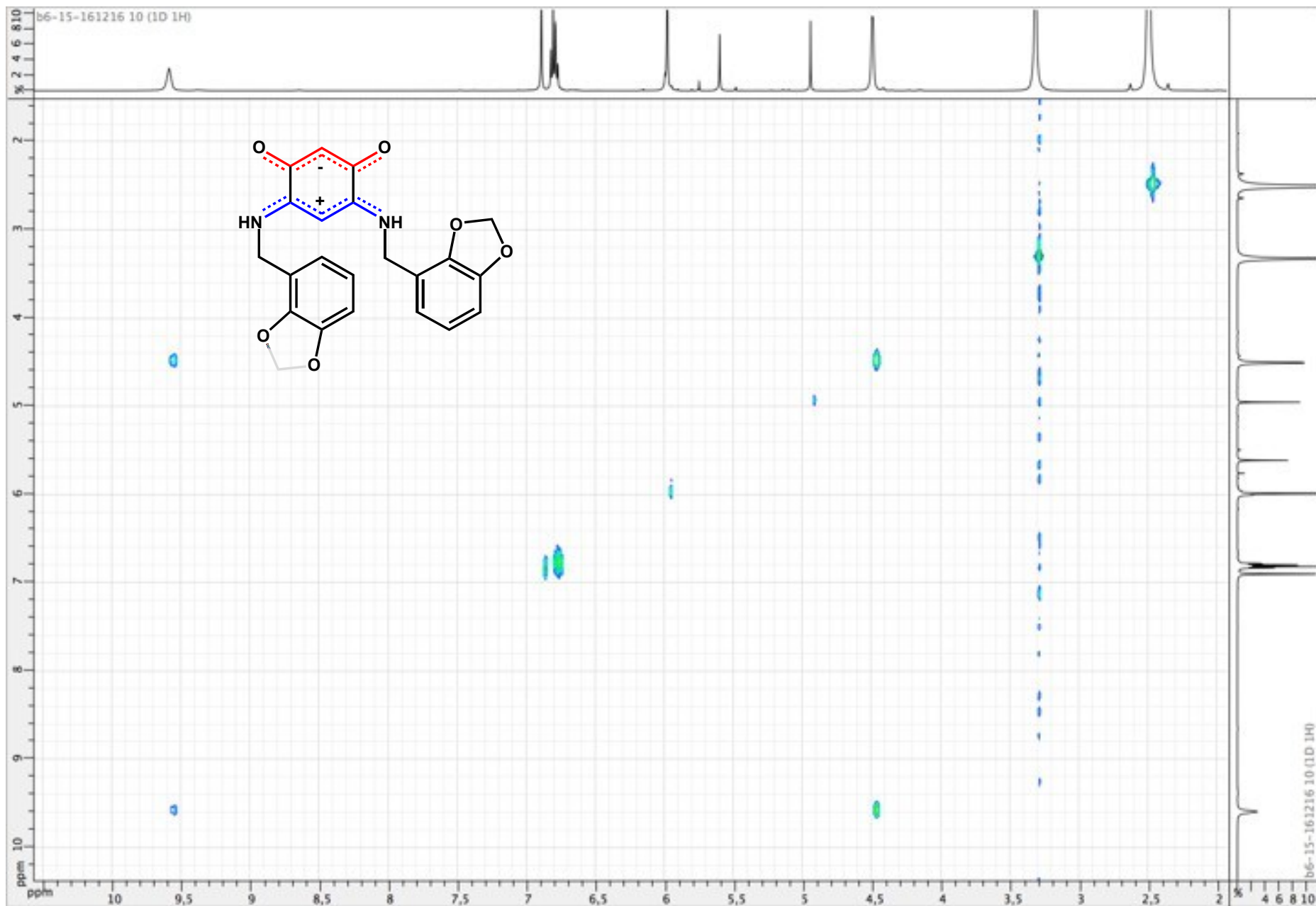


Figure S145. ¹H NMR spectrum of zwitterion **21** (CDCl₃; 500 MHz)

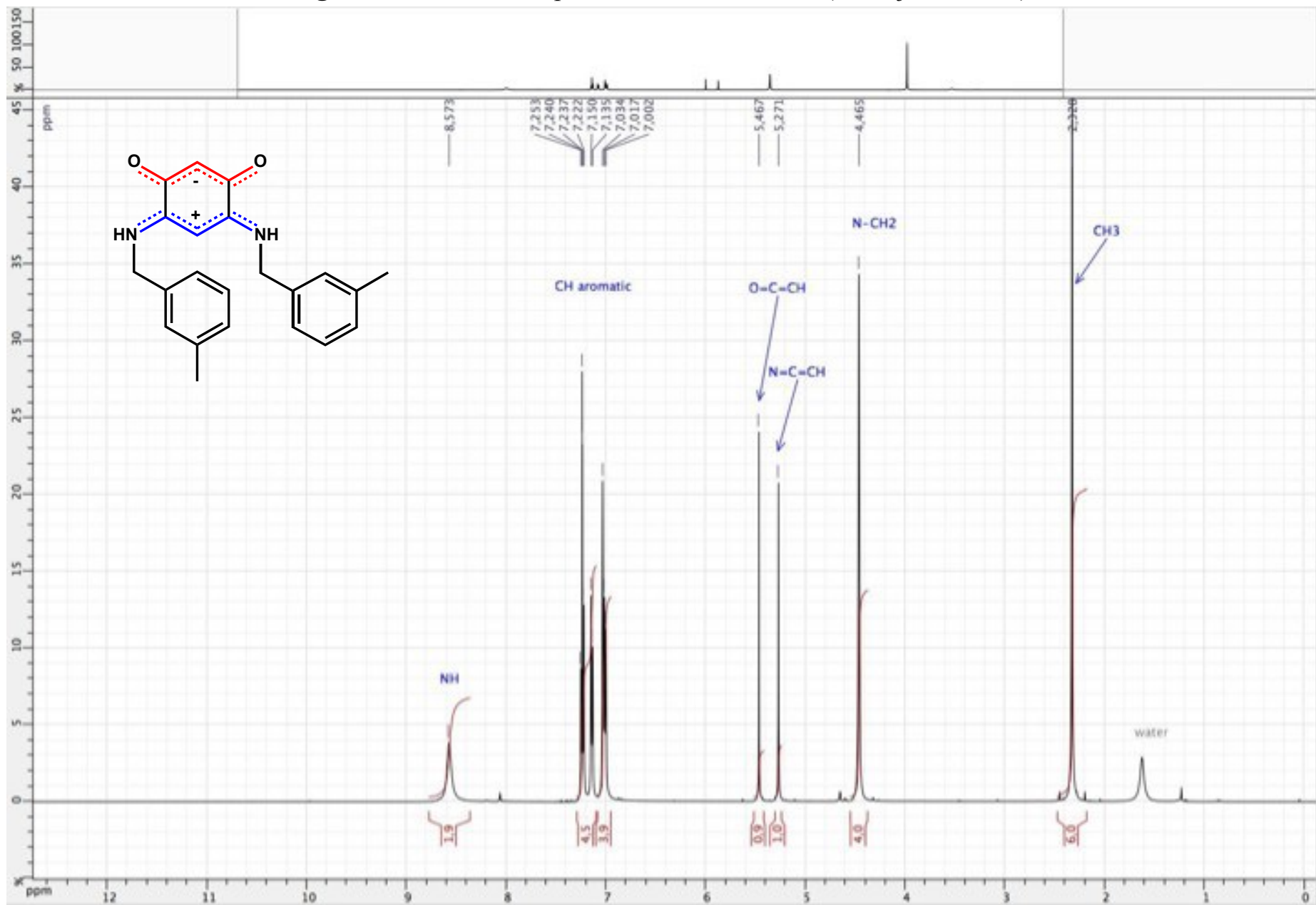


Figure S146. ^1H NMR spectrum of zwitterion **21** (CDCl_3 ; 500 MHz)

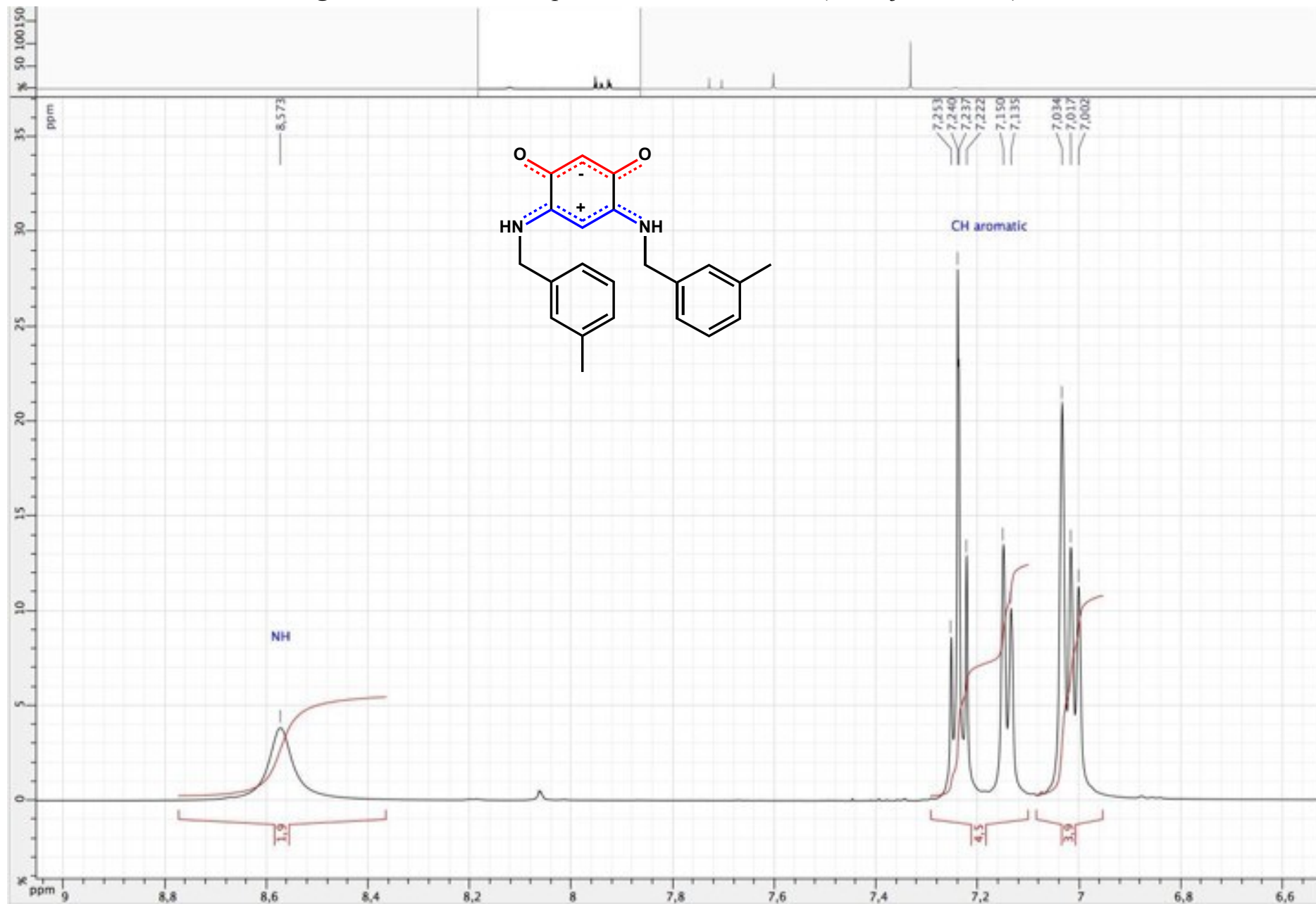


Figure S147. ^1H NMR spectrum of zwitterion **21** (CDCl_3 ; 500 MHz)

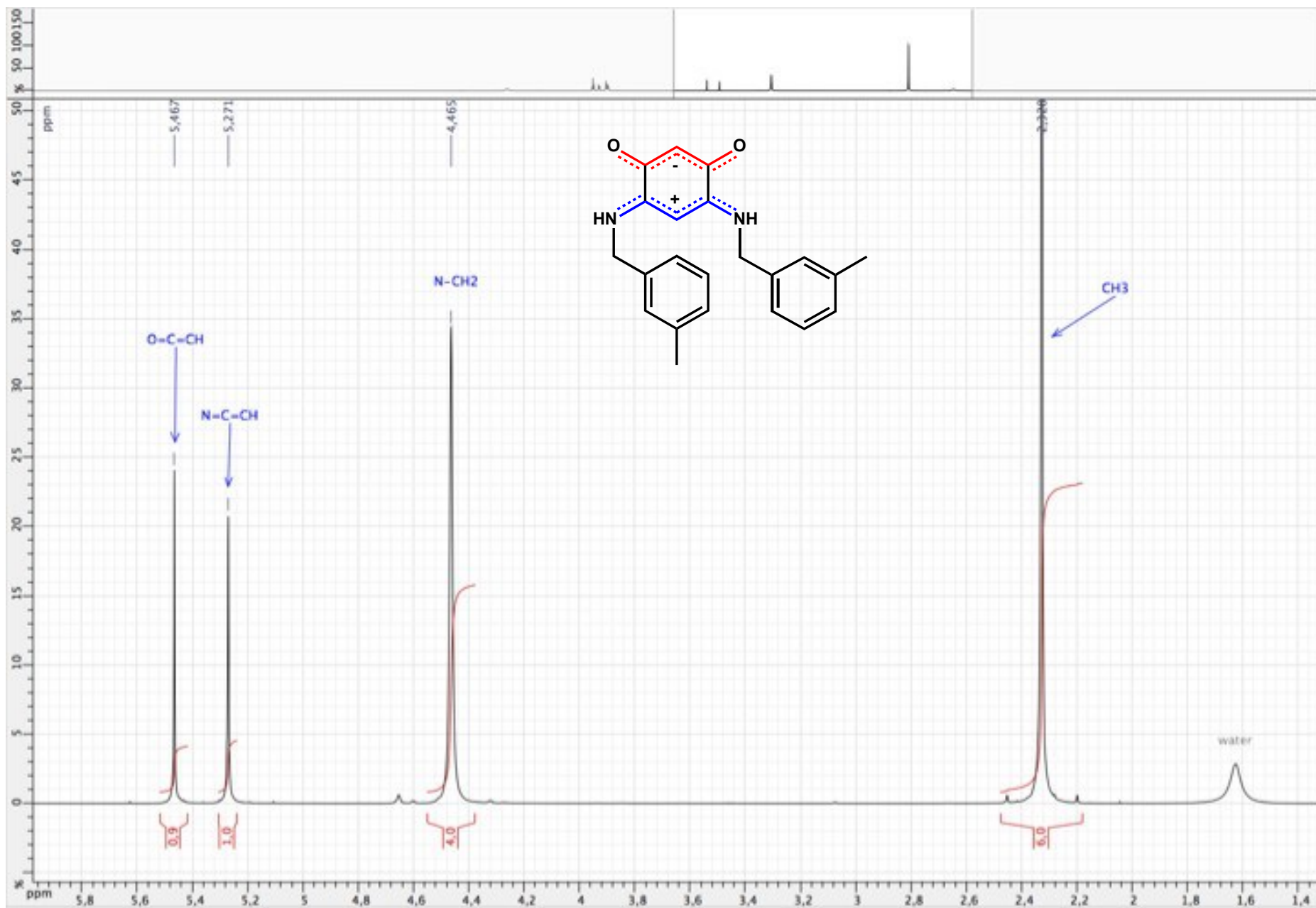


Figure S148. ^{13}C $\{^1\text{H}\}$ NMR spectrum of zwitterion **21** (CDCl_3 ; 125 MHz)

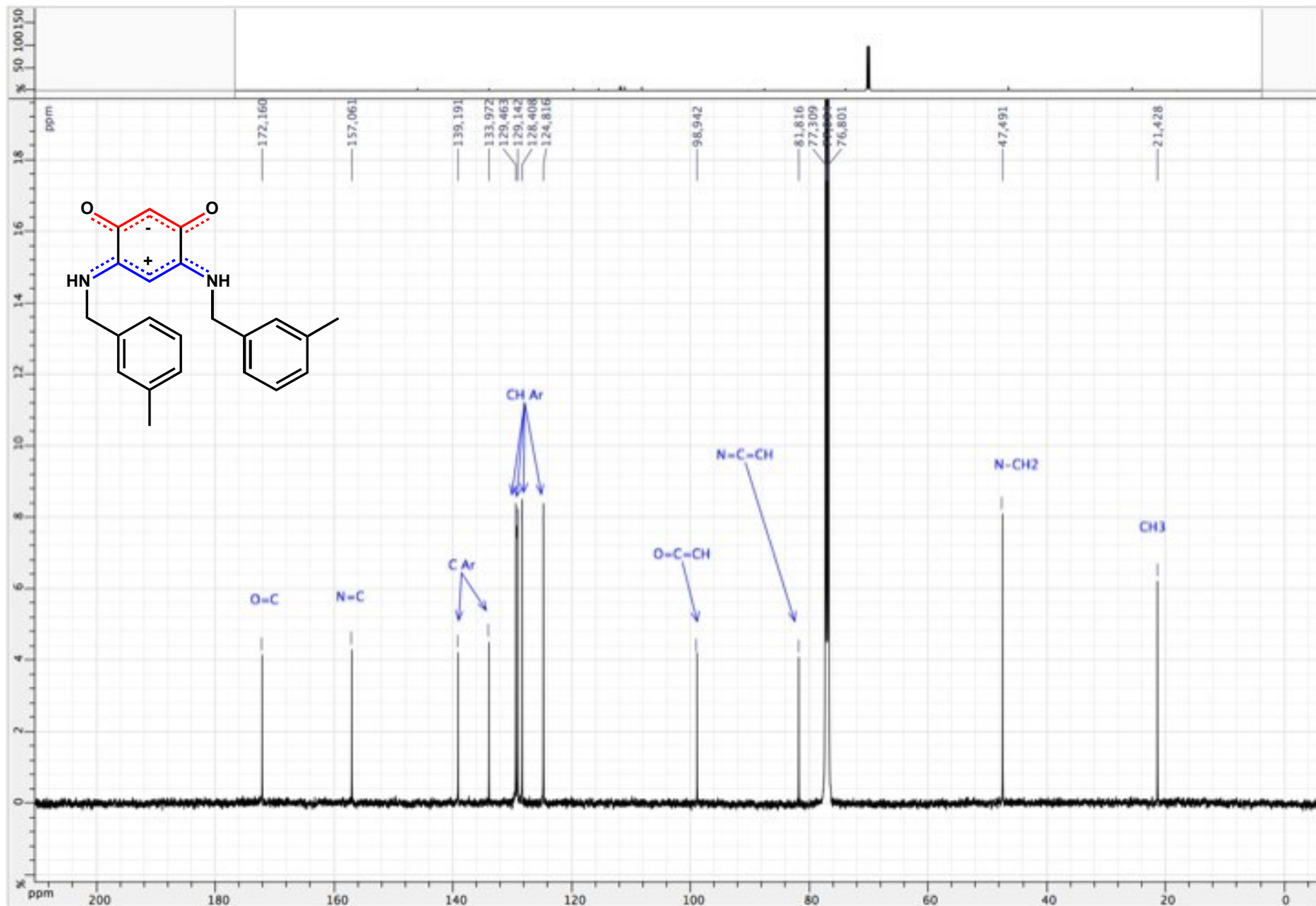


Figure S149. ^{13}C $\{^1\text{H}\}$ NMR spectrum of zwitterion **21** (CDCl_3 ; 125 MHz)

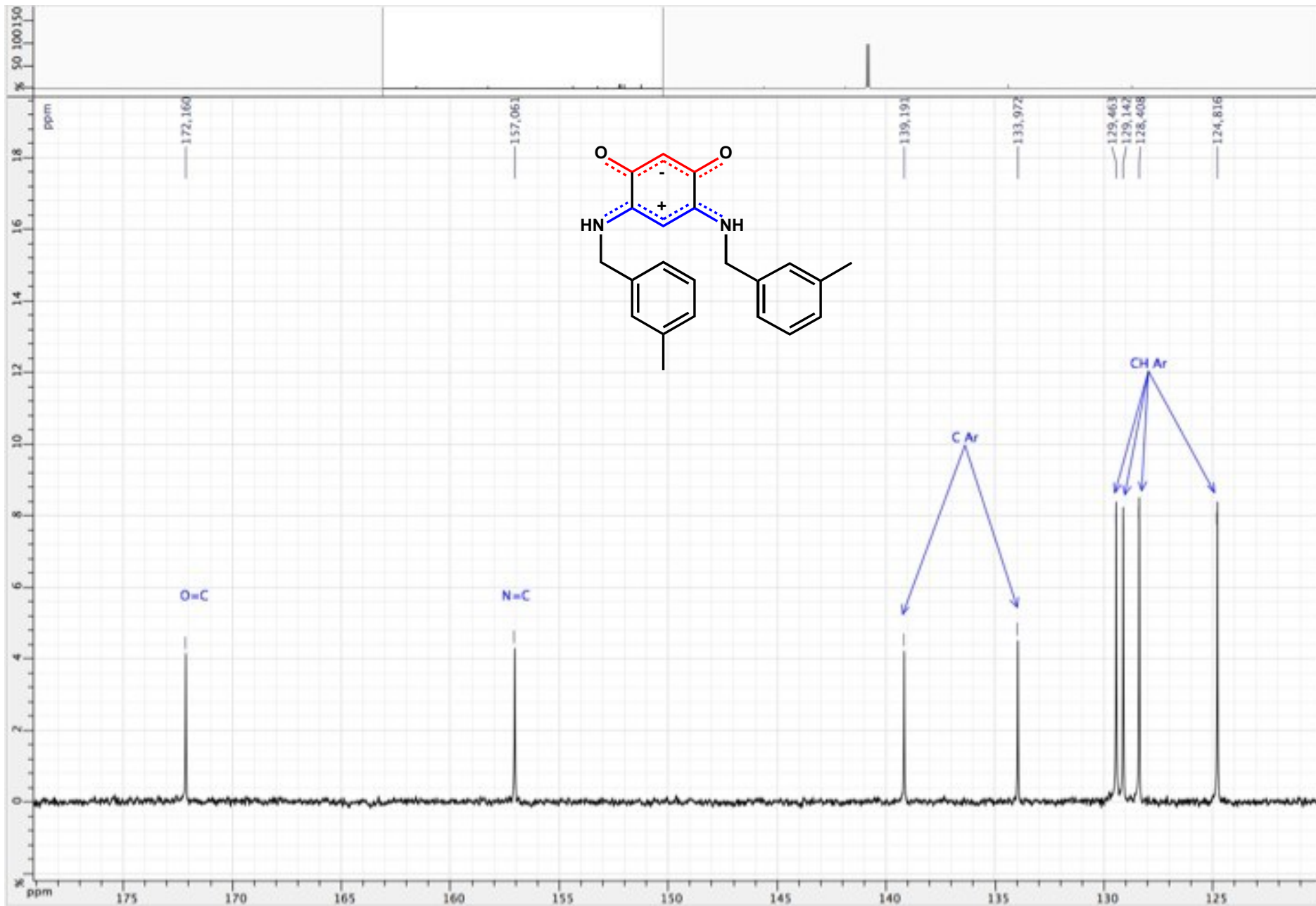


Figure S150. ^{13}C $\{^1\text{H}\}$ NMR spectrum of zwitterion **21** (CDCl_3 ; 125 MHz)

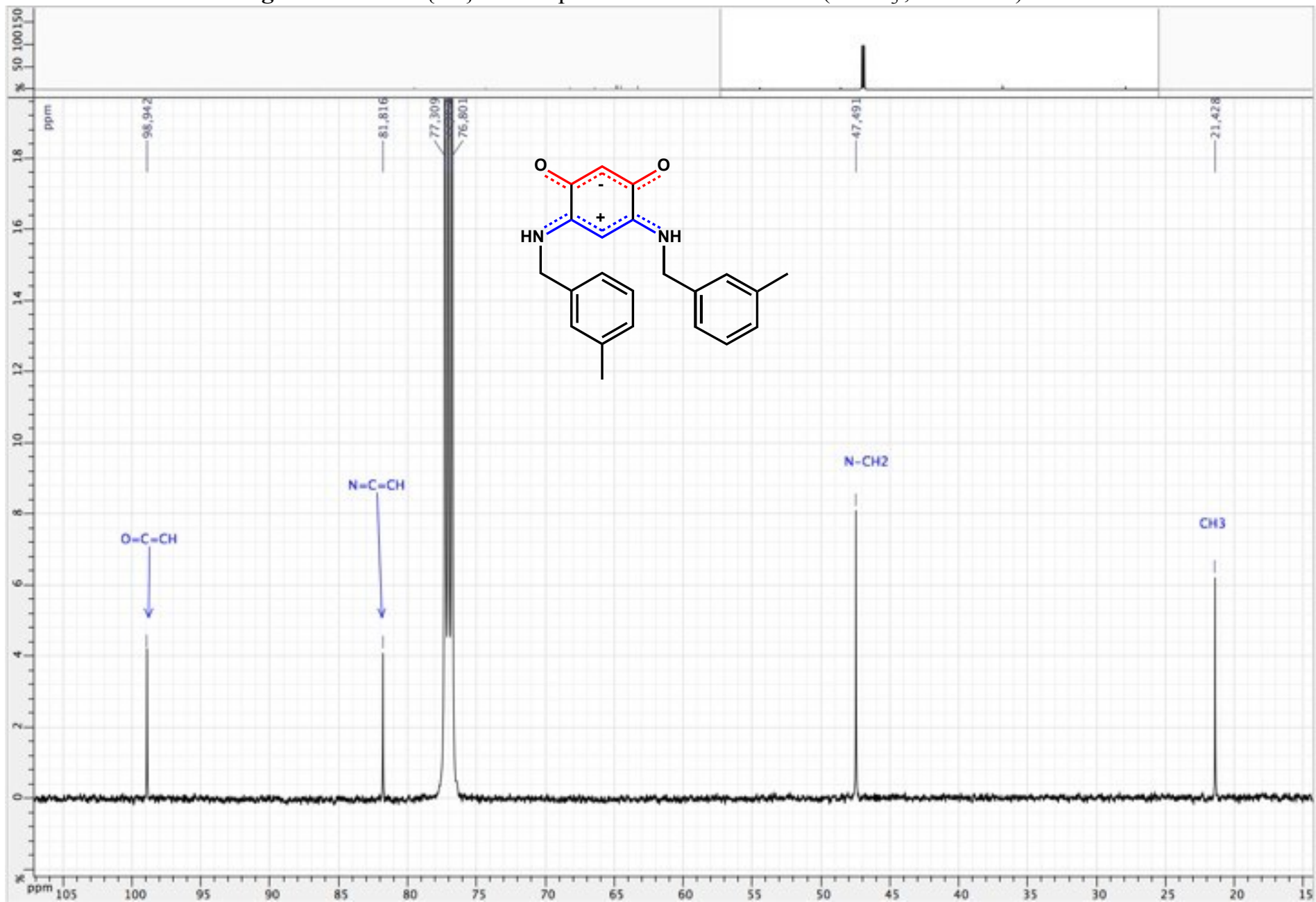


Figure S151. HSQC ($^1\text{H} / ^{13}\text{C} \{^1\text{H}\}$) spectrum of zwitterion **21** (CDCl_3 ; 500 / 125 MHz)

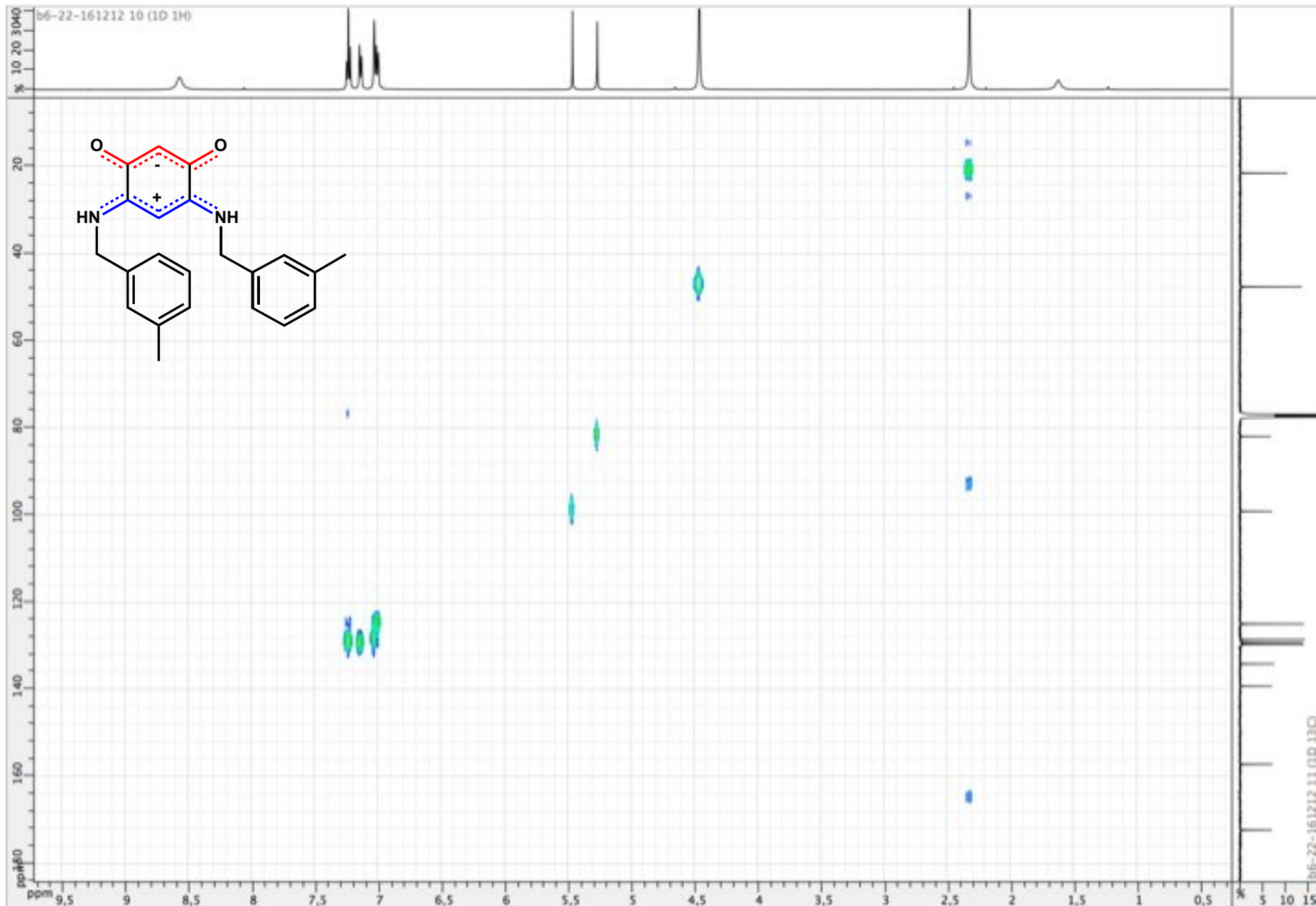


Figure S152. ^1H NMR spectrum of zwitterion **22** (CDCl_3 ; 500 MHz)

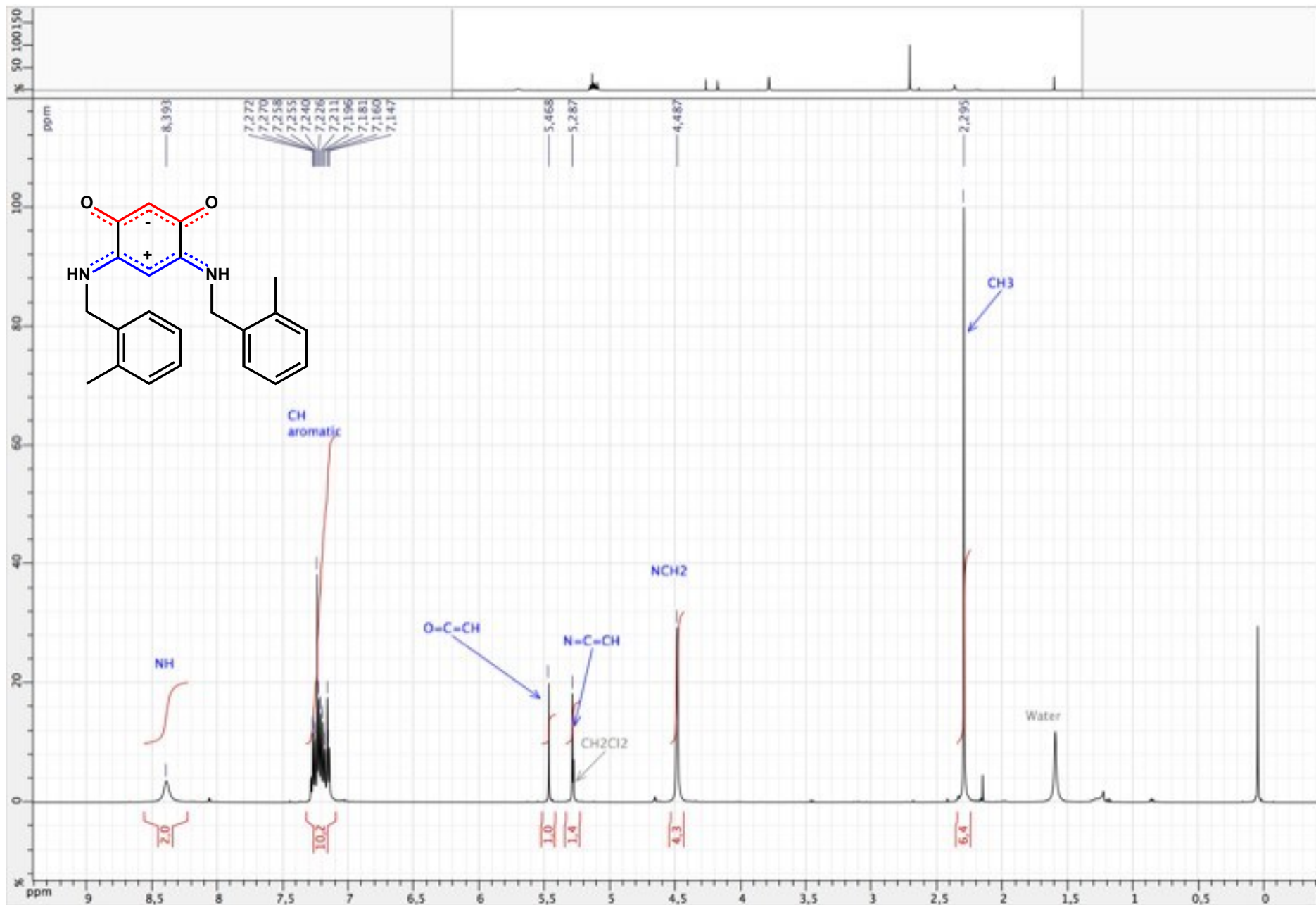


Figure S153. ^1H NMR spectrum of zwitterion **22** (CDCl_3 ; 500 MHz)

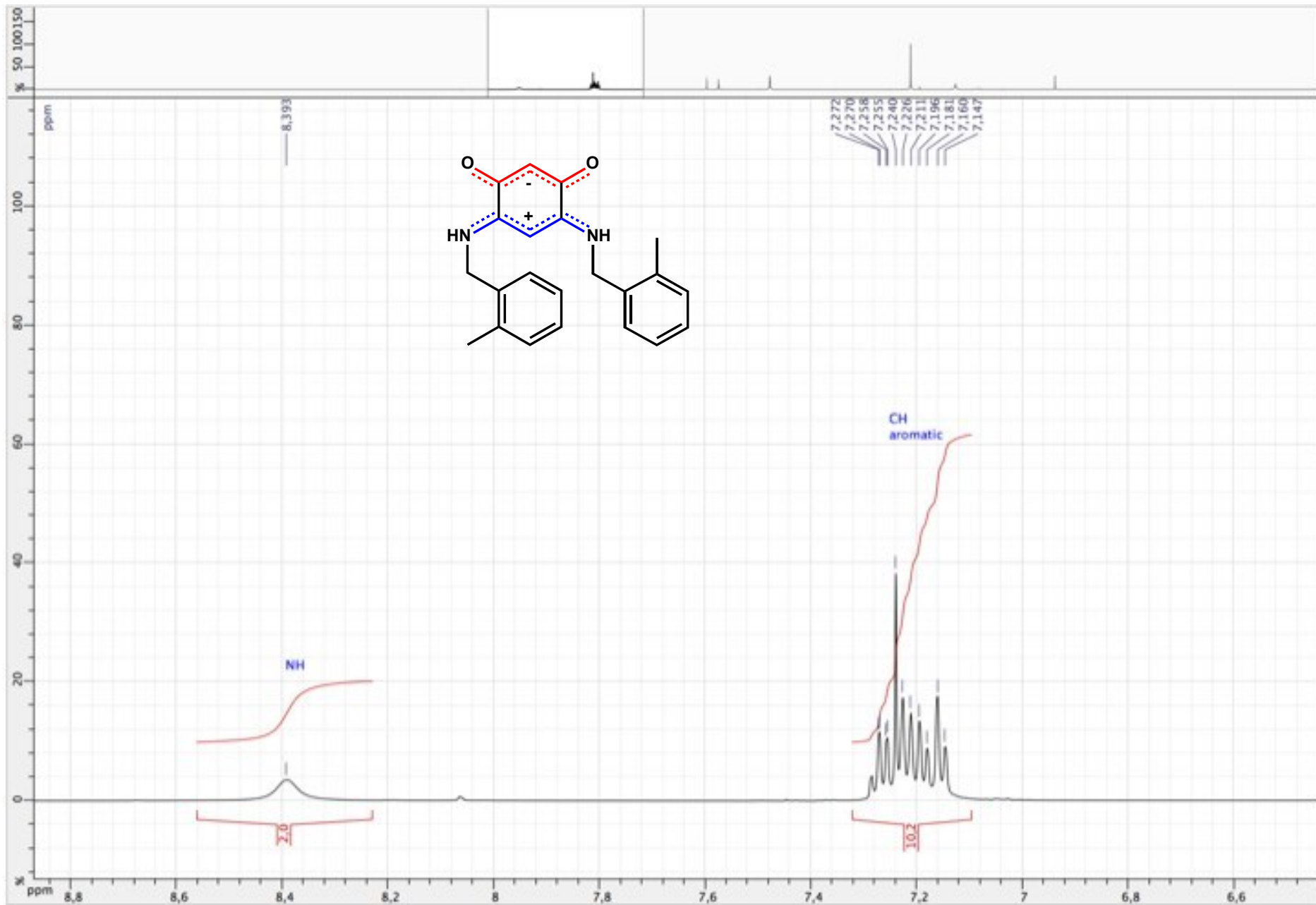


Figure S154. ^1H NMR spectrum of zwitterion **22** (CDCl_3 ; 500 MHz)

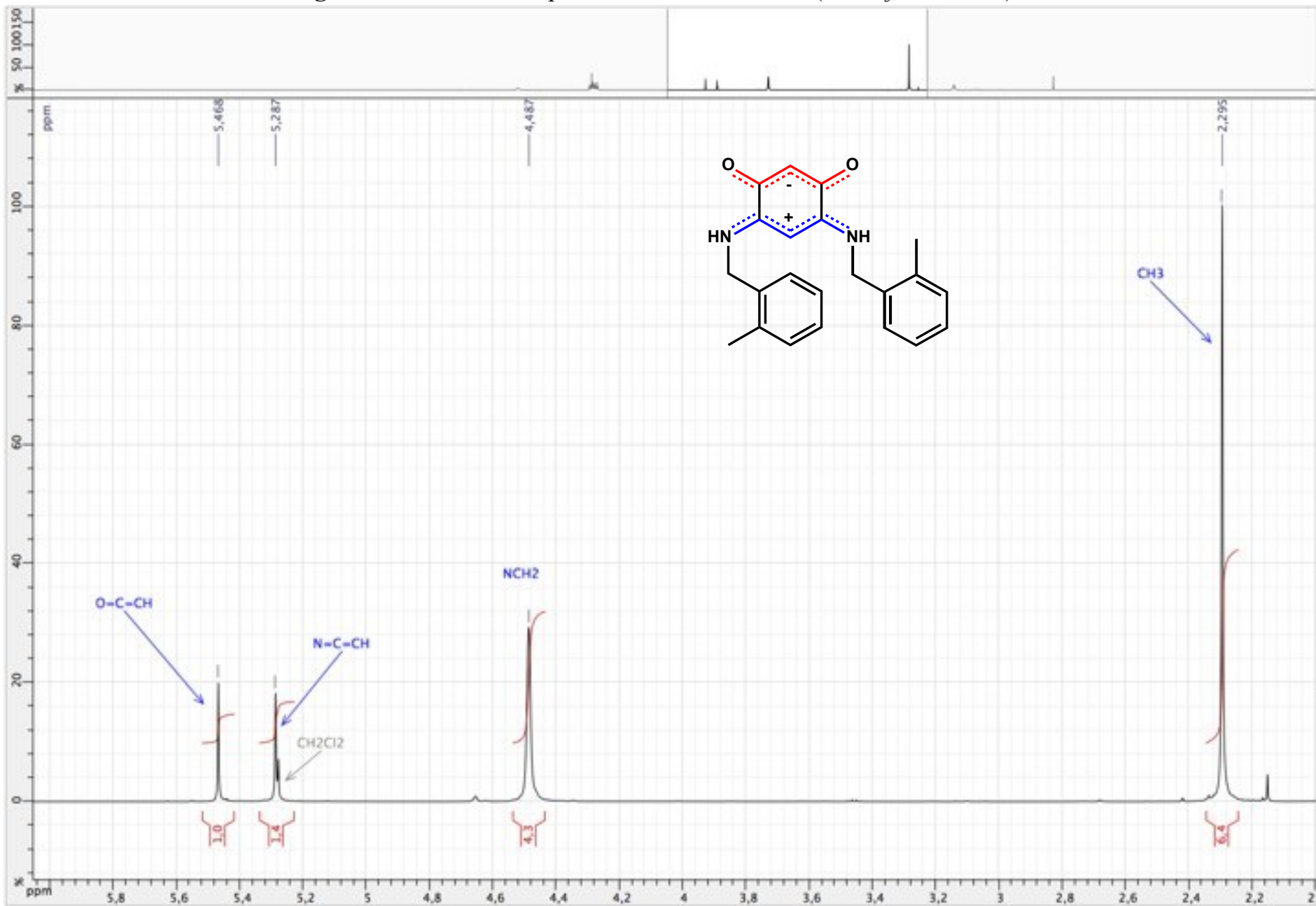


Figure S155. ^{13}C $\{^1\text{H}\}$ NMR spectrum of zwitterion **22** (CDCl_3 ; 125 MHz)

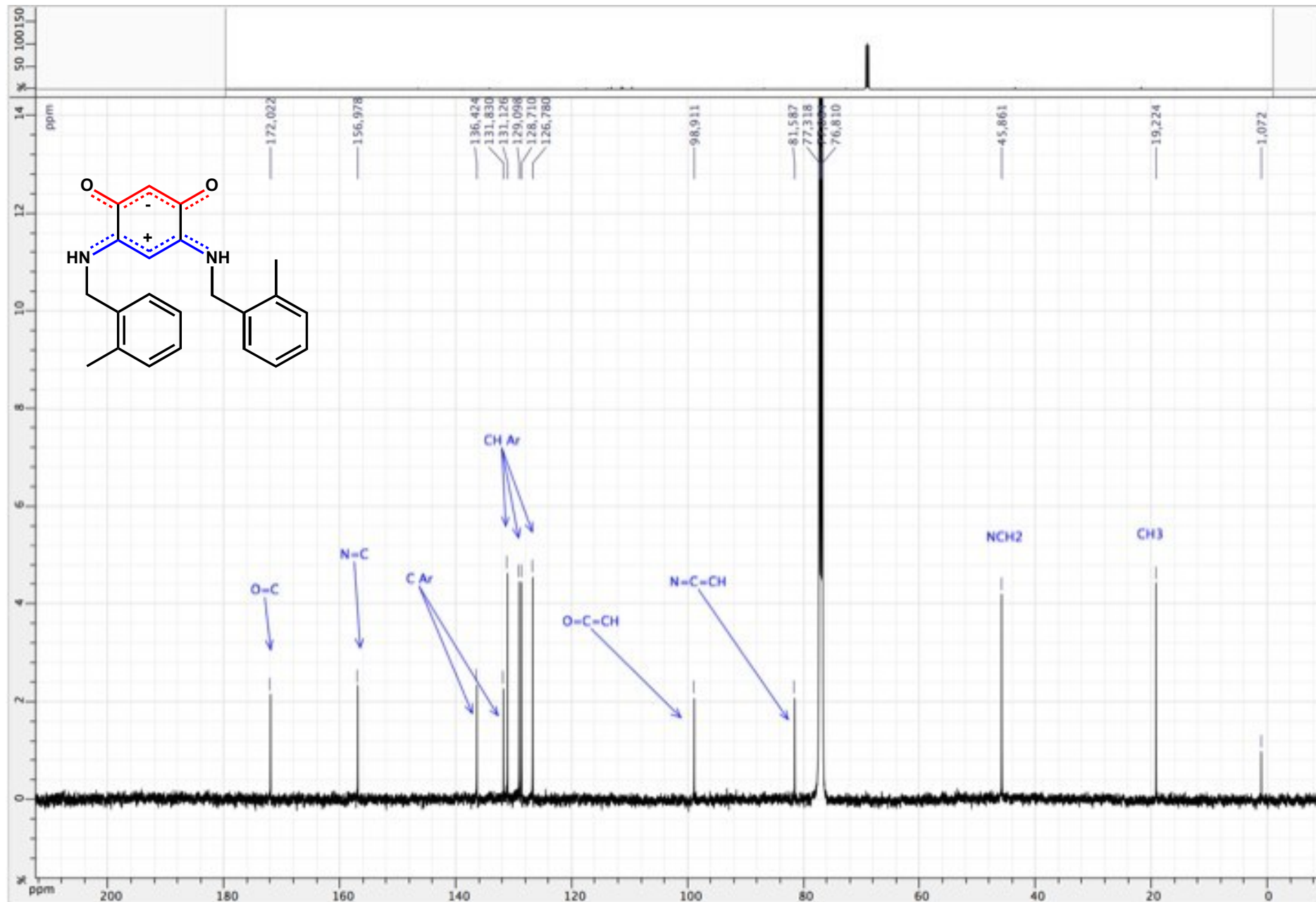


Figure S156. ^{13}C $\{^1\text{H}\}$ NMR spectrum of zwitterion **22** (CDCl_3 ; 125 MHz)

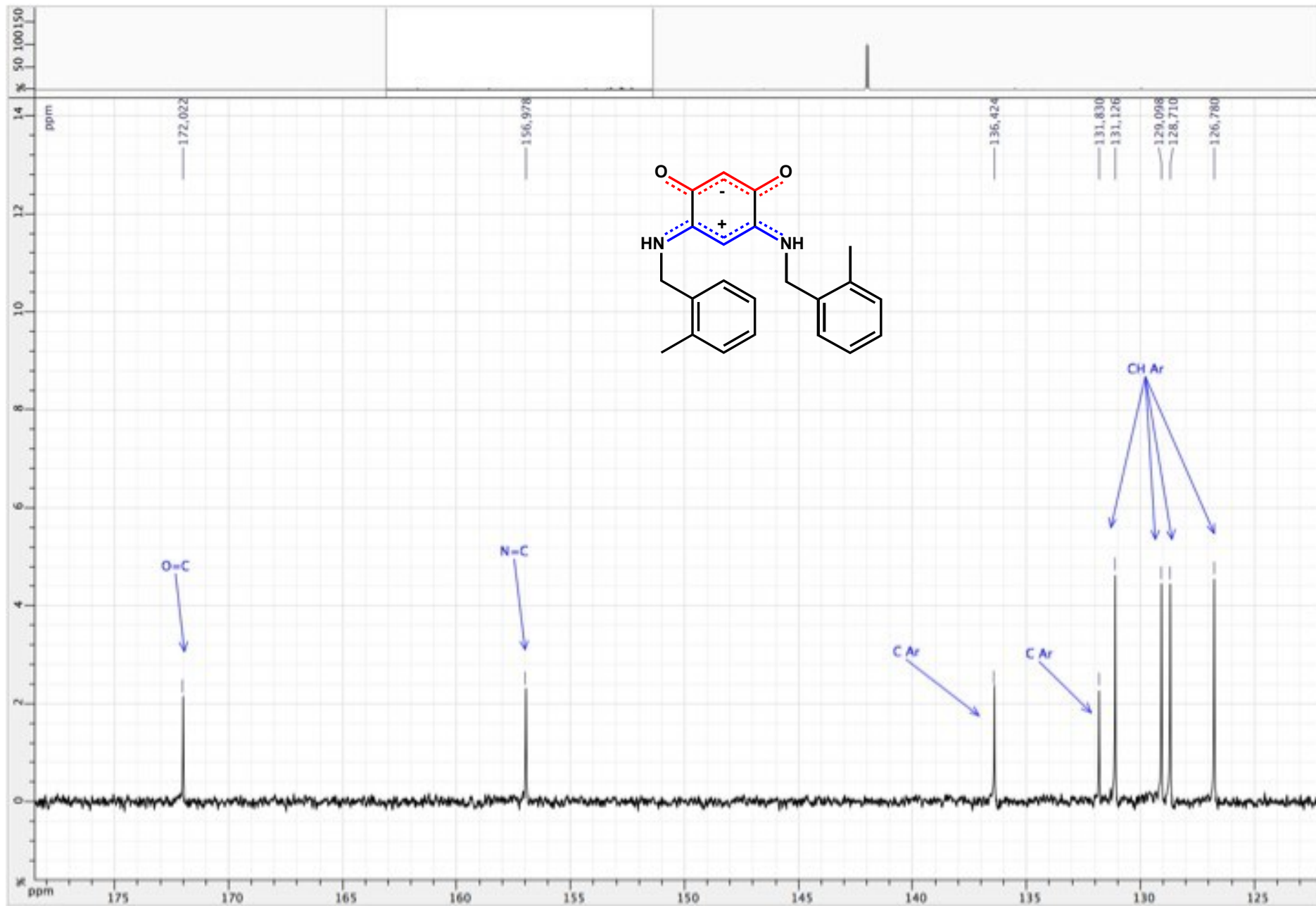


Figure S157. ^{13}C $\{^1\text{H}\}$ NMR spectrum of zwitterion **22** (CDCl_3 ; 125 MHz)

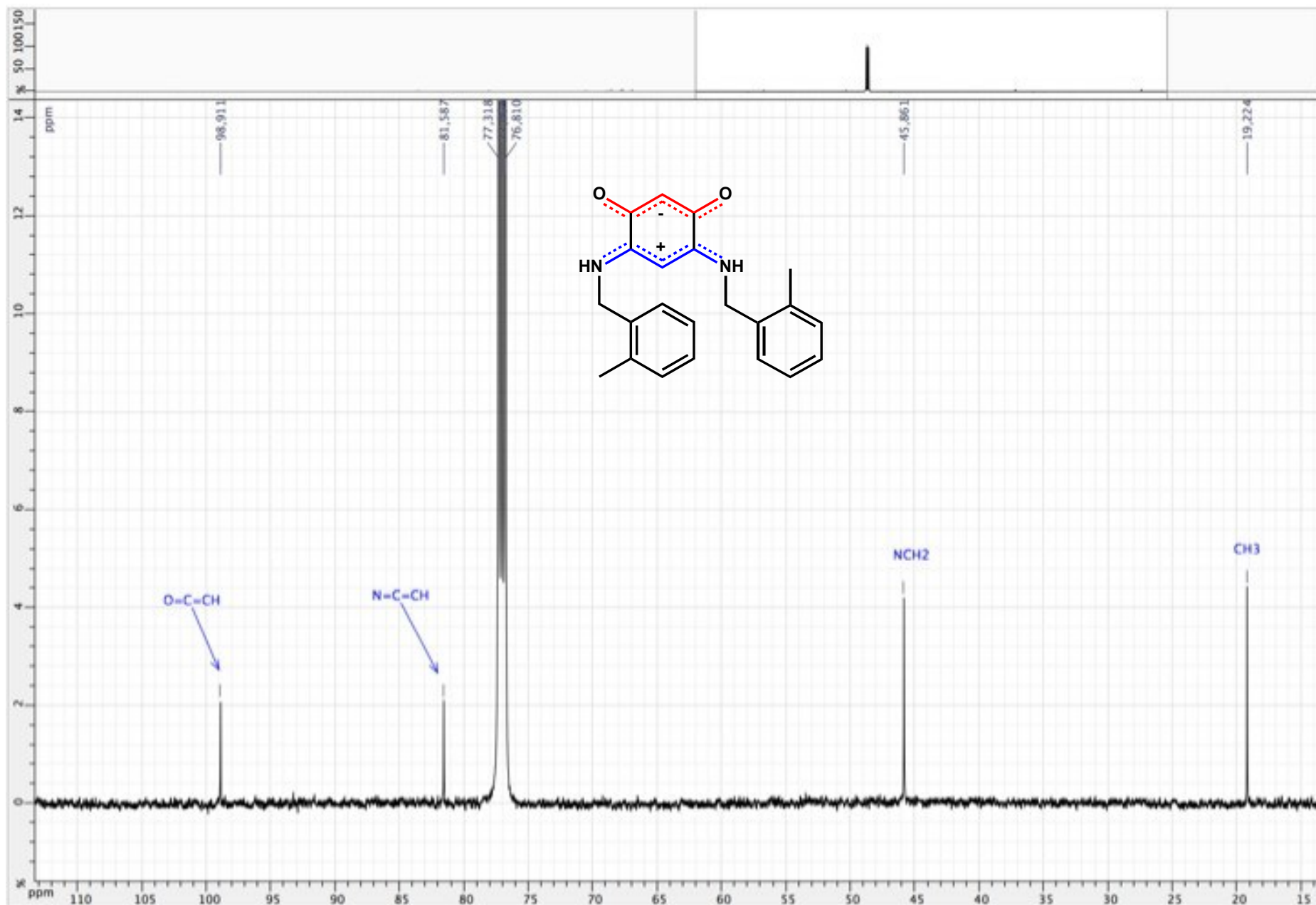


Figure S158. HSQC ($^1\text{H} / ^{13}\text{C} \{^1\text{H}\}$) spectrum of zwitterion **22** (CDCl_3 ; 500 / 125 MHz)

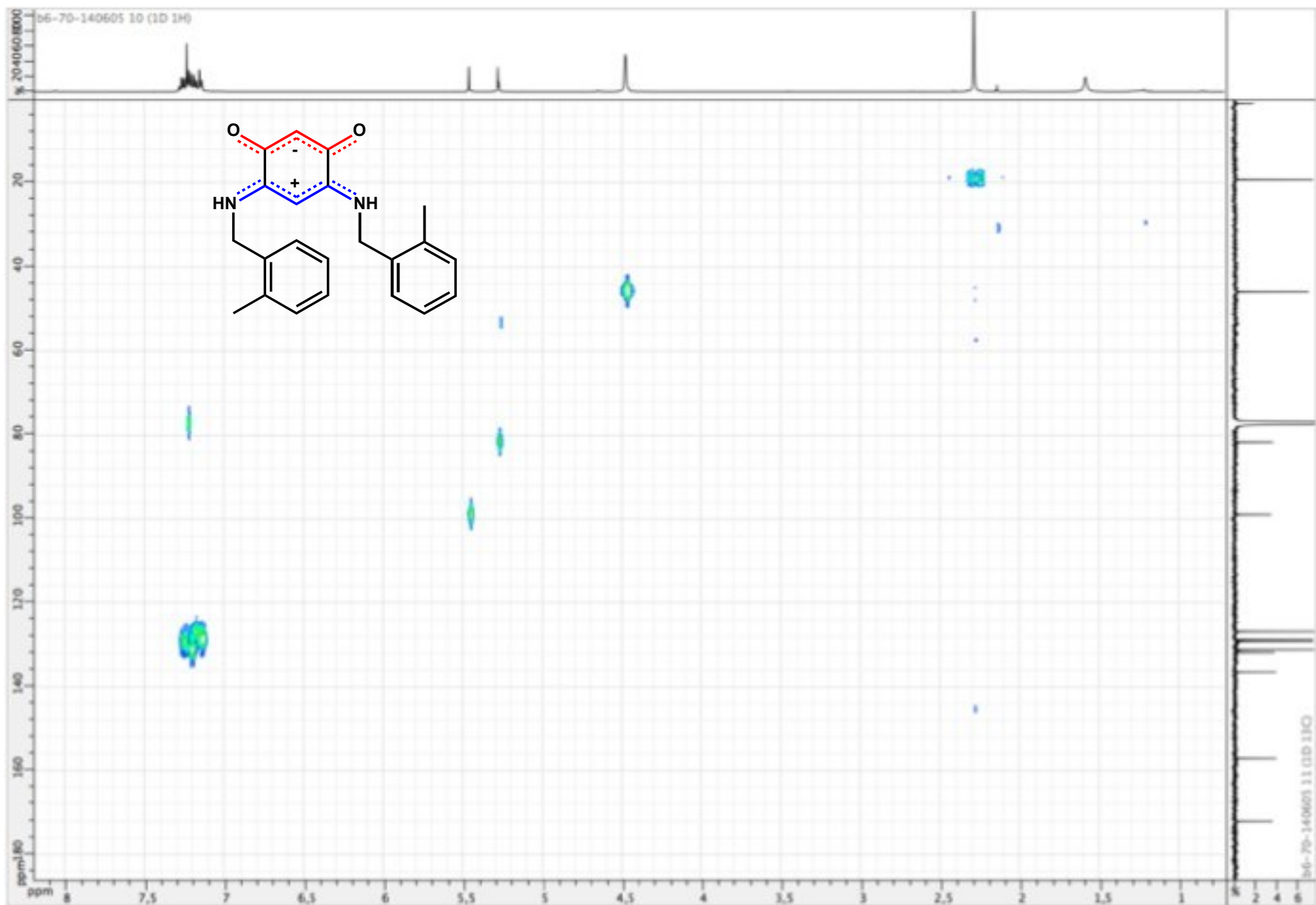


Figure S159. ¹H NMR spectrum of zwitterion **23** (CDCl₃; 500 MHz)

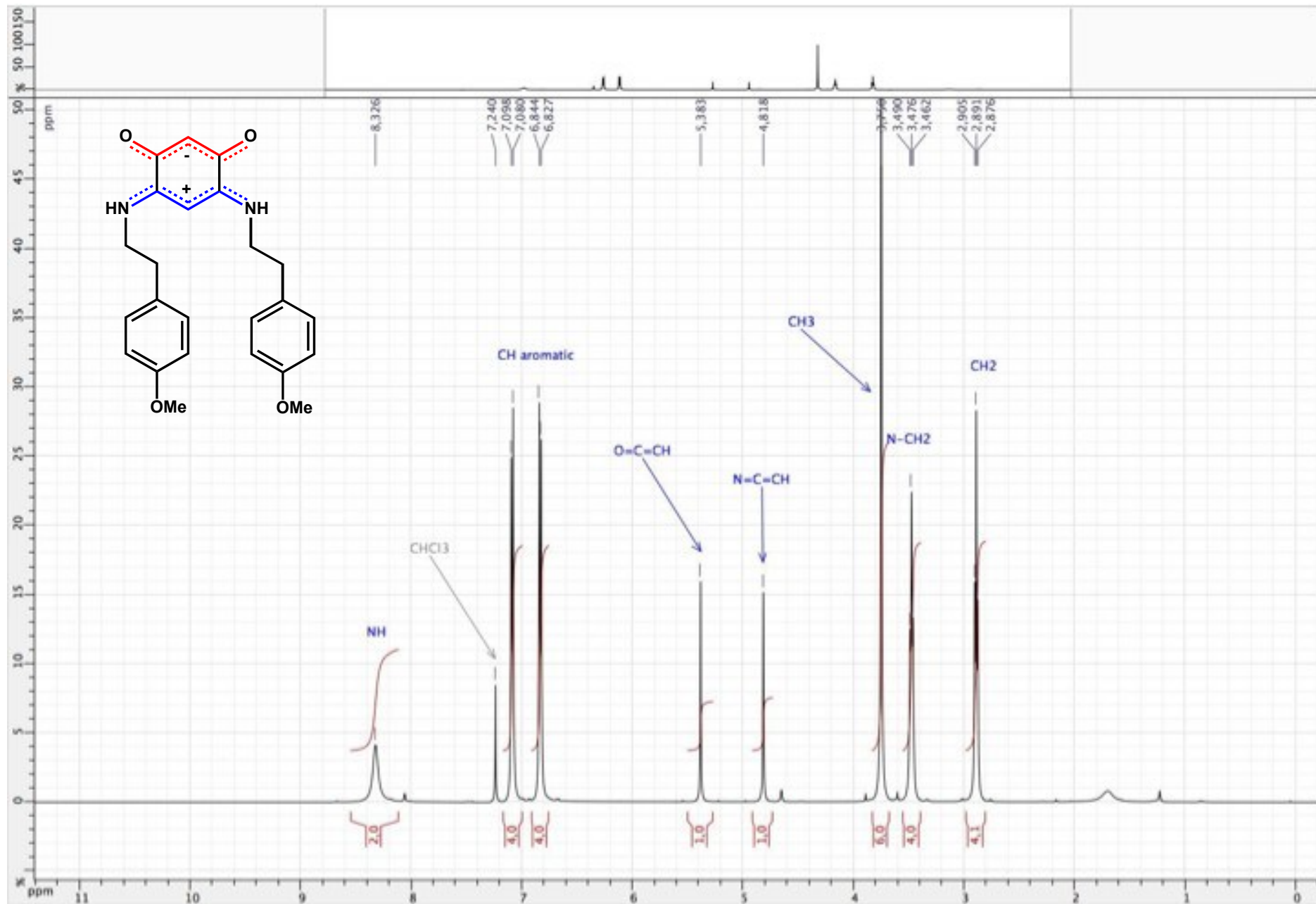


Figure S160. ^1H NMR spectrum of zwitterion **23** (CDCl_3 ; 500 MHz)

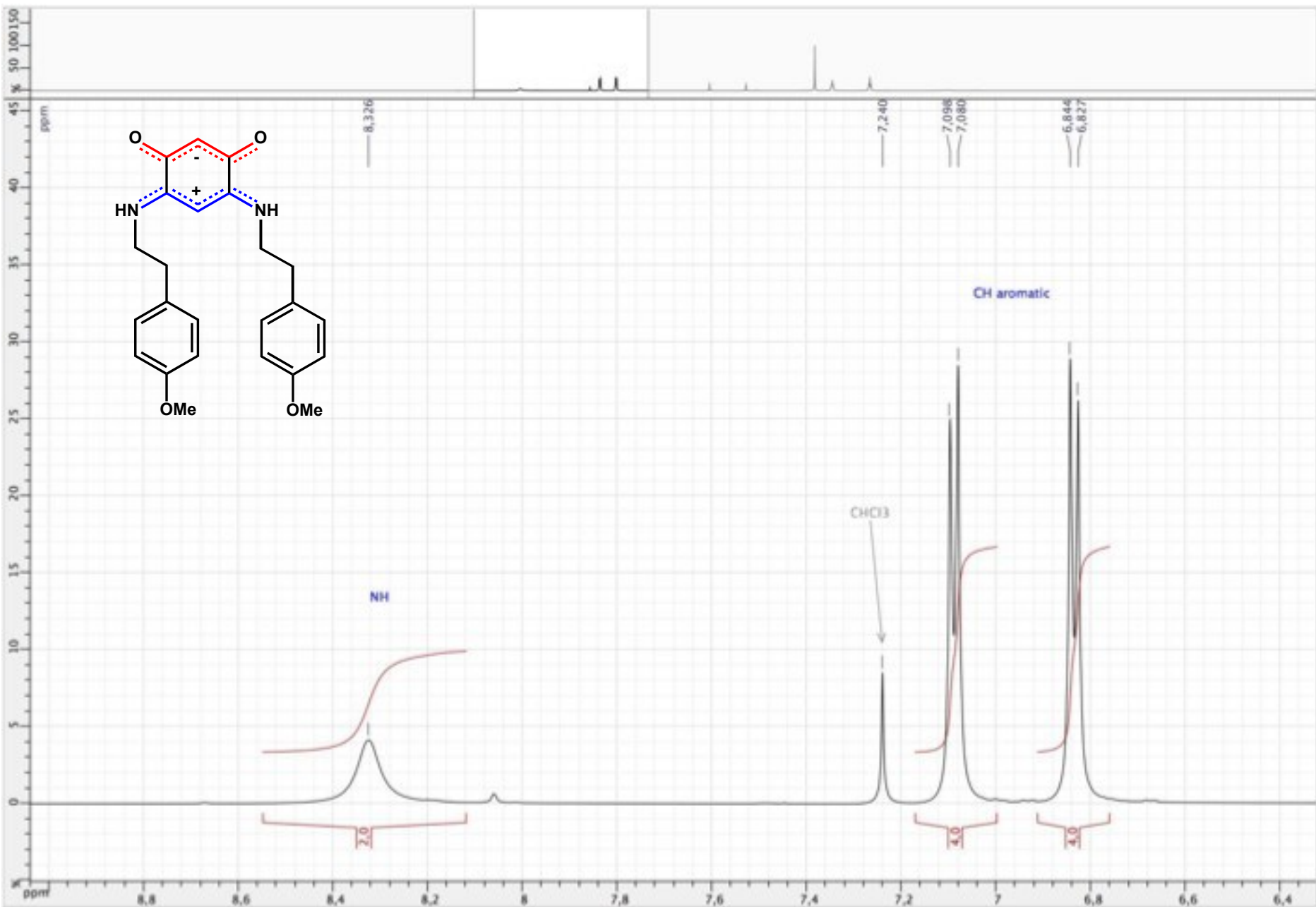


Figure S161. ^1H NMR spectrum of zwitterion **23** (CDCl_3 ; 500 MHz)

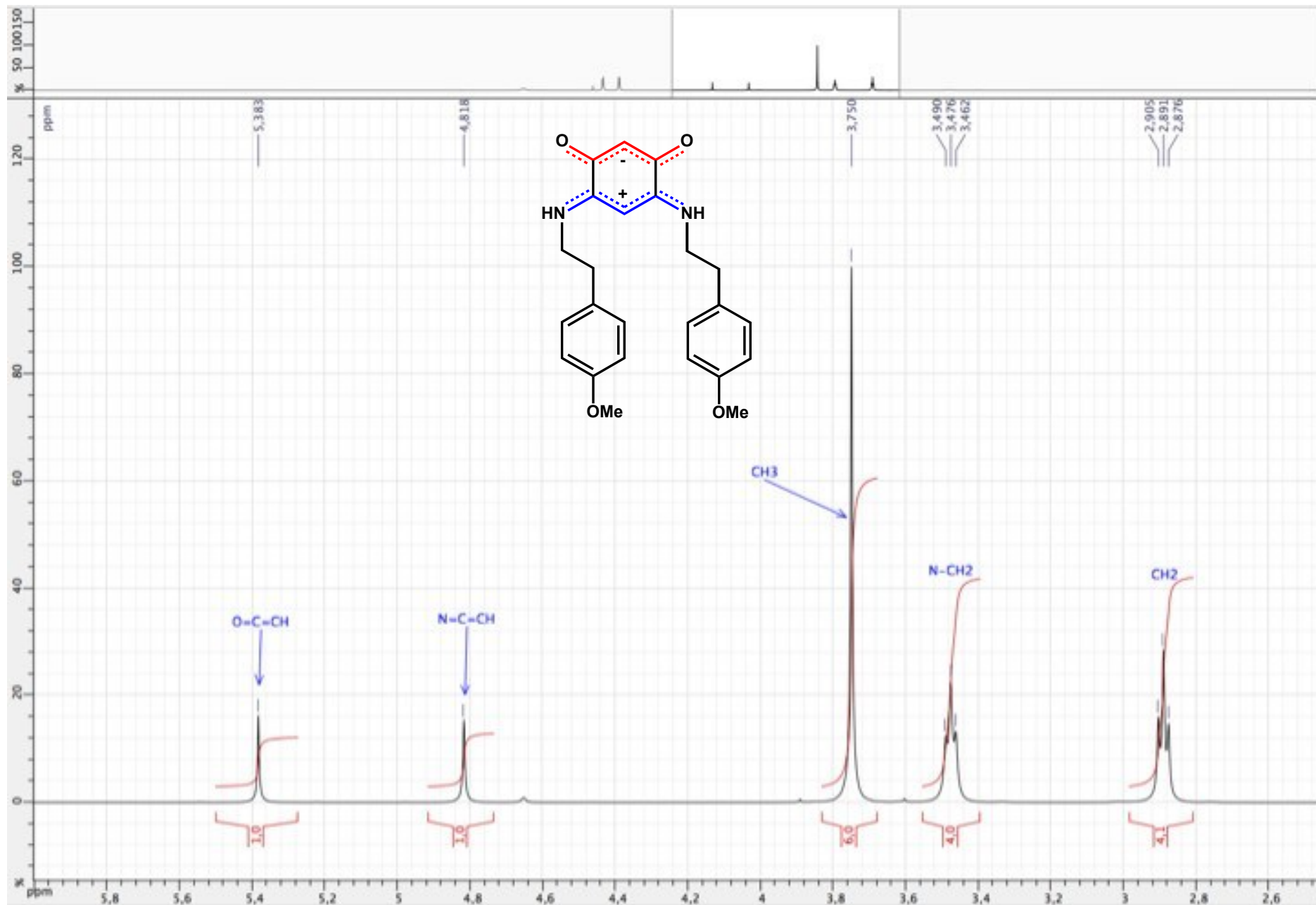


Figure S162. ^1H NMR spectrum of zwitterion **23** (CDCl_3 ; 500 MHz)

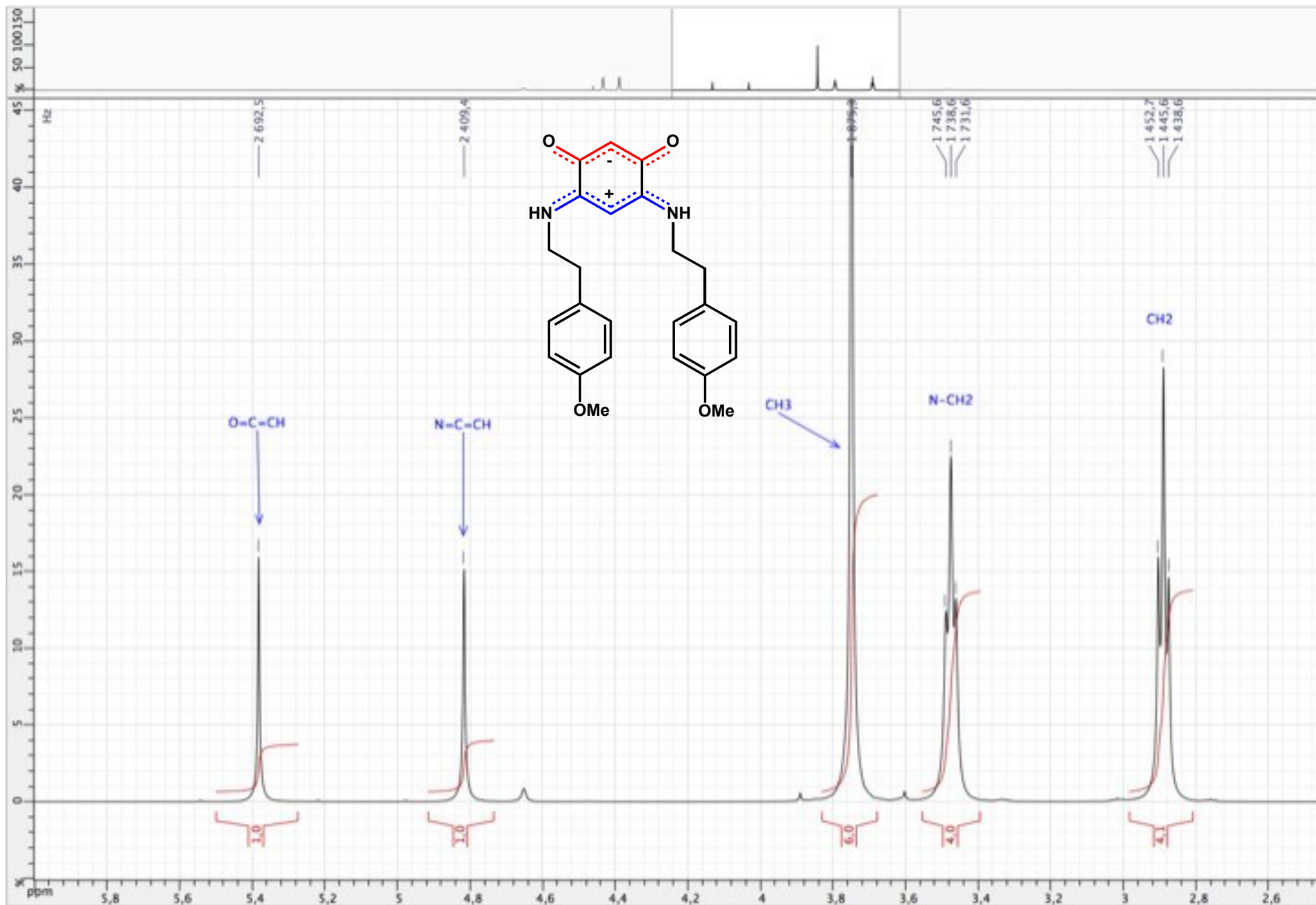


Figure S163. ^{13}C $\{^1\text{H}\}$ NMR spectrum of zwitterion **23** (CDCl_3 ; 125 MHz)

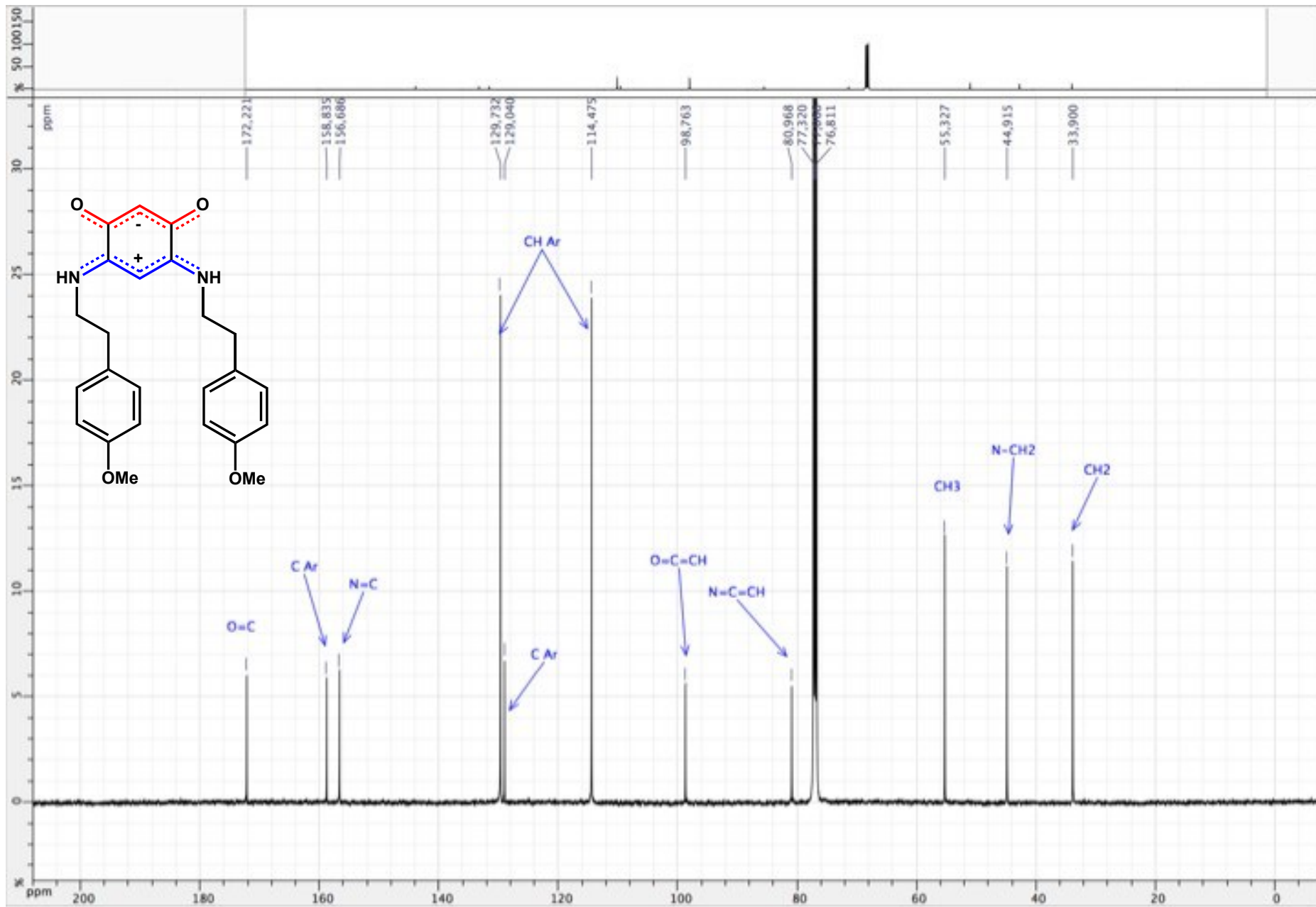


Figure S164. ^{13}C $\{^1\text{H}\}$ NMR spectrum of zwitterion **23** (CDCl_3 ; 125 MHz)

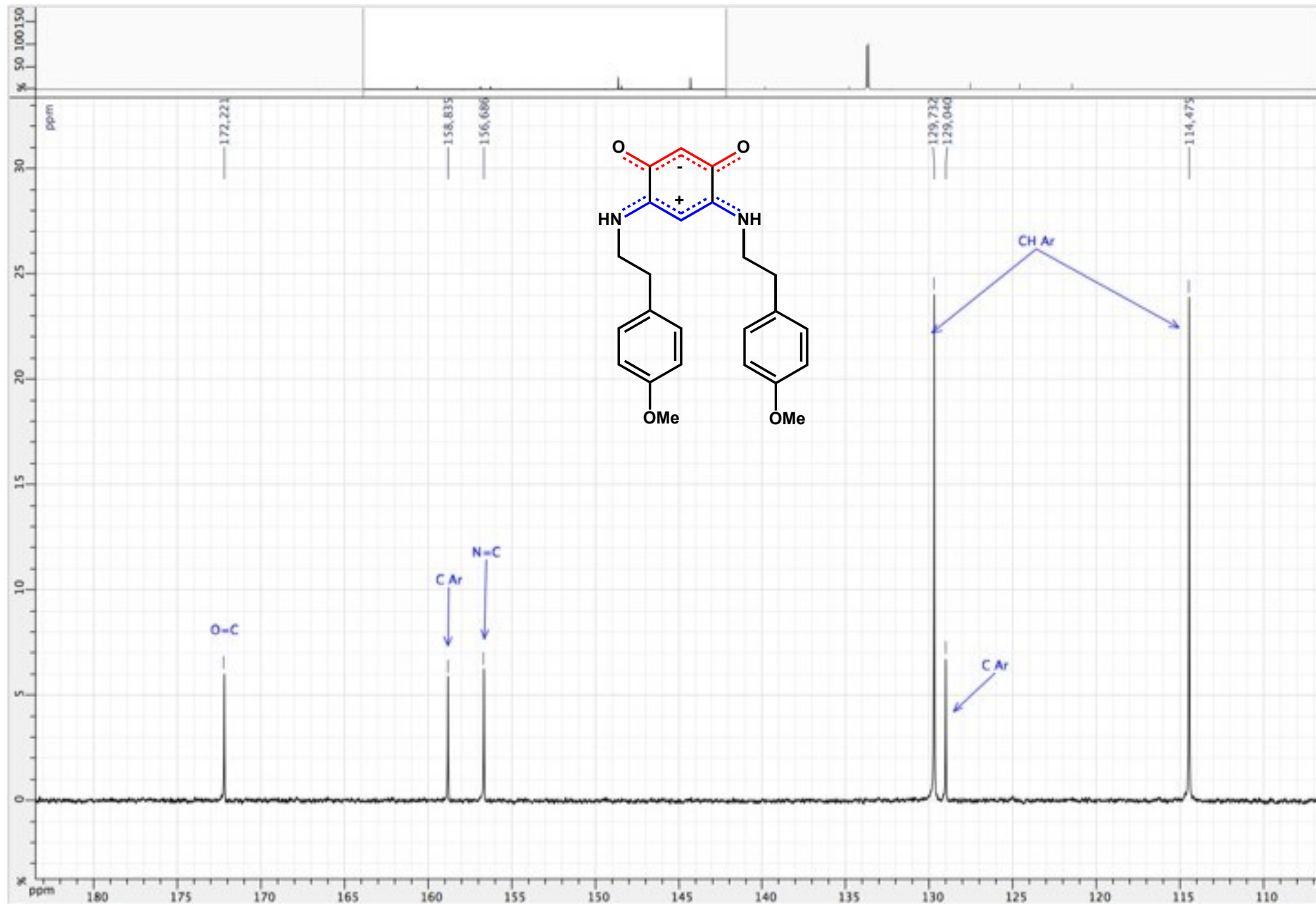


Figure S165. ^{13}C $\{^1\text{H}\}$ NMR spectrum of zwitterion **23** (CDCl_3 ; 125 MHz)

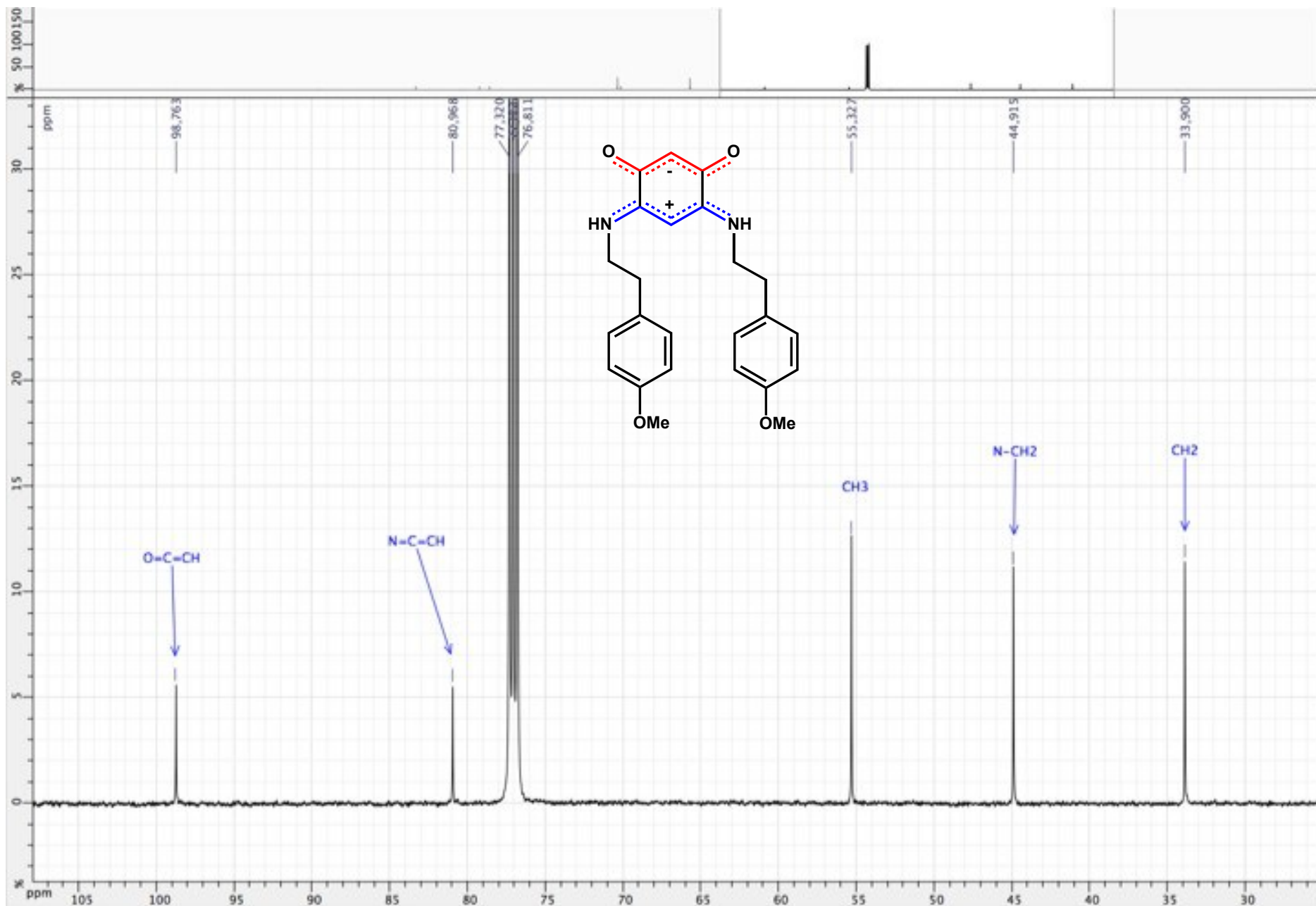


Figure S166. HSQC ($^1\text{H} / ^{13}\text{C} \{^1\text{H}\}$) spectrum of zwitterion **23** (CDCl_3 ; 500 / 125 MHz)

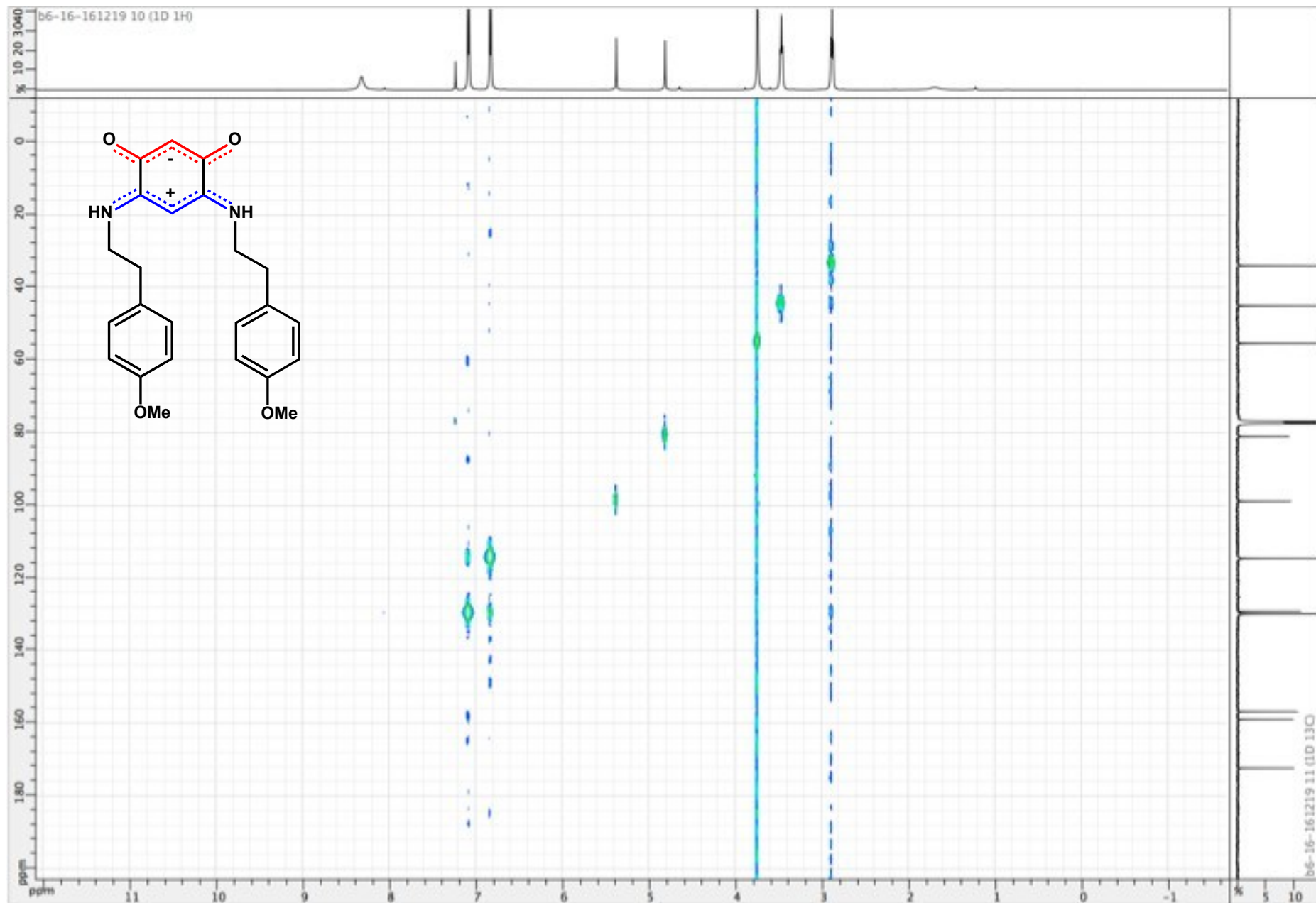


Figure S167. COSY ($^1\text{H} / ^1\text{H}$) spectrum of zwitterion **23** (CDCl_3 ; 500 MHz)

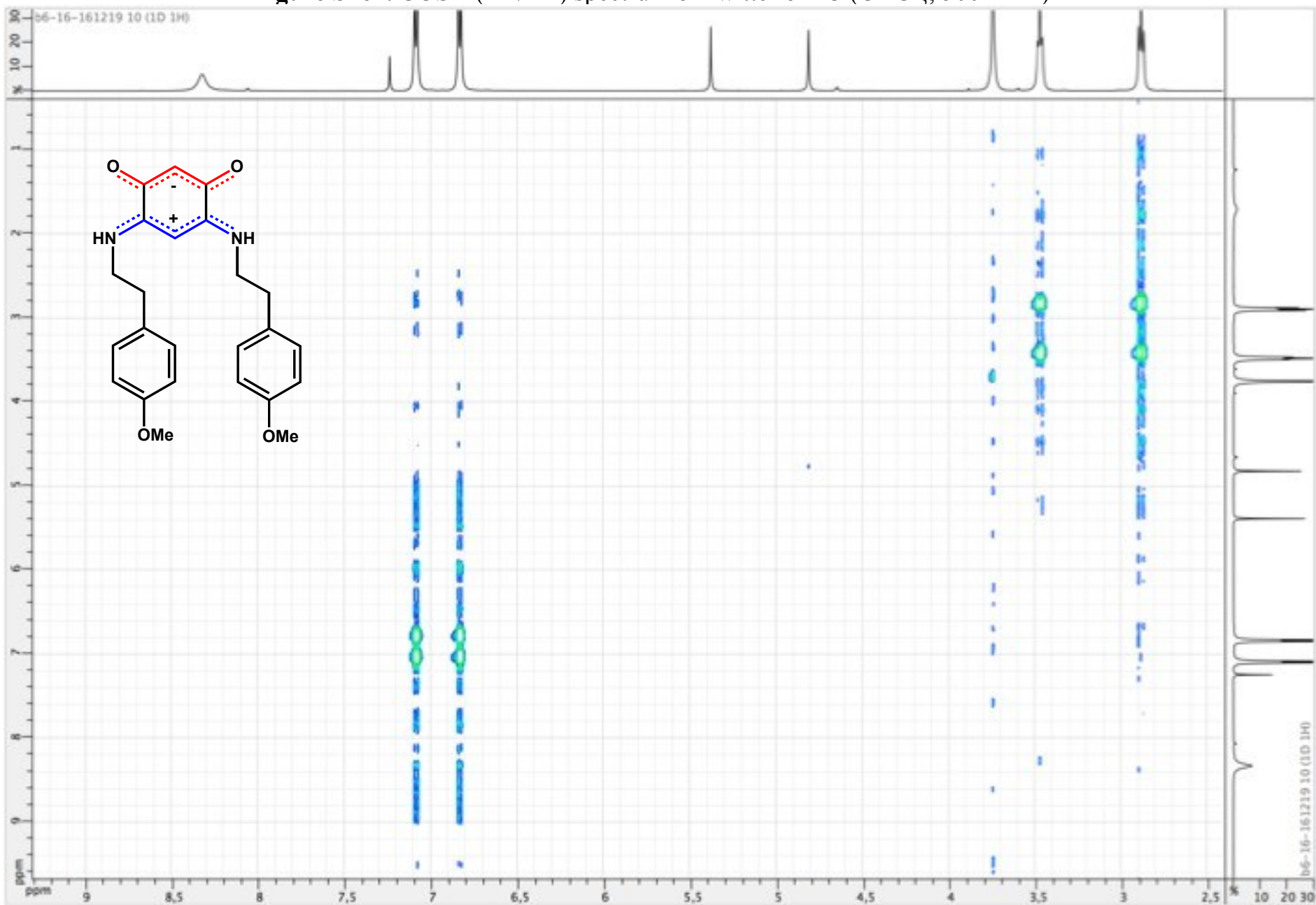


Figure S168. ¹H NMR spectrum of zwitterion **24** (CDCl₃; 500 MHz)

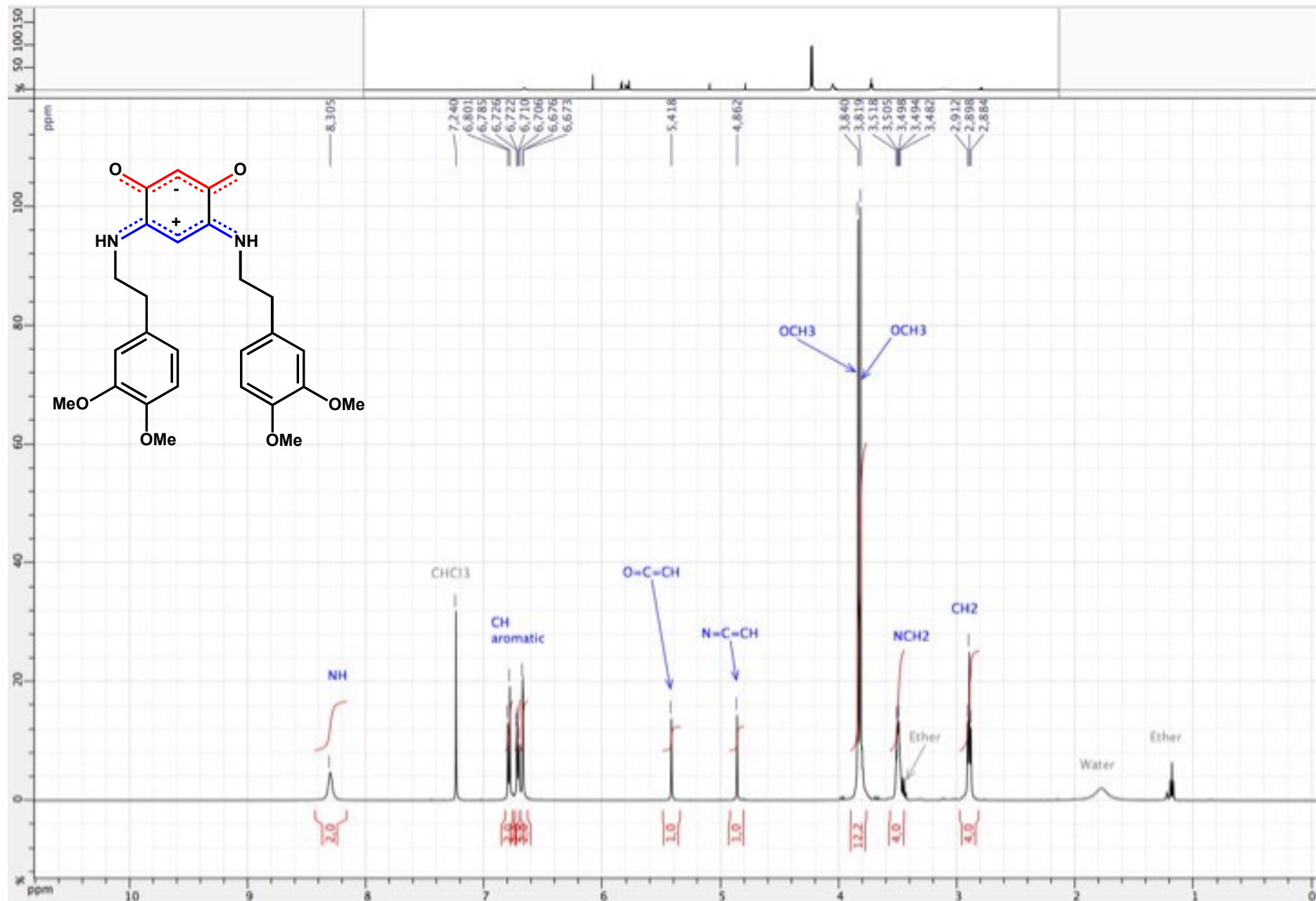


Figure S169. ^1H NMR spectrum of zwitterion **24** (CDCl_3 ; 500 MHz)

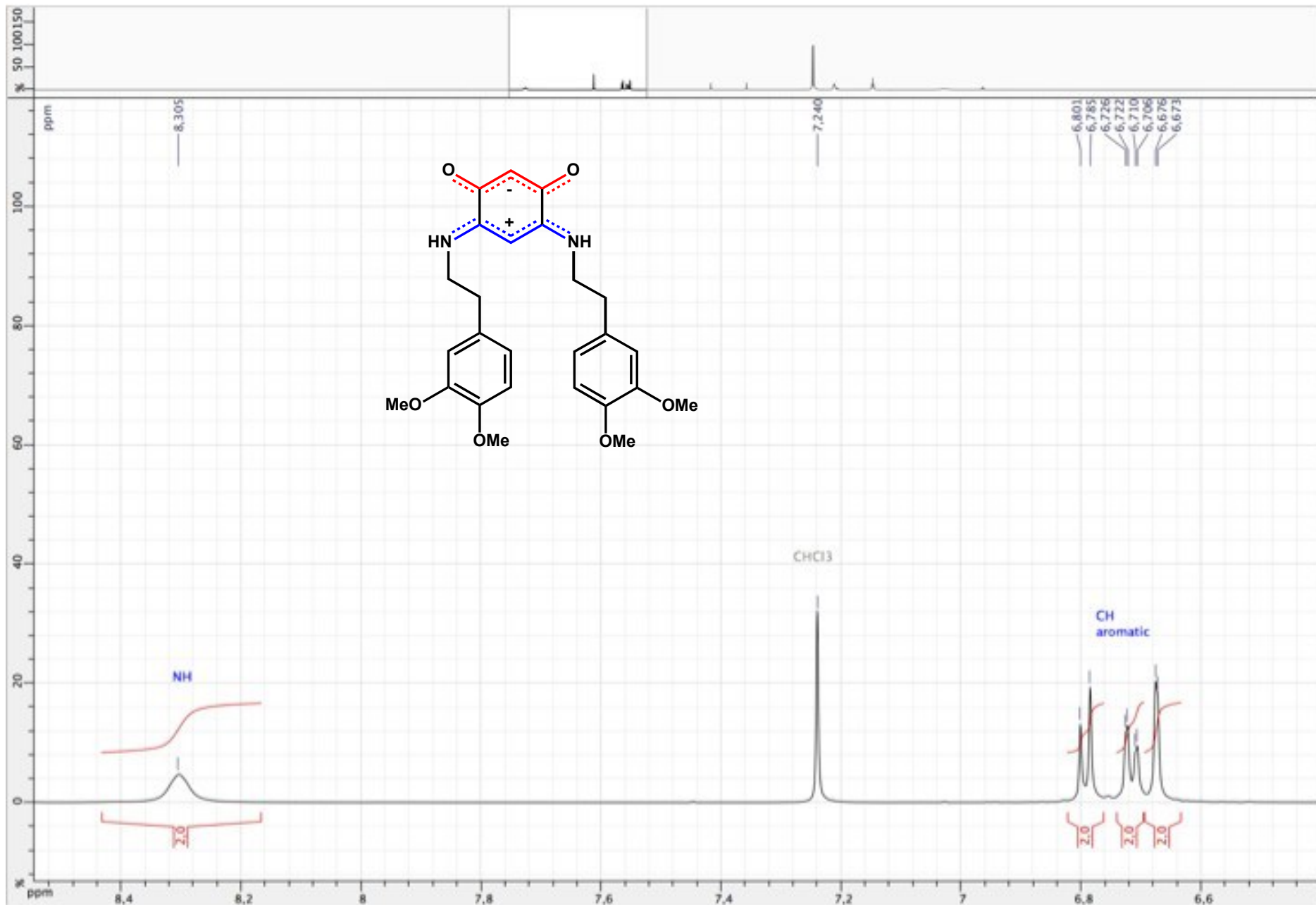


Figure S170. ^1H NMR spectrum of zwitterion **24** (CDCl_3 ; 500 MHz)

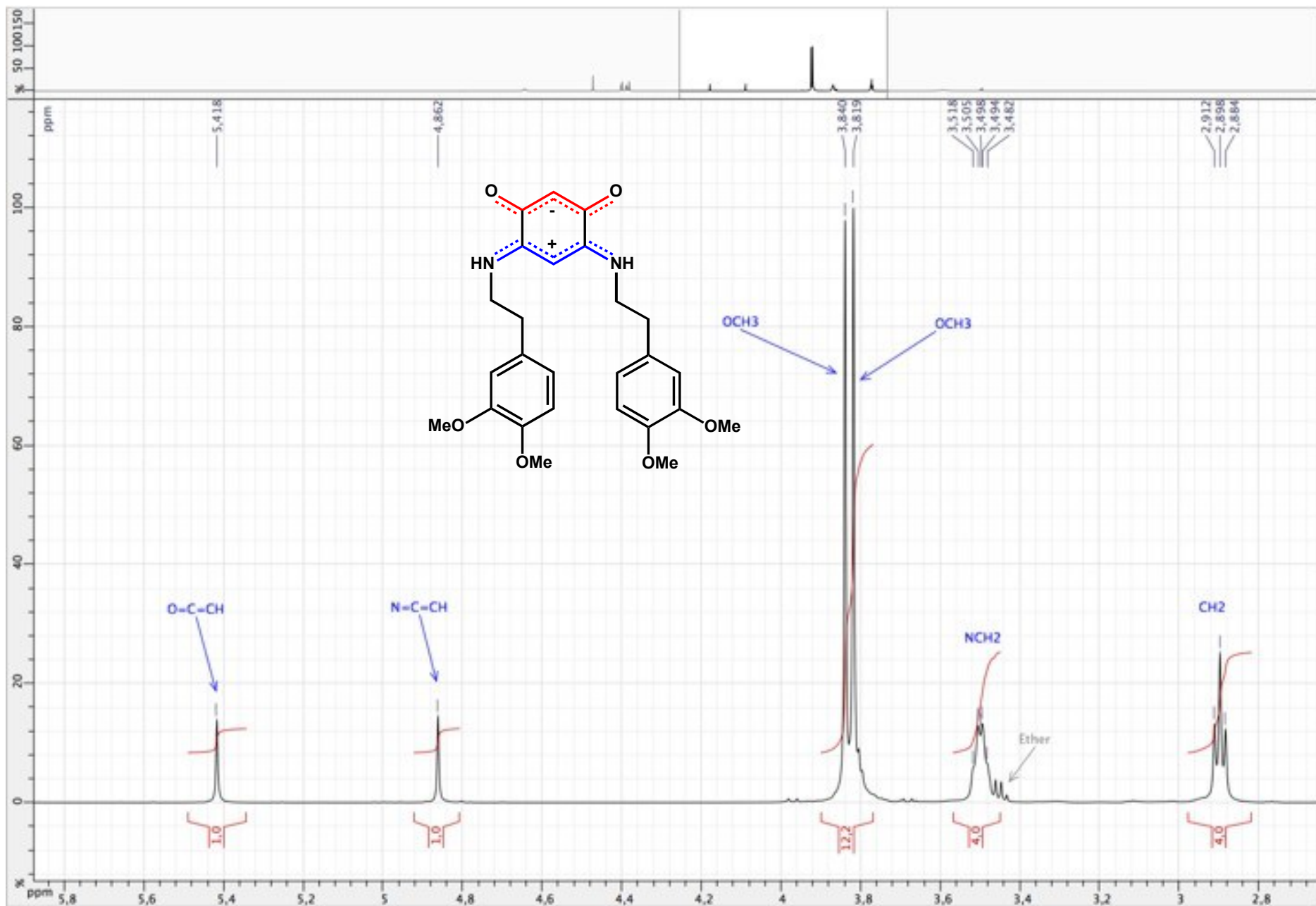


Figure S171. ^1H NMR spectrum of zwitterion **24** (CDCl_3 ; 500 MHz)

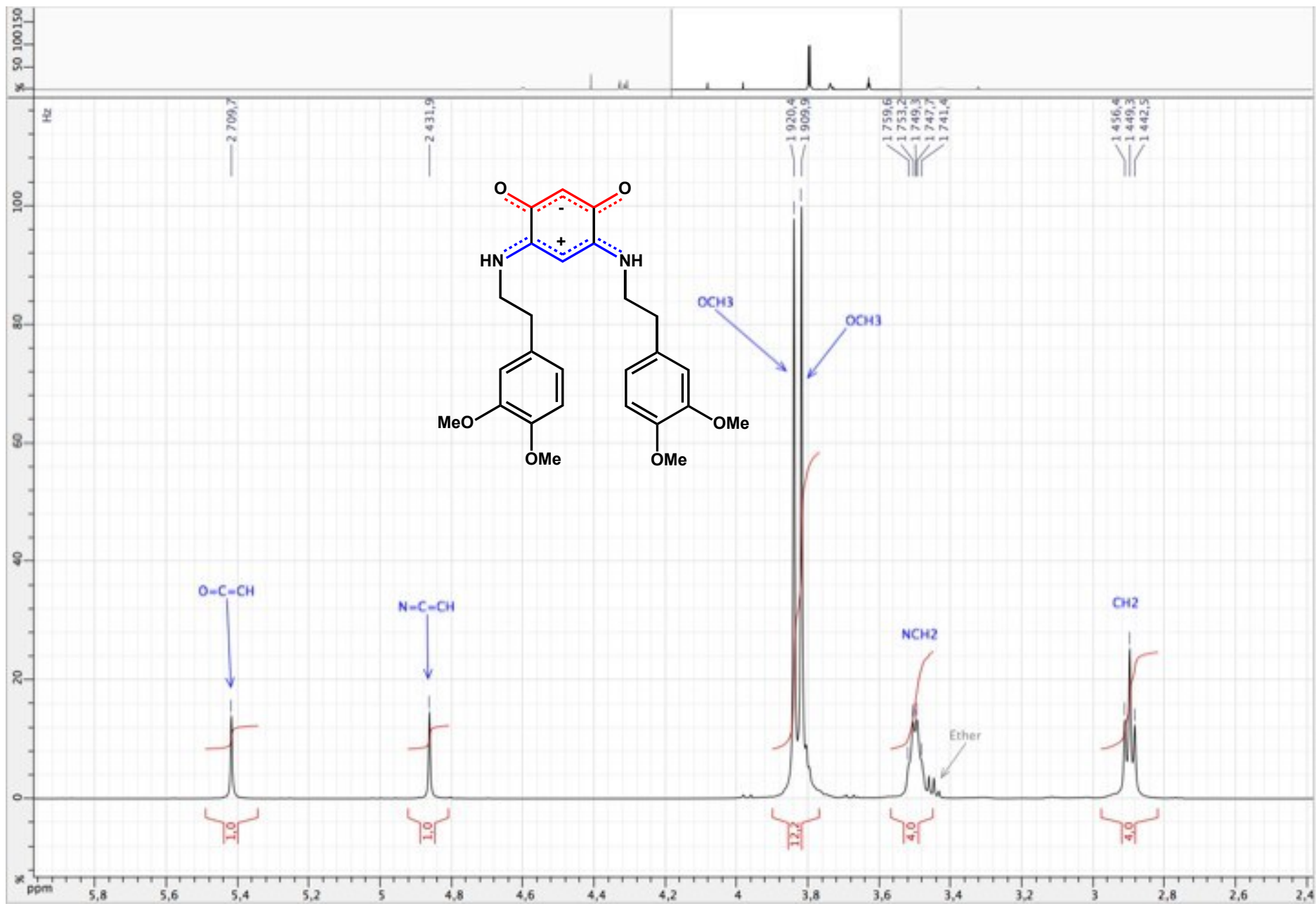


Figure S172. ^{13}C $\{^1\text{H}\}$ NMR spectrum of zwitterion **23** (CDCl_3 ; 125 MHz)

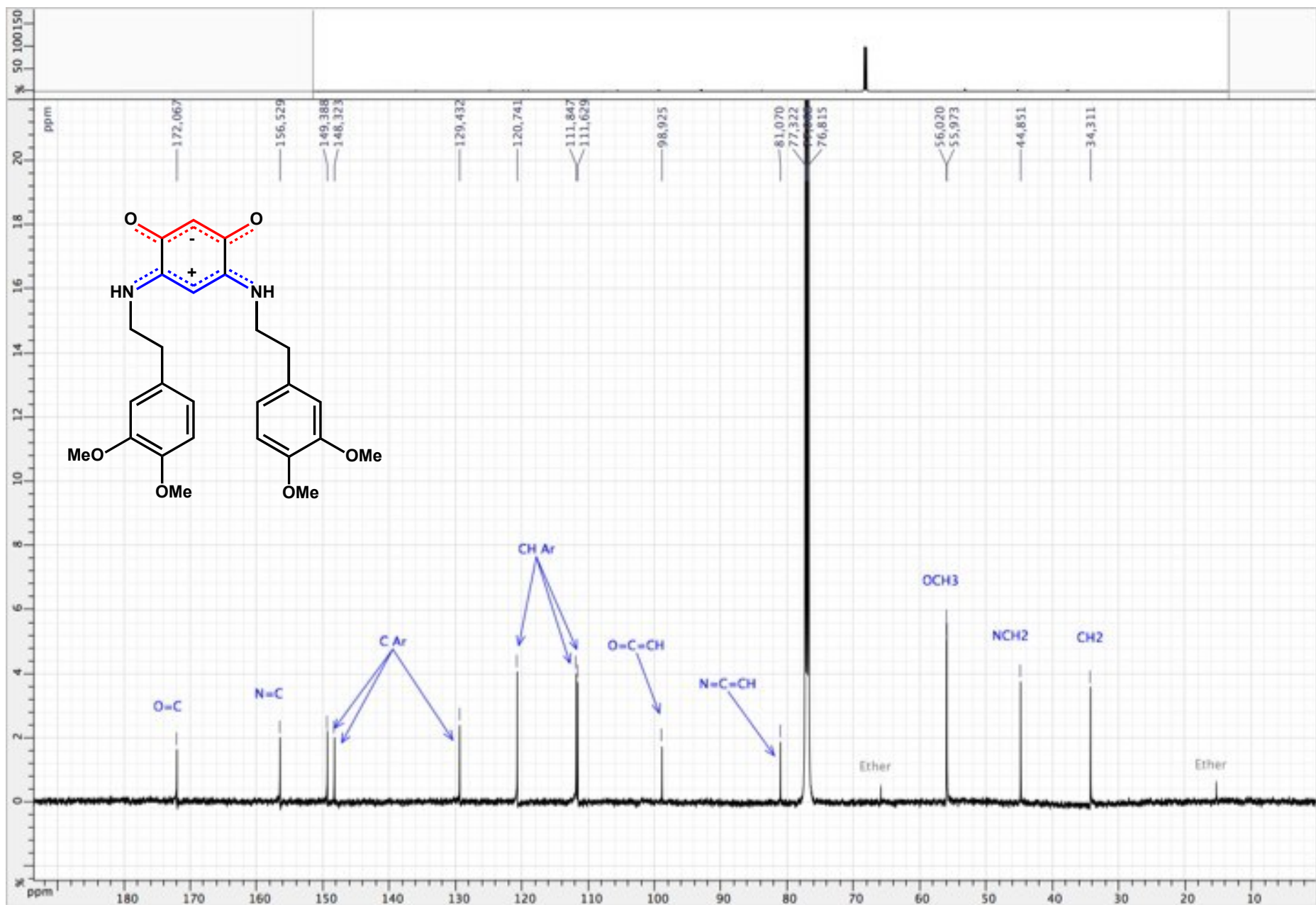


Figure S173. ^{13}C $\{^1\text{H}\}$ NMR spectrum of zwitterion **23** (CDCl_3 ; 125 MHz)

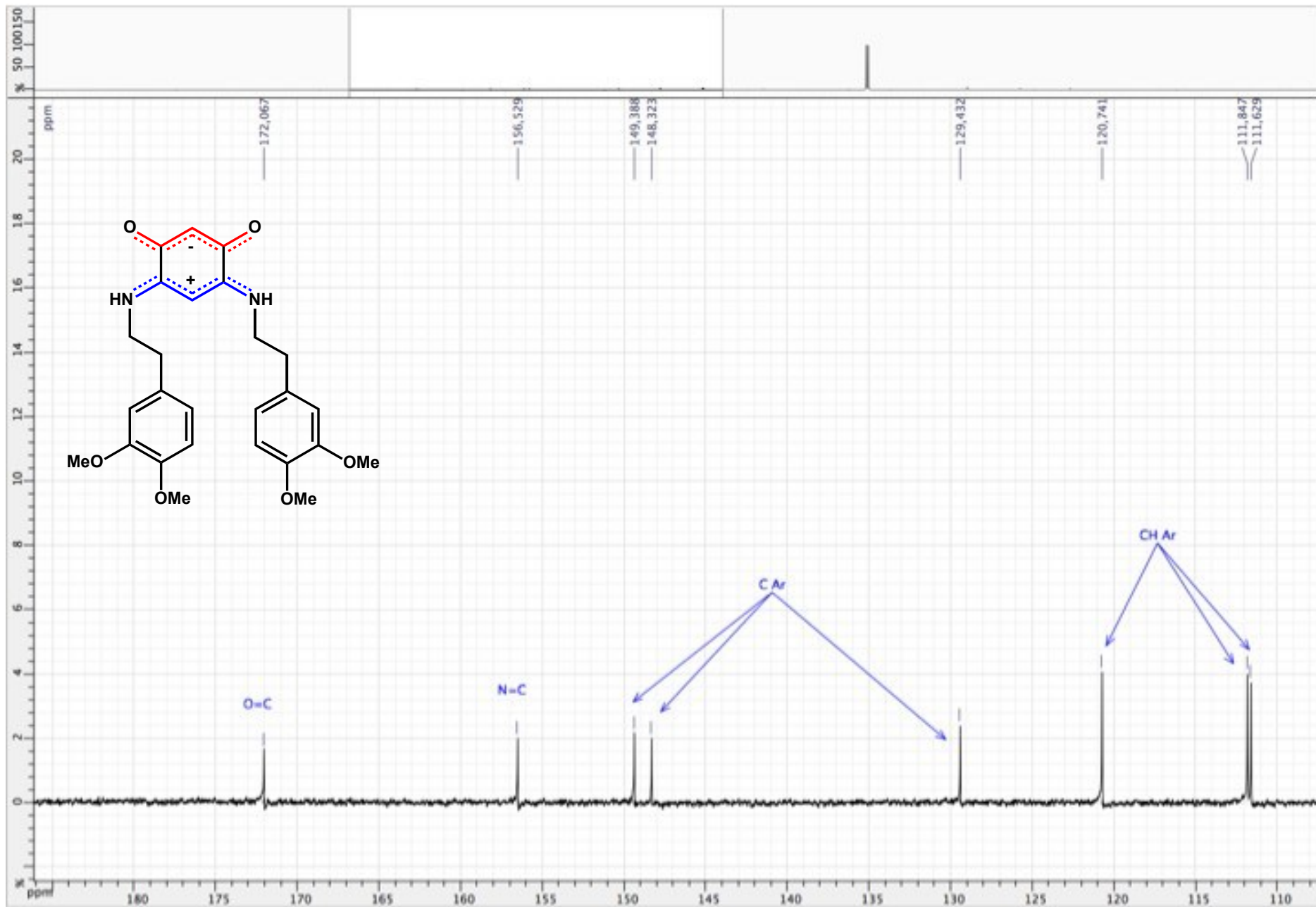


Figure S174. ^{13}C $\{^1\text{H}\}$ NMR spectrum of zwitterion **23** (CDCl_3 ; 125 MHz)

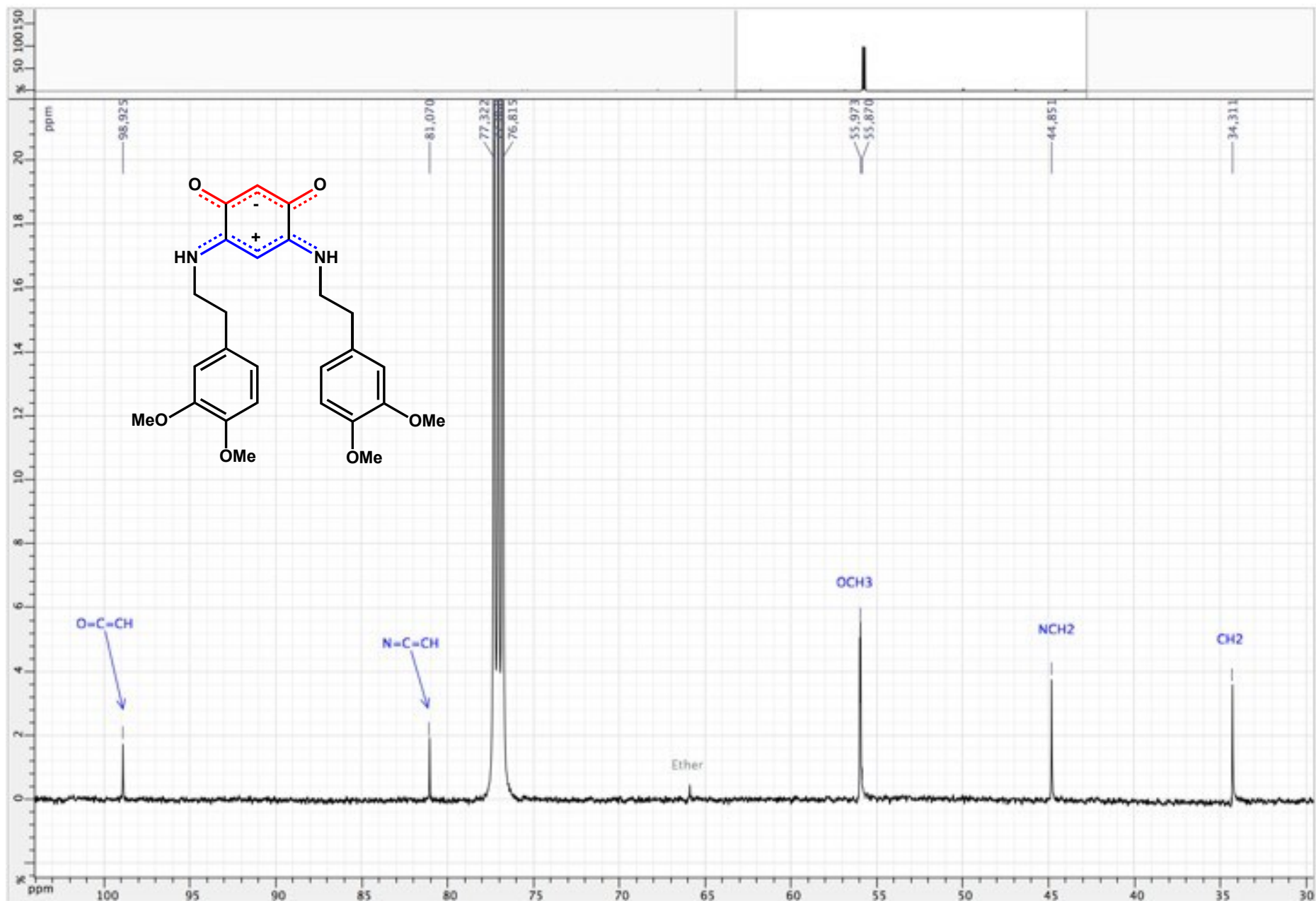


Figure S175. HSQC (^1H / ^{13}C { ^1H }) spectrum of zwitterion **24** (CDCl_3 ; 500 / 125 MHz)

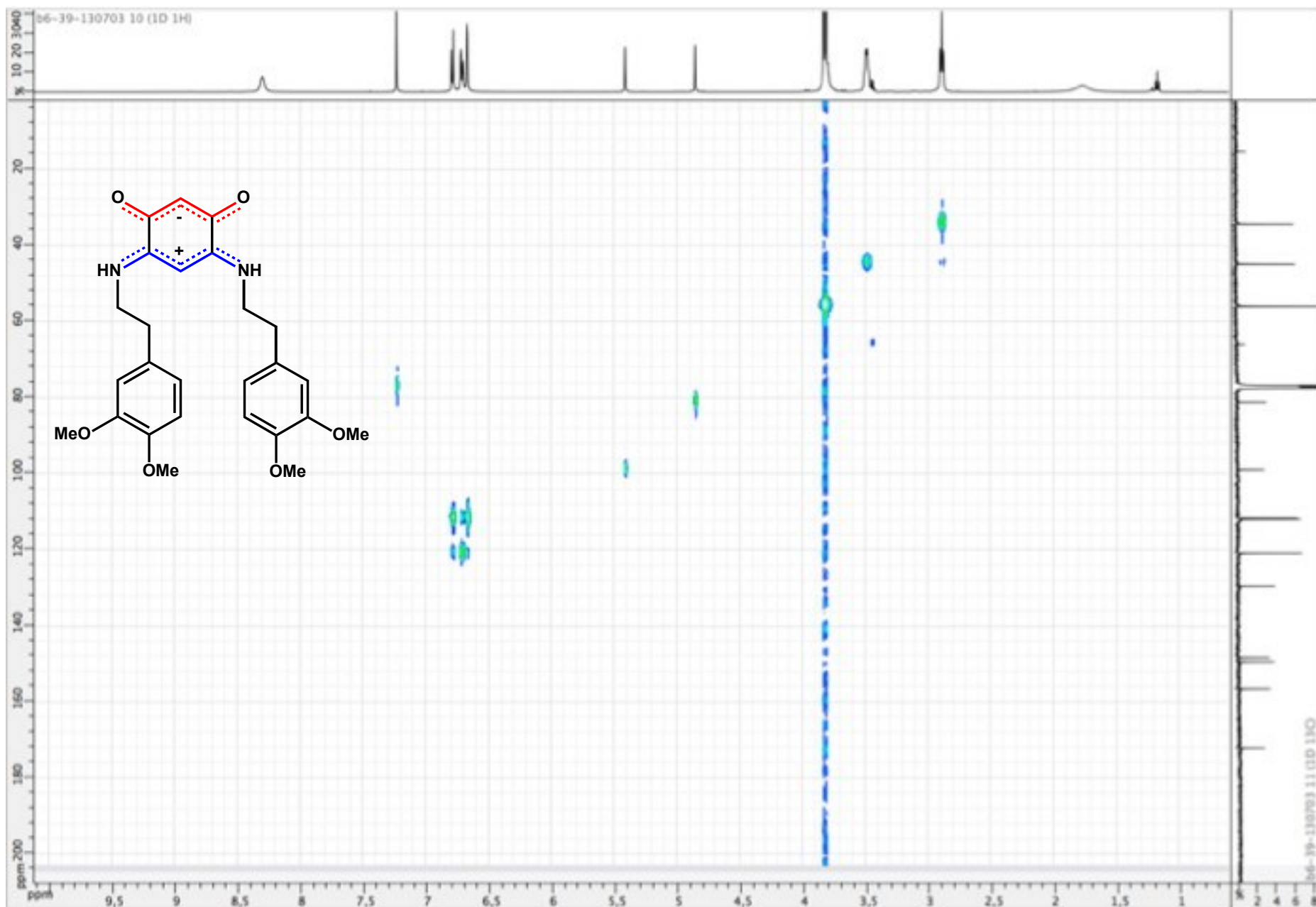


Figure S176. HSQC ($^1\text{H} / ^{13}\text{C} \{^1\text{H}\}$) spectrum of zwitterion **24** (CDCl_3 ; 500 / 125 MHz)

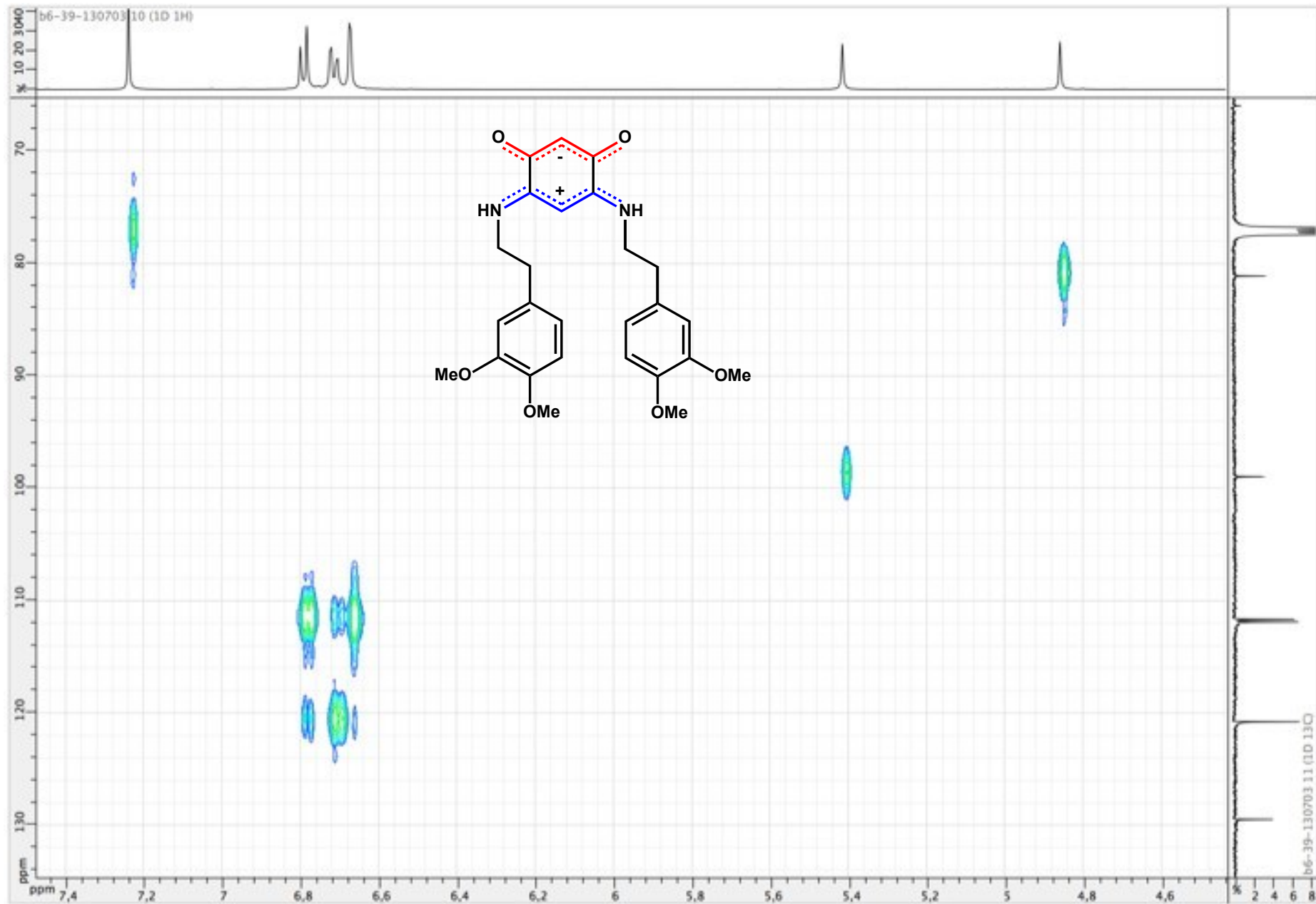


Figure S177. ^1H NMR spectrum of zwitterion **25** (DMSO d_6 ; 500 MHz)

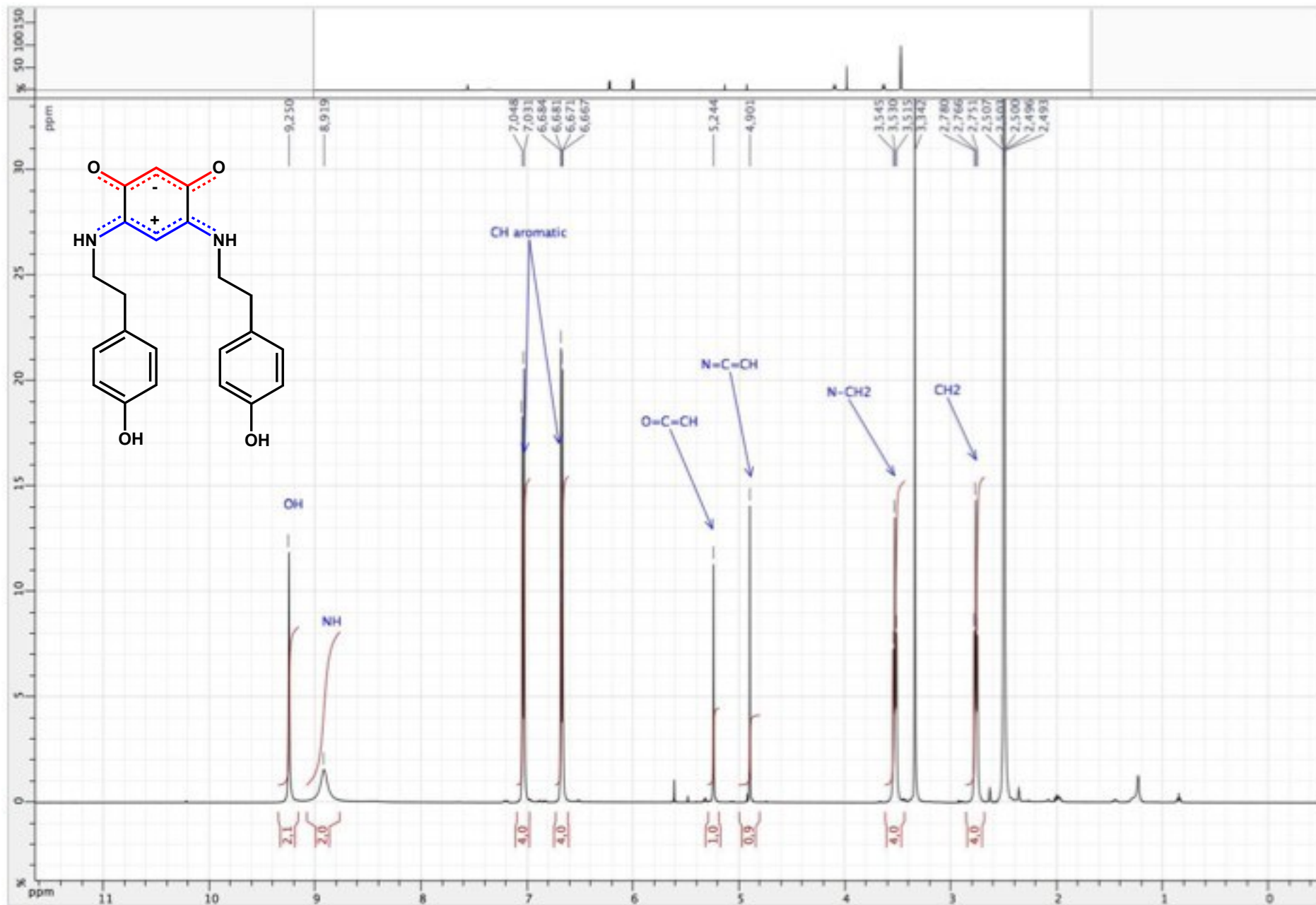


Figure S178. ^1H NMR spectrum of zwitterion **25** (DMSO d_6 ; 500 MHz)

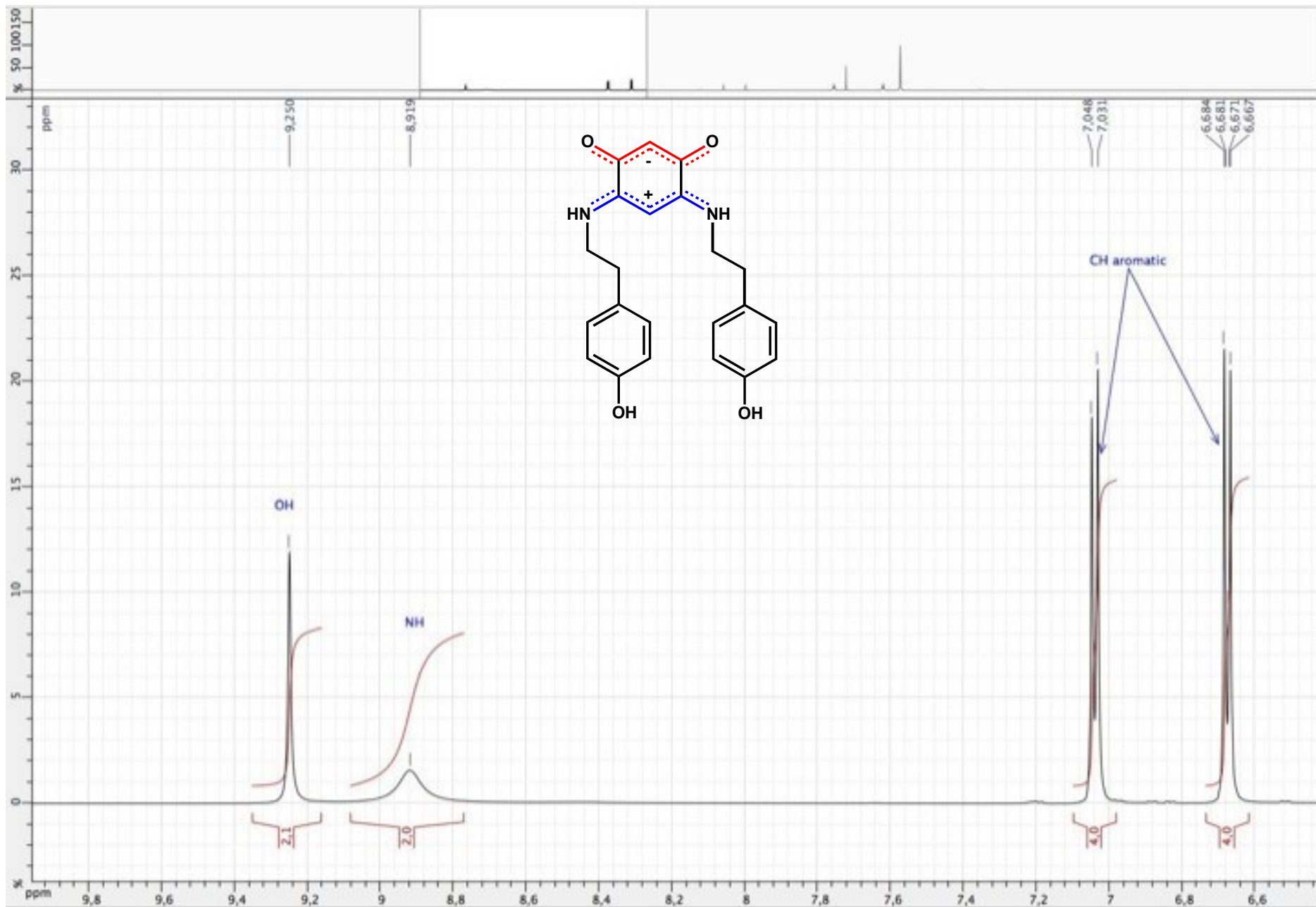


Figure S179. ^1H NMR spectrum of zwitterion **25** (DMSO d_6 ; 500 MHz)

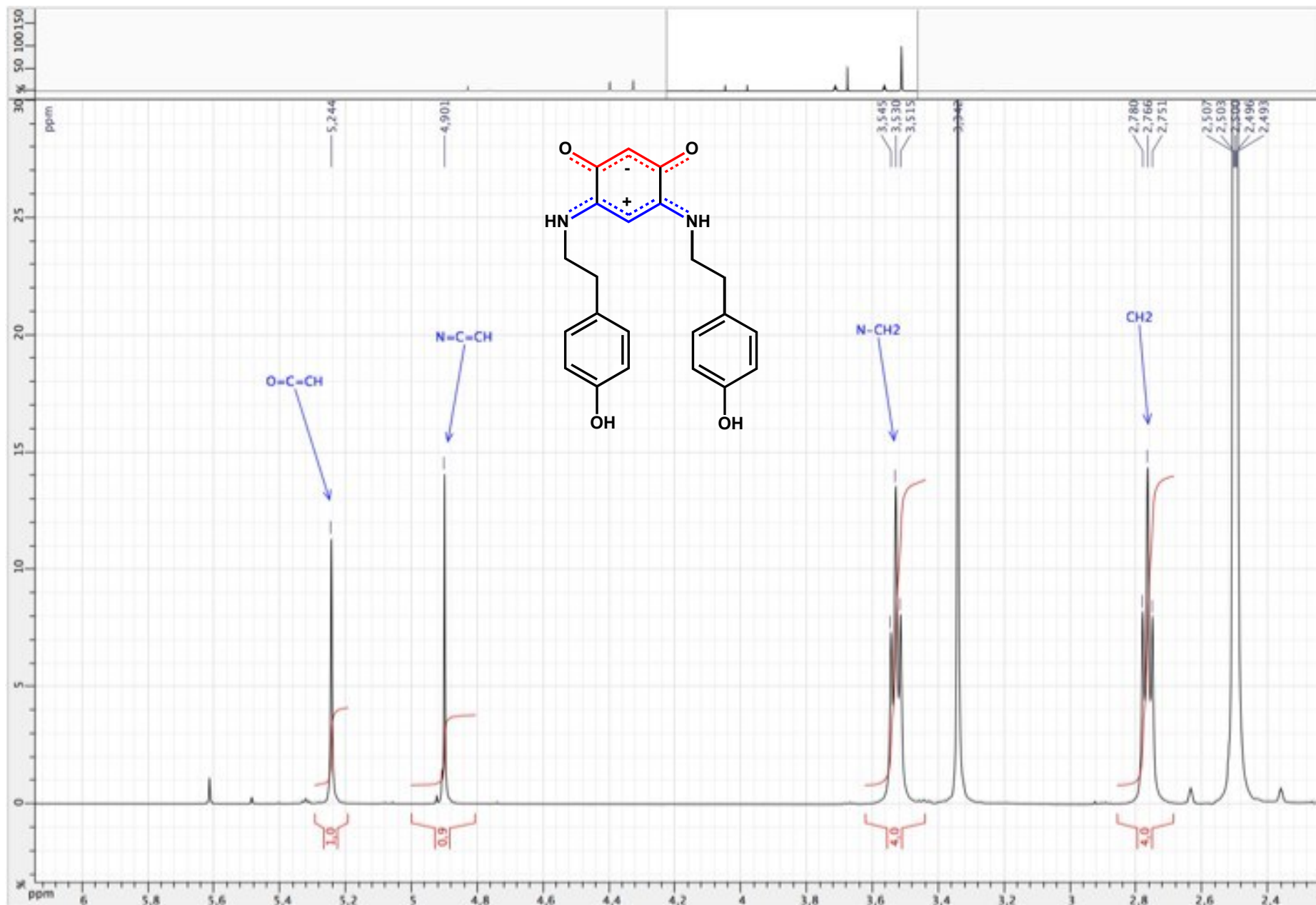


Figure S180. ^1H NMR spectrum of zwitterion **25** (DMSO d_6 ; 500 MHz)

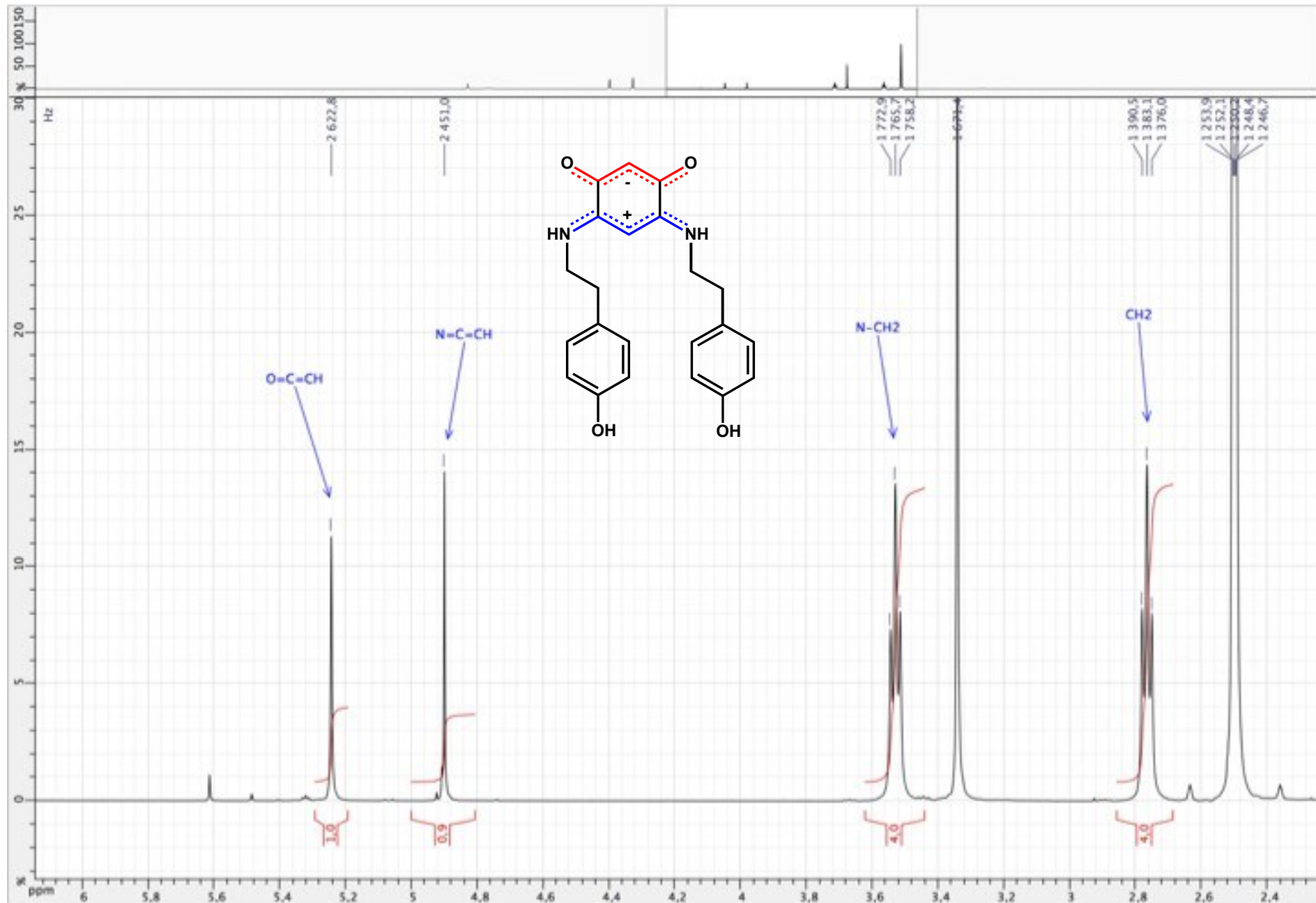


Figure S181. ^{13}C $\{^1\text{H}\}$ NMR spectrum of zwitterion **25** (DMSO d_6 ; 125 MHz)

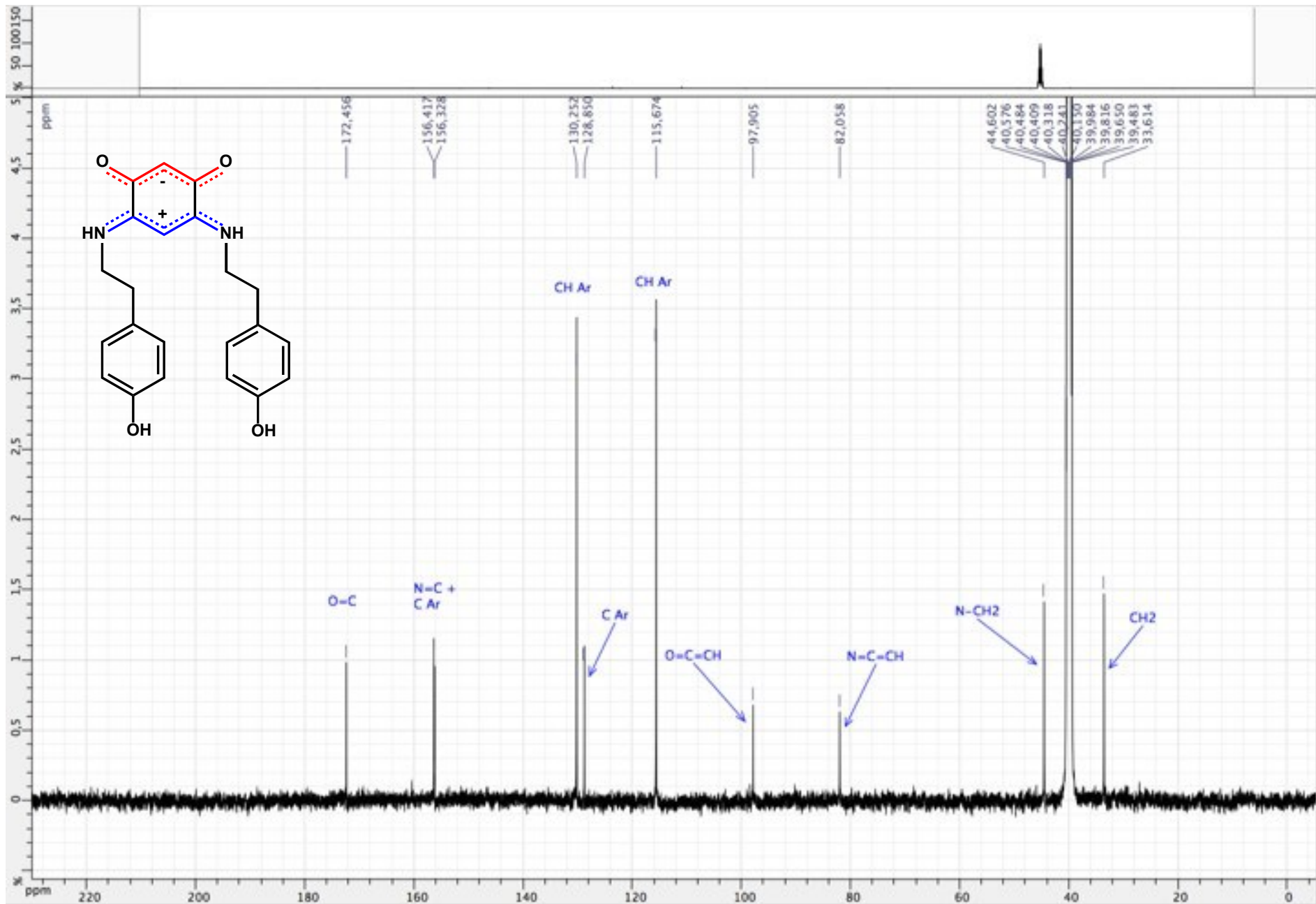


Figure S182. ^{13}C $\{^1\text{H}\}$ NMR spectrum of zwitterion **25** (DMSO d_6 ; 125 MHz)

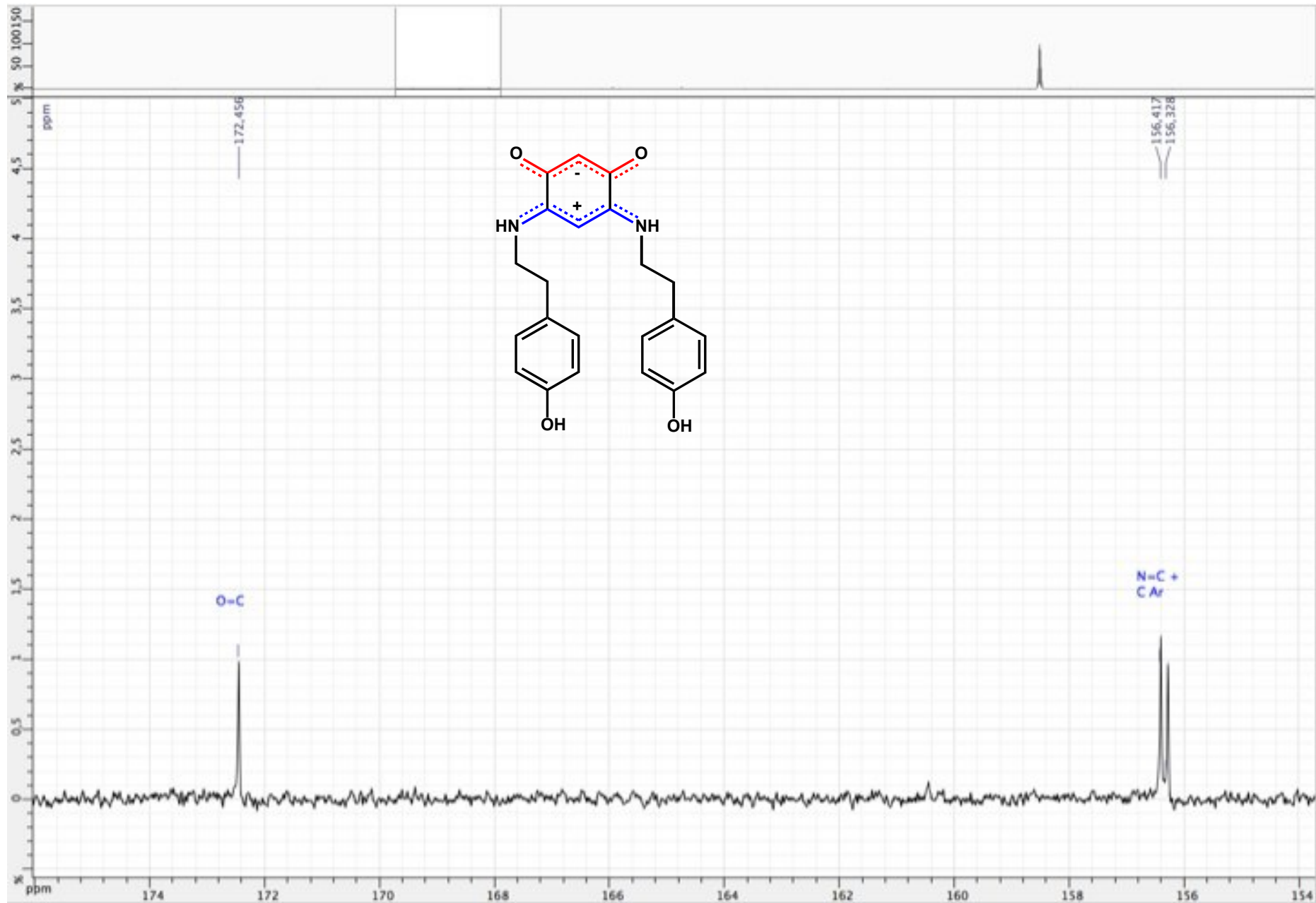


Figure S183. ^{13}C $\{^1\text{H}\}$ NMR spectrum of zwitterion **25** (DMSO d_6 ; 125 MHz)

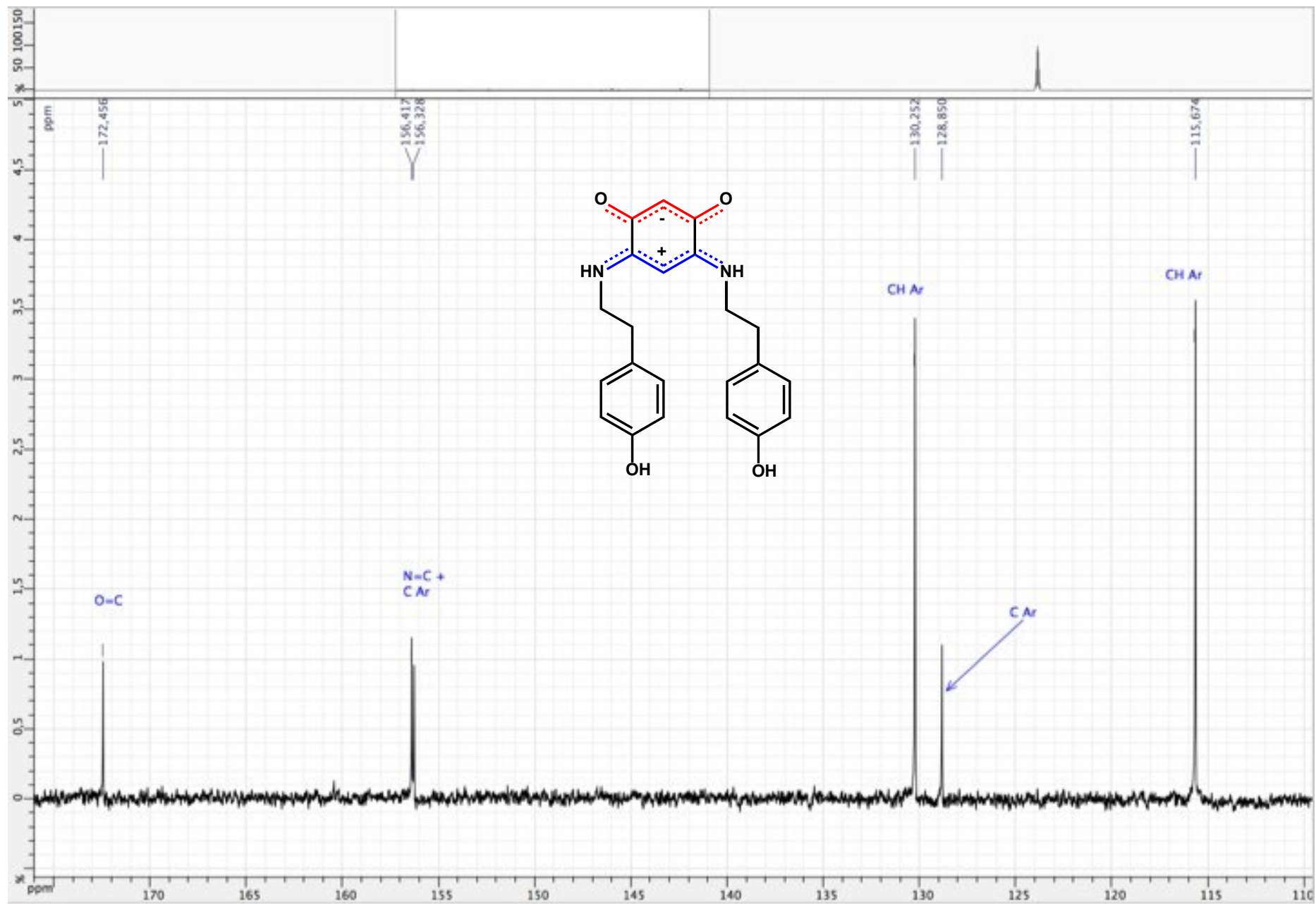


Figure S184. ^{13}C $\{^1\text{H}\}$ NMR spectrum of zwitterion **25** (DMSO d_6 ; 125 MHz)

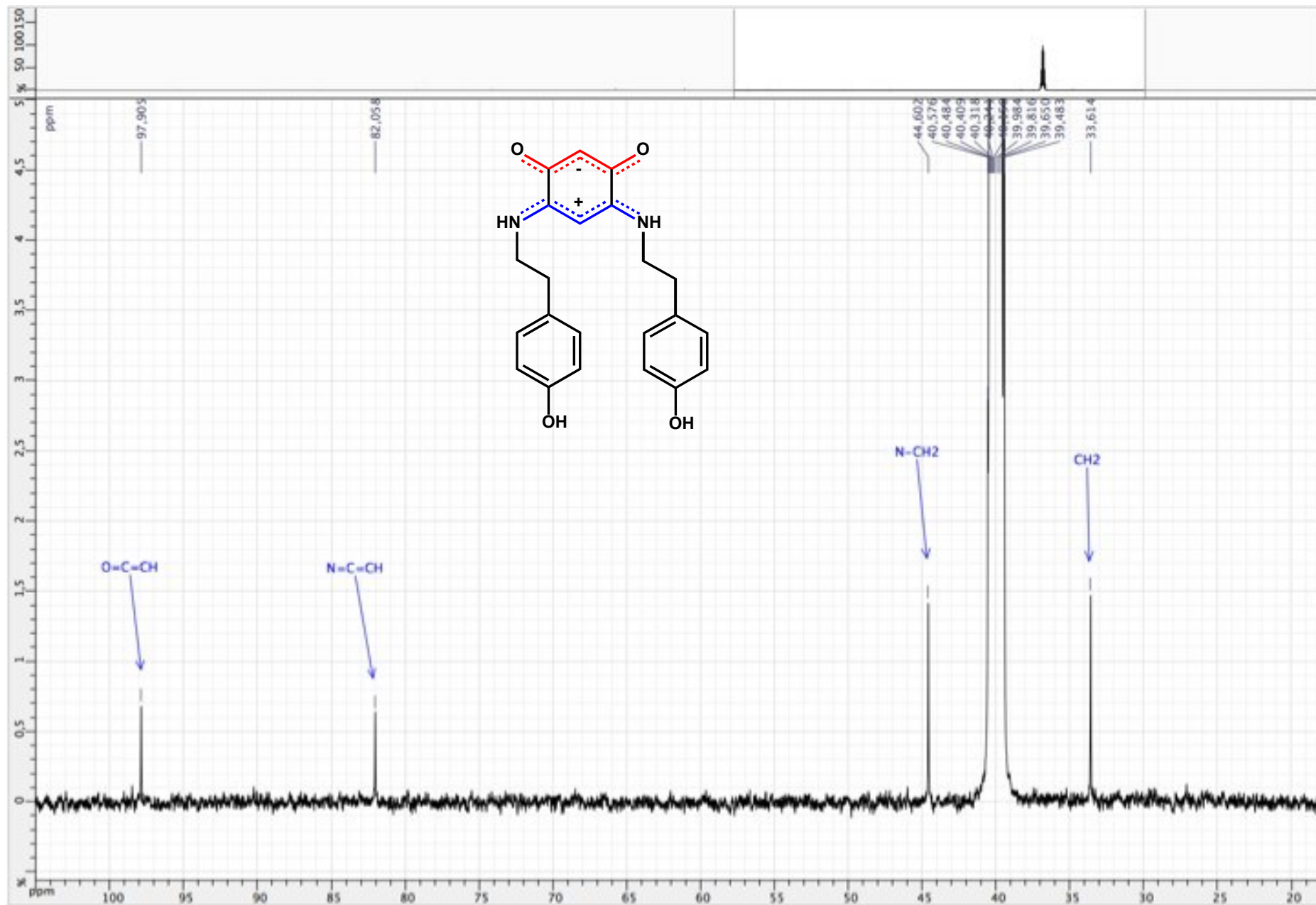


Figure S185. ¹H NMR spectrum of zwitterion 26 (DMSO d₆ ; 500 MHz)

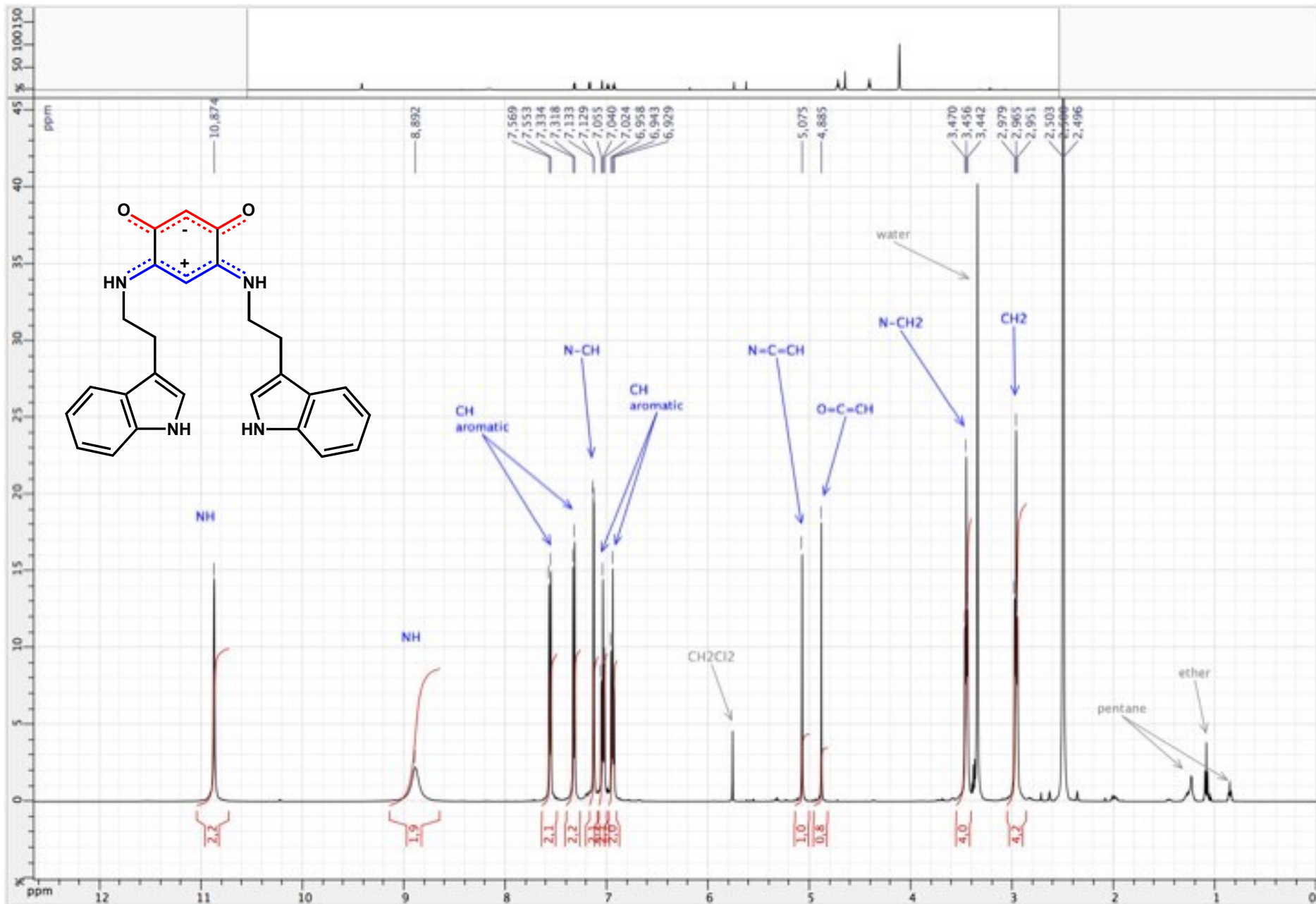


Figure S186. ¹H NMR spectrum of zwitterion 26 (DMSO d₆ ; 500 MHz)

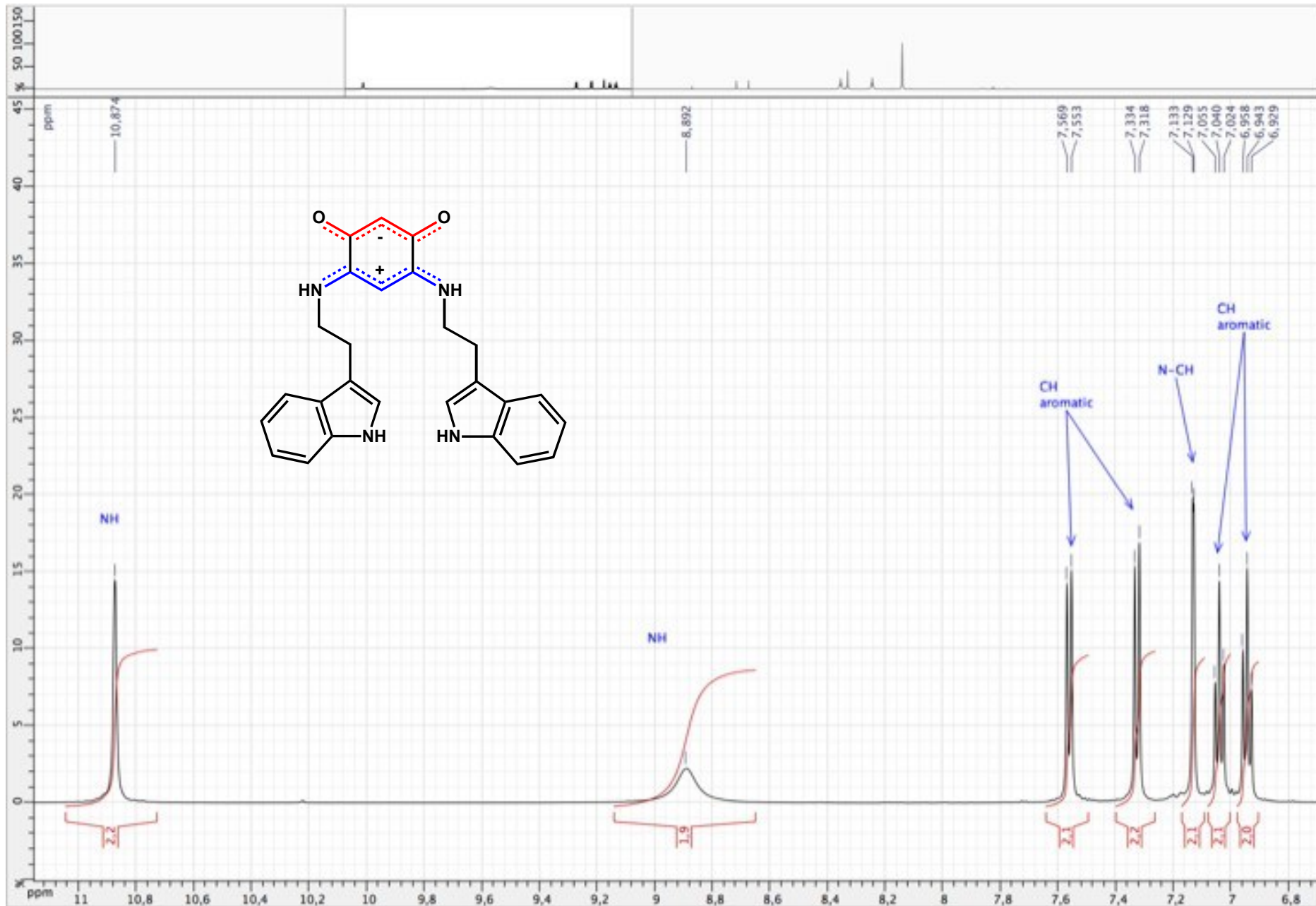


Figure S187. ¹H NMR spectrum of zwitterion 26 (DMSO d6 ; 500 MHz)

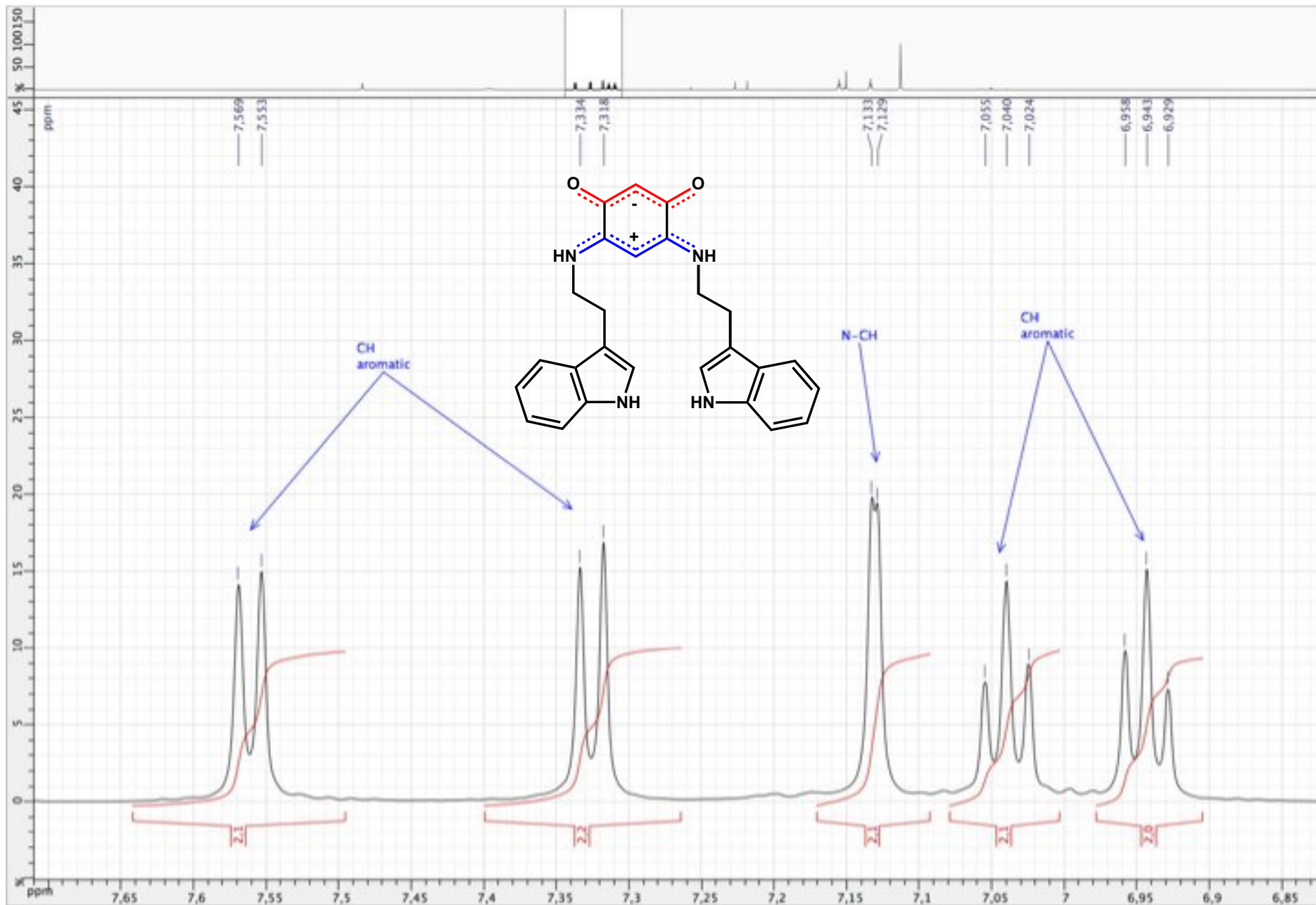


Figure S188. ^1H NMR spectrum of zwitterion **26** (DMSO d_6 ; 500 MHz)

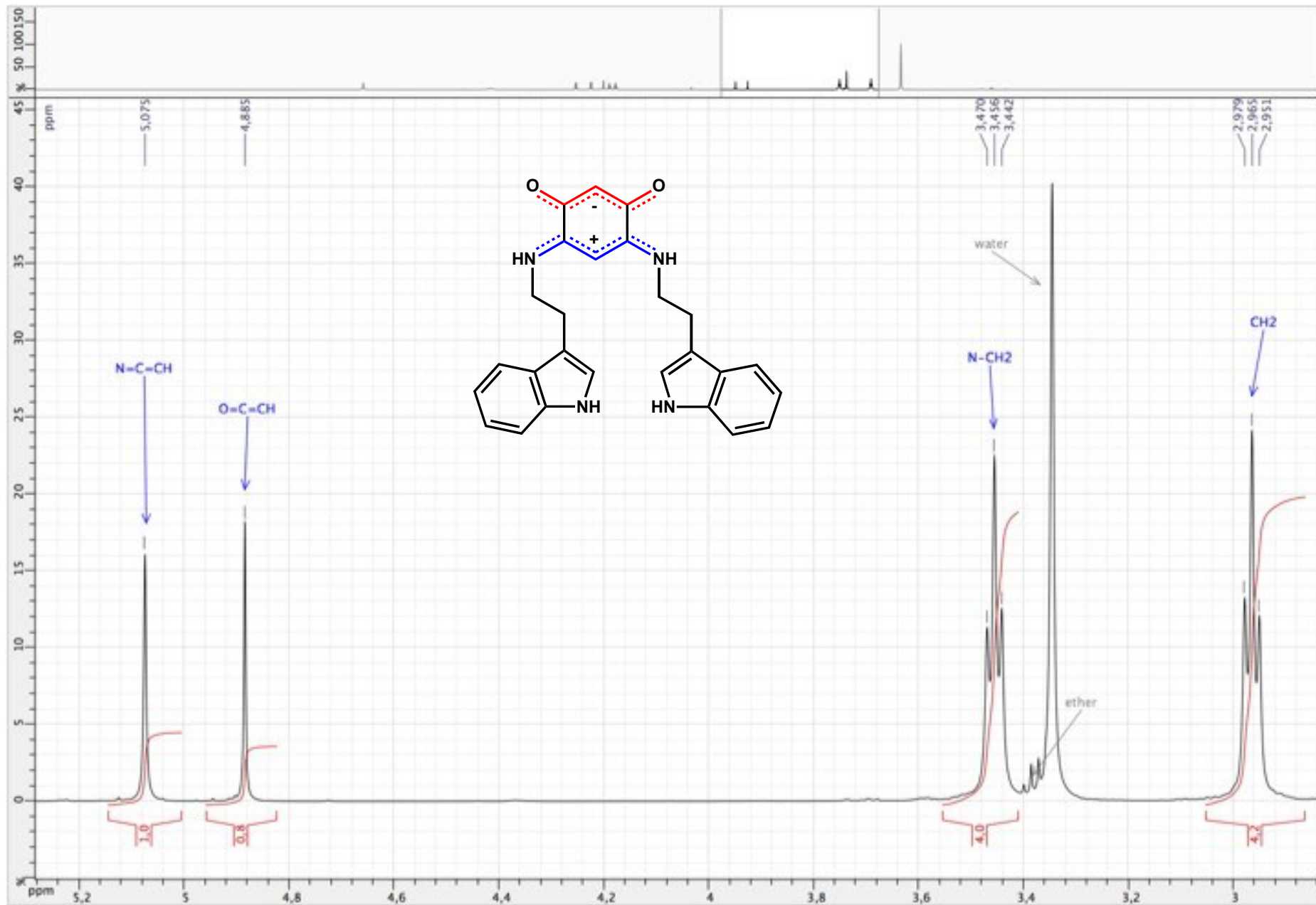


Figure S189. ¹H NMR spectrum of zwitterion 26 (DMSO d₆ ; 500 MHz)

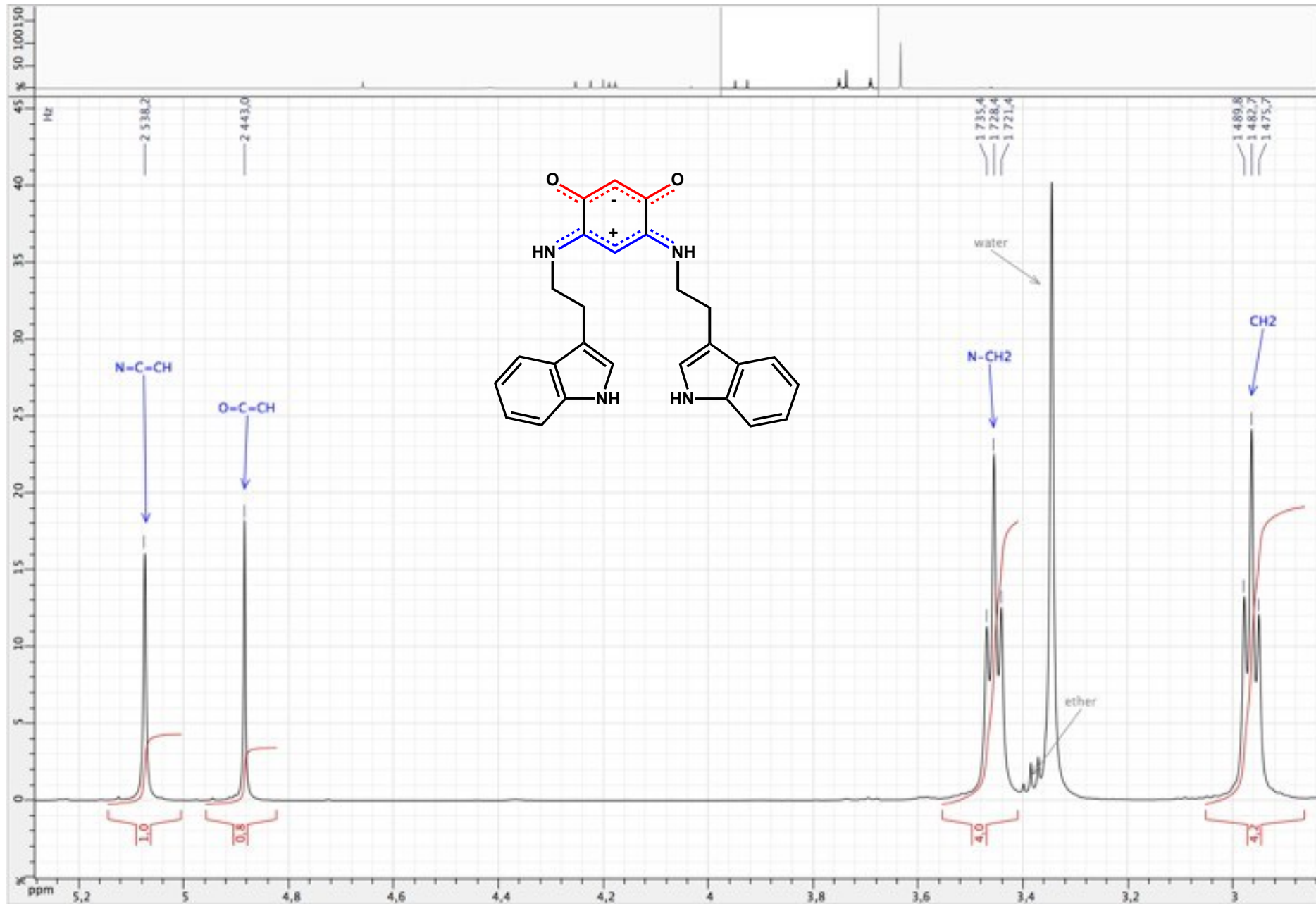


Figure S190. ^{13}C $\{^1\text{H}\}$ NMR spectrum of zwitterion **26** (DMSO d_6 ; 125 MHz)

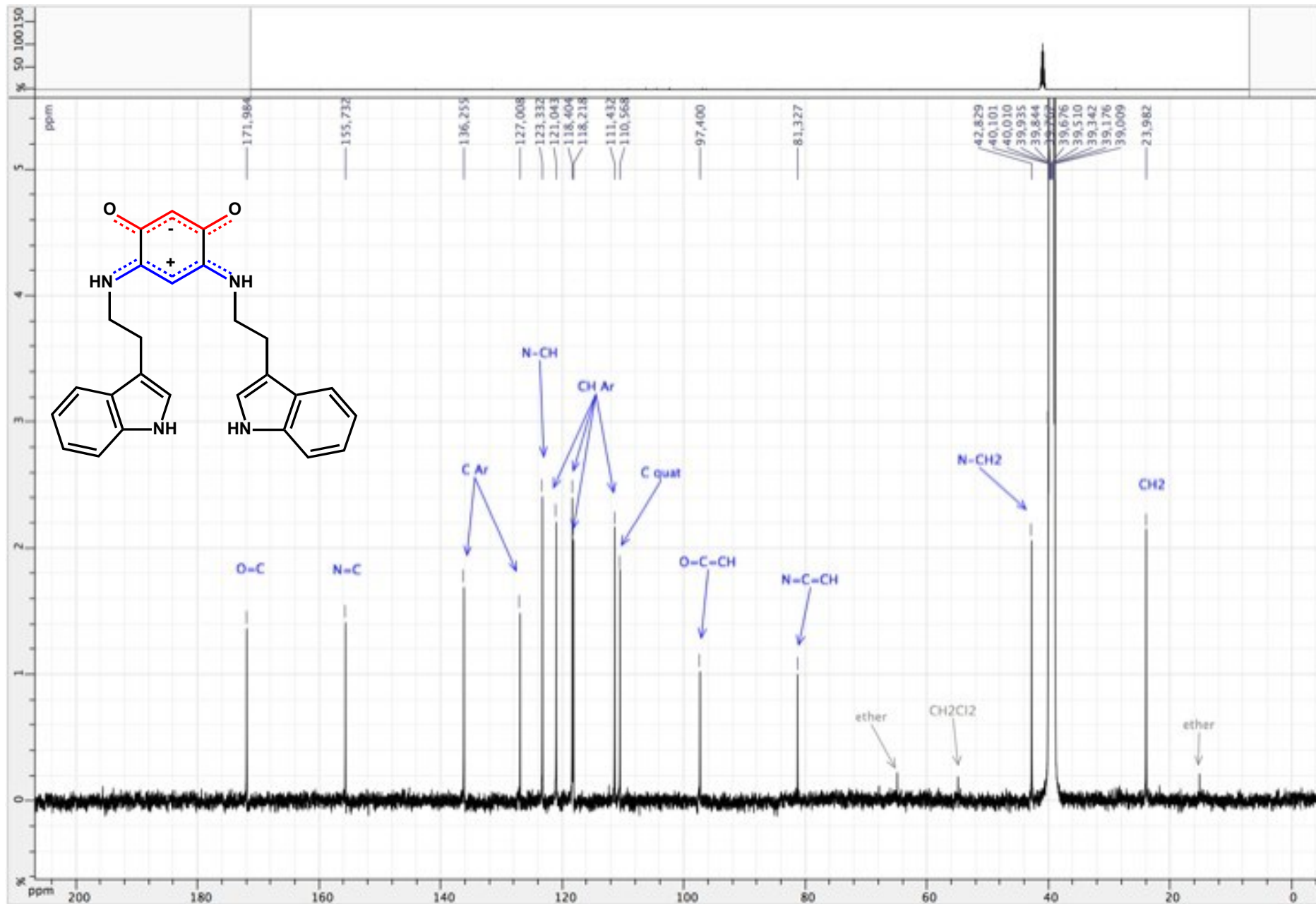


Figure S191. ^{13}C $\{^1\text{H}\}$ NMR spectrum of zwitterion **26** (DMSO d_6 ; 125 MHz)

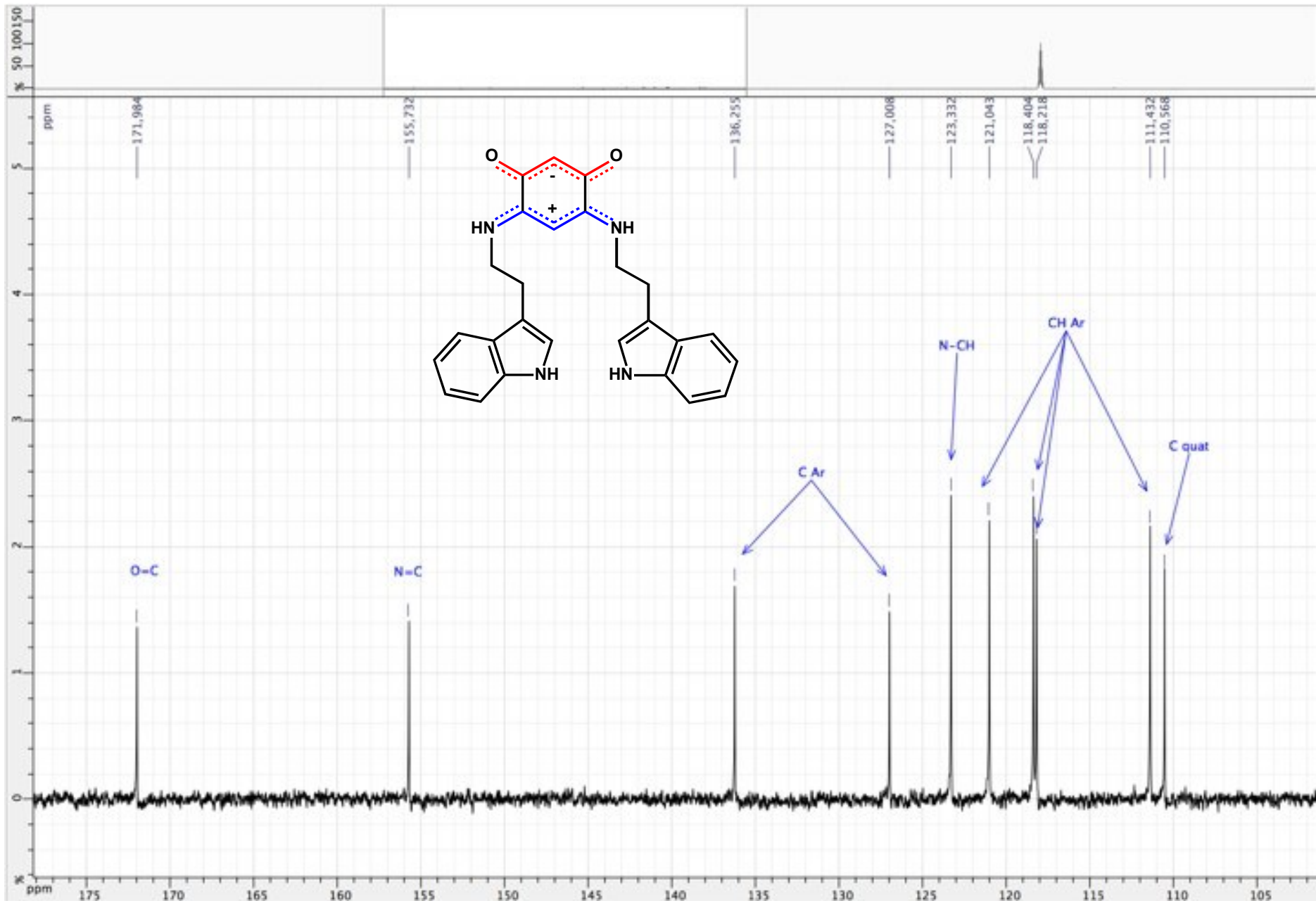


Figure S192. ^{13}C $\{^1\text{H}\}$ NMR spectrum of zwitterion **26** (DMSO d_6 ; 125 MHz)

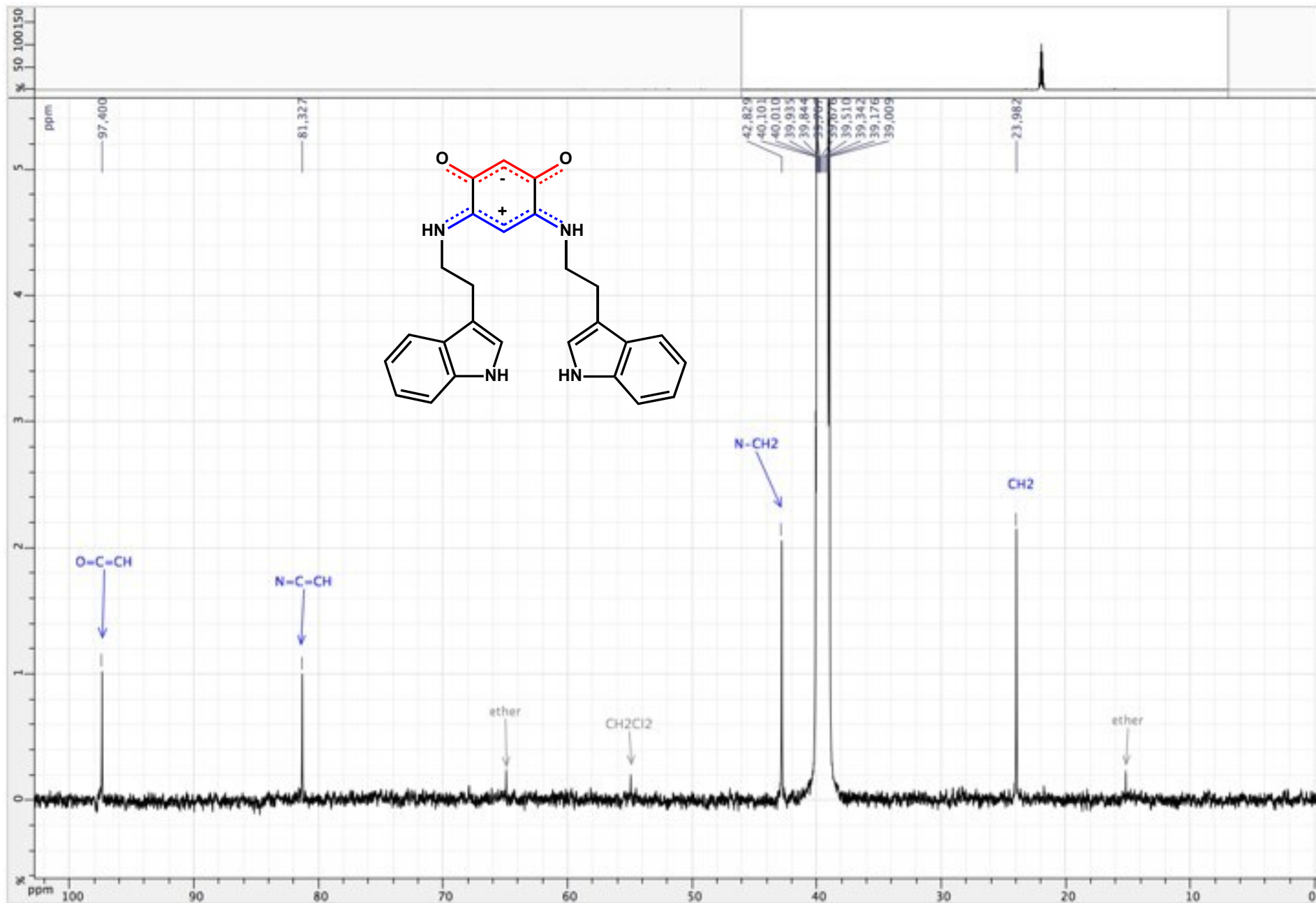


Figure S193. HSQC ($^1\text{H} / ^{13}\text{C} \{^1\text{H}\}$) spectrum of zwitterion **26** (DMSO d_6 ; 500 / 125 MHz)

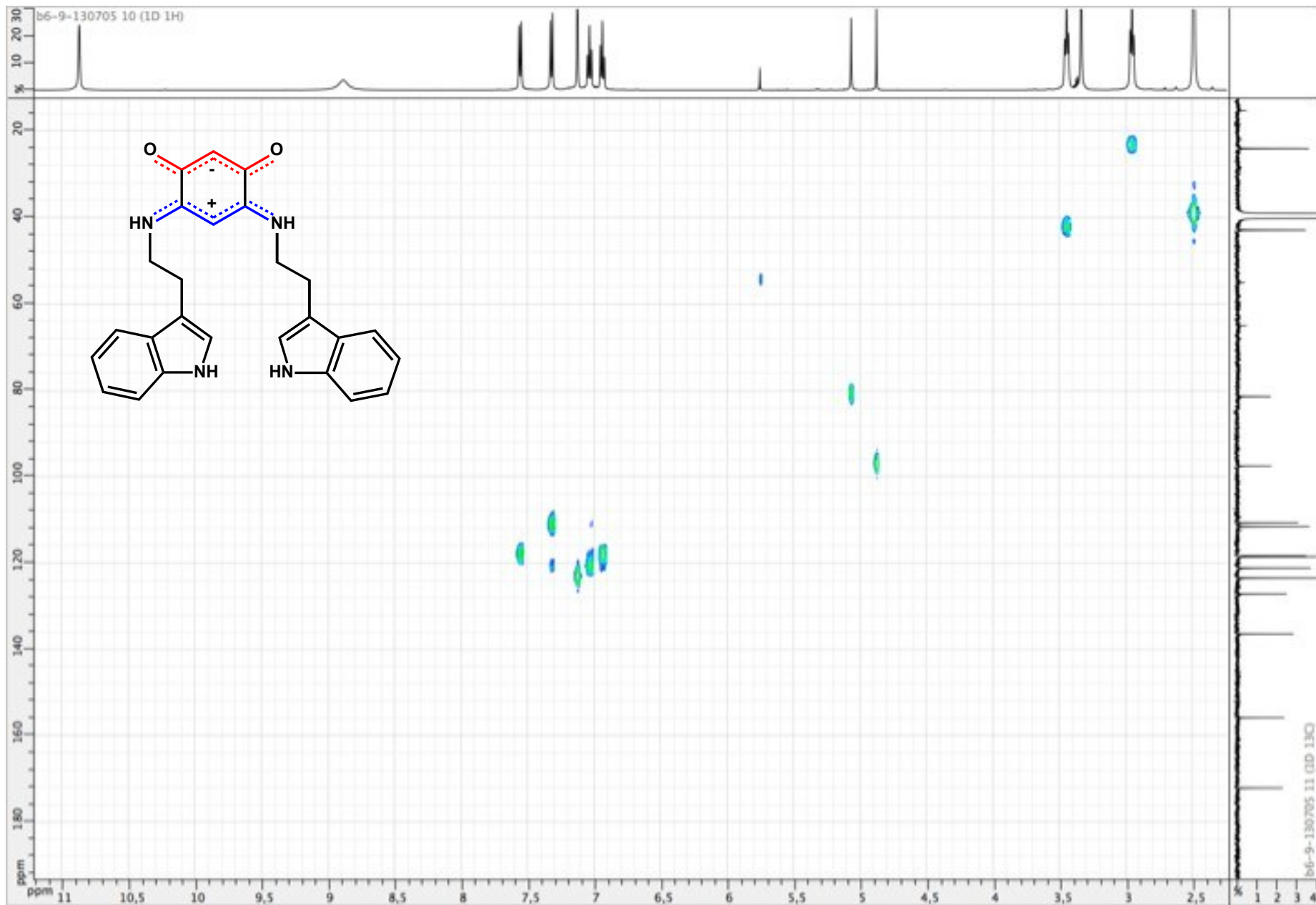


Figure S194. HSQC ($^1\text{H} / ^{13}\text{C} \{^1\text{H}\}$) spectrum of zwitterion **26** (DMSO d_6 ; 500 / 125 MHz)

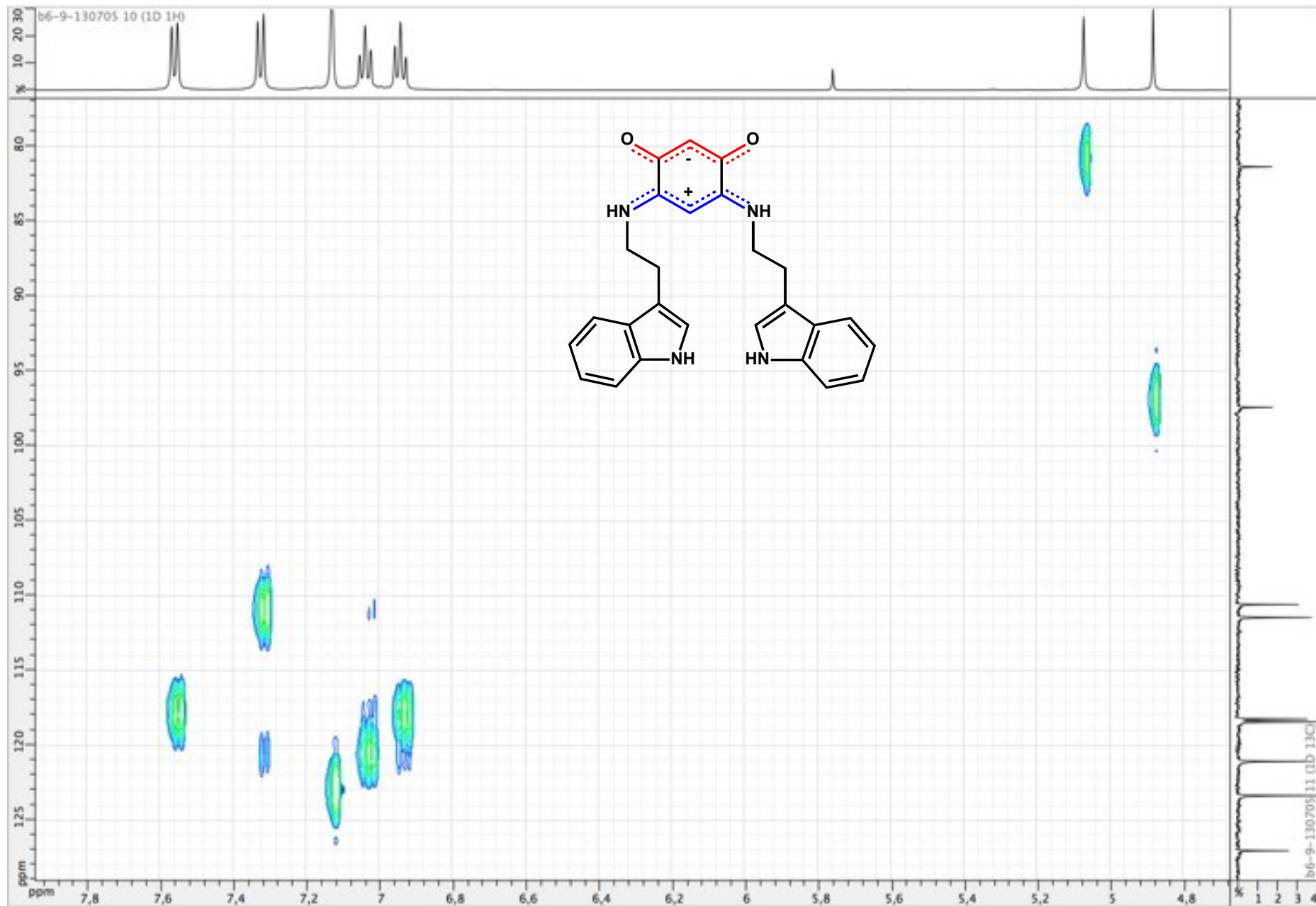


Figure S195. COSY ($^1\text{H} / ^1\text{H}$) spectrum of zwitterion **26** (DMSO d_6 ; 500 MHz)

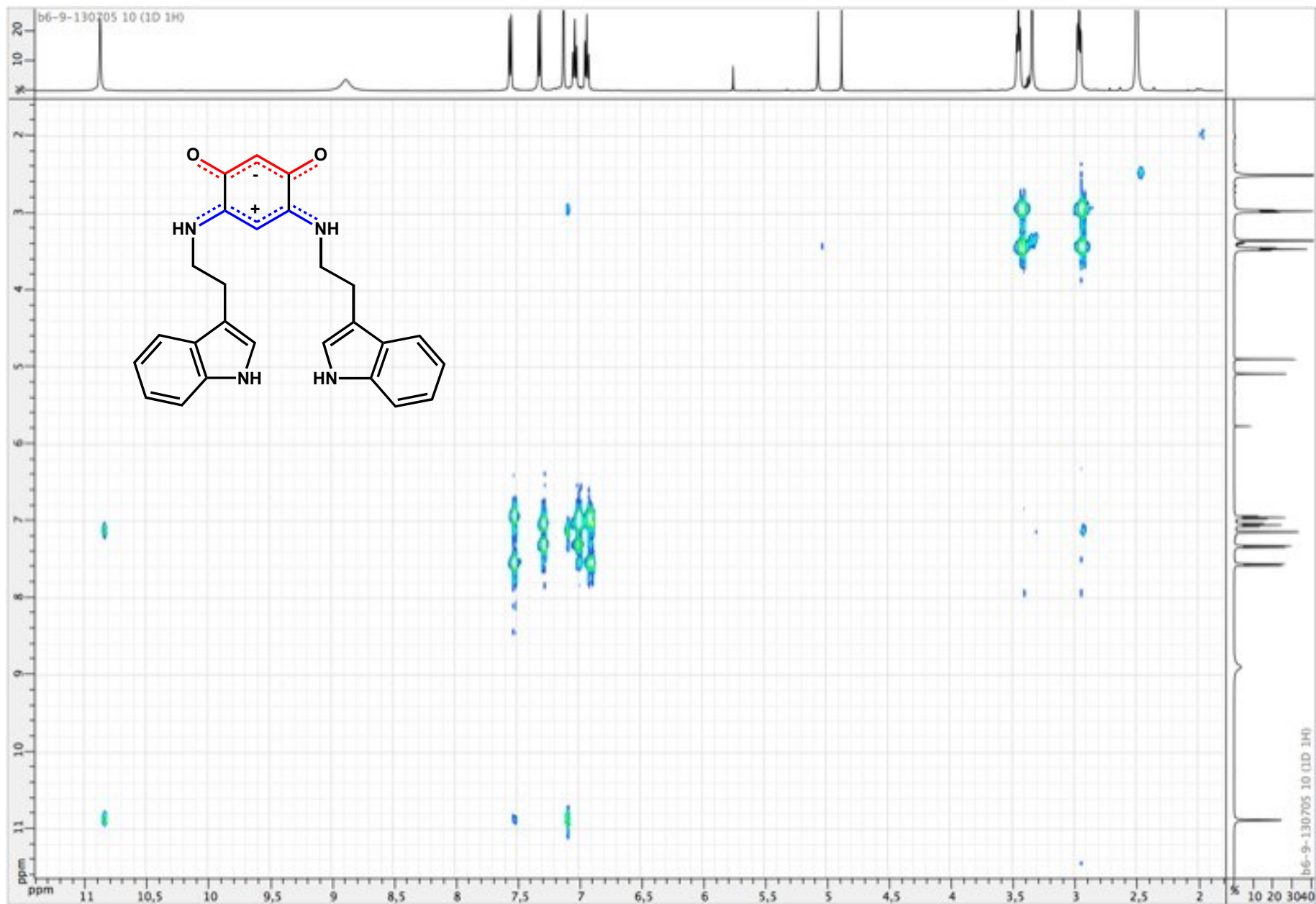


Figure S196. COSY ($^1\text{H} / ^1\text{H}$) spectrum of zwitterion **26** (DMSO d_6 ; 500 MHz)

